



UNIVERSITAT POLITÈCNICA
DE CATALUNYA

UNIVERSITAT POLITÈCNICA DE CATALUNYA
TEORIA DEL SENYAL I COMUNICACIONS

TRANSMISSION STRATEGIES FOR INTERFERING NETWORKS WITH FINITE RATE AND OUTDATED CHANNEL FEEDBACK

PhD Thesis

by MARC TORRELLAS SOCASTRO

Primary thesis advisor:
Adrian Agustin de Dios

Second thesis advisor:
Josep Vidal Manzano

Barcelona, December 2015

Abstract

The emergence of very capable mobile terminals, e.g. smartphones or tablets, has dramatically increased the demand of wireless data traffic in recent years. Current growth forecasts elucidate that wireless communication standards will not be able to afford future traffic demands, thus many research efforts have been oriented towards increasing the efficiency of wireless networks.

Wireless communications introduce many issues not present in wired systems, e.g. multipath effects or interference. Some of these issues may be tackled by the use of multiple antennas, i.e. MIMO technologies. This solution allows increasing not only the reliability and robustness of the communications, i.e. the diversity gain, but also its efficiency, i.e. the multiplexing gain or *degrees of freedom* (DoF). The DoF describe the slope of channel capacity at very high signal-to-noise-ratio (SNR) regime. For a point-to-point (P2P) communication, assuming that the wireless channel response is Rayleigh distributed (typical in urban environments with no dominant line of sight propagation), it is known that the DoF are equal to the minimum between the number of antennas at the transmitter and the receiver. Consequently, the throughput of a MIMO system may be scaled in a promising way, considerably boosting the efficiency of the system.

However, the DoF behavior for multi-user networks is still an open problem in general. This thesis focuses on the problem of characterizing the DoF of such networks, where a new problem comes into play: the interference. The most trivial way of tackling it is by means of orthogonalization of the transmission, i.e. the signals intended to each user are transmitted along different time slots. Although completely avoiding the problem of interference, with this solution resources are exploited by each user only a fraction of time inversely proportional to the number of users, i.e. each resource block is used only by one user.

As an alternative, the spatial dimensions provided by MIMO technologies may be exploited for orthogonalization, thus obtaining promising gains with reuse of time resources. Nevertheless, this approach implies sacrificing spatial dimensions in pursuit of managing the interference, i.e. instead of delivering more data symbols. Consequently, it is only advisable in case of an excess of antennas at the terminals. Since having a massive number of antennas may not be practical, especially at the user terminal, the *interference alignment* (IA) principle stands as a candidate for such dimensionally-limited systems. Introduced for the interference channel, with K transmitter-receiver pairs, a large number of applications of this concept have flooded the literature in the last years. In a nutshell, the IA approach allows having interference at the receiver under the constraint that interference terms are observed overlapped, which is achieved by smartly designing the transmitted signals. This way the number of dimensions occupied by interference can be reduced, thus increasing the number of symbols per user that can be delivered. Following this idea, one of the first works on IA showed the surprising result that in an

interference channel with an arbitrary number of transmitter-receivers pairs, “*each user gets half of the cake*”, where the *cake* refers to the number of degrees of freedom of the P2P channel.

At the beginning, the IA concept was exploited for scenarios where full channel state information is assumed to be available at the transmitter side (full CSIT), i.e. the information is acquired instantaneously, and with perfect quality. The first part of this thesis studies this case and completes the DoF characterization of the 3-user MIMO interference channel for some antenna configurations when channel coefficients are constant. For this case, the current approach in the literature, developed for time-varying channels, cannot reach the optimal DoF. In this regard, the first part of the dissertation describes a linear precoding strategy able to attain them regardless the channel dynamics.

In practice, CSIT should be obtained from channel feedback after a pilot-based training period, thus incurring delays and errors. Although the latter issue has been extensively studied, the requirement of having instantaneous CSIT is one of the critical aspects of IA. This is of special interest for implementation on networks with high channel dynamics, appearing on scenarios with high mobility, where the delay associated to channel feedback may be larger than the channel coherence time. In this regard, IA concepts were extended to networks with only past information of the channels, in a new framework known as *delayed CSIT*. This alternative form of IA is denoted as *retrospective interference alignment*, since the transmission is carried out in multiple phases, and signals may be aligned along space and the different phases. The second part of the thesis deepens into the DoF of two network topologies: the interference channel and interference broadcast channel, for which we propose linear precoding strategies where design employs only delayed CSIT. Moreover, for the interference channel we derive DoF-delay trade-offs, which are relevant as most strategies based on delayed CSIT entail long communication delays.

Finally, the last part of this thesis is focused on implementation issues. First, we define a common formulation relating the feedback procedure and settings to the feedback quality. Then, we study the performance of one scheme proposed in the second part (TDMA-groups scheme, or TG) for the downlink of a wireless scenario in terms of mean and outage rate, and with finite feedback parameters. After that, the effect of finite feedback quality is studied, by deriving its achievable DoF for the case of *imperfect delayed CSIT*.

The last contribution of the third part studies the net DoF, whereby the DoF are studied as a function of the coherence time (or user mobility), and taking into account all issues related to channel acquisition at both the transmitter and receiver side: consumption of resources for feedback transmission, consumption of resources for channel training, and feedback delays. Consequently, they represent the most accurate metric for analyzing the performance of transmission protocols. In this regard, we build two protocols upon the TG scheme, and evaluate its net DoF performance as a function of user mobility.

Acknowledgments

Aquesta tesi és la culminació d'una aventura que va començar fa més de nou anys, quan vaig entrar a l'UPC. Durant aquest temps, que curiosament representa exactament *un terç de la meva vida*, he tingut la sort de treballar durant aproximadament sis anys amb els meus tutors Adrian Agustín i Josep Vidal. I dic molta sort, perquè la seva qualitat no només professional sinó també humana ha estat clau per recolzar-me en el tobogan d'emocions que aquest viatge m'ha anat presentant pel camí. Perquè una tesi és un repte, i per superar-lo malgrat hi hagi il·lusió, sobretot el que cal tenir és molta paciència i perseverança. Per deixar els processos creatius en background i deixar que les idees apareguin quan els sembli, a la dutxa si cal. I és precisament en aquell moment, normalment sol i amb il·lusió però alhora intriga, quan s'ha d'estar preparat. Preparat per si només ha estat un error i has fet volar coloms, però també per si estirant d'aquell fil ets la primera persona al món que troba aquell resultat que probablement ningú ha pensat mai abans.

Per una banda, l'Adri, en el seu rol a baix nivell i proper, m'ha ajudat en els moments no tant bons, i sempre ha sabut trobar les paraules per motivar-me a tirar del fil d'aquells resultats o descobriments que en un primer moment em podia semblar que no valien la pena i eren massa triviais. És clar, sempre abans de donar-li dues o tres voltes més al tema. Amb tu he après una manera d'afrontar els problemes, de girar les coses per veure-les des d'un altre punt de vista, així com que les coses de forma visual entren molt millor, cosa que ha permès millorar notablement la qualitat dels meus articles.

Cobrint l'espai ortogonal i formant equip, el Josep ha posat al meu servei la seva intuïció, experiència, i també totes aquelles habilitats i actituds que em serviran molt profitosament d'ara en endavant, tant en la meva carrera professional, com en la meva vida en general. A més, vull agrair-li l'haver comptat sempre amb mi per a participar en altres activitats al llarg d'aquest període, tant les relacionades amb la tesi, com les que no, així com l'haver-me ajudat i orientat per encaminar el meu següent destí.

Respecte la gent amb qui he treballat, els meus agraïments cap als integrants de l'equip UPC en els projectes europeus TROPIC i TUCAN3G. De tot ells he après moltes coses. Especialment vull agrair a l'Olga Muñoz, que ha col·laborat en algunes de les publicacions que conformen aquesta tesi, i que sempre ha tingut bones paraules i bona disposició cap a mi.

Tornant quatre anys enrere, crec que se m'hagués fet difícil imaginar que tindria l'ambient de feina que he tingut al meu despatx, el D5-120. El meu reconeixement va per tots ells, ja que de cadascú de vosaltres he après alguna cosa, sigui o no a nivell tècnic. En el record ens quedarà per sempre el grup de fotos de pastissos, la Raspberry Pi, el "merendero", la constitució, les exclusives veganes, i mil i una més.

També vull recordar els meus amics de sempre, l'Albert Vicente i el Jordi Rius, que per sort conservo tot i el pas dels anys. Tanmateix, qui per sempre serà *el nen de repàs*, Ezequiel Lopez, de qui estic convençut haver après més que no pas haver-li ensenyat. Tant és així, que reconec que algunes de les nostres classes van servir-me per fer aquell 'click' que, inesperadament, em calia per avançar i desencallar certs moments de la tesi. I finalment la meva amiga Cris, perquè *esto no se para*.

Un agraïment molt especial se'n va cap a Cambridge, pel meu amic Pol Moreno i la seva (ara ja) promesa (i acomiadada) Mar González, a qui també tinc gran apreci. Per ser-hi quan ho he necessitat, encara que ara hagi de ser a través d'Skype. I també perquè en Pol és d'aquelles persones extraordinàries que he conegit en aquest últim terç de la meva vida, però que sempre ha cregut en mi i mai m'ha fallat. Els meus millors desitjos per aquesta feliç parella, a qui també pertany una petita porció d'aquesta tesi, doncs va ser en l'avió de la meva darrera visita on vaig desencallar la clau de la meva última publicació.

Però res de tot això hagués estat possible sense la meva família. I no només per l'haver-me finançat els estudis, sinó també per l'educació, confiança i tranquil·litat que m'han donat, i que m'han permès arribar aquí avui. Vull agrair especialment als meus pares Toni i Consol, que sempre hi són, i al meu germà Sergi, la meva cunyada Núria, i al petit Biel, que quan s'escriuen aquestes línies fa tan sols unes setmanes que està entre nosaltres; i finalment a tota la meva extensa família. Tot ells m'han donat força i comprensió per acabar de rematar-ho. Sempre han estat allà, sé que sempre hi seran, i reconec com de difícils han estat aquests anys per a tots ells. Us vull agrair el vostre suport i amor, i espero ser capaç de correspondre en un futur.

I per acabar però no menys important, la personeta que m'aguanta tots els dies. Vull expressar la meva gratitud a la vida per posar inesperadament a la meva parella Anna Foix en el meu camí. Ja que tot i que gairebé arribes al final del trajecte, la teva energia, bondat i amor m'han estat fonamentals per creure més en mi, per donar valor a les coses que realment tenen valor, i definitiva per fer escac i mat. Et vull agrair que des del primer moment hagis estat a l'alçada en aquesta etapa crítica de la meva vida. Perquè ens espera un futur prometedor junts, i perquè saps que *vull estar amb tu i junts, som molto fortos*.

Durant el desenvolupament d'aquesta tesi s'ha rebut finançament del Grup de Procesament de Senyal i Comunicacions (GPS) de l'UPC, del Govern de l'estat Espanyol a través de la beca FPI BES-2011-049197 associada al projecte MOSAIC TEC2010-19171, i a través d'ajudes associades als projectes europeus TROPIC FP7 ICT-2011-318784 i TUCAN3G FP7 ICT-2011-601102.

Contents

Acronyms and Abbreviations	viii
Notation	x
1 Introduction	1
1.1 Motivation	1
1.2 Thesis Focus and Organization	6
1.3 Research Contributions	8
2 System Model	10
2.1 General Topology	10
2.2 A Space-Time Linear Transmission-Reception Model	10
2.3 Channel Model: Dynamics and Acquisition	13
2.3.1 Type of Channels	15
2.3.2 CSIT with Delays	15
2.3.3 CSIT Feedback	16
2.3.4 Common Types of CSIT	17
2.4 Key Performance Metrics	17
2.4.1 Signal Space Matrix	17
2.4.2 Degrees of Freedom	18
2.4.3 Simplified DoF Analysis	19
2.4.4 DoF with Overheads	22
2.4.5 Net DoF	22
I Degrees of Freedom Analysis for Full CSIT	24
3 Preliminaries	25
3.1 Specific System Model	25
3.2 State-of-the-Art	25
3.2.1 IA for the Square Case	28
3.2.2 Subspace Alignment Chains	30
4 IC with Full CSIT	32
4.1 Main Contributions	32
4.2 Building a Proper Formulation	33
4.2.1 Precoding Matrices	33
4.2.2 Channels	33
4.2.3 Problem Formulation	34
4.3 The (2,3) Case	35

4.3.1	Precoding Matrix Design	35
4.3.2	Achievability Proof	36
4.4	The $(M, M + 1)$ Case with $M > 2$	38
4.4.1	Precoding Matrix Design	38
4.4.2	Achievability Proof	40
4.5	Numerical Results	42
4.6	Conclusion	42
Appendix		43
A	Additional Change of Basis at the Receiver Side	44
B	Proof of Lemma 4.1	45
C	Proof of Lemma 4.3	46
II	Degrees of Freedom Analysis for Delayed CSIT	49
5	Preliminaries	50
5.1	Specific System Model	50
5.1.1	Broadcast Channel	50
5.1.2	Interference Channel	51
5.1.3	Interference Broadcast Channel	51
5.1.4	Delayed CSIT Constraint	51
5.2	State-of-the-Art	51
5.2.1	MAT Scheme	54
5.2.2	RIA for the 3-user SISO IC	57
6	IC with Delayed CSIT	60
6.1	Main Contributions	60
6.1.1	Proposed Transmission Strategies	60
6.1.2	DoF-Delay Trade-Off	65
6.1.3	Achievable DoF for Constant Channels	65
6.2	Proposed Transmission Strategies	66
6.2.1	RIA Scheme ($M < N$)	66
6.2.2	TG Scheme ($M > N$)	72
6.2.3	3-user PSR Scheme ($M \approx N$)	77
6.3	DoF-Delay Trade-Off	84
6.3.1	RIA Scheme	85
6.3.2	TG Scheme	85
6.3.3	PSR Scheme	88
6.3.4	DoF with Limited Order of Symbols	88
6.4	Achievable DoF for Constant Channels	89
6.4.1	RIA Scheme	89
6.4.2	RIA Scheme with ACS	91
6.4.3	TG Scheme	92
6.4.4	3-user PSR Scheme	92
6.5	Conclusion	93
7	IBC with Delayed CSIT	95
7.1	Main Contribution	95
7.2	Proposed Transmission Strategy	97

7.2.1	Case M=4, N=1	97
7.2.2	Generalization to MIMO	103
7.3	Conclusion	105
III	Impact of Limited Feedback	106
8	Preliminaries	107
8.1	Specific System Model	107
8.1.1	MISO Interference Channel	107
8.1.2	Channel Feedback Quality	108
8.1.3	Net DoF	109
8.2	Feedback Methods	110
8.2.1	Digital Feedback	110
8.2.2	Analog Feedback	111
9	IC with Finite-Rate CSIT	113
9.1	Main Contributions	113
9.1.1	A Common Feedback Formulation	113
9.1.2	Analog vs Digital Feedback	113
9.1.3	Impact of Feedback Quality	113
9.1.4	Net DoF Analysis	114
9.2	A Common Feedback Formulation	114
9.3	Analog vs Digital Feedback	116
9.3.1	Review of eICIC	116
9.3.2	Problem Formulation	116
9.3.3	Simulation Results	117
9.4	Impact of Feedback Quality	119
9.4.1	Proof of Theorem 9.1	119
9.4.2	Simulation results for Finite SNR	122
9.5	Net DoF Analysis	122
9.5.1	Problem Formulation	122
9.5.2	A Per-Protocol Analysis	125
9.5.3	Numerical Results	127
9.6	Conclusion	130
	Discussion and Lines of Future Work	131
	Bibliography	136

Acronyms and Abbreviations

ACS	Asymmetric Complex Signaling
AFB	Analog Feedback
BC	Broadcast Channel
CB	Codebook
CSI	Channel State Information
CSIT	Channel State Information at the Transmitter side
CT	Channel Coherence Time
DoF	Degrees of Freedom
DFB	Digital Feedback
DT	Dedicated Training
EDT	Extra Dedicated Training
EIA	Ergodic Interference Alignment
FB	Feedback
FCT	Finite Coherence Time
i.i.d.	independent and identically distributed
IA	Interference Alignment
IBC	Interference Broadcast Channel
IC	Interference Channel
iff	if and only if
LC	Linear Combination
MAC	Multiple Access Channel
MAT	Maddah-Ali and Tse
MBR	Mean Bit-Rate
MIMO	Multiple-Input Multiple-Output

MISO	Multiple-Input Single-Output
MMSE	Minimum Mean Square Error
NS	Null-Steering
OIA	Opportunistic Interference Alignment
OR	Outage Rate
pdf	probability density function
PSR	Precoding, Scheduling and Redundancy
P2P	Point-to-Point
RIA	Retrospective Interference Alignment
s.t.	subject to
SAC	Subspace Alignment Chains
SISO	Single-Input Single-Output
SotA	State-of-the-Art
SNR	Signal-to-Noise-Ratio
SPB	Support Precoding Blocks
SSM	Signal Space Matrix
TDMA	Time Division Multiplex Access
TG	TDMA-Groups
w.r.t.	with respect to
ZF	Zero-Forcing
ZP	Zero Propagation

Notation

Vectors and Matrices

$[a, b]$	Two-component row vector. Scalar variables are written in italics.
$\underline{\mathbf{x}}$	Row vector (boldface underlined lowercase types).
\mathbf{x}	Column vector (boldface lowercase types).
\mathbf{X}	Matrix (boldface uppercase types).
$\mathbf{0}$	Matrix or vector of all zeros.
\mathbf{I}	Identity matrix.
$(\cdot)^T$	Transpose operator for vectors/matrices.
$(\cdot)^H$	Transpose and conjugate operator for vectors/matrices.
$\text{trace}(\mathbf{X})$	Trace of matrix \mathbf{X} , i.e. the sum of the entries in its main diagonal.
$ \mathbf{X} $	Determinant of matrix \mathbf{X} .
\otimes	Kronecker product.
$\mathbf{x} \propto \mathbf{y}$	The two vectors are proportional, i.e. there exists a constant λ such that $\mathbf{x} = \lambda \mathbf{y}$. The same operator also applies for row vectors.
$\mathbf{x}(a : b)$	Given an N -component vector $\mathbf{x} = [x(1), x(2), \dots, x(N)]^T$, the subset of components from a to b of \mathbf{x} , i.e: $[x(a), x(a+1), \dots, x(b)]^T$.
$\mathbf{X}_{a:b}$	Given an N -column matrix $\mathbf{X} = [\mathbf{x}_1, \mathbf{x}_2, \dots, \mathbf{x}_N]$, the subset of columns from a to b of \mathbf{X} , i.e:

$$\mathbf{X}_{a:b} = [\mathbf{x}_a, \mathbf{x}_{a+1}, \dots, \mathbf{x}_b] .$$

stack (\mathbf{X}, \mathbf{Y}) The matrix obtained from stacking the matrix \mathbf{Y} below \mathbf{X} , i.e:

$$\text{stack}(\mathbf{X}, \mathbf{Y}) = \begin{bmatrix} \mathbf{X} \\ \mathbf{Y} \end{bmatrix}.$$

bdiag (\mathbf{X}, \mathbf{Y}) The matrix obtained from the block diagonal composition of \mathbf{X} with \mathbf{Y} , i.e:

$$\text{bdiag}(\mathbf{X}, \mathbf{Y}) = \begin{bmatrix} \mathbf{X} & \mathbf{0} \\ \mathbf{0} & \mathbf{Y} \end{bmatrix}.$$

Sets and Linear subspaces

$\{a, b\}$ Two-element set.

\mathcal{X} Set or subspace (calligraphic uppercase types).

$\text{lcm}(\mathcal{X})$ Lowest common multiple of all the elements in \mathcal{X} , i.e. the smallest possible integer that is divisible by all of the elements in \mathcal{X} .

$\text{span}(\mathbf{X})$ The *column subspace* of matrix \mathbf{X} , containing all possible linear combinations (LCs) of its columns.

$\text{rspan}(\mathbf{X})$ The *row subspace* of matrix \mathbf{X} . If, for context, there exists a matrix \mathbf{X} , then \mathcal{X} denotes its row subspace.

$\text{rank}(\mathbf{X})$ The dimension of the set $\mathcal{X} = \text{rspan}(\mathbf{X})$, also denoted as $\dim(\mathcal{X})$.

$\mathbf{X} \doteq \mathbf{Y}$ Equality of row spans, i.e. short for $\text{rspan}(\mathbf{X}) = \text{rspan}(\mathbf{Y})$. Notice that for vectors, $\mathbf{x} \doteq \mathbf{y}$ is equivalent to $\mathbf{x} \propto \mathbf{y}$.

$\mathcal{X} \subset \mathcal{Y}$ The set \mathcal{X} is a subset of \mathcal{Y} . When they are linear subspaces, it denotes that the elements in \mathcal{X} can be generated as LCs of the elements in \mathcal{Y} .

\mathcal{X}^\perp Complementary set.

$\mathcal{X} + \mathcal{Y}$ The *sum subspace*, containing all the elements that can be generated using the elements of \mathcal{X} and \mathcal{Y} . Notice that the operator $\text{stack}(\cdot)$ produces a matrix whose rows span the sum of row subspaces.

$\mathcal{X} \cap \mathcal{Y}$ The intersection subspace, given by the elements that belong to both \mathcal{X} and \mathcal{Y} . A basis for the intersection subspace can be bound by exploiting the fact that operations over Linear Subspaces form a Boolean Algebra. Hence, we have:

$$\bigcap_{i=1 \dots N} \mathcal{X}_i = \left(\sum_{i=1 \dots N} \mathcal{X}_i^\perp \right)^\perp.$$

$\mathcal{X} \setminus \mathcal{Y}$ The set/subspace containing the elements that belong to \mathcal{X} but not to \mathcal{Y} .

Other notation

\mathbb{R} Field of real numbers.

\mathbb{C} Field of complex numbers.

\mathbb{Z}^+ Field of positive integer numbers.

\mathbb{E} Expectation operator.

$\mathbb{1}$ Indicator function.

$\lceil \cdot \rceil$ Ceiling operator, i.e. the smallest following integer.

$\lfloor \cdot \rfloor$ Floor operator, i.e. the largest previous integer.

$\langle \cdot \rangle$ Modulo- K operator, where K is the number of users. Moreover, all indices are assumed to be in the set $\{1, 2, \dots, K\}$, applying the modulo- K operation only if necessary.

$(a)^+$ $\max(a, 0)$.

$a \wedge b$ $\min(a, b)$.

Introduction

1

1.1 Motivation

Research on wireless communications has been significantly active during the last three decades. Many issues appear in wireless links which are not present in wired communications, e.g. interference or fast fading. The problem of interference in the first mobile networks, oriented to support voice services, was primarily addressed by means of three methods, depending if transmitters or receivers act against it. First, receivers can ignore the interference and treat it as noise. Second, transmitters can adjust its transmission power in pursuit of limiting/controlling the generated interference, what is usually known as power control procedures [KML04]. And third, the interference can be addressed by orthogonalizing the access, either in time or frequency domain, and trivially turning the multi-user networks into independent point-to-point (P2P) channels. Notice that both two first strategies are not advisable for very dense scenarios or in case high transmission power is available at the transmitters. One the one hand, if the interference is ignored, the level of generated interference turns to collapse the rate performance achieved over the network. On the other hand, in such scenario where interference is the main bottleneck, only a small portion of the available transmission power will be employed, thus a large amount of resources will be wasted. Therefore, the best solution appears to be the orthogonalization approach.

Regarding the fast fading effects due to multi-path propagation, one of the main tools that has been envisioned to combat it is the smart use of multiple antennas [G⁺07]. Interestingly, for the P2P channel, it is known that compared to the single-antenna case (SISO), multiple-input multiple-output (MIMO) technologies allow increasing the reliability of the communications, i.e. the outage error probability, whose decaying rate is usually referred to as the *diversity gain*. Moreover, MIMO technologies have been also identified as one of the main drivers for increasing the efficiency of the communication, i.e. the transmitted rate. One of the seminal works in this matter is [Tel99], where Telatar proved that for a MIMO P2P channel the capacity scales linearly with the minimum between the number of antennas at the transmitter and the receiver. This scaling factor is usually known as the *multiplexing gain*. Beyond describing the communication capability with only the diversity or the multiplexing gains, Tse [TV05] showed that the intuitive trade-off between reliability and efficiency, or error probability and data rate, can be translated into a diversity-multiplexing region of operation.

So far the reader could think that the combination of MIMO with orthogonalization is the best and a sufficient candidate to combat (and exploit) interference and fading in wireless interference-limited networks. However, its performance is still not enough for nowadays customers' needs, demanding to be connected with a minimum quality of service

anywhere and at anytime. Furthermore, a dramatic growth has been experienced in the last years on traffic demands, especially for data traffic, due to the apparition of ever more capable mobile terminals, e.g. smartphones or tablets. For example, the average monthly traffic per smartphone in United States was 76 MB in 2009, whereas it grew to 1.8 GB in 2014 [SR15]. One simple solution is to increase the channel bandwidth to provide higher throughput. However, bandwidth is a scarce resource, and it cannot be ensured to what extent, if this traffic growth persists, current networks will be able to satisfy user demands.

In this context, the orthogonalization in time/frequency has been identified as possibly one of the bottlenecks for improving system performance, since each user has access to the channel only a fraction of time/frequency inversely proportional to the total number of users. Indeed, orthogonalization means that each resource is assigned and thus exploited by only a single user. Then, it is being investigated the best way of reusing time/frequency resources, allowing that the signals captured at the receivers contain interference, and how the transmitters and receivers can act to manage such interference, with the aim of boosting the efficiency achieved over the network. As will be explained later, one of the solutions envisioned is *spatial orthogonalization*, whereby the spatial dimensions provided by the use of multiple antennas are exploited for allowing multiple simultaneous transmissions.

Information theory literature has organized the characterization of this problem by defining a number of multi-user channels [GK12, Part II], and depending on the role and the number of terminals involved in the communication, assuming that the rest of potential actors use an orthogonal channel. In this respect, the scenarios considered in this thesis may be subsumed by the interference broadcast channel (IBC), shown in Fig. 1.1. The K_u -user K_c -cell IBC defines a cellular communication system, where each cell contains one transmitter and K_u users, and each transmitter aims to deliver independent messages to the K_u users located in its cell. Then, the system consists of K_c transmitters and $K = K_u \cdot K_c$ users. The more interesting aspect of the IBC topology is that it presents two different types of interference: inter-cell and intra-cell interference. In the former case, each receiver suffers from interference containing information intended to the out-of-cell users, whereas in the latter the information is intended to in-cell users, and transmitted by the same transmitter who is serving that user.

Notice that although the IBC naturally models the downlink (DL) transmission in cellular systems, it is not restricted to it and can be applied to other more general settings where transmitter and receiver do not have necessarily to be identified as the base-station and user equipment. Furthermore, we will use in the sequel the terms *receiver* and *user* almost indistinctly, with preference for the former to refer to signals, i.e. in a physical layer sense, and for the latter to refer to symbols, i.e. in a higher-level layer sense.

While the IBC captures the essence of many multi-user communications systems, usually research advances are first devised for canonical scenarios, which are easily obtained by decomposing the IBC in more complex settings by means of orthogonalization. In this regard, Fig. 1.2 depicts two of the canonical multi-user channels considered in the literature: broadcast channel (BC) and interference channel (IC). The BC models a single-cell ($K_c = 1$) transmission, which can be achieved in the IBC by assigning orthogonal time/frequency resources to the transmissions in each cell, thus obtaining a K_u -user BC. On the other hand, the IC models the scenario where K_c transmitters serve only

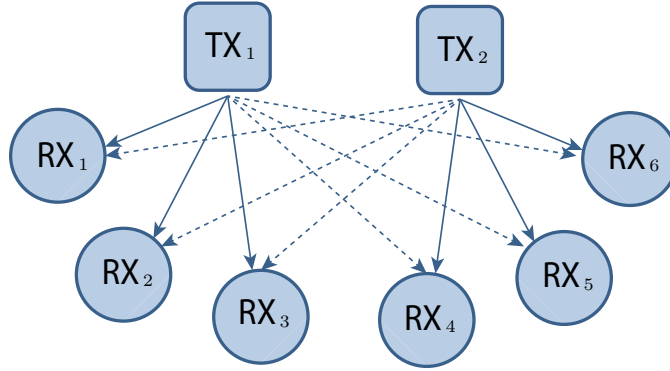


Figure 1.1: The K_u -user K_c -cell Interference Broadcast Channel, subsuming all the topologies studied in this dissertation. This example specifically shows the 3-user 2-cell IBC, where two transmitters serve three users each. Solid lines represent links containing intended information, and dashed lines represent links containing only unintended information.

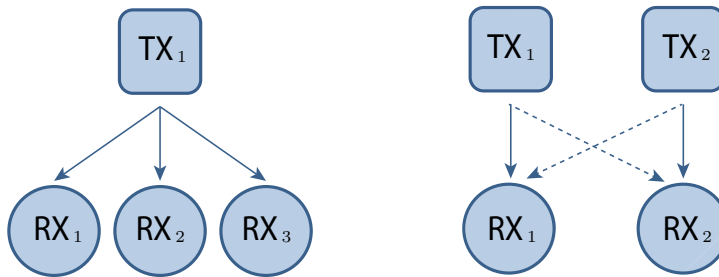


Figure 1.2: Canonical channels derived from the Interference Broadcast Channel: Broadcast Channel (left) and Interference Channel (right). This example specifically shows the 3-user BC and 2-user IC. Solid lines represent links containing intended information, and dashed lines represent links containing only unintended information.

one user ($K_u = 1$) per cell at the same time. This can be achieved in the IBC by assigning orthogonal time/frequency resources to the users of each cell, and applying such assignment for the rest of cells.

The study of the capacity region for the K -user MIMO *Gaussian*¹ BC was established few years ago in [WSS06]. In contrast, for the Gaussian IC capacity region just a few number of settings are fully characterized. The first result was found by Carleial over 30 years ago in [Car75], who established the channel capacity region for the 2-user IC under *very strong* interference. Later on, Han and Kobayashi extended the work of Carleial in [HK81], characterizing the capacity region of the 2-user IC for all cases where the ratio between cross and direct channels² is greater than one, denoted as the *strong* interference case. While some results have appeared along the years, the next work providing optimal capacity characterization took place just few years ago with the appearance of [MK09], where the sum capacity of the 2-user IC in case of *weak* interference was established for

¹In this dissertation, Gaussian channels will be always assumed, where the received signals are corrupted by additive white gaussian noise.

²We will repeatedly use the following extended convention: the links between a transmitter and its served users are denoted as the *direct channels*, whereas the rest of links are denoted as the *cross-channels*.

some cases. Moreover, [MK09] characterized the sum capacity of the *mixed* IC. While the very strong and very weak (noisy) interference regimes have been also characterized for the K -user IC in terms of sum-capacity, see [S⁺08] and [AV09], respectively, in spite of four decades of research the capacity region for an arbitrary interference regime remains open. In addition, the characterization for multiple antennas has recently been initiated in [KV14].

While the challenge of characterizing channel capacity in general remains open, its study for the IC and other more complicated scenarios as the IBC is usually restricted to the high signal-to-noise-ratio (SNR) regime, and in terms of *degrees of freedom* (DoF). This assumption implies that the effect of noise is negligible, and interference becomes the major bottleneck of the network. The design is then focused on how interference is managed, and allows simplifying the mathematical analysis, as well as drawing some interesting and promising conclusions at the expenses of having a partial characterization of the channel capacity.

In recent years, the DoF have emerged as one of the most important metrics for characterizing interference networks. In contrast to channel capacity, the DoF have became popular in part because they allow getting insights and drawing conclusions easily for a large number of topologies and under many different settings, e.g. line-of-sight links with finite diversity [BT09], constant or time-correlated channel coefficients [Jaf10, Y⁺13], multiple antennas at the transmitter and/or receiver sides [GJ10], multicast [L⁺12], general message demands [VVK14], transmission with privacy constraints [K⁺11], transmission with a cognitive helper [WS13], coexistence of primary and cognitive secondary networks [AEKN11]. In some of these cases the DoF characterization is the only available way known to approach the characterization of capacity.

It is known that the DoF of wireless channels are dramatically boosted if channel state information (CSI) at the transmitter side (CSIT) is available [Tel99][VV12a]. This is because it allows properly designing and managing the interference, which is the main bottleneck in the DoF analysis framework. Many different types of CSIT have been defined in the literature, starting from the *full CSIT* case, where it is assumed that transmitters are aware of the channel state instantaneously and with perfect accuracy. Exploiting such information, interference can be spatially orthogonalized by means of the well-known *null-steering* or *zero-forcing* principles [SSH04]. In both cases, the idea is to exploit the dimensions provided by multiple antennas at the transmitter or receiver side, respectively. Therefore, the received signals contain no interference, and the multi-user network may be treated as multiple parallel P2P channels. Both approaches have been proved to be optimal in DoF terms when there are many more antennas at the transmitter side than at the receiver side, or viceversa. However, they are not feasible or give a poor performance for dimensionally-limited systems. In this context, the *interference alignment* (IA) principle [MAMK08, CJ08] comes into play as a generalization of the two previous approaches. In this case, receivers use their antennas to zero-force the interference, but with the help of transmitters make zero-forcing at the receiver side optimal for most antenna settings. Specifically, the transmitted signals are designed to reduce the dimension of the subspace occupied by interference at the each receiver, thus releasing more dimensions to allocate desired signals, which are retrieved by applying zero-forcing concepts on the received signals.

Although many promising advances have been achieved on the DoF characterization of

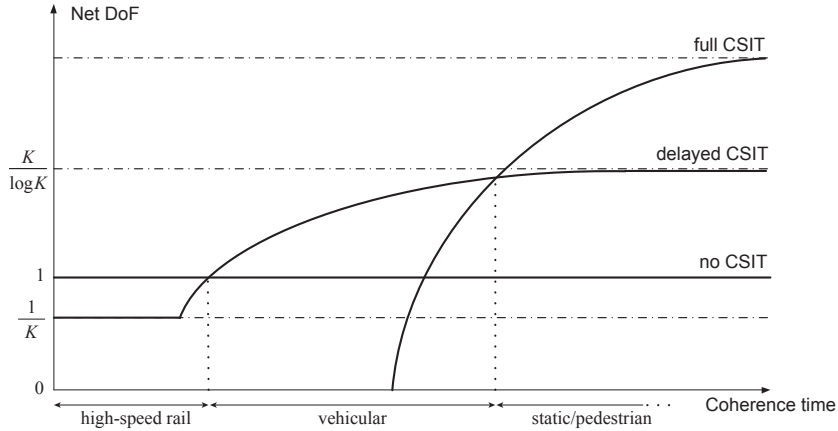


Figure 1.3: The net DoF of the K -user BC as a function of the coherence time, accounting not only for the gains, but also the cost of having feedback. Three different types of CSIT are considered: full, delayed or no CSIT. Each of them stands as the best option for a different coherence time regime.

wireless networks with full CSIT, there are still many topologies to be fully characterized. Furthermore, in recent years a research area has focused on studying more practical issues, e.g. where the channel feedback (FB) report provides the CSIT with delay and errors. On the first hand, delay on feedback has usually been treated in the literature by assuming a time-correlated model, which is especially suited for networks with short feedback delay. But, what if the channel has completely changed when the feedback report is available at the transmitter side? Can the feedback report still be useful when the feedback delay is larger than the channel coherence time, and hence the channel estimate is totally outdated? This situation is denoted in the literature as *delayed CSIT* and with [MAT12] as its starting point, the question was answered positively. Interestingly, having delayed CSIT may be exploited by applying the IA principle, but adapted for the scenario with delayed CSIT, which is known as *retrospective interference alignment* (RIA). In short, thanks to delayed CSIT transmitters are able to elucidate the generated interference during the past transmissions, and then design the current transmitted signals to achieve a form of IA over the space-time domain. This means that, surprisingly, past and current interference may be aligned without any knowledge of current channel coefficients. Built upon this principle, the BC and IC with two users have been fully characterized in DoF terms. However, little is known about the DoF of other topologies, especially when there are multiple transmitters.

On the other hand, taking into account errors due to finite precision on feedback has been majorly studied for the case of full CSIT (imperfect current CSIT) [Jin06, AH12], and more recently also for the case with delayed CSIT (imperfect delayed CSIT) [XAJ12]. In this context, one of the more interesting research directions is the analysis of the *net DoF* of wireless networks. The net DoF generalize the DoF metric by analyzing the multiplexing gain as a function of the coherence time, and taking into account all the issues associated to channel acquisition: errors and delays on feedback reports, and network resources not dedicated to data transmission, e.g. training periods or feedback overheads. This is interesting because it provides a net measure describing the existing trade-off between the gain provided by having CSIT, and the cost of its acquisition, both as a function of channel dynamics. As an illustrative example, and without any statement of optimality, the DoF of some schemes for the BC were analyzed in [XAJ12], summarized

in Fig. 1.3. Taking into account that the coherence time is inversely proportional to the terminal velocity, some interesting conclusions may be drawn. First, it is observed that the techniques for full CSIT are useful when channels have long coherence time or, equivalently, for low-speed terminals. Otherwise, for very rapid channel dynamics or high-speed terminals, the gains obtained from feedback acquisition does not compensate its cost, thus it is preferable to employ strategies assuming no CSIT. Finally, there is an intermediate regime where the channels change in a fashion where the techniques developed assuming delayed CSIT provide the best trade-off. All these conclusions were obtained for the K -user MISO BC, but it is not known to what extent they are also applicable to other scenarios.

1.2 Thesis Focus and Organization

This thesis studies interference wireless networks in terms of DoF and, mostly in its last part, also in terms of achievable bit-rates. The research contributions are grouped in three parts, see Fig. 1.4, depending on the topologies and CSIT model assumed, as follows:

- **Part I:** IC with full CSIT and constant channel coefficients.
- **Part II:** IC and IBC with (perfect) delayed CSIT.
- **Part III:** IC with CSIT obtained after a finite-rate feedback report.

Chapter 2 describes the system model, taking into account the different models assumed throughout the thesis. Although some of the definitions and formulation will be repeated when necessary for the sake of readability, the aim of this chapter is to 1) give a common signal model, 2) describe all the channel and CSIT models assumed along the thesis, and 3) to precisely define the performance metrics that will be used for evaluation of the proposed transmission strategies, and comparison to state-of-the-art.

The first part of the dissertation entails Chapters 3 and 4. First, Chapter 3 describes the specific system model for this part, and reviews the associated state-of-the-art (SotA), with special focus on two fundamental tools in the literature: interference alignment and subspace alignment chains. While the latter will be only useful for the full CSIT case, the former constitutes one of the main tools of this work. The SotA review concludes that for the case of full CSIT and constant channels some antenna settings cannot be resolved with current linear strategies. In this regard, Chapter 4 tackles this problem and fully characterizes all except the single-antenna setting, that remains open. Our main contribution is the application of asymmetric complex signaling concepts into the subspace alignment chains framework.

Part II addresses the analysis of wireless networks with multiple transmitters when only delayed CSIT is assumed. First, Chapter 5 provides the specific system model for the BC, the IC and the IBC with delayed CSIT, and reviews the associated state-of-the-art. In this case, two strategies are reviewed from the literature, constituting the generalization of IA to the delayed CSIT setting, i.e. RIA. These two strategies are relevant to understand our contribution in this matter.

Chapter 6 deals with the IC, proposing three linear precoding strategies, formulated as a function of the antenna setting and the number of users, thus applicable to the general K -user (M, N) MIMO IC, with all transmitters having M antennas, and all

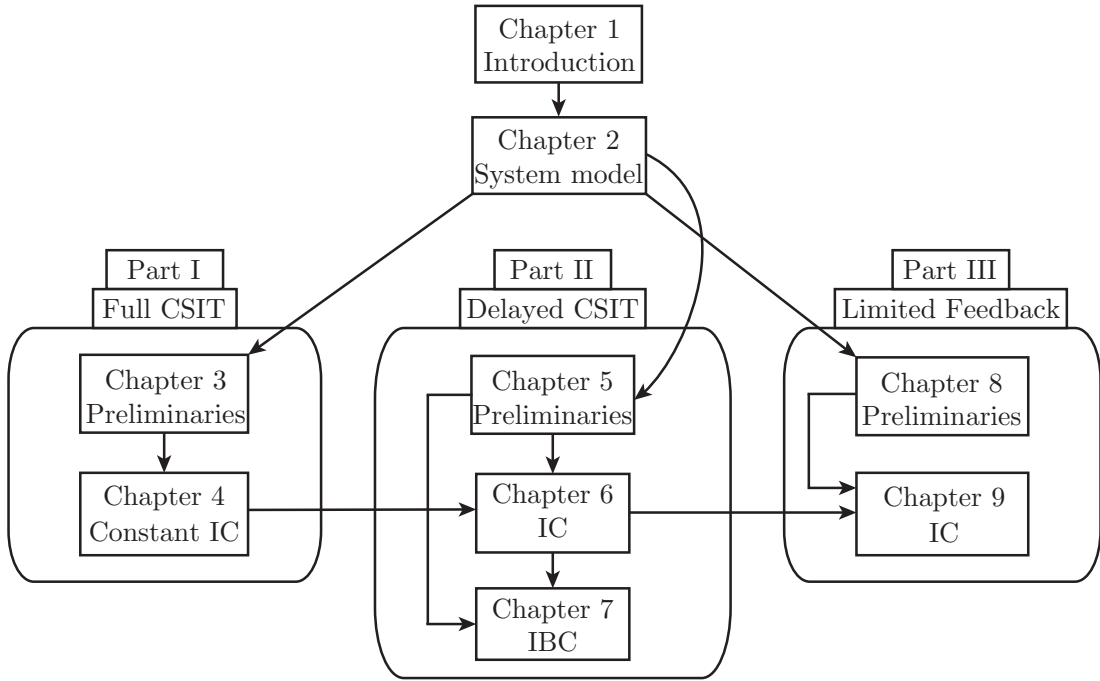


Figure 1.4: Thesis organization. Arrows specify connected chapters, in the sense that some tools developed for one chapter have inspired or been applied to the other.

receivers having N antennas. The given formulation allows to derive the achievable DoF as a function of the transmission delay, thus elucidating its achievable DoF-delay trade-off. This is especially useful because most schemes using delayed CSIT require long transmission delays to provide the promised DoF gains. Then, we evaluate to what extent the increase of complexity is worth the DoF improvement. Finally, we consider the case of delayed CSIT with constant channels, and show that the application of asymmetric complex signaling concepts (as in Chapter 4) is required to ensure DoF achievability in the single-antenna case.

Chapter 7 studies the IBC with 2 cells and 2 user per cell. In this case, both inter-cell and intra-cell interference appear. Inspired by the optimal scheme for the BC and the lessons learned in Chapter 6 for the IC, we propose a linear precoding scheme improving the current knowledge about achievable DoF.

The last part of this thesis, part III, addresses all the contributions devoted to study the practical costs and gains in case the TDMA-groups scheme proposed in Chapter 6 for the MISO IC with delayed CSIT would be implemented. In this regard, Chapter 8 reviews all the state-of-the-art and background necessary for this part.

Next, Chapter 9 analyzes the impact of limited feedback in the MISO IC when the TDMA-groups scheme, proposed in Chapter 6, is employed. First, and before the analysis, a common formulation for the feedback quality is proposed, subsuming any of the two existing feedback procedures. Second, the performance to the scheme is evaluated and compared when using digital or analog feedback, and compared to non-CSIT-based strategies. Conclusions are drawn thanks to the common feedback formulation framework. Next, the performance of the system is evaluated when a fixed feedback quality is set for all SNR values, independently of the feedback procedure. Finally, the net DoF

of two protocols based on the TDMA-groups scheme are derived, and compared to other protocols. Moreover, sum-rate results are provided as a function of the SNR for different user velocities.

1.3 Research Contributions

The contributions in terms of technical papers or documents is next summarized for each part the thesis:

Part I

M. Torrellas, A. Agustin, J. Vidal and O. Muñoz, "The degrees of freedom of the 3-user $(p, p+1)$ MIMO Interference Channel", IEEE Trans. on Communications, pp. 3842-3853, November 2014.

Part II

M. Torrellas, A. Agustin, and J. Vidal, "Retrospective Interference Alignment for the 3-user MIMO Interference Channel", IEEE ICASSP, Florence, May 2014.

M. Torrellas, A. Agustin, and J. Vidal, "On the degrees of freedom of the K -user MISO Interference Channel With Delayed CSIT", IEEE ICASSP, Florence, May 2014.

M. Torrellas, A. Agustin, and J. Vidal, "DoF-Delay Trade-Off for the K -user MIMO Interference Channel With Delayed CSIT", submitted to the IEEE Transactions on Information Theory, June 2015.

M. Torrellas, A. Agustin, and J. Vidal, "Retrospective Interference Alignment for the MIMO Interference Broadcast Channel", IEEE ISIT, Hong Kong, June 2015.

Part III

M. Torrellas, A. Agustin, and J. Vidal, "On the degrees of freedom of the K -user MISO Interference Channel With Delayed CSIT", IEEE ICASSP, May 2014.

M. Torrellas, A. Agustin, and J. Vidal, "Performance Analysis of Inter-cell Interference Co-ordination in Small-Cell Networks with long feedback delays", Poster at EuCNC, Bologna, June 2014.

M. Torrellas, A. Agustin, and J. Vidal, "Net DoF analysis for the K -user MISO IC with outdated and imperfect channel feedback", EuCNC, Paris, June 2015.

Other contributions not included in this dissertation

M. Torrellas, A. Agustin, and J. Vidal, "Coordinated beamforming access for interfering half-duplex relay networks", IEEE ICC Communications Workshops, Budapest, June 2013

A. Agustin, J. Vidal, M. Torrellas, S. Lagen, S. Barbarossa, S. Sardellitti, P. Di Lorenzo, A. Baiocchi, M. Sarkiss, F. Jardel, M. Kamoun, M. Fiorito, S. Sezginer , G. Vivier,

M. Goldhamer, P. Mach, L. Klozar, Z. Becvar, “MP2MP communication systems for LTE-A HeNB deployments”, deliverable of the EC project TROPIC FP7 ICT-2011-8-318784, May 2014, <http://ict-tropic.eu>

System Model

2

This chapter provides a general framework capturing the essence of all the network topologies and settings studied throughout the dissertation. In this regard, the objective is to describe the general interference broadcast channel with the more general transmission procedure, and 1) give a common received signal and transmission model, 2) describe all the channel and CSIT models assumed along the thesis, and 3) to precisely define the performance metrics that will be used for evaluation of the proposed transmission strategies.

2.1 General Topology

The K_u -user K_c -cell (M, N) IBC, see as an example Fig. 1.1 with $K_u = 3$ and $K_c = 2$, subsumes all the topologies studied in this dissertation: BC, IC and the IBC itself. In this general model, K_c transmitters and $K = K_u \cdot K_c$ receivers coexist in the same frequency band. Transmitters are equipped with M antennas, whereas receivers are equipped with N antennas. Transmitter TX_i serves all users with $c(j) = i$, where

$$c(j) = \left\lceil \frac{j}{K_u} \right\rceil \in \{1, \dots, K_c\}, \quad (2.1)$$

indexes the serving transmitter for RX_j , with $j \in \{1, \dots, K\}$.

2.2 A Space-Time Linear Transmission-Reception Model

The objective of the transmission is that each transmitter TX_i delivers b independent symbols to each receiver RX_j in its cell. The transmission is carried out in P phases, and each phase p is in turn divided in R_p rounds of S_p time slots each, see Fig. 2.1. According to this, the total number of time slots used for data transmission is

$$\tau = \sum_{p=1}^P \tau_p, \quad \tau_p = R_p S_p. \quad (2.2)$$

This methodology aims at dedicating each round to only a specific group of users, whose benefits will be explained later. Then, the (p, r) th round, i.e. the round r of the phase p , is dedicated to all users in the group $\mathcal{G}^{(p,r)}$. All groups of each phase have the same cardinality, with $G_p = |\mathcal{G}^{(p,r)}|, \forall r$.

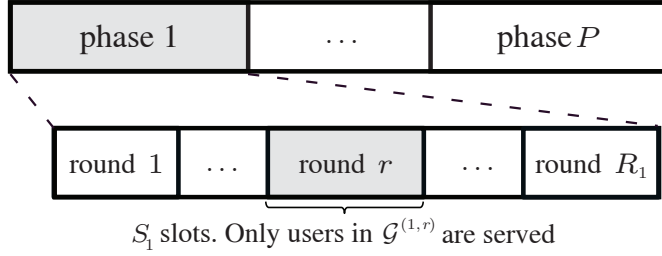


Figure 2.1: General transmission frame. There are P phases, where the phase p is divided in R_p rounds. All rounds of the phase p are in turn divided in S_p time slots. During each round (p, r) one different group of G_p users is served, predefined by the set $\mathcal{G}^{(p,r)}$.

During the (p, r) th round, the received signal model at RX_j writes as

$$\mathbf{y}_j^{(p,r)} = \mathbf{d}_j^{(p,r)} + \mathbf{i}_j^{(p,r)} + \mathbf{n}_j^{(p,r)} \quad (2.3a)$$

$$= \mathbf{H}_{j,c(j)}^{(p,r)} \mathbf{V}_j^{(p,r)} \mathbf{x}_j + \mathbf{H}_{j,c(j)}^{(p,r)} \sum_{\substack{i|i \neq j \\ c(i)=c(j)}} \mathbf{V}_i^{(p,r)} \mathbf{x}_i + \sum_{i|c(i) \neq c(j)} \mathbf{H}_{j,c(i)}^{(p,r)} \mathbf{V}_i^{(p,r)} \mathbf{x}_i + \mathbf{n}_j^{(p,r)}, \quad (2.3b)$$

relating $\mathbf{y}_j^{(p,r)} \in \mathbb{C}^{NS_p \times 1}$ as the vector representing the signals observed at RX_j , and all vectors $\mathbf{x}_i \in \mathbb{C}^{b \times 1}$ containing the b uncorrelated unit-powered complex-valued data symbols intended to each user i . It is worth pointing out that linear combinations (LCs) of the same b symbols are transmitted during all phases, linearly decoded at the end of the communication.

The model in (2.3) provides a two-level description of the input-output relationship of the system. In a first level, (2.3a) formulates the received signal as the sum of the three terms $\mathbf{d}_j^{(p,r)}$, $\mathbf{i}_j^{(p,r)}$, and $\mathbf{n}_j^{(p,r)}$ denoting the signal containing the desired symbols, the interference signal containing other user's symbols, and the unit-powered noise term, respectively. The components of the noise vector are i.i.d. as $\mathcal{CN}(0, 1)$.

In a second level, (2.3b) describes the each of those terms in lower level terms, separating interference as the sum of the inter-cell and intra-cell contribution.

The channel matrix $\mathbf{H}_{j,k}^{(p,r)} \in \mathbb{C}^{NS_p \times MS_p}$ ($k = c(i)$) in (2.3b) collects the link gains from each antenna of TX_k to each antenna of RX_j for all time slots of the (p, r) th round. Let $\mathbf{H}_{j,k}^{(p,r,\vartheta)} \in \mathbb{C}^{N \times M}$ denote the matrix collecting the links gains for each time slot ϑ of the round, whose distribution in terms of probability and dynamics will be described in the next section. Then, we write

$$\mathbf{H}_{j,c(i)}^{(p,r)} = \text{bdiag} \left(\mathbf{H}_{j,c(i)}^{(p,r,1)}, \dots, \mathbf{H}_{j,c(i)}^{(p,r,S_p)} \right), \quad (2.4a)$$

$$\mathbf{H}_{j,c(i)}^{(p)} = \text{bdiag} \left(\mathbf{H}_{j,c(i)}^{(p,1)}, \mathbf{H}_{j,c(i)}^{(p,2)}, \dots, \mathbf{H}_{j,c(i)}^{(p,R_p)} \right), \quad (2.4b)$$

$$\mathbf{H}_{j,c(i)} = \text{bdiag} \left(\mathbf{H}_{j,c(i)}^{(1)}, \dots, \mathbf{H}_{j,c(i)}^{(P)} \right), \quad (2.4c)$$

as the equivalent channel matrices for all the slots of the (p, r) th round, all the rounds of the p th phase, and for the complete communication, respectively.

The precoding matrix employed during the (p, r) th round, and carrying the vector of symbols \mathbf{x}_i desired by the i th user, is denoted by $\mathbf{V}_i^{(p,r)} \in \mathbb{C}^{MS_p \times b}$, with

$$\mathbf{V}_i^{(p,r)} = \mathbf{0}, \forall i \notin \mathcal{G}^{(p,r)}. \quad (2.5)$$

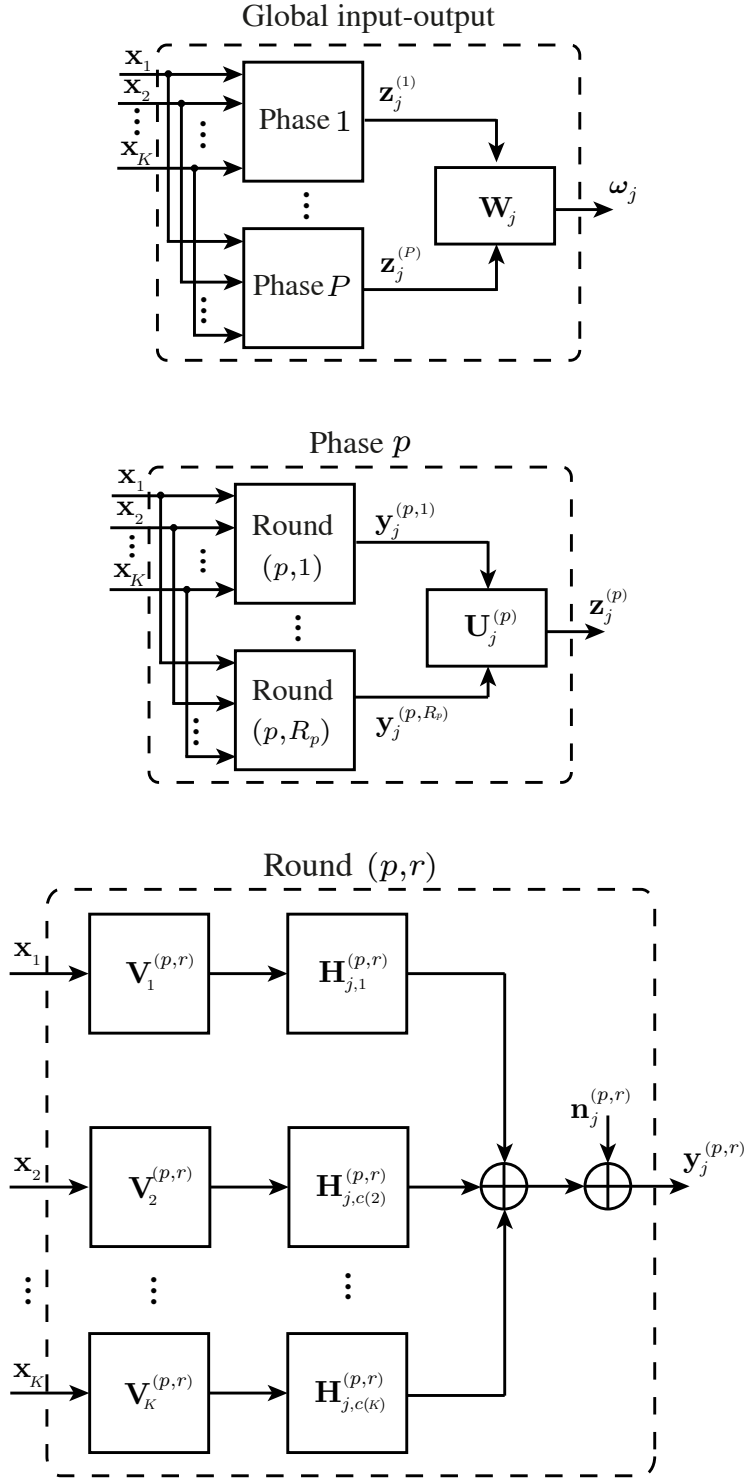


Figure 2.2: Block diagram for the general transmission and reception model considered, divided in phases, in turn divided in rounds. From top to bottom, each of the diagrams is related to equations (2.9), (2.8) and (2.3), describing the global input-output relationship of the system (top), the processed signal per phase (middle), and received signal per round (bottom), respectively.

It is designed at the beginning of each phase according to the available channel state information at the transmitter side, for which different models are assumed throughout this dissertation and described in the next section. Also, its design takes into account the constraint of maximum transmission power P_T per transmitter and channel use, given by:

$$\sum_{c(i)=k} \text{trace} \left(\left(\mathbf{V}_i^{(p,r)} \right) \left(\mathbf{V}_i^{(p,r)} \right)^H \right) \leq S_p \cdot P_T, \quad k = 1, \dots, K_c, \quad (2.6)$$

where the sum is for all precoding matrices of users served by TX_k during S_p slots of the (p,r) th round. Notice that since noise is normalized, the average SNR per user is given by $\frac{P_T}{K_u}$. Moreover, we can write the following compact precoding matrices:

$$\mathbf{V}_i^{(p)} = \text{stack} \left(\mathbf{V}_i^{(p,1)}, \mathbf{V}_i^{(p,2)}, \dots, \mathbf{V}_i^{(p,R_p)} \right), \quad (2.7a)$$

$$\mathbf{V}_i = \text{stack} \left(\mathbf{V}_i^{(1)}, \dots, \mathbf{V}_i^{(P)} \right). \quad (2.7b)$$

Remark: All the indices of precoding or channel matrices are subject to some degree of simplification in some parts of the dissertation if, for example, there is only one round for a given phase. Those simplifications will be done only when they can be trivially understood thanks to the context.

In the sequel, the compact formulation for channels and precoding matrices above will be exploited to write the global input-output relationship of the system, as depicted in the block diagrams of Fig. 2.2. First, notice that (2.3) is summarized in Fig. 2.2-bottom. Now, assume that the received signals from all rounds of phase p are jointly processed at RX_j , as in Fig. 2.2-middle, thus obtaining

$$\mathbf{z}_j^{(p)} = \mathbf{U}_j^{(p)} \mathbf{y}_j^{(p)}, \quad (2.8a)$$

$$= \mathbf{U}_j^{(p)} \text{stack} \left(\mathbf{y}_j^{(p,1)}, \dots, \mathbf{y}_j^{(p,R_p)} \right), \quad (2.8b)$$

$$= \mathbf{U}_j^{(p)} \left(\sum_i \mathbf{H}_{j,c(i)}^{(p)} \mathbf{V}_i^{(p)} \mathbf{x}_i + \mathbf{n}_j^{(p)} \right), \quad (2.8c)$$

where $\mathbf{U}_j^{(p)}$ is the linear filter at RX_j for phase p , whose design will be detailed for each case. Similarly, RX_j collects the signals along all the communication, as in Fig. 2.2-top, such that the global input-output relationship of the system is written in compact form as

$$\boldsymbol{\omega}_j = \mathbf{W}_j \mathbf{z}_j, \quad (2.9a)$$

$$= \mathbf{W}_j \text{stack} \left(\mathbf{z}_j^{(1)}, \dots, \mathbf{z}_j^{(P)} \right), \quad (2.9b)$$

where $\boldsymbol{\omega}_j \in \mathbb{C}^{b \times 1}$ is the estimation of \mathbf{x}_j at RX_j , and \mathbf{W}_j is the global receiving filter applied to the global processed signal \mathbf{z}_j , whose dimensions depend on each transmission strategy.

2.3 Channel Model: Dynamics and Acquisition

A block fading channel model is assumed with coherence time T_C , see Fig. 2.3, measured in number of time slots. In this model, the channel state remains constant for every block

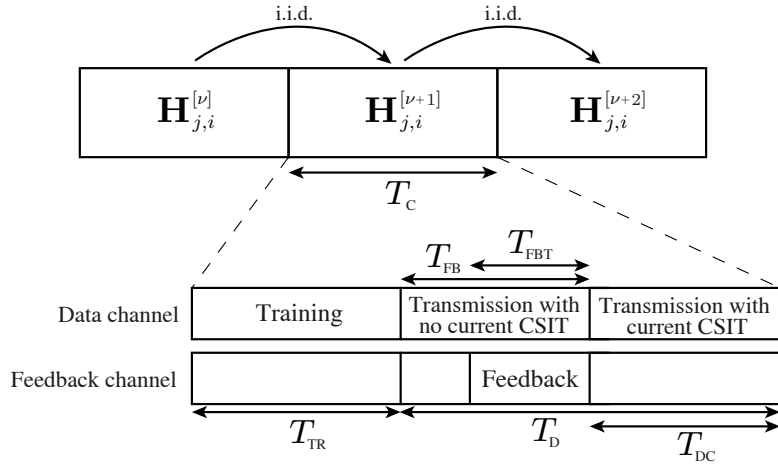


Figure 2.3: Block fading channel model. The channel remains constant in blocks of duration T_C time slots. Every time the channel changes of state, it is estimated by means of a training phase of duration T_{TR} time slots. This information is then fed back through the feedback channel, centered in an orthogonal channel, e.g. another frequency carrier. The transmission of the feedback lasts for T_{FBT} slots, although we assume that the feedback delay is system-fixed and equal to T_{FB} . During this waiting time, the transmitter can use the channel to transmit data without resorting to the current CSIT, i.e. with delayed or without CSIT. Finally, the remaining time of the block (T_{DC}) can be used for transmission exploiting the available information about the current channel state at the transmitter side. The total time of the block that can be used to transmit data is denoted by T_D .

of duration T_C time slots, and then it instantaneously changes to a new channel state i.i.d. as $\mathcal{CN}(0, 1)$. Now, it is worth pointing out that the model in (2.3) indexes the time slots from the point of view of the transmission strategy, but does not take into account the block fading model. Therefore, the time slots (p, r, ϑ) and $(p, r, \vartheta + 1)$ correspond to consecutive time slots of the same instance of the transmission strategy, i.e. the same deployment and set of symbols per user are considered, but those two time slots may or not be adjacent in time, being a decision to be taken in case of implementation.

In this regard, we next introduce an alternative signal model, describing the transmitted and received signals in the time domain. This will be useful for the last part of the thesis. Let $\mathbf{y}_j^{[t,\nu]}$ denote the received signal at RX_j for each time slot t of the block ν , formulated as

$$\mathbf{y}_j^{[t,\nu]} = \sum_i \mathbf{H}_{j,i}^{[\nu]} \mathbf{s}_i^{[t,\nu]} + \mathbf{n}_j^{[t,\nu]}, t = 1, \dots, T_C, \quad (2.10)$$

where $\mathbf{H}_{j,i}^{[\nu]}$ denotes the channel for *all* time slots of the block with state ν , and $\mathbf{s}_i^{[t,\nu]}$ and $\mathbf{n}_j^{[t,\nu]}$ denote the signal transmitted by TX_i, and the noise signal at RX_j, for *each* time slot t of the block ν .

Every time the channel state changes, a training period is scheduled providing channel state estimations at the receiver side after T_{TR} time slots. For all this dissertation it is assumed perfect quality for the estimations of CSI at the receiver side. This information is reported to the transmitted side by means of a feedback report through the feedback channel, such that the transmitter must wait for T_{FB} time slots before being able to transmit with current CSIT. Therefore, we define the following two quantities:

$$T_D = (T_C - T_{\text{TR}})^+, \quad T_{\text{DC}} = (T_D - T_{\text{FB}})^+, \quad (2.11)$$

where T_D denotes the number of time slots where data can be transmitted (in general), whereas T_{DC} represents the number of time slots where data can be transmitted exploiting

the *current CSIT*, thanks to the feedback report information. Depending on the value of these parameters and the quality and delay of feedback, we will distinguish among different particular situations often considered in the literature, summarized in Table 2.1, and described in the next sections.

2.3.1 Type of Channels

Two different types of channel will be defined: constant or time-varying channel. Those categories arise from the transmitter's point of view, and they are function of the duration of the communication, and how the transmission is carried out. In order to avoid confusion they are next defined:

Definition 1. *The channel will be denoted as constant throughout all this thesis if the same channel realization is present during all the transmission time τ of a transmission experience.*

Definition 2. *The channel will be denoted as time-varying if all time slots of the transmission experience correspond to different channel states. Recall that although the channel coherence time may be long, if a transmission strategy requires different channel states for each channel use, the time slots of one transmission experience can be assigned to different coherence time blocks, as long as the system may support the generated latency. In any case, the channel has to be considered as time-varying whether if $T_D = 1$ or $T_{DC} = 1$ (if the transmission strategy requires current CSIT) .*

Table 2.1: Type of channel as a function of its dynamics, and type of CSIT as a function of the feedback delay and quality. Conditions for these extreme cases are specified in the last column. Variables τ , T_C , and T_{FB} are written in multiples of time slots.

	Feature	Particular case	Mathematical condition
Type of channel	Dynamics	Constant	—
		Time-varying	—
Type of CSIT	FB delay	Delayed CSIT	$T_{TR} + T_{FB} > T_C$ or $T_{DC} = 0$
		Current CSIT	$T_{TR} + T_{FB} < T_C$ or $T_{DC} > 0$
	FB quality	Useless CSIT	$\epsilon = 0$
		Perfect CSIT	$\epsilon = 1$

2.3.2 CSIT with Delays

In some scenarios, e.g. when users have high mobility, channel coherence time is short and may be comparable to the time lag needed for channel feedback. Then, two extreme cases are often assumed in the literature, and also in this work: current and delayed CSIT. Since usually $T_{FB} \gg T_{TR}$ ¹, both types of CSIT basically depend on how long is the feedback delay T_{FB} w.r.t. the coherence time T_C .

¹As specified later, the training process consists in transmitting pilot sequences, allowing the receivers to estimate their channels in parallel. However, T_{FB} accounts not only for the time of transmitting the channels from the receivers to the transmitters, but also for the time of processing the channel estimates. In addition, the feedback transmission is carried out with very limited information about the feedback channel. Therefore, it incurs a much longer time lag compared to the duration of the training process.

In case of current CSIT, it is assumed that channels are available at the transmitter side early enough to be exploited, thus $T_{\text{DC}} > 0$. On the other hand, in case of delayed CSIT the feedback report is obtained at the transmitter side after the channel has changed, thus $T_{\text{DC}} = 0$. Consequently, in case of delayed CSIT the feedback report gives only information about previous channel states, but none about the current one. When delayed CSIT is assumed for transmission, it is assumed that at the beginning of each phase p , each transmitter has access to

$$\{\mathbf{H}_{j,i}^{(\varrho)}\}_{\varrho=1}^{p-1}, \forall i, j,$$

i.e. the channel matrices for all links during all phases previous to phase p , whereas for current CSIT the channels for phase p would be also available.

2.3.3 CSIT Feedback

Let us write the channel matrix of each link for each coherence time block ν as the stacking of its N rows as

$$\mathbf{H}_{j,i}^{[\nu]} = \text{stack}\left(\underline{\mathbf{h}}_{j,i}^{[\nu]}(1), \dots, \underline{\mathbf{h}}_{j,i}^{[\nu]}(N)\right). \quad (2.12)$$

Two procedures exist in the literature for reporting the channel estimations from the receiver to the transmitter side. Although more details will be given in Part III, here we briefly review them, and introduce some notation related to the measure of quality of CSIT. On the one hand, in the *digital feedback* framework [Jin06], the channel information is quantized using a codebook available at all the nodes, and transmitted digitally. We will assume that this transmission consumes resources on the feedback channel, but does not introduce more errors than those associated to binary quantization, due to the finite number of bits. One possibility for implementation is to send the data through almost error-free control channels usually reserved in wireless networks.

On the other hand, in the *analog feedback* framework [AH12], the channel information is sent through a feedback channel, i.e. the same channel for which the receivers would communicate with the transmitters if the roles were reversed. In this case, the quality of the estimations at the transmitter side depends only on the feedback transmission power, since the noise is assumed unitary. Therefore, both procedures introduce some errors on the channel knowledge at the transmitters.

Let $\hat{\mathbf{h}}_{j,i}^{[\nu]}(n)$ denote the estimation available at the transmitter side for the n th receiving antenna exact channel $\underline{\mathbf{h}}_{j,i}^{[\nu]}(n)$. This estimation is distributed as a Gaussian variable for both procedures. In case of digital feedback, this results from the use of a codebook containing Gaussian distributed codewords. Otherwise, $\hat{\mathbf{h}}_{j,i}^{[\nu]}(n)$ is an MMSE estimate of a Gaussian variable corrupted by Gaussian noise, thus it is also Gaussian distributed. According to this, the feedback error is given by

$$\tilde{\mathbf{h}}_{j,i}^{[\nu]}(n) = \underline{\mathbf{h}}_{j,i}^{[\nu]}(n) - \hat{\mathbf{h}}_{j,i}^{[\nu]}(n) \sim \mathcal{CN}(0, P_{\text{T}}^{-\epsilon}), \quad (2.13)$$

where the exponent $\epsilon \in [0, 1]$ defines the FB quality. The formulation of the FB quality by one single parameter ϵ independently of the FB procedure will be addressed in Section 9.2. Recall that the quality is determined by the decaying rate of the error variance w.r.t. P_{T} : $\epsilon = 1$ implies perfect CSIT, whereas $\epsilon = 0$ entails useless or completely inaccurate CSIT,

such that the feedback knowledge gives no information about the actual channel. This definition of quality arises from the context of DoF analysis, which studies the channel at high SNR. Therefore, $\epsilon = 1$ makes the error to vanish as P_T grows, whereas $\epsilon = 0$ makes the error to be as strong as the channel itself.

2.3.4 Common Types of CSIT

In terms of feedback and delay, three relevant types of CSIT are usually assumed in the literature, next defined:

Definition 3. We denote by full CSIT the case where the CSIT is current and perfect, i.e. it has no errors and it is instantaneously available.

Definition 4. We denote by delayed CSIT the case where perfect but totally outdated CSI is available, i.e. it has no errors, but cannot be exploited for the current channel block. If nothing is stated, delayed CSIT denotes the case without errors, i.e. perfect delayed CSIT, whereas the case with errors will be specifically denoted as imperfect delayed CSIT.

Definition 5. We denote by no CSIT the case where CSI is only available at the receivers. It is worth pointing out that when errors are severe, i.e. useless CSIT, this information is considered as useful as not having CSI.

In practice, after the training period, receivers report the feedback to its associated transmitters. Therefore, the following two distinctions are also made in terms of the specific channels that are available (either for current/delayed, and perfect/imperfect cases) at each transmitter:

Definition 6. We denote by local CSIT the case where each transmitter has only access to the CSI where it is acting as the source. In other words, if TX_i has local CSIT of any type, then only the channels $\mathbf{H}_{j,i}^{(p)}, \forall j$, are available at that transmitter, for the corresponding phases and quality.

Definition 7. In contrast, we denote by global CSIT the situation where all CSI is available at all transmitters. Notice that the acquisition of global CSIT requires extra overheads with respect to local CSIT, which can be very detrimental in case of several transmitters.

Similarly, local/global CSIR may be defined, i.e. local/global knowledge at the receivers. In any case, we will assume that global CSI is available at both transmitter and receiver sides, and clearly state when local CSIT is sufficient.

2.4 Key Performance Metrics

2.4.1 Signal Space Matrix

To the best of the author's knowledge, the idea of formulating a matrix to capture all the signal spaces available at the receiver, was first proposed in [PD12], denoted as the signal space matrix (SSM). This matrix will be useful to compactly write the sum-rate and DoF in the sequel, and also allows writing the estimation of \mathbf{x}_j at RX_j in (2.9) as:

$$\boldsymbol{\omega}_j = \mathbf{W}_j \left(\boldsymbol{\Omega}_j \text{stack}(\mathbf{x}_1, \dots, \mathbf{x}_K) + \mathbf{U}_j \mathbf{n}_j \right), \quad (2.14)$$

where \mathbf{U}_j collects all the per-phase filters, and $\boldsymbol{\Omega}_j$ denotes the SSM at RX_j, defined as follows:

$$\boldsymbol{\Omega}_j = [\boldsymbol{\Omega}_j^{\text{des}} \quad \boldsymbol{\Omega}_j^{\text{int}}] = \mathbf{U}_j [\mathbf{H}_{j,1} \mathbf{V}_1, \dots, \mathbf{H}_{j,K_c} \mathbf{V}_K], \quad (2.15)$$

where $\boldsymbol{\Omega}_j^{\text{des}} = \mathbf{U}_j \mathbf{H}_{j,c(j)} \mathbf{V}_j$, and $\boldsymbol{\Omega}_j^{\text{int}}$ contains the columns of $\boldsymbol{\Omega}_j$ related to the interference, i.e. the ones not in $\boldsymbol{\Omega}_j^{\text{des}}$.

Taking into account those definitions, the covariance matrices for desired and interference signals are given by:

$$\mathbf{Q}_j^{\text{des}} = (\mathbf{W}_j \boldsymbol{\Omega}_j^{\text{des}}) (\mathbf{W}_j \boldsymbol{\Omega}_j^{\text{des}})^H, \quad \mathbf{Q}_j^{\text{int}} = (\mathbf{W}_j \boldsymbol{\Omega}_j^{\text{int}}) (\mathbf{W}_j \boldsymbol{\Omega}_j^{\text{int}})^H. \quad (2.16)$$

Then, the achievable sum bit-rate is given by [TV05]:

$$B = \sum_j B_j = \sum_j \frac{1}{\tau} \log_2 \left| \mathbf{I} + (\mathbf{Q}_j^{\text{int}} + \mathbf{W}_j \mathbf{W}_j^H)^{-1} \mathbf{Q}_j^{\text{des}} \right|, \quad (2.17)$$

where we have applied the assumption of i.i.d. noise with unit variance.

2.4.2 Degrees of Freedom

Channel capacity of the BC has been extensively studied and many results are available in the literature, see for instance [WSS06]. However, the study of the IC channel capacity has been open for over 30 years [Car75], and it is only closed for some special cases [S⁺08][AV09].

In recent years, the DoF, also known as the *multiplexing gain*, have emerged as one of the most important metrics for characterizing multi-user networks where channel capacity is too challenging. The DoF analysis assumes arbitrarily high SNR regime, such that the effect of noise becomes negligible, and interference becomes the major bottleneck of the network. The design is then focused on interference management, and allows simplifying the mathematical analysis, as well as drawing some interesting and promising conclusions.

Definition

Let $C(P_T)$ denote the channel capacity, i.e. the maximum sum bit-rate that can be employed with vanishing error probability [CT06] at SNR P_T . Then,

$$d = \lim_{P_T \rightarrow \infty} \frac{C(P_T)}{\log_2 P_T}, \quad (2.18)$$

denotes the *channel DoF* [MAMK08][CJ08]. The DoF describe how the system bit-rate scales with the logarithm of the SNR at the high SNR regime, i.e. they are the slope of channel capacity when plotted as a function of the logarithm of the SNR. Alternatively, they can be understood as the number of signal dimensions independently available per channel use. The study of the DoF reveals how different conditions on the network, e.g. deploying additional antennas, considering multiple time/frequency transmissions or having different levels of channel knowledge, provides a different number of signal dimensions that can be exploited for bit-rate gains.

Linear DoF

This thesis studies the DoF under linear encoding/decoding strategies, by proposing different designs for the covariance matrices $\{\mathbf{Q}_j^{\text{des}}, \mathbf{Q}_j^{\text{int}}\}$. For a given choice, the DoF value achieved $d^{(\text{in})} \triangleq d^{(\text{in})}(\{\mathbf{Q}_j^{\text{des}}, \mathbf{Q}_j^{\text{int}}\})$ represents an *inner bound*, and it may be formulated as follows:

$$d^{(\text{in})} = \lim_{P_T \rightarrow \infty} \frac{B(P_T, \{\mathbf{Q}_j^{\text{des}}, \mathbf{Q}_j^{\text{int}}\})}{\log P_T} \leq d^{(\text{lin})} \leq d \leq d^{(\text{out})}, \quad (2.19)$$

where $d^{(\text{out})}$ denotes an *outer bound*, i.e. a DoF value which is known to be greater or equal than the channel DoF. Notice that we refer to d as the *channel DoF*, corresponding to the maximum DoF that can be achieved. Usually, the methodology employed to characterize them is to propose DoF inner bounds and outer bounds until two of them match. In such a case, the DoF value obtained corresponds to the channel DoF.

Finally, $d^{(\text{lin})}$ represents the channel *linear* DoF, i.e. the maximum DoF that can be achieved using linear strategies. One cannot assume that in general $d^{(\text{lin})} = d$, although for most cases the literature has revealed that this statement holds.

DoF per user and time-sharing

In this dissertation, we assume symmetrical users, i.e. all users obtain the same DoF. Consequently, the DoF per user write as

$$d_j = \frac{1}{K}d.$$

Notice that the same definition applies for all types of DoF defined above, i.e. channel DoF, linear DoF, and DoF inner and outer bound.

In a similar fashion, we denote by time-sharing the procedure for exploiting a scheme designed to work with $L < K$ users for a scenario with K users. Although the concept also applies for the IBC, let us for simplicity describe it for the IC. In such a case, the procedure consists in applying this scheme independently to each possible group of L users, such that all users are served the same number of times.

Let assume that $\tilde{d}_j^{(\text{in})}$ DoF are achieved by each of L users of a L -user IC along $\tilde{\tau}$ slots. Then, the equivalent DoF per user and total duration of the communication when it is used for the K -user case write as

$$d_j^{(\text{in})} = \frac{L}{K} \tilde{d}_j^{(\text{in})}, \quad \tau = \binom{K}{L} \tilde{\tau}. \quad (2.20)$$

2.4.3 Simplified DoF Analysis

As anticipated at the beginning of this section, the DoF formulation allows approaching to the channel capacity characterization, and simplifying the mathematical analysis. Three properties of the DoF are next explained to this end: computation of the DoF with no interference, spatially-normalized DoF, and DoF reciprocity.

DoF with no interference

Since the DoF analysis entails studying the capacity at high SNR, the interference becomes the major bottleneck. Decoding the desired symbols having very strong interference dramatically decreases the achieved rate. Therefore, the interference must be removed, which in turn simplifies the DoF computation as next shown.

Assume that the precoding matrices and receiving filters are designed such that $\mathbf{Q}_j^{\text{int}} = \mathbf{0}$ or, alternatively:

$$\mathbf{W}_j \mathbf{U}_j \mathbf{H}_{j,c(i)} \mathbf{V}_i = \mathbf{0}, \quad \forall i \neq j. \quad (2.21)$$

This general design can be the result of the coordination of transmitter and receiver side, or simply be achieved by one of the two sides. On the one hand, the idea of precoding matrices designed such that

$$\mathbf{H}_{j,c(i)} \mathbf{V}_i = \mathbf{0}, \quad \forall i \neq j, \quad (2.22)$$

is usually denoted in the literature as null-steering (NS) or zero-forcing (ZF) at the transmitter side. This is because (2.22) can be interpreted as transmitting through the angular directions where the radiation pattern diagram vanishes. Otherwise, having

$$\mathbf{W}_j \mathbf{U}_j \mathbf{H}_{j,c(i)} = \mathbf{0}, \quad \forall i \neq j, \quad (2.23)$$

is usually known as ZF at the receiver side or simply ZF, and can be interpreted as filtering the angular directions where the interference is received from.

In any case, if (2.21) holds, using standard derivations [TV05] it is found that (2.18) can be expressed as

$$d_j^{(\text{in})} = \frac{1}{\tau} \text{rank} (\mathbf{W}_j \boldsymbol{\Omega}_j^{\text{des}}) \stackrel{(a)}{\leq} \frac{b}{\tau} \quad (2.24)$$

where (a) is satisfied with equality only if after the projection \mathbf{W}_j the rank of the desired signals is equal to the number of transmitted symbols b . In other words, each receiver should be able to retrieve b independent and interference-free LCs or observations of its desired symbols. Since usually the precoding matrices are designed to manage the interference, direct channels do not take part on the precoding matrix design. Therefore, it is often conjectured that since channels are generic inequality (a) will be satisfied with equality with probability one. However, this is not always true and a rigorous proof may be required, which is the motivation of the work described in the first part of the thesis (Chapter 4) for the 3-user MIMO IC.

The equivalence of the DoF with the rank of the SSM matrix eases the DoF derivation, and gives some interesting conclusions. For example, it is straightforward to see that for a P2P channel the channel DoF are equal to $\min(M, N)$, i.e. the minimum between the number of antennas at the transmitters and the receivers. This is usually referred in the literature as the single-user DoF value.

Spatially-normalized DoF

All the schemes proposed in this thesis are studied in terms of spatially-normalized DoF. In order to avoid cumbersome notation, the same notation as for the non-normalized DoF

will be used, i.e. $d_j^{(\text{in})}$ refers from now on to the normalized DoF per user inner bound, and similarly for d_j , $d_j^{(\text{out})}$, and $d_j^{(\text{lin})}$. Assuming that one scheme allows to decode all the transmitted symbols b , i.e. inequality (a) in (2.24) is satisfied, then they are defined as follows:

$$d_j^{(\text{in})} \triangleq \frac{b}{N\tau}. \quad (2.25)$$

The normalized DoF allow us to study the channel DoF as a function of its *antenna ratio*, defined as follows:

$$\rho = \frac{M}{N}, \quad (2.26)$$

such that, unless otherwise stated, it is assumed that the DoF scale with a factor α if M and N are also scaled by α . Consequently, studying the channel for a given ρ reduces the DoF characterization task, since all antenna settings with the same ratio should be analyzed only for one case.

DoF reciprocity

When both the transmitter and receiver sides have the same type of CSI, i.e. in our case only for full CSIT, a step further can be done by generalizing the antenna ratio in (2.26) to

$$\rho = \frac{\min(M, N)}{\max(M, N)}. \quad (2.27)$$

Hence, the DoF characterization challenge can be highly alleviated, because only half the number of antenna settings should be considered, since now ρ depends only on the maximum and minimum between M and N . This generalization is built upon the concept of *DoF reciprocity of wireless networks* [GCJ08], next stated:

Theorem 2.1. *Consider a wireless network with full CSIT defined by its topology, the number of antennas at the transmitters and receivers (M and N , respectively). Then, its reciprocal setting, i.e. a network where M and N are exchanged, has exactly the same sum DoF.*

Proof: The proof follows from the DoF expression as a rank of a matrix in (2.24), here rewritten for reader's convenience:

$$d_j^{(\text{in})} = \frac{1}{\tau} \text{rank} (\mathbf{W}_j \boldsymbol{\Omega}_j^{\text{des}}) = \frac{1}{\tau} \text{rank} (\mathbf{W}_j \mathbf{H}_{j,j} \mathbf{V}_j), \quad (2.28)$$

where we assume without loss of generality and to simplify notation that no per-phase filters are used, i.e. $\mathbf{U}_j = \mathbf{I}$.

Now, consider using the data channel in the reverse direction, i.e. with transmitters acting as receivers and viceversa. In such a case, $\tilde{\mathbf{W}}_j \in \mathbb{C}^{b \times M}$, $\tilde{\mathbf{H}}_{j,j} \in \mathbb{C}^{M \times N}$, and $\tilde{\mathbf{V}}_j \in \mathbb{C}^{N \times b}$ denote the receiving filter used at TX_j, the channel matrix from RX_j to TX_j, and the precoding matrix used at RX_j, respectively. Therefore, the achievable DoF in case of using the data channel in the reverse direction would be given by:

$$\tilde{d}_j^{(\text{in})} = \frac{1}{\tau} \text{rank} (\tilde{\mathbf{W}}_j \tilde{\mathbf{H}}_{j,j} \tilde{\mathbf{V}}_j). \quad (2.29)$$

Showing the equivalence of (2.28) and (2.29), recall that wireless propagation channels have *reciprocity* [TV05], i.e:

$$\tilde{\mathbf{H}}_{j,j} = (\mathbf{H}_{j,j})^H, \quad (2.30)$$

since the complex channel gain from one antenna to another is equal to its conjugate when considering the reverse direction. Now, taking the design

$$\tilde{\mathbf{W}}_j = \mathbf{V}_j^H, \quad \tilde{\mathbf{V}}_j = \mathbf{W}_j^H, \quad (2.31)$$

the same achievable DoF value is achieved in both cases. Finally, it is worth pointing out that this property does not hold for networks with delayed or no CSIT, because in such a case the design in (2.31) cannot be realized, since transmitters and receivers have different type of CSI. \square

2.4.4 DoF with Overheads

The effect of the block fading model on the DoF has been neglected in the previous definitions, but may decrease the throughput of the network especially for channels with high dynamics. Then, it is necessary to account for the overheads due to *i*) training, and *ii*) feedback periods, since they reduce the percentage of the block that can be dedicated to data transmission. While other more complicated cases will be dealt in Part III, consider here the most simple case where only one block is used, thus $\tau < T_C$. Then, we define the *overhead factor*, as follows

$$\Gamma_{\text{OH}} = \frac{T_{\text{DC}}}{T_C} = \frac{(T_C - T_{\text{TR}} - T_{\text{FB}})^+}{T_C}, \quad (2.32)$$

such that the achievable DoF are computed as

$$d^{(\text{in})} = K \cdot \Gamma_{\text{OH}} \cdot \frac{b}{\tau}. \quad (2.33)$$

Notice that this multiplicative factor is usually neglected since as long as $T_C \gg T_{\text{TR}} + T_{\text{FB}}$, Γ_{OH} converges to 1, thus the DoF with or without overheads are almost equal. Similar expressions are derived for the case where the report of the current channel is not required.

2.4.5 Net DoF

The net DoF were introduced in [XAJ12] to measure the DoF taking into account all the issues related to channel acquisition. While the overhead described in the preceding section accounts for the cost of having CSIT in terms of occupancy of the data channel for the current block, two other issues must be taken into account:

- The *dedicated training* periods, representing the procedures required to deliver extra CSI to the receivers. Actually, notice that the training process only provides to RX_j its *local* channels, i.e. $\mathbf{H}_{j,i}^{[\nu]}, \forall i$, as defined in Section 2.3.4. However, some strategies require having non-local channels (or a function of them) at the receivers, whose transmission is denoted as the dedicated training process.
- The amount of resources consumed on the feedback channel to deliver the report of the current block. Notice that it is relevant not only the wait required to acquire the feedback, but also the consumption of resources on the feedback channel which could have been used for transmission of data from receivers to transmitters.

In the sequel, assume that $d^{(\text{in})}$ includes the overheads due to training, feedback waits, and dedicated training. The objective the rest of this section is to describe how feedback is accounted, and formally define the net DoF. In this regard, let F denote the FB rate, i.e. the amount of resources consumed on the feedback channel to deliver the CSI. Then, the feedback DoF are defined as

$$d^{(\text{FB})} = \lim_{P_T \rightarrow \infty} \frac{F}{\log_2 P_T}. \quad (2.34)$$

According to this, the net DoF and net bit-rate are defined as

$$d^{(\text{net})} = d^{(\text{in})} - d^{(\text{FB})} = \lim_{P_T \rightarrow \infty} \frac{B^{(\text{net})}}{\log_2 P_T}, \quad B^{(\text{net})} = B - F, \quad (2.35)$$

where $d^{(\text{in})}$ accounts for the overheads as in (2.33).

Part I

Degrees of Freedom Analysis for Full CSIT

The DoF of the 3-user MIMO IC with full CSIT and constant channel coefficients are investigated. First, state-of-the-art for the MIMO Interference Channel is reviewed, introducing the relevant concepts of *interference alignment* and *subspace alignment chains*. From this review, it is observed that the previous works cannot attain the DoF outer bound when $(p, p+1)$ antennas and constant channels are considered. In short, our contribution consists in formally proving that the achievability of the DoF outer bound is attained using linear methods, thereby avoiding the use of the more complex rational dimensions framework. The proposed transmission scheme exploits asymmetric complex signaling together with symbol extensions in time and space interference alignment concepts. While only the cases $p = 2, 3, \dots, 6$ are considered, providing the specific transmit and receive filters, we also provide the tools needed for proving the achievability of the optimal DoF for $p > 6$, whose DoF characterization is conjectured.

Technical paper/s related to this part:

M. Torrellas, A. Agustin, J. Vidal and O. Muñoz, "The degrees of freedom of the 3-user $(p, p+1)$ MIMO Interference Channel", IEEE Transactions on Communications, pp. 3842-3853, Nov. 2014.

Preliminaries

3

This chapter reviews some background related to the 3-user IC with full CSIT, studied along this part of the thesis. First, the specific system model for the 3-user MIMO IC is explained. Second, the state-of-the-art of the DoF characterization for the IC with full CSIT is addressed.

3.1 Specific System Model

The 3-user IC presents only one user per cell, thus the serving transmitter has always the same index as the user. Therfeore, for the IC we have

$$K_u = 1, \quad K = K_c = 3, \quad c(j) = j, \forall j. \quad (3.1)$$

Furthermore, all the strategies reviewed and proposed in this part of the thesis have only one phase and one round, with all users being served, i.e:

$$P = 1, \quad R = 1, \quad \tau = S_1, \quad G = 3. \quad (3.2)$$

The received signal at RX_j generally expressed in (2.3) simplifies to

$$\mathbf{y}_j = \mathbf{H}_{j,j} \mathbf{V}_j \mathbf{x}_j + [\mathbf{H}_{j,j-1} \mathbf{V}_{j-1}, \mathbf{H}_{j,j+1} \mathbf{V}_{j+1}] \begin{bmatrix} \mathbf{x}_{j-1} \\ \mathbf{x}_{j+1} \end{bmatrix} + \mathbf{n}_j, \quad (3.3)$$

where $\mathbf{y}_j, \mathbf{n}_j \in \mathbb{C}^{N\tau \times 1}$, $\mathbf{H}_{j,i} \in \mathbb{C}^{N\tau \times M\tau}$, and $\mathbf{V}_i \in \mathbb{C}^{M\tau \times b}$, with $\tau = S_1$. We remark that all variables with supraindices have been omitted since only one round is scheduled, thus those supraindices may be therefore reused for other notation. Moreover, all indexes are written modulo K unless otherwise stated.

3.2 State-of-the-Art

The channel DoF of the BC with full CSIT at all terminals may be attained by a combination of ZF, either at the transmitter or the receiver side [Jaf05], and time-sharing concepts. However, this approach is optimal for the IC only when the number of antennas at either the transmitter or the receiver side is much larger than at the other, i.e. $M \gg N$ or $M \ll N$. Otherwise, the study of the DoF not only for the IC, but also for many interference wireless networks, has been intimately connected to the emergence and development of the interference alignment concept. The main purpose of IA is to divide the task described in (2.21) of canceling the interference by coordinating the operations at the transmitter and receiver side. One the one hand, it is assumed that the receiver projects the received signal onto the orthogonal-to-interference subspace by means of ZF concepts, as in (2.23). On the other hand, the transmit filters are designed in such a

way that there exists some intersection among the generated interference terms. Consequently, their sum subspace occupies less dimensions at the receiver signal space or, equivalently, its orthogonal-to-interference subspace can allocate desired signals of higher dimension. It is important to remark that projecting the desired signals onto the null space of the interference will always reduce the power of the desired signals, but this effect is neglected in this context since the DoF analysis assumes an arbitrarily high SNR regime.

The IA concept was originally proposed in the context of index coding in [BK98], while it crystallized later on for the 2-user MIMO X-channel in [MAMK08] and for the K -user SISO IC with $K > 2$ in [CJ08]. Surprisingly, Cadambe and Jafar [CJ08] proposed a linear precoding/decoding scheme that provides *each user half the cake*, i.e. half the DoF compared to the single-user case, thus a total of $K/2$ sum DoF. Additionally, the authors showed that this result generalizes to the square MIMO case, i.e. when all nodes are equipped with M antennas, obtaining $KM/2$ total DoF. This approach will be reviewed for the 3-user case with 2 antennas per node in Section 3.2.1. For both SISO and square MIMO cases, the achievability of fractional DoF relies on a single-round transmission with multiple time slots on a time-varying channel. However, it fails when considering a constant SISO channel. This is because the equivalent channel matrices result on scaled identity matrices with not enough diversity as compared to the case where channel variations or multiple antennas are employed. This limitation revealed that when the channel coefficients are constant the signal dimensions provided by deploying additional antennas (referred in [WGJ14] as space extensions) provide more diversity than the signal dimensions obtained through time/frequency extensions.

The case of different number of antennas at transmitters and receivers in a IC has been extensively analyzed by applying the original IA concept, see for example [RLL12, GJ10, WGJ14, WSJ14, GCJ08, CJW10]. Beyond that, many extensions of the disrupting idea of IA have appeared in the literature. A very extensive survey can be found in [Jaf11]. Summarizing, there are two different frameworks for developing IA-based transmit precoders: lattice level IA [MMK10] (*lattice alignment*), and space level IA [MAMK08, CJ08], (*space alignment*), see Fig. 3.1. These two approaches arise from the choice between structured or random codes, respectively. Lattice alignment-based techniques are non-linear and use structured coding, e.g. lattice codes, to align the interference on the signal scale level. This idea was first exploited in the context of the rational dimensions framework by Mota-hari *et al.* in [M⁺14]. Following this line of research, Ghasemi *et al.* [GMK10] showed that the DoF outer bound may be attained for any user and antenna settings. Nevertheless, its rate performance is extremely degraded at medium SNR values [OE13]. In contrast, space alignment techniques provide a better rate performance at moderate SNR regimes, but when the channel coefficients are constant they cannot attain optimality for certain antenna configurations.

All the schemes proposed in this thesis follow the conventional IA approach, denoted hereafter as *linear IA*, under the space alignment framework. In turn, under this framework two other types of IA were proposed: ergodic IA (EIA) [N⁺12] and opportunistic IA (OIA) [LC13, LCR13]. First, EIA relies on repeating the same transmission along two time slots with complementary channel states, i.e. two channel realizations such that the interference is canceled by simply summing up the signals received from both time slots. The surprising result in [N⁺12] was that the optimal $\frac{K}{2}$ DoF value can be attained in a K -user SISO IC. However, time-varying channels is a fundamental feature for applying

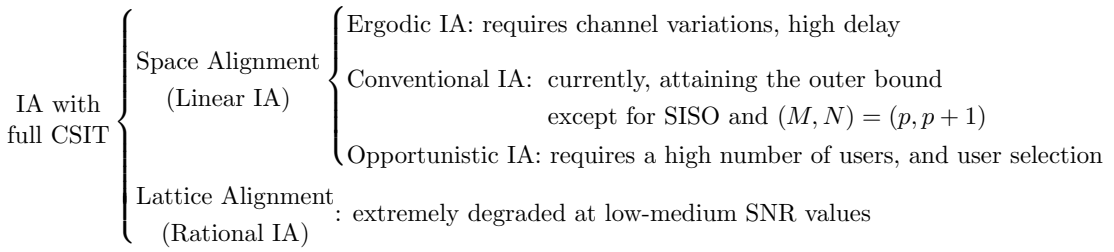


Figure 3.1: Different types of IA with full CSIT appeared in the literature

EIA, whereas linear IA applies to almost all settings either if channels change over time or not. Second, OIA exploits the diversity provided by a large amount of users, let say *user dimension*, through scheduling. The idea is to combine the benefits of opportunistic beamforming and IA. The transmitters select a random precoding design, and transmit pilot signals. Then, taking into account the signals obtained at the receivers, the best subset, i.e. the subset of receivers where the interference has been aligned using such design, is selected. Consequently, no CSIT is required, which allows a significant reduction of the control plane information sharing. Although interesting for some scenarios, a more generic case where users cannot be selected and its channels are given will be assumed, thus OIA will not be considered in this thesis.

In the sequel, the most relevant results in terms of DoF for the 3-user MIMO IC are briefly exposed, summarized in Fig. 3.2. First, for the SISO case, the best known inner bound was proposed by Cadambe *et al.* in [CJW10]. The authors proposed a linear scheme able to achieve 1.2 DoF, thanks to the *asymmetric complex signaling* (ACS) concept, reviewed in Section 4.2.2. In short, the idea is to exploit the existing diversity on complex numbers to transform the complex channel into a real one with a more sophisticated structure than simply scaled identity matrices. This tool has shown to be useful also for the 4-user SISO IC in [LS13].

Second, for the MIMO case, Wang *et al.* characterized the DoF of the 3-user MIMO IC in [WGJ14]. Their work provide two new ingredients to this research area: the *change of basis* (CoB) and *subspace alignment chains* (SAC) concepts. On the one hand, the CoB operation was useful to derive the DoF outer bound, since it allows writing the equivalent channels in such a way that the appropriate genie signals to be provided to each receiver can be more easily identified. This approach will be reviewed in Section 4.2.2, and allows deriving the DoF outer bound for the 3-user MIMO IC, proved to be tight in [WGJ14] thanks to the lattice alignment approach in [MMK10]. Moreover, the CoB operation has been found to be useful also to derive inner and outer bounds for other settings, e.g. the MIMO rank-deficient IC in [Z⁺14]. On the other hand, the proposed DoF inner bound flows from the SAC concept. This linear approach will be reviewed in Section 3.2.2, and allows stating equivalence of linear and channel DoF for almost all antenna settings.

Nevertheless, when $M = N = 1$ or $\rho = \frac{M}{M+1}$ with $M > 1$,¹, the work in [WGJ14] does not clarify if the DoF outer bound can be attained using linear schemes when the channel coefficients are constant, see [WGJ14, Section VIII.C]. Actually, optimality of the case $\rho = \frac{M}{M+1}$ was later claimed in [WGJ11] by means of *asymmetric complex signaling* and *subspace alignment chains* concepts, but the result is just sustained on numerical exper-

¹The case $M = 1$ was previously addressed in [GJ10].

N/M	1	2	3	4	5	6
1	[0.4, 0.5] ACS					
2	2/3 ○ △	1 ○ □	3			
3	1 ○ △	6/5 ●	3/2 ○ □	4		
4	1 ○ △	4/3 ○ △	12/7 ●	2 ○ □	5	
5	1 ○ △	5/3 ○ △	2 ○ △	20/9 ●	5/2 ○ □	6
6	1 ○ △	2 ○ △	2 ○ △	12/5 ○ △	30/11 ●	3 ○ □

□ CJ
 △ SAC
 ○ already solved
 ● solved in the next chapter

Figure 3.2: Current knowledge about the linear DoF per user of the 3-user MIMO IC with constant channel coefficients for all transmitters and receivers equipped with $M, N = 1 \dots 6$ antennas, respectively. The channel DoF may be attained using rational alignment for all antenna settings. However, only those with empty circles may be currently attained using linear alignment techniques, either with the CJ or the SAC approaches, reviewed in Sections 3.2.1 and 3.2.2, respectively. This work shows that all other settings except SISO can be handled using linear alignment without the need of lattice alignment. Consequently, only the linear DoF for SISO remain unknown.

iments. Therefore, to the best of the authors' knowledge, there is not a formal proof in the literature.

3.2.1 IA for the Square Case

The original scheme proposed by Cadambe and Jafar (CJ) in [CJ08] is here reviewed for the 3-user MIMO IC, with $M = N = 2$ antennas per node. In this case, a single-slot transmission is required, i.e. $\tau = 1$, where each transmitter delivers $b = 1$ symbol to its associated receiver. According to this, the received signal at RX_j writes as

$$\mathbf{y}_j = \mathbf{H}_{j,j} \mathbf{v}_j x_j + [\mathbf{H}_{j,j-1} \mathbf{v}_{j-1}, \mathbf{H}_{j,j+1} \mathbf{v}_{j+1}] \begin{bmatrix} x_{j-1} \\ x_{j+1} \end{bmatrix} + \mathbf{n}_j, \quad (3.4)$$

where $\mathbf{y}_j, \mathbf{v}_j, \mathbf{n}_j \in \mathbb{C}^{2 \times 1}$, $\mathbf{H}_{j,i} \in \mathbb{C}^{2 \times 2}$. Notice that since $b = 1$ the precoding matrices have only one column, thus become column vectors.

The idea of IA is to force the two interference terms at each receiver to be enclosed on the same dimensional subspace, as shown in Fig. 3.3, where the two interference terms at each receivers lie on a line. To this end, the precoding matrix design should satisfy the following set of constraints:

$$\text{span}(\mathbf{H}_{j,j-1} \mathbf{v}_{j-1}) = \text{span}(\mathbf{H}_{j,j+1} \mathbf{v}_{j+1}), \quad j = 1, 2, 3. \quad (3.5)$$

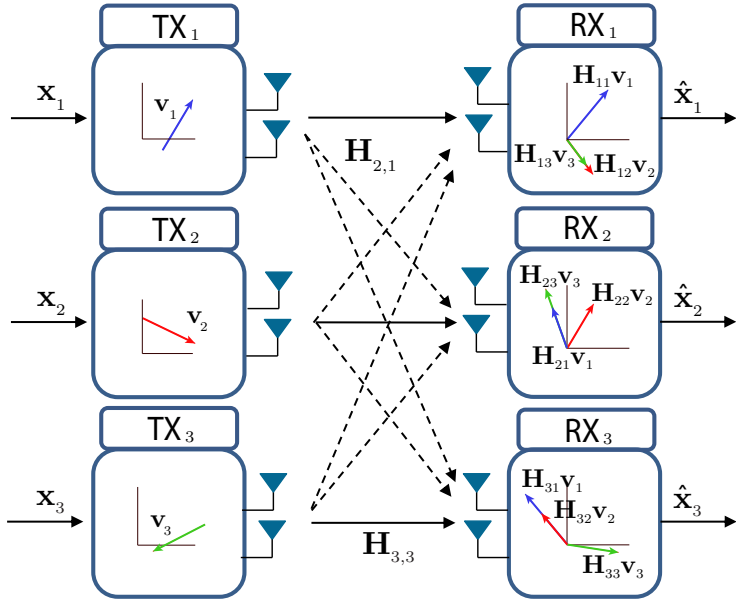


Figure 3.3: Signal subspaces using the original interference alignment approach, when all terminals are equipped with $M = N = 2$ antennas. Colors identify users.

One easy way to ensure this, is to force equality without the $\text{span}(\cdot)$ operators, i.e:

$$\mathbf{H}_{1,3}\mathbf{v}_3 = \mathbf{H}_{1,2}\mathbf{v}_2, \quad (3.6a)$$

$$\mathbf{H}_{2,1}\mathbf{v}_1 = \mathbf{H}_{2,3}\mathbf{v}_3, \quad (3.6b)$$

$$\mathbf{H}_{3,2}\mathbf{v}_2 = \mathbf{H}_{3,1}\mathbf{v}_1, \quad (3.6c)$$

or in compact form:

$$\begin{bmatrix} \mathbf{0} & \mathbf{H}_{1,2} & -\mathbf{H}_{1,3} \\ \mathbf{H}_{2,1} & \mathbf{0} & -\mathbf{H}_{2,3} \\ \mathbf{H}_{3,1} & -\mathbf{H}_{3,2} & \mathbf{0} \end{bmatrix} \begin{bmatrix} \mathbf{v}_1 \\ \mathbf{v}_2 \\ \mathbf{v}_3 \end{bmatrix} = \mathbf{0}. \quad (3.7)$$

Note that this is a more restrictive set of conditions than (3.5), but it will be sufficient to attain DoF-optimality.

Now, let \mathbf{e}_1 denote one of the two eigenvectors of the matrix $\mathbf{H}_{1,2}\mathbf{H}_{2,1}^{-1}\mathbf{H}_{2,3}\mathbf{H}_{3,2}^{-1}\mathbf{H}_{3,1}\mathbf{H}_{1,3}^{-1}$. Then, it is easy to see that the following design ensures IA [CJ08]:

$$\mathbf{v}_1 = \mathbf{e}_1, \quad (3.8a)$$

$$\mathbf{v}_2 = \mathbf{H}_{3,2}^{-1}\mathbf{H}_{3,1}\mathbf{v}_1 = \mathbf{H}_{3,2}^{-1}\mathbf{H}_{3,1}\mathbf{e}_1, \quad (3.8b)$$

$$\mathbf{v}_3 = \mathbf{H}_{2,3}^{-1}\mathbf{H}_{2,1}\mathbf{v}_1 = \mathbf{H}_{2,3}^{-1}\mathbf{H}_{2,1}\mathbf{e}_1, \quad (3.8c)$$

such that the interference subspace collapses to 1 dimension, as shown in Fig. 3.3. Consequently, there exists one available dimension in the two-dimensional receiver subspace to allocate the signals carrying desired symbols, which can be retrieved by means of ZF concepts.

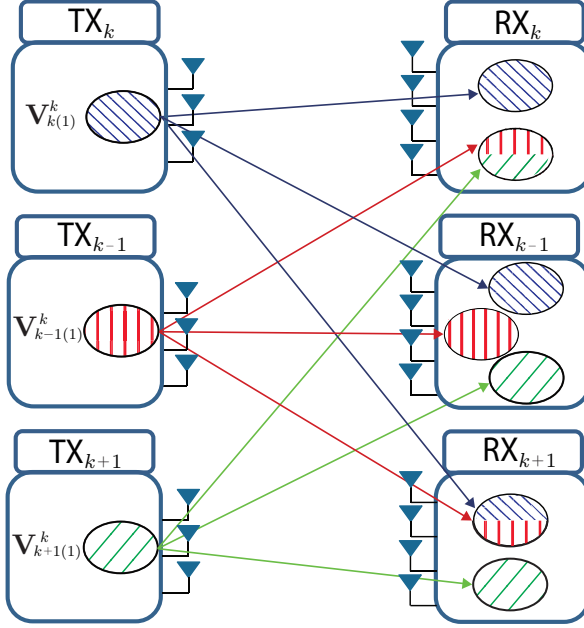


Figure 3.4: Occupation of receivers for the signals designed using alignment chain k ($M = 3, N = 4$ case). Ovals represent different subspaces at transmitters and receivers. Colors/Line patterns identify users.

3.2.2 Subspace Alignment Chains

IA proposes a linear transmitter design intertwined among users through the alignment, see (3.6), where each precoding vector should satisfy two conditions, i.e. appears in two equations. This can be interpreted as a chain, as follows:

$$\mathbf{v}_3 \xleftrightarrow{\text{RX}_1} \mathbf{v}_2 \xleftrightarrow{\text{RX}_3} \mathbf{v}_1 \xleftrightarrow{\text{RX}_2} \mathbf{v}_3, \quad (3.9)$$

where the design of the precoding vectors at TX_3 and TX_2 are connected by the alignment constraint at RX_1 . At the same time, the design of \mathbf{v}_2 is connected to \mathbf{v}_1 due to the alignment constraint at RX_3 . Finally, the chain is closed by the alignment constraint at RX_1 .

For the case $M \neq N$, this concept is generalized by means of the SAC approach [WGJ14]. In the sequel, the SAC concepts applied to attain optimal DoF are described for the case $N = M + 1$ with time-varying channels. For that case, the precoding matrix of each user is divided in M column sub-blocks per user, as follows:

$$\mathbf{V}_i = \left[\mathbf{V}_{i,(1)}^1 \cdots \mathbf{V}_{i,(U_i^1)}^1 \mid \mathbf{V}_{i,(1)}^2 \cdots \mathbf{V}_{i,(U_i^2)}^2 \mid \mathbf{V}_{i,(1)}^3 \cdots \mathbf{V}_{i,(U_i^3)}^3 \right], \quad (3.10)$$

where $\mathbf{V}_{i,(u)}^k \in \mathbb{R}^{\tau M \times (M+1)}$ denotes the u th sub-block carrying the $M(M+1)$ symbols of user i , designed by means of the k th alignment chain, and $U_i^1 + U_i^2 + U_i^3 = M$, whose specific values will be specified later. Notice that the supraindex has been used to specify the associated alignment chain since only one phase and one round are considered, as in previous section.

Now, for any value of M , three alignment chains, similar to (3.9), are built:

$$\mathbf{V}_{k,(1)}^k \xleftrightarrow{\text{RX}_{k+1}} \mathbf{V}_{k-1,(1)}^k \xleftrightarrow{\text{RX}_k} \mathbf{V}_{k+1,(1)}^k \xleftrightarrow{\text{RX}_{k-1}} \mathbf{V}_{k,(2)}^k \xleftrightarrow{\text{RX}_{k+1}} \cdots \xleftrightarrow{\text{RX}_{\eta_k}} \mathbf{V}_{\eta_k+1,(U_{\eta_k+1}^k)}^k \quad (3.11)$$

which mathematically is formulated as follows:

$$\text{span}(\mathbf{H}_{k+1,k} \mathbf{V}_{k,(1)}^k) = \text{span}(\mathbf{H}_{k+1,k-1} \mathbf{V}_{k-1,(1)}^k), \quad (3.12a)$$

$$\text{span}(\mathbf{H}_{k,k-1} \mathbf{V}_{k-1,(1)}^k) = \text{span}(\mathbf{H}_{k,k+1} \mathbf{V}_{k+1,(1)}^k), \quad (3.12b)$$

$$\text{span}(\mathbf{H}_{k-1,k+1} \mathbf{V}_{k+1,(1)}^k) = \text{span}(\mathbf{H}_{k-1,k} \mathbf{V}_{k,(2)}^k), \quad (3.12c)$$

⋮

$$\text{span}(\mathbf{H}_{\eta_k,\eta_k-1} \mathbf{V}_{\eta_k-1,(U_{\eta_k-1}^k)}^k) = \text{span}(\mathbf{H}_{\eta_k,\eta_k+1} \mathbf{V}_{\eta_k+1,(U_{\eta_k+1}^k)}^k), \quad (3.12d)$$

describing the alignment constraints to be satisfied by the sub-blocks with supraindex k , where $k = 1, 2, 3$ identifies each chain, $\eta_k = k - M$ is the last receiver of the k th chain, and the value U_i^k denotes the number of sub-blocks corresponding to the i th user designed according to the k th alignment chain. Taking into account that there are 3 users and $3M$ sub-blocks, it may be expressed in closed form as

$$U_i^k = \left\lceil \frac{M - \langle k - i \rangle}{3} \right\rceil. \quad (3.13)$$

The meaning of (3.11) or (3.12) is next conceptually described, and depicted for $M = 3$ in Fig. 3.4, where ovals represent at each transmitter/receiver the subspaces for the k th alignment chain, and each color/line pattern identifies each user's signals. First, (3.12a) states that the subspace occupied by the sub-block $\mathbf{V}_{k,(1)}^k$ should be the same as that for the sub-block $\mathbf{V}_{k-1,(1)}^k$ at the $(k + 1)$ th receiver, see Fig. 3.4. This will be expressed as the *alignment* between sub-block $\mathbf{V}_{k,(1)}^k$ and sub-block $\mathbf{V}_{k-1,(1)}^k$ at RX_{k+1} . Next, (3.12b) ensures that this latter sub-block is, *at the same time*, aligned with $\mathbf{V}_{k+1,(1)}^k$ at the k th receiver. This process continues as long as there exists a subspace at each receiver where signals can be aligned. The existence of such subspace can be guaranteed by means of basic linear algebra properties (see [WGJ14] for details), and defines the length of the alignment chain, corresponding to the number of sub-blocks designed according to such chain. Notice that in contrast to (3.9), here the chain has finite length. Consequently, the first and last sub-blocks in each chain participate only in the first and the last alignment conditions, respectively. This can be observed in Fig. 3.4 at RX_{k-1} .

As for the square case, equations (3.12) are tackled by dropping the $\text{span}(\cdot)$ operators:

$$\begin{bmatrix} \mathbf{H}_{k+1,k} & -\mathbf{H}_{k+1,k-1} & \mathbf{0} & \dots & \mathbf{0} \\ \mathbf{0} & \mathbf{H}_{k,k-1} & -\mathbf{H}_{k,k-2} & & \vdots \\ \vdots & \ddots & \ddots & \ddots & \mathbf{0} \\ \mathbf{0} & \dots & \mathbf{0} & \mathbf{H}_{\eta_k,\eta_k-1} & -\mathbf{H}_{\eta_k,\eta_k+1} \end{bmatrix} \begin{bmatrix} \mathbf{V}_{k,(1)}^k \\ \mathbf{V}_{k-1,(1)}^k \\ \mathbf{V}_{k-2,(1)}^k \\ \mathbf{V}_{k,(2)}^k \\ \vdots \\ \mathbf{V}_{\eta_k+1,(U_{\eta_k+1}^k)}^k \end{bmatrix} = \mathbf{0}, \quad (3.14)$$

where the precoding matrices may be obtained as the null space of the matrix at the left hand side above. Using this precoding matrix design in conjunction with ZF receiving filters, it can be seen that there are enough dimensions to allocate the desired signals, and all desired symbols can be linearly decoded.

IC with Full CSIT

4

When channel state is constant in time, the approach explained in the previous section does not always attain the channel DoF of the IC defined in (2.18). The reason is: even when the interference is aligned and there exist enough dimensions to allocate the desired signals, the linear combinations of desired symbols obtained after projection are not necessarily independent. In other words, $\text{rank}(\mathbf{W}_j \boldsymbol{\Omega}_j^{\text{des}}) < b$. This occurs for all antenna settings with $N = M = 1$, or $\rho = \frac{M}{M+1}$, with $M > 1$. Recall that for full CSIT, the property of reciprocity, described in Section 2.4.3, inspires a generalization of the antenna ratio definition, here repeated for reader's convenience:

$$\rho = \frac{\min(M, N)}{\max(M, N)}.$$

The goal of this chapter is to formally prove that the channel DoF can be achieved using linear transmit-receive filters, and coincide with the DoF outer bound for the 3-user $(M, M + 1)$ MIMO IC if $M > 1$ even assuming constant channel coefficients. Notice that such proof is also useful for the case $N = M - 1$ since both cases have equal antenna ratio. To this end, a linear scheme is proposed based on SAC (see Section 3.2.2), a one-phase one-round multi-slot transmission, and ACS [CJW10].

4.1 Main Contributions

Three main items summarize this chapter contribution:

- It is proved that the 3-user MIMO IC with constant channel coefficients has exactly $\frac{\rho}{\rho+1}$ linear DoF per user for $\rho = \frac{M}{M+1}$ and $M = 2, 3 \dots 6$, see Theorem 4.2 and Theorem 4.4, see Sections 4.3 and 4.4, respectively.
- The proposed transmit precoding matrices present a specific structure that can be generalized for any value of M . It is characterized by two properties: *i*) there are some elements equal to zero, and *ii*) all transmit precoders are defined as a function of 3 matrices, denoted as the *support precoding blocks*. Inspired by this structure, we propose an iterative algorithm able to find the structure of each precoding matrix for any value of M , thus simplifying the analysis.
- The methodology followed for the proof is also generalized for any value of M . Based on this, we conjecture that the value $\frac{\rho}{\rho+1}$ corresponds also to the normalized linear DoF for any $M \geq 7$, which has been also checked through numerical results.

4.2 Building a Proper Formulation

This section introduces some operations and definitions built upon the original input-output model in (3.4). This is one of the key aspects of our contribution: the construction of a formulation able to prove the feasibility of SAC for constant channels.

4.2.1 Precoding Matrices

The precoding matrix of each user is written as a function of M sub-block matrices of the form $\mathbf{V}_{i,(u)}^k \in \mathbb{R}^{2M\tau \times 2(M+1)}$ (whose objective was explained in Section 3.2.2), separated in three groups. This methodology is similar to the case without using ACS, but notice that now the entries of $\mathbf{V}_{i,(u)}^k$ instead of complex are real numbers, and each sub-block carries $2(M+1)$ real symbols instead of $M+1$ complex symbols. Moreover, for the sake of simplifying future descriptions, we introduce a permutation matrix $\mathbf{\Pi}_i \in \mathbb{R}^{2M \times 2M}$. Therefore, each precoding matrix when ACS is employed is given by

$$\mathbf{V}_i = \left[\mathbf{V}_{i,(1)}^1 \cdots \mathbf{V}_{i,(U_i^1)}^1 \mid \mathbf{V}_{i,(1)}^2 \cdots \mathbf{V}_{i,(U_i^2)}^2 \mid \mathbf{V}_{i,(1)}^3 \cdots \mathbf{V}_{i,(U_i^3)}^3 \right] \mathbf{\Pi}_i. \quad (4.1)$$

Furthermore, for convenience in the analysis each $\mathbf{V}_{i,(u)}^k$ is in turn divided in M blocks by rows, as follows:

$$\mathbf{V}_{i,(u)}^k = \text{stack} \left(\mathbf{V}_{i,(u)}^{k,1}, \mathbf{V}_{i,(u)}^{k,2}, \dots, \mathbf{V}_{i,(u)}^{k,M} \right), \quad (4.2)$$

where each $\mathbf{V}_{i,(u)}^{k,m} \in \mathbb{R}^{2\tau \times 2(M+1)}$ corresponds to one of the $m = 1 \dots M$ transmit antennas.

4.2.2 Channels

The channel matrix in model (3.4) stands for the equivalent channel matrix from TX_i to RX_j after applying:

- a multi-slot transmission
- asymmetric complex signaling
- change of basis

as detailed next. All three operations provide a more sophisticated structure to the channel matrices, and become the proper framework to prove achievability for the case of interest.

Let $\bar{\mathbf{H}}_{j,i} \in \mathbb{C}^{(M+1) \times M}$ be the original spatial channel matrix from the i th transmitter to the j th receiver, and assume a transmission over τ channel uses. Then, taking into account that the channel is constant, the $\text{bdiag}(\cdot)$ operation used in (2.4) may be written as follows:

$$\mathsf{T}(\bar{\mathbf{H}}_{j,i}) = \mathbf{I}_\tau \otimes \bar{\mathbf{H}}_{j,i}, \quad (4.3)$$

where $\mathbf{I}_\tau \in \mathbb{R}^{\tau \times \tau}$ is the identity matrix, and \otimes denotes the Kronecker product.

In addition to transmit through multiple time slots, now consider ACS, i.e. separate the design of real and imaginary parts of the transmitted signals, as in [CJW10]. In contrast, here the concept will be applied to each particular channel coefficient. Then, the extended form for each channel element is defined as:

$$\text{ACS} \left(\bar{h}_{j,i}^{n,m} \right) = \left| \bar{h}_{j,i}^{n,m} \right| \bar{\Phi} \left(\bar{\phi}_{j,i}^{n,m} \right) \in \mathbb{R}^{2 \times 2}, \quad (4.4)$$

where $\bar{h}_{j,i}^{n,m}$ is the *complex* channel gain between the m th antenna of TX_i and the n th antenna of RX_j , $\bar{\phi}_{j,i}^{n,m}$ is the phase of the complex number $\bar{h}_{j,i}^{n,m}$, and $\bar{\Phi} \left(\bar{\phi}_{j,i}^{n,m} \right) \in \mathbb{R}^{2 \times 2}$ is an unitary matrix given by:

$$\bar{\Phi} \left(\bar{\phi}_{j,i}^{n,m} \right) = \begin{bmatrix} \cos \left(\bar{\phi}_{j,i}^{n,m} \right) & -\sin \left(\bar{\phi}_{j,i}^{n,m} \right) \\ \sin \left(\bar{\phi}_{j,i}^{n,m} \right) & \cos \left(\bar{\phi}_{j,i}^{n,m} \right) \end{bmatrix}, \quad (4.5)$$

with some interesting properties that will be used in the sequel, for example:

$$\bar{\Phi} \left(q \right) \bar{\Phi} \left(r \right) = \bar{\Phi} \left(q + r \right), \quad \bar{\Phi} \left(q \right)^{-1} = \bar{\Phi} \left(-q \right), \quad (4.6)$$

for any arbitrary phases $q, r \in [0, 2\pi]$. For the sake of clarity, let us write the equivalent channel matrix $\hat{\mathbf{H}}_{j,i} \in \mathbb{R}^{2\tau(M+1) \times 2\tau M}$ if the two previous concepts are together applied, given by

$$\hat{\mathbf{H}}_{j,i} = \begin{bmatrix} \mathbf{C} \left(\bar{h}_{j,i}^{1,1} \right) & \dots & \mathbf{C} \left(\bar{h}_{j,i}^{1,M} \right) \\ \vdots & \ddots & \vdots \\ \mathbf{C} \left(\bar{h}_{j,i}^{M+1,1} \right) & \dots & \mathbf{C} \left(\bar{h}_{j,i}^{M+1,M} \right) \end{bmatrix}, \quad (4.7)$$

with $\mathbf{C} \left(\bar{h}_{j,i}^{n,m} \right) = \left| \bar{h}_{j,i}^{n,m} \right| \mathbf{I}_\tau \otimes \bar{\Phi} \left(\bar{\phi}_{j,i}^{n,m} \right)$. Now the last step to obtain the system model in (3.4) consists in applying a *change of basis* operation [WGJ14]:

$$\mathbf{H}_{j,i} = \text{CoB}(\hat{\mathbf{H}}_{j,i}) = \boldsymbol{\Xi}_j \hat{\mathbf{H}}_{j,i} \boldsymbol{\Theta}_i, \quad (4.8)$$

where $\boldsymbol{\Xi}_j \in \mathbb{R}^{2\tau(M+1) \times 2\tau(M+1)}$ and $\boldsymbol{\Theta}_i \in \mathbb{R}^{2\tau M \times 2\tau M}$ are invertible linear transformations applied at the transmitters and the receivers. This way the resulting equivalent channel becomes a rotation of $\hat{\mathbf{H}}_{j,i}$ that contains zeros at some specific antenna elements, see [WGJ14] for details.

In our case, the same CoB as in [WGJ14] is applied, as well as some additional operations at the receiver side described in Appendix A. This way channel matrices present a simplified structure which helps in the precoding design based on SAC, as well as the achievability proof.

Remark: Notice that matrices $\boldsymbol{\Xi}_j$ and $\boldsymbol{\Theta}_i$ are applied at the transmitter and the receiver, respectively. Therefore, the final linear filters at TX_i and RX_j are $\mathbf{W}_j \boldsymbol{\Xi}_j$ and $\boldsymbol{\Theta}_i \mathbf{V}_i$, respectively.

4.2.3 Problem Formulation

The objective of this chapter is to show that for the 3-user MIMO IC with antenna ratio $\rho = \frac{M}{M+1}$,

$$d_j^{(\text{in})} \stackrel{(a)}{=} \frac{\rho}{\rho + 1} \stackrel{(b)}{=} d_j^{(\text{lin})} = d_j \stackrel{(c)}{=} d_j^{(\text{out})}, \quad (4.9)$$

While equality (c) above was previously proved using rational IA, here we specifically prove equality (a), i.e. the achievable DoF. Then, since $d_j^{(\text{in})}$ match d_j , equality (b) follows, thus the channel DoF may be attained by means of linear strategies. The achievable DoF value is proved by proposing a transmission scheme where $b = 2M(M + 1)$ real-valued symbols per user are delivered along 2τ equivalent channel uses thanks to the use of ACS during $\tau = 2M + 1$ time slots.

In this case, $\mathbf{z}_j = \mathbf{y}_j$ (see (2.8)) since there is only one phase, thus $\mathbf{U}_j = \mathbf{I}$, and all the receive processing is carried out by the global filter \mathbf{W}_j . The objective of this filter is to remove the interference by projecting onto its orthogonal subspace, but without reducing the rank of the desired signals. To this end, it is necessary that desired and interference subspaces are linearly independent. Moreover, it is required that the rank of the desired signals before and after projection is equal to b , if linear feasibility is to be ensured. In this regard, let us denote

$$I = \text{rank}(\Omega_j^{\text{int}}), \quad D = \text{rank}(\Omega_j^{\text{des}}) \leq b, \quad (4.10)$$

where Ω_j^{des} and Ω_j^{int} were introduced in (2.15), and define matrices $\bar{\Omega}_j^{\text{des}} \in \mathbb{R}^{2\tau(M+1) \times D}$ and $\bar{\Omega}_j^{\text{int}} \in \mathbb{R}^{2\tau(M+1) \times I}$ such that

$$\text{span}(\bar{\Omega}_j^{\text{des}}) = \text{span}(\Omega_j^{\text{des}}), \quad \text{span}(\bar{\Omega}_j^{\text{int}}) = \text{span}(\Omega_j^{\text{int}}), \quad (4.11)$$

i.e. basis of Ω_j^{des} and Ω_j^{int} , respectively, as well as

$$\bar{\Omega}_j = [\bar{\Omega}_j^{\text{des}} \quad \bar{\Omega}_j^{\text{int}}] \in \mathbb{R}^{2\tau(M+1) \times (D+I)}. \quad (4.12)$$

When using SAC for the case $N = M + 1$, it turns out that $D + I = (M + 1)\tau$, thus $\bar{\Omega}_j$ is a square matrix. Then, a sufficient condition to ensure linear independence between desired and interference subspaces is that the SSM in (4.12) is full-rank with probability one for any possible channel realization.

4.3 The (2, 3) Case

This section characterizes the linear DoF of the (2, 3) constant MIMO IC. The proposed precoding scheme allows each transmitter to deliver $b = 12$ real-valued symbols to its intended receiver along $2\tau = 10$ equivalent channel uses, thus attaining the DoF outer bound of $6/5$ in (4.9). First, the precoding matrices are obtained for this antenna deployment in Section 4.3.1, designed according to minorly modified conditions from the ones shown in (3.14). Next, Section 4.3.2 derives the SSM $\bar{\Omega}_j$ in (4.12), providing the achievability proof for the proposed precoding scheme.

4.3.1 Precoding Matrix Design

According to definitions (4.1) and (4.2), each precoding matrix can be written as

$$\mathbf{V}_i = [\mathbf{V}_i^1 \quad \mathbf{V}_i^2] \boldsymbol{\Pi}_i, \quad \mathbf{V}_i^k = \begin{bmatrix} \mathbf{V}_i^{k,1} \\ \mathbf{V}_i^{k,2} \end{bmatrix}, \quad (4.13)$$

with $\mathbf{V}_i \in \mathbb{R}^{20 \times 12}$, $\mathbf{V}_i^k \in \mathbb{R}^{20 \times 6}$, $\mathbf{V}_i^{k,q} \in \mathbb{R}^{10 \times 6}$, $\boldsymbol{\Pi}_i \in \mathbb{R}^{6 \times 6}$. Notice that for ease of notation the second subindex (u) appearing in (4.1) has been dropped. From (3.14), the three

alignment chains follow. Let us focus on the first alignment chain, given by

$$[\mathbf{H}_{2,1}, -\mathbf{H}_{2,3}] \begin{bmatrix} \mathbf{V}_1^1 \\ \mathbf{V}_3^1 \end{bmatrix} = \mathbf{0}.$$

By plugging the particular structure of equivalent channels (see Appendix A), it reduces to

$$\begin{bmatrix} \mathbf{C}(h_{2,1}^{1,1}) & \mathbf{0} & \mathbf{0} & \mathbf{0} \\ \mathbf{0} & \mathbf{C}(h_{2,1}^{2,2}) & \mathbf{C}(h_{2,3}^{2,1}) & \mathbf{0} \\ \mathbf{0} & \mathbf{0} & \mathbf{0} & \mathbf{C}(h_{2,3}^{3,2}) \end{bmatrix} \begin{bmatrix} \mathbf{V}_1^{1,1} \\ \mathbf{V}_1^{1,2} \\ \mathbf{V}_3^{1,1} \\ \mathbf{V}_3^{1,2} \end{bmatrix} = \mathbf{0}.$$

Using properties in (4.6) and taking into account that non-zero blocks are full-rank with probability one, since channels are drawn from a continuous distribution, one obtains

$$\mathbf{V}_1^{1,1} = \mathbf{0}, \quad \mathbf{V}_3^{1,1} = \mathbf{C}\left(\frac{h_{2,1}^{2,2}}{h_{2,3}^{2,1}}\right)\mathbf{V}_1^{1,2}, \quad \mathbf{V}_3^{1,2} = \mathbf{0}.$$

The other alignment chains are similarly solved, thus at the end we have

$$\begin{aligned} \mathbf{V}_1 &= \begin{bmatrix} \mathbf{0} & \mathbf{C}\left(\frac{h_{3,2}^{2,2}}{h_{3,1}^{2,1}}\right)\mathbf{V}_2^{1,2} \\ \mathbf{V}_1^{1,2} & \mathbf{0} \end{bmatrix} \boldsymbol{\Pi}_1, \quad \mathbf{V}_2 = \begin{bmatrix} \mathbf{0} & \mathbf{C}\left(\frac{h_{1,3}^{2,2}}{h_{12}^{2,1}}\right)\mathbf{V}_3^{2,2} \\ \mathbf{V}_2^{1,2} & \mathbf{0} \end{bmatrix} \boldsymbol{\Pi}_2, \\ \mathbf{V}_3 &= \begin{bmatrix} \mathbf{C}\left(\frac{h_{2,1}^{2,2}}{h_{2,3}^{2,1}}\right)\mathbf{V}_1^{1,2} & \mathbf{0} \\ \mathbf{0} & \mathbf{V}_3^{2,2} \end{bmatrix} \boldsymbol{\Pi}_3. \end{aligned}$$

Now we will make use of the permutation matrices $\boldsymbol{\Pi}_i$ in order to obtain the same structure for all precoding matrices. Notice that reordering the columns of the precoders does not affect to the interference alignment. Furthermore, notice that there are only three non-zero precoding sub-blocks. Hereafter, they will be referred to as the *support precoding blocks* (SPBs) and denoted as $\mathbf{T}_1, \mathbf{T}_2$ and \mathbf{T}_3 . Therefore, the j th precoding matrix for $j = 1, 2, 3$ generally writes as follows:

$$\mathbf{V}_j = \begin{bmatrix} \mathbf{C}\left(\frac{h_{j-1,j+1}^{2,2}}{h_{j-1,j}^{2,1}}\right)\mathbf{T}_{j+1} & \mathbf{0} \\ \mathbf{0} & \mathbf{T}_j \end{bmatrix}. \quad (4.14)$$

4.3.2 Achievability Proof

This section derives the SSM $\bar{\boldsymbol{\Omega}}_j$ as a function of the SPBs $\mathbf{T}_1, \mathbf{T}_2$, and \mathbf{T}_3 . Then, a design for those matrices is proposed easing the achievability proof, formalized in Theorem 4.2, and based on Lemma 4.1, both presented at the end of this section.

$$\bar{\Omega}_j = \begin{bmatrix} \mathbf{C}(h_{j,j}^{1,1}) \mathbf{T}_{j+1} & \mathbf{C}(h_{j,j}^{1,2}) \mathbf{T}_j & \mathbf{C}\left(\frac{h_{j,j-1}^{1,1} h_{j+1,j}^{2,2}}{h_{j+1,j-1}^{2,1}}\right) \mathbf{T}_j & \mathbf{0} & \mathbf{0} \\ \mathbf{C}(h_{j,j}^{2,1}) \mathbf{T}_{j+1} & \mathbf{C}(h_{j,j}^{2,2}) \mathbf{T}_j & \mathbf{0} & \mathbf{C}(h_{j,j-1}^{2,2}) \mathbf{T}_{j-1} & \mathbf{0} \\ \mathbf{C}(h_{j,j}^{3,1}) \mathbf{T}_{j+1} & \mathbf{C}(h_{j,j}^{3,2}) \mathbf{T}_j & \mathbf{0} & \mathbf{0} & \mathbf{C}(h_{j,j+1}^{3,2}) \mathbf{T}_{j+1} \end{bmatrix} \quad (4.15)$$

For the proper derivation of the SSM, let us compute

$$\mathbf{H}_{j,j+1} \mathbf{V}_{j+1} = \begin{bmatrix} \mathbf{0} & \mathbf{0} \\ \mathbf{C}(h_{j,j-1}^{2,2}) \mathbf{T}_{j-1} & \mathbf{0} \\ \mathbf{0} & \mathbf{C}(h_{j,j+1}^{3,2}) \mathbf{T}_{j+1} \end{bmatrix}, \quad (4.16)$$

$$\mathbf{H}_{j,j-1} \mathbf{V}_{j-1} = \begin{bmatrix} \mathbf{C}\left(\frac{h_{j,j-1}^{1,1} h_{j+1,j}^{2,2}}{h_{j+1,j-1}^{2,1}}\right) \mathbf{T}_j & \mathbf{0} \\ \mathbf{0} & \mathbf{C}(h_{j,j-1}^{2,2}) \mathbf{T}_{j-1} \\ \mathbf{0} & \mathbf{0} \end{bmatrix}, \quad (4.17)$$

defining the subspaces of received interference at RX_j, see (4.12). Notice that the first block column of (4.16) is aligned with the last block column of (4.17), which is actually forced by the (j + 1)th alignment chain. As a result, the basis for the interference space $\bar{\Omega}_j^{\text{int}}$ is defined by the three linearly independent block columns of (4.16)-(4.17), and the SSM $\bar{\Omega}_j$ may be written as in (4.15).

The SSM in (4.15) is similar to the equivalent matrix obtained in [WGJ11, Equation 16]. Even though in this case the full-rank condition for the SSM can be ensured by picking entries of the SPBs randomly (as pointed out by [WGJ11]), we next present a formal proof that is also useful for the $M > 2$ case.

To this end, define $\boldsymbol{\lambda}_i^j \in \mathbb{R}^{6 \times 1}$, $i = 1 \dots 5$, $j = 1, 2, 3$, hereafter referred to as the *rank descriptors*. Then, one may ensure that the SSM is full-rank iff the only solution for

$$\bar{\Omega}_j \left[(\boldsymbol{\lambda}_1^j)^T \dots (\boldsymbol{\lambda}_5^j)^T \right]^T = \mathbf{0} \quad (4.18)$$

is to set all rank descriptors to zero. To this end, let also define an arbitrary orthonormal basis $\mathbf{F} = [\mathbf{f}_1 \mathbf{f}_2 \dots \mathbf{f}_{10}] \in \mathbb{R}^{10 \times 10}$. We propose the following design:

$$\begin{aligned} \mathbf{T}_1 &= [\mathbf{F}_{1:2} \quad \mathbf{F}_{3:5} \quad \mathbf{F}_6], \quad \mathbf{T}_2 = [\mathbf{F}_{1:2} \quad \mathbf{F}_{7:9} \quad \mathbf{F}_{10}], \\ \mathbf{T}_3 &= [\mathbf{F}_{3:5} \quad \mathbf{F}_{7:9}], \end{aligned} \quad (4.19)$$

where $\mathbf{F}_{p:q}$ takes all columns of \mathbf{F} from p to q . The following lemma states the DoF achievability:

Lemma 4.1 ($\bar{\Omega}_j$ full-rank for $M = 2$). *Considering (4.15) and the SPBs chosen as in (4.19), then the only possible solution for (4.18) is $\boldsymbol{\lambda}_i^j = \mathbf{0}, \forall i, j$.*

Proof: See Appendix B. □

Finally, the optimal DoF are settled by means of Theorem 4.2, next stated:

Theorem 4.2 (DoF for the $(2,3)$ case). *The 3-user $(2,3)$ MIMO IC with constant channel coefficients has exactly $2/5$ spatially-normalized linear DoF per user.*

Proof: Each user transmits $b = 12$ real-valued symbol streams along $\tau = 5$ time slots, considering ACS, and the described precoding scheme. According to Lemma 4.1, the SSM defined in (4.15) is full-rank, thus interference and desired signals become linearly independent, and the desired symbols can linearly be decoded. Since the DoF outer bound in (4.9) and the achievable DoF attained by the proposed scheme match, this value corresponds to the optimal linear DoF. \square

4.4 The $(M, M + 1)$ Case with $M > 2$

This section addresses the $(M, M + 1)$ MIMO IC with constant channel coefficients and $M \geq 3$. The proposed precoding scheme allows each user to obtain $b = 2M(M + 1)$ real-valued data symbols over $2\tau = 2(2M + 1)$ equivalent channel uses, thus attaining the DoF outer bound of $\frac{\rho}{\rho+1}$ in (4.9).

Unfortunately, the number of conditions used for the precoder design, see (3.14), increases proportionally to M^2 . Therefore, the approach used for the $M = 2$ case gets complicated as M grows. This section presents a methodology to simplify the resolution of such matrix equation system, which will be illustrated for the $M = 3$ case. The core of this methodology is the *zero propagation algorithm*, to be presented next, which allows to obtain the structure of the transmit and receive filters for any value of M .

4.4.1 Precoding Matrix Design

Out of the three alignment chains, let us consider the first alignment chain ($k = 1$) given by (4.21), shown at the top of the next page. The remaining alignment chains are handled similarly.

Thanks to the obtained structure of matrix \mathbf{E} , one observes that some sub-blocks of \mathbf{J} are forced to be zero. For example, consider the fifth block row element of $\mathbf{E} \cdot \mathbf{J}$:

$$\mathbf{C}(h_{1,3}^{1,1})\mathbf{V}_{3,(1)}^{1,1} = \mathbf{0}. \quad (4.20)$$

Clearly, the only solution above is $\mathbf{V}_{3,(1)}^{1,1} = \mathbf{0}$ with probability one. Hence, other equations where this variable participates are simplified. Each of these events is denoted as a *zero propagation* (ZP) and give the possibility of finding which blocks are zero for \mathbf{J} in (4.21). Inspired by this idea, we present the ZP algorithm, see Algorithm 4.1¹. This algorithm allows simplifying the alignment chain conditions in (4.21), reducing the number of blocks to be designed in (4.22). Moreover, by writing the remaining equations it turns out that

¹We use Matlab notation to simplify the description of the algorithm. The function `zeros(p, q)` produces an all-zeros $p \times q$ matrix, while $\mathbf{E}(p, :)$ and $\mathbf{E}(:, q)$ refer to the p th row and the q th column, respectively, of matrix \mathbf{E} .

$$\begin{bmatrix} \mathbf{C}(h_{2,1}^{1,1}) & \mathbf{0} \\ \mathbf{0} & \mathbf{C}(h_{2,1}^{2,2}) & \mathbf{C}(h_{2,1}^{2,3}) & \mathbf{C}(h_{2,3}^{2,1}) & \mathbf{0} & \mathbf{0} & \mathbf{0} & \mathbf{0} & \mathbf{0} \\ \mathbf{0} & \mathbf{0} & \mathbf{C}(h_{2,1}^{3,3}) & \mathbf{C}(h_{2,3}^{3,1}) & \mathbf{C}(h_{2,3}^{3,2}) & \mathbf{0} & \mathbf{0} & \mathbf{0} & \mathbf{0} \\ \mathbf{0} & \mathbf{0} & \mathbf{0} & \mathbf{0} & \mathbf{0} & \mathbf{C}(h_{2,3}^{4,3}) & \mathbf{0} & \mathbf{0} & \mathbf{0} \\ \mathbf{0} & \mathbf{0} & \mathbf{0} & \mathbf{C}(h_{1,3}^{1,1}) & \mathbf{0} & \mathbf{0} & \mathbf{0} & \mathbf{0} & \mathbf{0} \\ \mathbf{0} & \mathbf{0} & \mathbf{0} & \mathbf{0} & \mathbf{C}(h_{1,3}^{2,2}) & \mathbf{C}(h_{1,3}^{2,3}) & \mathbf{C}(h_{1,2}^{2,1}) & \mathbf{0} & \mathbf{0} \\ \mathbf{0} & \mathbf{0} & \mathbf{0} & \mathbf{0} & \mathbf{0} & \mathbf{C}(h_{1,3}^{3,3}) & \mathbf{C}(h_{1,2}^{3,1}) & \mathbf{C}(h_{1,2}^{3,2}) & \mathbf{0} \\ \mathbf{0} & \mathbf{C}(h_{1,2}^{4,3}) \end{bmatrix} \begin{bmatrix} \mathbf{V}_{1,(1)}^{1,1} \\ \mathbf{V}_{1,(1)}^{1,2} \\ \mathbf{V}_{1,(1)}^{1,3} \\ \mathbf{V}_{3,(1)}^{1,1} \\ \mathbf{V}_{3,(1)}^{1,2} \\ \mathbf{V}_{3,(1)}^{1,3} \\ \mathbf{V}_{2,(1)}^{1,1} \\ \mathbf{V}_{2,(1)}^{1,2} \\ \mathbf{V}_{2,(1)}^{1,3} \end{bmatrix} = \mathbf{0}$$

$\mathbf{E} \cdot \mathbf{J} = \mathbf{0}$ (4.21)

$$\begin{bmatrix} \mathbf{C}(h_{2,1}^{2,2}) & \mathbf{C}(h_{2,1}^{2,3}) & \mathbf{0} & \mathbf{0} & \mathbf{0} \\ \mathbf{0} & \mathbf{C}(h_{2,1}^{3,3}) & \mathbf{C}(h_{2,3}^{3,2}) & \mathbf{0} & \mathbf{0} \\ \mathbf{0} & \mathbf{0} & \mathbf{C}(h_{1,3}^{2,2}) & \mathbf{C}(h_{1,2}^{2,1}) & \mathbf{0} \\ \mathbf{0} & \mathbf{0} & \mathbf{0} & \mathbf{C}(h_{1,2}^{3,1}) & \mathbf{C}(h_{1,2}^{3,2}) \end{bmatrix} \begin{bmatrix} \mathbf{V}_{1,(1)}^{1,2} \\ \mathbf{V}_{1,(1)}^{1,3} \\ \mathbf{V}_{3,(1)}^{1,2} \\ \mathbf{V}_{3,(1)}^{1,1} \\ \mathbf{V}_{2,(1)}^{1,1} \\ \mathbf{V}_{2,(1)}^{1,2} \end{bmatrix} = \mathbf{0} (4.22)$$

Algorithm 4.1: Zero Propagation

Consider the matrix equation system given by $\mathbf{E} \cdot \mathbf{J} = \mathbf{0}$, with $\mathbf{J} \in \mathbb{R}^{J_{\text{BR}} \cdot J_{\text{R}} \times J_{\text{BC}}}$ and $\mathbf{E} \in \mathbb{R}^{E_{\text{BR}} \cdot E_{\text{R}} \times J_{\text{BR}} \cdot J_{\text{R}}}$, where $J_{\text{R}} (E_{\text{R}})$ defines the number of block rows of \mathbf{J} (\mathbf{E}). Moreover, J_{BC} (J_{BR}) defines the size of each block column (row) \mathbf{J} , and E_{BR} defines the size of each block row of \mathbf{E} . The blocks of \mathbf{J} that can be set to zero may be obtained by computing the following steps:

Step 1: Find one block row in \mathbf{E} containing only one non-zero element, located at the $[\alpha, \beta]$ th block position.

Step 2: Set $\begin{cases} \mathbf{E}(\alpha, :) = \text{zeros}(E_{\text{BR}}, J_{\text{BR}} \cdot J_{\text{R}}) \\ \mathbf{E}(:, \beta) = \text{zeros}(E_{\text{BR}} \cdot E_{\text{R}}, J_{\text{BR}}) \end{cases}$

Step 3: Set $\mathbf{J}(\beta, :) = \text{zeros}(J_{\text{BR}}, J_{\text{BC}})$.

Step 4: Repeat Steps 1-3 until Step 1 provides no more block rows.

Step 5: Remove the all-zeros block columns and all-zeros block rows in \mathbf{E} and \mathbf{J} .

each precoding matrix can be written as a function of three SPBs, as follows:

$$\mathbf{V}_i = \begin{bmatrix} \mathbf{C}(\theta_{i,(1)}^{i-1,1}) \mathbf{T}_{i-1} & \mathbf{0} & \mathbf{0} \\ \mathbf{C}(\theta_{i,(1)}^{i-1,2}) \mathbf{T}_{i-1} & \mathbf{C}(\theta_{i,(1)}^{i+1,2}) \mathbf{T}_{i+1} & \mathbf{C}(\theta_{i,(1)}^{i,2}) \mathbf{T}_i \\ \mathbf{0} & \mathbf{0} & \mathbf{T}_i \end{bmatrix}, \quad (4.23)$$

where $\theta_{i,(1)}^{q,r}$ stands for the complex value obtained from the q th alignment chain and located at the r th block row of \mathbf{V}_i . They can be obtained by computing a null space basis from (4.22). Note that the number of unknown sub-block matrices per precoding matrix is reduced from 9 to 1. In general, the $3M^2$ variables (sub-blocks) involved in the alignment chains can be written as in (4.23) as a function of the three SPBs $\mathbf{T}_i \in \mathbb{C}^{2(2M+1) \times 2(M+1)}$, $i = 1, 2, 3$. Hence, after applying the ZP algorithm the problem reduces to the design of the three SPBs.

4.4.2 Achievability Proof

This section derives the SSM for the $M = 3$ case, and generalizes the ideas for $M > 3$. First, a design for the three SPBs in (4.23) is proposed, generalizing (4.19) for any value of M . Second, the SSM is shown to be full-rank, allowing to state the optimal linear DoF by means of Theorem 4.4, presented at the end of this section.

In order to build $\bar{\Omega}_j$, it is necessary to compute a basis for the sum space defined by the received interference and desired signals. Regarding the desired signals, it can be easily seen that $\bar{\Omega}_j^{\text{des}} = \mathbf{H}_{j,j} \mathbf{V}_j$. On the other hand, since some of the interference is aligned it is necessary to first calculate the products $\mathbf{H}_{j,j-1} \mathbf{V}_{j-1}$ and $\mathbf{H}_{j,j+1} \mathbf{V}_{j+1}$. Next, we will see that this task can be highly alleviated. Note that the ZP algorithm output in (4.22) not only states which sub-blocks of each \mathbf{V}_i are actually zero, but also which conditions should be satisfied by the remaining sub-blocks. For example, (4.22) forces

$$\mathbf{C}(h_{2,1}^{2,2}) \mathbf{V}_{1,(1)}^{1,2} + \mathbf{C}(h_{2,1}^{2,3}) \mathbf{V}_{1,(1)}^{1,3} = \mathbf{0}. \quad (4.24)$$

Interestingly, this is indeed one of the elements resulting from the product $\mathbf{H}_{2,1} \mathbf{V}_1$. Taking into account all other conditions where there are only elements managed by one unique transmitter, the products $\mathbf{H}_{j,j-1} \mathbf{V}_{j-1}$ and $\mathbf{H}_{j,j+1} \mathbf{V}_{j+1}$ can be further simplified, obtaining (4.25)-(4.26), where $\bar{\theta}_{j,i}^{q,r}$ is the corresponding complex number for the (q,r) th position of $\mathbf{H}_{j,i} \mathbf{V}_i$, $i \neq j$. Note that in this case due to alignment conditions, we will have $\bar{\theta}_{j,j-1}^{q,q} = \bar{\theta}_{j,j+1}^{q,q-1}$ with $q = 2, 3$, i.e. columns $\{2, 3\}$ of $\mathbf{H}_{j,j+1} \mathbf{V}_{j+1}$ are aligned with columns $\{1, 2\}$ of $\mathbf{H}_{j,j-1} \mathbf{V}_{j-1}$, respectively. Therefore, in this case the SSM is given by (4.27)-(4.28), where $\Omega_j^{\text{des}}(q, r)$ and $\hat{\theta}_j^{q,r}$ are the matrix and the complex number corresponding to the (q,r) th block position of $\bar{\Omega}_j^{\text{des}}$ and $\bar{\Omega}_j^{\text{int}}$, respectively. For Ω_j^{des} , we write the blocks $\Omega_j^{\text{des}}(q, r)$, because they are linear combinations of some extended channel elements, e.g.

$$\Omega_j^{\text{des}}(1, 2) = \mathbf{C}(h_{1,1}^{1,1}) - \mathbf{C}\left(\frac{h_{1,1}^{2,2} h_{3,1}^{3,1}}{h_{3,1}^{3,2}}\right).$$

In contrast to (4.15), now it is not clear if the SSM for this case is full-rank by just taking the SPBs randomly. Next, we provide the proof to verify that $\bar{\Omega}_j$ is full-rank. All

$$\mathbf{H}_{j,j-1} \mathbf{V}_{j-1} = \begin{bmatrix} \mathbf{C}(\bar{\theta}_{j,j-1}^{1,1}) \mathbf{T}_{j+1} & \mathbf{0} & \mathbf{0} \\ \mathbf{C}(\bar{\theta}_{j,j-1}^{2,1}) \mathbf{T}_{j+1} & \mathbf{C}(\bar{\theta}_{j,j-1}^{2,2}) \mathbf{T}_j & \mathbf{0} \\ \mathbf{0} & \mathbf{0} & \mathbf{C}(\bar{\theta}_{j,j-1}^{3,3}) \mathbf{T}_{j-1} \\ \mathbf{0} & \mathbf{0} & \mathbf{0} \end{bmatrix} \quad (4.25)$$

$$\mathbf{H}_{j,j+1} \mathbf{V}_{j+1} = \begin{bmatrix} \mathbf{0} & \mathbf{0} & \mathbf{0} \\ \mathbf{C}(\bar{\theta}_{j,j+1}^{2,1}) \mathbf{T}_j & \mathbf{0} & \mathbf{0} \\ \mathbf{0} & \mathbf{C}(\bar{\theta}_{j,j+1}^{3,2}) \mathbf{T}_{j-1} & \mathbf{C}(\bar{\theta}_{j,j+1}^{3,3}) \mathbf{T}_{j+1} \\ \mathbf{0} & \mathbf{0} & \mathbf{C}(\bar{\theta}_{j,j+1}^{4,3}) \mathbf{T}_{j+1} \end{bmatrix} \quad (4.26)$$

$$\bar{\Omega}_j^{\text{des}} = \begin{bmatrix} \Omega_j^{\text{des}}(1,1) \mathbf{A}_{j-1} & \Omega_j^{\text{des}}(1,2) \mathbf{A}_{j+1} & \Omega_j^{\text{des}}(1,3) \mathbf{A}_j \\ \Omega_j^{\text{des}}(2,1) \mathbf{A}_{j-1} & \Omega_j^{\text{des}}(2,2) \mathbf{A}_{j+1} & \Omega_j^{\text{des}}(2,3) \mathbf{A}_j \\ \Omega_j^{\text{des}}(3,1) \mathbf{A}_{j-1} & \Omega_j^{\text{des}}(3,2) \mathbf{A}_{j+1} & \Omega_j^{\text{des}}(3,3) \mathbf{A}_j \\ \Omega_j^{\text{des}}(4,1) \mathbf{A}_{j-1} & \Omega_j^{\text{des}}(4,2) \mathbf{A}_{j+1} & \Omega_j^{\text{des}}(4,3) \mathbf{A}_j \end{bmatrix} \quad (4.27)$$

$$\bar{\Omega}_j^{\text{int}} = \begin{bmatrix} \mathbf{C}(\hat{\theta}_j^{1,1}) \mathbf{A}_{j+1} & \mathbf{0} & \mathbf{0} & \mathbf{0} \\ \mathbf{C}(\hat{\theta}_j^{2,1}) \mathbf{A}_{j+1} & \mathbf{C}(\hat{\theta}_j^{2,2}) \mathbf{A}_j & \mathbf{0} & \mathbf{0} \\ \mathbf{0} & \mathbf{0} & \mathbf{C}(\hat{\theta}_j^{2,3}) \mathbf{A}_{j-1} & \mathbf{C}(\hat{\theta}_j^{2,4}) \mathbf{A}_{j+1} \\ \mathbf{0} & \mathbf{0} & \mathbf{0} & \mathbf{C}(\hat{\theta}_j^{3,4}) \mathbf{A}_{j+1} \end{bmatrix} \quad (4.28)$$

vectors and matrices are defined for a general value of M , and all possible procedures are generalized.

As for the (2,3) case, the SSM may be shown to be full-rank iff the only solution for

$$\bar{\Omega}_j \left[(\boldsymbol{\lambda}_1^j)^T \dots (\boldsymbol{\lambda}_{2M+1}^j)^T \right]^T = \mathbf{0} \quad (4.29)$$

is to set all $\boldsymbol{\lambda}_i^j \in \mathbb{R}^{2(2M+1) \times 1}$, $i = 1 \dots 2M + 1$, $j = 1, 2, 3$ equal to zero. In this regard, define an orthonormal basis $\mathbf{F} = [\mathbf{f}_1, \mathbf{f}_2 \dots \mathbf{f}_{2(2M+1)}] \in \mathbb{R}^{2(2M+1) \times 2(2M+1)}$ and

$$\begin{aligned} \mathcal{X}_1 &= \{3, 4, \dots, M + 3\}, \\ \mathcal{X}_2 &= \{M + 4, M + 5, \dots, 2M + 2\}, \\ \mathcal{Y}_1 &= \{2M + 3, \dots, 3M + 3\}, \\ \mathcal{Y}_2 &= \{3M + 4, \dots, 4M + 2\}, \\ \mathcal{Z} &= \{1, 2\}. \end{aligned} \quad (4.30)$$

Hereafter, we use these sets to arrange columns of \mathbf{F} , e.g. $\mathbf{F}_{\mathcal{X}_2} = \mathbf{F}_{M+4:2M+2}$. Accordingly,

we set:

$$\begin{aligned}\mathbf{T}_1 &= [\mathbf{F}_{\mathcal{Z}} \quad \mathbf{F}_{\mathcal{X}_1} \quad \mathbf{F}_{\mathcal{X}_2}], \quad \mathbf{T}_2 = [\mathbf{F}_{\mathcal{Z}} \quad \mathbf{F}_{\mathcal{Y}_1} \quad \mathbf{F}_{\mathcal{Y}_2}], \\ \mathbf{T}_3 &= [\mathbf{F}_{\mathcal{X}_1} \quad \mathbf{F}_{\mathcal{Y}_1}].\end{aligned}\tag{4.31}$$

Given these definitions, the following lemma states the DoF achievability:

Lemma 4.3 ($\bar{\Omega}_j$ full-rank for $M < 6$). *For the $3 \leq M \leq 6$ cases, the SSM defined as in (4.27)-(4.28) with SPBs chosen as in (4.31) is full-rank with probability one.*

Proof: See Appendix C. \square

Finally, the DoF characterization for $M = 3, 4, 5, 6$ follows from Lemma 4.3, and it is formalized as follows:

Theorem 4.4 (DoF of the $(M, M+1)$ IC, $M = 3, 4, 5, 6$). *The 3-user $(M, M+1)$ MIMO IC with $M = 3, 4, 5, 6$ and constant channel coefficients has exactly $\frac{\rho}{\rho+1}$ spatially-normalized linear DoF per user.*

Proof: The proof is analogous to the proof of Theorem 4.2. In general, the optimal linear DoF are achieved by using the proposed transmission scheme, delivering $b = 2M(M+1)$ symbol streams to each user along $2\tau = 2(2M+1)$ equivalent channel uses. \square

Remark: Due to the similarity of the different cases, but the difficulty of generalization, only the cases $M = 2, 3, 4, 5, 6$ have been analytically proved. Nonetheless, based on the explained methodology and some numerical results (see next section), we conjecture that the full-rank SSMs are obtained for $M > 6$, and hence the optimal DoF can be attained and proved:

Conjecture 4.5 (DoF for the general $(M, M+1)$ IC). *The 3-user $(M, M+1)$ MIMO IC with constant channel coefficients has exactly $\frac{M(M+1)}{2M+1}$ linear DoF per user for $M > 6$, and they can be achieved by means of the proposed multi-slot transmission designed using SAC and ACS.*

4.5 Numerical Results

In order to validate the contributions of this work, as well as increase the strength of Conjecture 4.5, we simulate the cases $M = 2, 3, 5, 6, 8, 9$ for the 3-user MIMO IC. Two schemes are simulated, the one proposed in this chapter, and the design in [WGJ14] not considering ACS. In both cases, we apply the CoB operation and the additional transformations explained in Appendix A. Results are shown in Fig. 4.1, where solid/dashed lines denote the two schemes with/without ACS. It can be seen that the former improves the slope achieved at high SNR for each case. Moreover, for the cases $M > 6$ simulated, the slope at high SNR follows Conjecture 4.5.

4.6 Conclusion

This work has investigated the linear DoF of the 3-user $(M, M+1)$ MIMO Interference Channel with constant channel coefficients and full channel state information at both

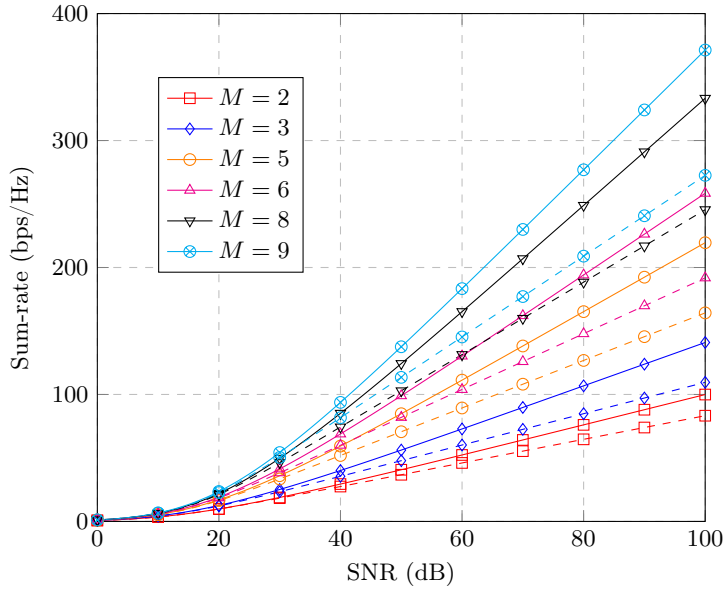


Figure 4.1: Comparison of using a multi-slot transmission based on SAC and ACS (solid lines) w.r.t. not using ACS (dashed lines).

sides. By means of the proposed precoding scheme, the optimal linear DoF achievability has been proved for the cases $M = 2 \dots 6$. Moreover, a methodology has been presented easing the proof for the cases $M > 6$, where we conjecture that the optimal linear DoF can also be attained. This conjecture has been numerically checked.

The contribution of this part of the dissertation has been twofold. On the one hand, we have shown that the use of asymmetric complex signaling together with the previous state-of-the-art approach in [WGJ14] allows characterizing the linear DoF of this channel. Therefore, we have provided a formal proof, and uncoupled the achievability statement from numerical experiments. On the other hand, our results revealed that, except for the SISO case, the channel DoF can be achieved using either linear or rational IA.

Appendix

A Additional Change of Basis at the Receiver Side

The CoB operation [WGJ14] is a tool that provides a predetermined structure for the cross-channel matrices. In particular, it forces zeros at some specific antenna elements. For example, the equivalent cross-channel matrices $\{\bar{\mathbf{H}}_{j,j-1}, \bar{\mathbf{H}}_{j,j+1}\}$ for $M = 3$ after performing the original CoB described in [WGJ14] are given by

$$[\bar{\mathbf{H}}_{j,j-1}, \bar{\mathbf{H}}_{j,j+1}] = \begin{bmatrix} \mathbf{C}(\bar{h}_{j,j-1}^{1,1}) & \mathbf{0} & \mathbf{0} & \mathbf{0} & \mathbf{0} & \mathbf{0} \\ \mathbf{C}(\bar{h}_{j,j-1}^{2,1}) & \mathbf{C}(\bar{h}_{j,j-1}^{2,2}) & \mathbf{C}(\bar{h}_{j,j-1}^{2,3}) & \mathbf{C}(\bar{h}_{j,j+1}^{2,1}) & \mathbf{0} & \mathbf{C}(\bar{h}_{j,j+1}^{2,3}) \\ \mathbf{C}(\bar{h}_{j,j-1}^{3,1}) & \mathbf{0} & \mathbf{C}(\bar{h}_{j,j-1}^{3,3}) & \mathbf{C}(\bar{h}_{j,j+1}^{3,1}) & \mathbf{C}(\bar{h}_{j,j+1}^{3,2}) & \mathbf{C}(\bar{h}_{j,j+1}^{3,3}) \\ \mathbf{0} & \mathbf{0} & \mathbf{0} & \mathbf{0} & \mathbf{0} & \mathbf{C}(\bar{h}_{j,j+1}^{4,3}) \end{bmatrix}.$$

Here we assume that the CoB at the receiver Θ_j is the product of two matrices: the original CB and an additional combining matrix $\Upsilon_j \in \mathbb{R}^{2\tau(M+1) \times 2\tau(M+1)}$ such that

$$\Upsilon_j [\bar{\mathbf{H}}_{j,j-1}, \bar{\mathbf{H}}_{j,j+1}] = \begin{bmatrix} \mathbf{C}(h_{j,j-1}^{1,1}) & \mathbf{0} & \mathbf{0} & \mathbf{0} & \mathbf{0} & \mathbf{0} \\ \mathbf{0} & \mathbf{C}(h_{j,j-1}^{2,2}) & \mathbf{C}(h_{j,j-1}^{2,3}) & \mathbf{C}(h_{j,j+1}^{2,1}) & \mathbf{0} & \mathbf{0} \\ \mathbf{0} & \mathbf{0} & \mathbf{C}(h_{j,j-1}^{3,3}) & \mathbf{C}(h_{j,j+1}^{3,1}) & \mathbf{C}(h_{j,j+1}^{3,2}) & \mathbf{0} \\ \mathbf{0} & \mathbf{0} & \mathbf{0} & \mathbf{0} & \mathbf{0} & \mathbf{C}(h_{j,j+1}^{4,3}) \end{bmatrix}$$

is satisfied. Then, each block row of $\Upsilon_j = [\mathbf{v}_{j,1}^T, \dots, \mathbf{v}_{j,4}^T]^T$ is derived as follows:

$$\begin{aligned} \mathbf{v}_{j,1} &= [\mathbf{I}_{2\tau} \quad \mathbf{0}], \\ \mathbf{v}_{j,2} &= \text{null}([\bar{\mathbf{H}}_{j,j-1}(:,1), \bar{\mathbf{H}}_{j,j+1}(:,2:3)]), \\ \mathbf{v}_{j,3} &= \text{null}([\bar{\mathbf{H}}_{j,j-1}(:,1:2), \bar{\mathbf{H}}_{j,j+1}(:,3)]), \\ \mathbf{v}_{j,4} &= [\mathbf{0} \quad \mathbf{I}_{2\tau}], \end{aligned}$$

where $\mathbf{A}(:, p : q)$ gives the matrix resulting from picking the entries of \mathbf{A} from block column p to q , and $\mathbf{I}_{2\tau} \in \mathbb{R}^{2\tau \times 2\tau}$, $\mathbf{0} \in \mathbb{R}^{2\tau \times 2\tau M}$ are the identity and all-zero matrices.

B Proof of Lemma 4.1

We will prove the lemma for the system of equations defined for $j = 1$. The cases $j = 2, 3$ can be similarly handled, and they are omitted to avoid redundancy. Therefore, we drop the supraindex j and write $\lambda_i, i = 1, \dots, 5$ to simplify notation. Additionally, some rank-preserving transformations will be applied to $\bar{\Omega}_j$. Consequently, the matrix equation system in (4.18) for $j = 1$ can be written as follows:

$$\mathbf{C}(h_{1,1}^{1,1})\mathbf{T}_2\lambda_1 + \mathbf{T}_1\lambda_3 = \mathbf{0}, \quad (\text{B.1a})$$

$$\mathbf{C}(h_{1,1}^{2,1})\mathbf{T}_2\lambda_1 + \mathbf{C}(h_{1,1}^{2,2})\mathbf{T}_1\lambda_2 + \mathbf{T}_3\lambda_4 = \mathbf{0}, \quad (\text{B.1b})$$

$$\mathbf{C}(h_{1,1}^{3,2})\mathbf{T}_1\lambda_2 + \mathbf{T}_2\lambda_5 = \mathbf{0}, \quad (\text{B.1c})$$

which can be simplified by introducing (4.19), and by means of linear independence among the vectors \mathbf{f}_i , as explained next. For instance, consider all equations corresponding to $\mathbf{F}_{1:2}$ in (B.1), given by:

$$\mathbf{C}(h_{1,1}^{1,1})\mathbf{f}_q\lambda_1(q) + \mathbf{f}_q\lambda_3(q) = \mathbf{0}, \quad (\text{B.2a})$$

$$\mathbf{C}(h_{1,1}^{2,1})\mathbf{f}_q\lambda_1(q) + \mathbf{C}(h_{1,1}^{2,2})\mathbf{f}_q\lambda_2(q) = \mathbf{0}, \quad (\text{B.2b})$$

$$\mathbf{C}(h_{1,1}^{3,2})\mathbf{f}_q\lambda_2(q) + \mathbf{f}_q\lambda_5(q) = \mathbf{0}, \quad (\text{B.2c})$$

with $q = 1, 2$. Each of such equations can be simplified as follows. Let us define:

$$\bar{\mathbf{f}}_q = \begin{bmatrix} f_q(1) + j f_q(2) \\ f_q(3) + j f_q(4) \\ \vdots \\ f_q(9) + j f_q(10) \end{bmatrix} \quad (\text{B.3})$$

where $\mathbf{f}_q = \text{stack}(f_q(1), \dots, f_q(10))$, $j = \sqrt{-1}$ stands here for the imaginary unit, and $q = 1, 2$. Then, as in [CJW10], we can write (B.2) in terms of $\bar{\mathbf{f}}_q$. For instance, (B.2a) can be rewritten as follows:

$$\begin{aligned} \left| h_{1,1}^{1,1} \right| e^{j\phi_{1,1}^{1,1}} \bar{\mathbf{f}}_q \lambda_1(q) + \bar{\mathbf{f}}_q \lambda_3(q) &= \mathbf{0}, \\ \left| h_{1,1}^{1,1} \right| e^{j\phi_{1,1}^{1,1}} \lambda_1(q) + \lambda_3(q) &= 0, \end{aligned} \quad (\text{B.4})$$

with $q = 1, 2$. Hence, equating real and imaginary parts of each equation to zero, we have:

$$\left| h_{1,1}^{1,1} \right| \sin(\phi_{1,1}^{1,1}) \lambda_1(q) = 0, \quad (\text{B.5a})$$

$$\left| h_{1,1}^{1,1} \right| \cos(\phi_{1,1}^{1,1}) \lambda_1(q) + \lambda_3(q) = 0, \quad (\text{B.5b})$$

with $q = 1, 2$. The set containing all the possible values such that $\left| h_{1,1}^{1,1} \right| \sin(\phi_{1,1}^{1,1}) = 0$ is a countable set, thus it has zero measure [CK99]. Then, by randomness arguments the only solution is $\lambda_r(q) = 0, r = 1, 3, q = 1, 2$. Applying this methodology to all equations derived from all groups of columns of \mathbf{F} , one finds out that all rank descriptors are equal to zero.

An alternative way to prove that the rank descriptors associated to $\mathbf{F}_{1:2}$ must be zero is next shown. Instead of developing (B.2a) only, consider all equations in (B.2) in the form of (B.5). Then, equating imaginary parts to zero, we have

$$\begin{bmatrix} \left|h_{1,1}^{1,1}\right| \sin(\phi_{1,1}^{1,1}) & 0 \\ \left|h_{1,1}^{2,1}\right| \sin(\phi_{1,1}^{2,1}) & \left|h_{1,1}^{2,2}\right| \sin(\phi_{1,1}^{2,2}) \\ 0 & \left|h_{1,1}^{3,2}\right| \sin(\phi_{1,1}^{3,2}) \end{bmatrix} \begin{bmatrix} \lambda_1(q) \\ \lambda_2(q) \end{bmatrix} = \mathbf{0}. \quad (\text{B.6})$$

We will refer to the 3×2 matrix at the left-hand side of (B.6) as an *elimination matrix*. As long as we can ensure it has no right null space, all rank descriptors in (B.6) must be set to zero. In this case, this is trivially ensured by means of randomness arguments and the matrix dimensions. Likewise, using the real counterpart of (B.6), we have $\lambda_i(q) = 0, i = 3, 5, q = 1, 2$. By the same rationale applied to each group of columns of \mathbf{F} , we obtain an elimination matrix for each case, and it is easy to check that none of them has right null space, thus all rank descriptors are definitely equal to zero.

So far we have proved that considering ACS is sufficient for achieving a full rank SSM. In what follows, we explain why it is necessary when using the scheme based on alignment chains. To this end, we next write the equivalent set of equations (B.2) in case of employing only symbol extensions in time:

$$h_{1,1}^{1,1} \lambda_1(q) + \lambda_3(q) = 0, \quad (\text{B.7a})$$

$$h_{1,1}^{2,1} \lambda_1(q) + h_{1,1}^{2,2} \lambda_2(q) = 0, \quad (\text{B.7b})$$

$$h_{1,1}^{3,2} \lambda_2(q) + \lambda_5(q) = 0, \quad (\text{B.7c})$$

written in matrix form as

$$\begin{bmatrix} h_{1,1}^{1,1} & 0 & 1 & 0 \\ h_{1,1}^{2,1} & h_{1,1}^{2,2} & 0 & 0 \\ 0 & h_{1,1}^{3,2} & 0 & 1 \end{bmatrix} \begin{bmatrix} \lambda_1(q) \\ \lambda_2(q) \\ \lambda_3(q) \\ \lambda_5(q) \end{bmatrix} = \mathbf{0}, \quad (\text{B.8})$$

with $q = 1, 2$. Note that the matrices $\mathbf{C}(\cdot)$ disappear. This is because when only symbol extensions in time are applied, each channel element becomes a scaled identity matrix, see (4.3). Also, notice that the rank descriptors contain now complex values. Therefore, the elimination matrix is a 3×4 full-row rank matrix having a one-dimensional null space. Consequently, the SSM becomes rank deficient, since there are some rank descriptors different from zero and desired signals cannot be linearly separated from interference.

C Proof of Lemma 4.3

Due to similarity with the proof for $M = 2$, we elaborate a sketch of the proof for $M = 3$ and provide intuition of the proof for cases $M = 4, 5, 6$ by means of examples of its elimination matrices.

The SSM for $M = 3$ is constructed by using (4.25)-(4.26). As before, without loss of generality we consider \mathbf{RX}_1 only. In this case, after applying some full-rank linear transformations to the SSM, the following system of four equations is obtained:

$$\begin{aligned}
& \left[\mathbf{C}(h_{1,1}^{1,1}) - \mathbf{C}(\alpha_{1,1}^{\text{des}}) \right] \mathbf{T}_3 \boldsymbol{\lambda}_1 + \mathbf{C}(h_{1,1}^{1,2}) \mathbf{T}_2 \boldsymbol{\lambda}_2 + \left[\mathbf{C}(h_{1,1}^{1,3}) - \mathbf{C}(\alpha_{1,2}^{\text{des}}) \right] \mathbf{T}_1 \boldsymbol{\lambda}_3 + \mathbf{C}(h_{1,3}^{1,1}) \mathbf{T}_2 \boldsymbol{\lambda}_4 = \mathbf{0}, \\
& \left[\mathbf{C}(h_{1,1}^{2,1}) - \mathbf{C}(\alpha_{2,1}^{\text{des}}) \right] \mathbf{T}_3 \boldsymbol{\lambda}_1 + \mathbf{C}(h_{1,1}^{2,2}) \mathbf{T}_2 \boldsymbol{\lambda}_2 - \mathbf{C}(\alpha_1^{\text{int}}) \mathbf{T}_2 \boldsymbol{\lambda}_4 + \mathbf{T}_1 \boldsymbol{\lambda}_5 = \mathbf{0}, \\
& \mathbf{C}(h_{1,1}^{3,2}) \mathbf{T}_2 \boldsymbol{\lambda}_2 + \left[\mathbf{C}(h_{1,1}^{3,3}) - \mathbf{C}(\alpha_{3,2}^{\text{des}}) \right] \mathbf{T}_1 \boldsymbol{\lambda}_3 + \mathbf{T}_3 \boldsymbol{\lambda}_6 - \mathbf{C}(\alpha_2^{\text{int}}) \mathbf{T}_2 \boldsymbol{\lambda}_7 = \mathbf{0}, \\
& \left[\mathbf{C}(h_{1,1}^{4,1}) - \mathbf{C}(\alpha_{4,1}^{\text{des}}) \right] \mathbf{T}_3 \boldsymbol{\lambda}_1 + \mathbf{C}(h_{1,1}^{4,2}) \mathbf{T}_2 \boldsymbol{\lambda}_2 + \left[\mathbf{C}(h_{1,1}^{4,3}) - \mathbf{C}(\alpha_{4,2}^{\text{des}}) \right] \mathbf{T}_1 \boldsymbol{\lambda}_3 + \mathbf{C}(h_{1,2}^{4,3}) \mathbf{T}_2 \boldsymbol{\lambda}_7 = \mathbf{0},
\end{aligned} \tag{C.1}$$

where the SPBs are chosen as in (4.31), i.e:

$$\mathbf{T}_1 = \begin{bmatrix} \mathbf{F}_{1:2} & \mathbf{F}_{3:6} & \mathbf{F}_{7:8} \end{bmatrix}, \quad \mathbf{T}_2 = \begin{bmatrix} \mathbf{F}_{1:2} & \mathbf{F}_{9:12} & \mathbf{F}_{13:14} \end{bmatrix}, \quad \mathbf{T}_3 = \begin{bmatrix} \mathbf{F}_{3:6} & \mathbf{F}_{9:12} \end{bmatrix},$$

and

$$\begin{aligned}
\alpha_{q,1}^{\text{des}} &= \frac{h_{1,1}^{q,2} h_{3,1}^{3,1}}{h_{3,1}^{3,2}}, & \alpha_{q,2}^{\text{des}} &= \frac{h_{1,1}^{q,2} h_{2,1}^{2,3}}{h_{2,1}^{2,2}}, \\
\alpha_1^{\text{int}} &= \frac{h_{1,3}^{2,2} h_{2,3}^{3,1}}{h_{2,3}^{3,2}}, & \alpha_2^{\text{int}} &= \frac{h_{1,2}^{3,2} h_{3,1}^{2,3}}{h_{3,1}^{2,2}}.
\end{aligned}$$

A full-rank SSM is obtained as long as all rank descriptors $\boldsymbol{\lambda}_i, i = 1, \dots, 7$ are equal to the zero vector. For instance, consider the elimination matrix in (C.2), obtained for the group \mathcal{Z} (see (4.30)) after applying similar steps as in Appendix B, and equating imaginary parts to zero. Notice that this elimination matrix is full rank almost surely, since each row contains at least one element of the direct channel. Therefore, all rank descriptors involved in (C.2) are equal to zero.

Similar ideas apply to cases $M = 4, 5, 6$. For the sake of brevity, we show only the elimination matrix analogous to (C.2) for each of those cases at the next page, see (C.3)-(C.5). Following similar arguments discussed above, it can be ensured that all the elimination matrices are full rank, they have no right null space, and thus all involved rank descriptors are equal to zero. Note that to simplify notation we have used the function $\psi(a, b)$, defined as the sum of the sinusoidal functions corresponding to the position (a, b) of each elimination matrix.

$$\begin{bmatrix} \left|h_{1,1}^{1,2}\right| \sin(\phi_{1,1}^{1,2}) & \left|h_{1,1}^{1,3}\right| \sin(\phi_{1,1}^{1,3}) - |\alpha_{1,2}^{\text{des}}| \sin(\alpha_{1,2}^{\text{des}}) & \left|h_{1,3}^{1,1}\right| \sin(\phi_{1,3}^{1,1}) & 0 \\ \left|h_{1,1}^{2,2}\right| \sin(\phi_{1,1}^{2,2}) & 0 & -|\alpha_1^{\text{int}}| \sin(\alpha_1^{\text{int}}) & 0 \\ \left|h_{1,1}^{3,2}\right| \sin(\phi_{1,1}^{3,2}) & \left|h_{1,1}^{3,3}\right| \sin(\phi_{1,1}^{3,3}) - |\alpha_{3,2}^{\text{des}}| \sin(\alpha_{3,2}^{\text{des}}) & -|\alpha_1^{\text{int}}| \sin(\alpha_1^{\text{int}}) - |\alpha_2^{\text{int}}| \sin(\alpha_2^{\text{int}}) & \lambda_4(q) \\ \left|h_{1,1}^{4,2}\right| \sin(\phi_{1,1}^{4,2}) & \left|h_{1,1}^{4,3}\right| \sin(\phi_{1,1}^{4,3}) - |\alpha_{4,2}^{\text{des}}| \sin(\alpha_{4,2}^{\text{des}}) & \left|h_{1,2}^{4,3}\right| \sin(\phi_{1,2}^{4,3}) & 0 \end{bmatrix} = \mathbf{0} \quad (\text{C.2})$$

$M = 4 :$

$$\begin{bmatrix} 0 & \psi(1,2) & \psi(1,3) & 0 \\ \psi(2,1) & 0 & \psi(2,3) & 0 \\ 0 & \psi(3,2) & 0 & \psi(3,4) \\ \psi(4,1) & \psi(4,2) & \psi(4,3) & \psi(4,4) \\ \psi(5,1) & 0 & \psi(5,3) & \psi(5,4) \end{bmatrix} \begin{bmatrix} \lambda_1(q) \\ \lambda_3(q) \\ \lambda_4(q) \\ \lambda_9(q) \end{bmatrix} = \mathbf{0} \quad (\text{C.3})$$

$M = 5 :$

$$\begin{bmatrix} \psi(1,1) & 0 & 0 & 0 & \psi(1,5) & 0 \\ \psi(2,1) & \psi(2,2) & \psi(2,3) & \psi(2,4) & \psi(2,5) & 0 \\ 0 & \psi(3,2) & 0 & \psi(3,4) & \psi(3,5) & 0 \\ \psi(4,1) & 0 & \psi(4,3) & 0 & 0 & \psi(4,6) \\ \psi(5,1) & \psi(5,2) & \psi(5,3) & \psi(5,4) & 0 & \psi(5,6) \\ 0 & \psi(6,2) & 0 & 0 & 0 & \psi(6,6) \end{bmatrix} \begin{bmatrix} \lambda_1(q) \\ \lambda_2(q) \\ \lambda_4(q) \\ \lambda_5(q) \\ \lambda_9(q) \\ \lambda_{11}(q) \end{bmatrix} = \mathbf{0} \quad (\text{C.4})$$

$M = 6 :$

$$\begin{bmatrix} 0 & 0 & 0 & \psi(1,4) & \psi(1,5) & 0 & 0 \\ 0 & 0 & \psi(2,3) & 0 & \psi(2,5) & \psi(2,6) & 0 \\ \psi(3,1) & \psi(3,2) & \psi(3,3) & \psi(3,4) & \psi(3,5) & \psi(3,6) & 0 \\ 0 & \psi(4,2) & 0 & \psi(4,4) & 0 & \psi(4,6) & 0 \\ \psi(5,1) & 0 & \psi(5,3) & 0 & 0 & 0 & \psi(5,7) \\ \psi(6,1) & \psi(6,2) & \psi(6,3) & \psi(6,4) & 0 & 0 & \psi(6,7) \\ 0 & \psi(7,2) & 0 & \psi(7,4) & 0 & 0 & \psi(7,7) \end{bmatrix} \begin{bmatrix} \lambda_2(q) \\ \lambda_3(q) \\ \lambda_5(q) \\ \lambda_6(q) \\ \lambda_7(q) \\ \lambda_8(q) \\ \lambda_{13}(q) \end{bmatrix} = \mathbf{0} \quad (\text{C.5})$$

Part II

Degrees of Freedom Analysis for Delayed CSIT

So far we have considered the IC under full CSIT, i.e. all nodes have perfect and instantaneous CSI. This second part addresses the case of delayed CSIT, where the transmitters have only access to the information about previous channel states. First, a review of the literature and some background is described in Chapter 5, as a way of introducing the reader to this change of paradigm. Then, the IC and IBC are studied in terms of DoF in Chapters 6 and 7, respectively. For each case, we propose transmission strategies achieving the best DoF to date for some antenna settings.

Technical paper/s related to this part:

M. Torrellas, A. Agustin, and J. Vidal, "Retrospective Interference Alignment for the 3-user MIMO Interference Channel", IEEE ICASSP, Florence, May 2014.

M. Torrellas, A. Agustin, and J. Vidal, "On the degrees of freedom of the K -user MISO Interference Channel With Delayed CSIT", IEEE ICASSP, Florence, May 2014.

M. Torrellas, A. Agustin, and J. Vidal, "DoF-Delay Trade-Off for the K -user MIMO Interference Channel With Delayed CSIT", submitted to the IEEE Transactions on Information Theory, June 2015.

M. Torrellas, A. Agustin, and J. Vidal, "Retrospective Interference Alignment for the MIMO Interference Broadcast Channel", IEEE ISIT, Hong Kong, June 2015.

Preliminaries

5

The required background related to networks with delayed CSIT is reviewed next. First, the specific system model is explained, particularizing the general system model presented in Chapter 2. Second, the current state-of-the-art of the DoF characterization for this type of networks is addressed, reviewing two relevant strategies that motivate the contributions addressed in the next chapters.

5.1 Specific System Model

As it will be explained in the next section, most of the literature on delayed CSIT corresponds to the BC. This is because having only one transmitter with knowledge of all messages eases the interference management. We study the IC and IBC scenarios, which are more challenging cases with multiple transmitters.

For all three cases, and in contrast to the previous part I of the thesis, here we consider multi-phase transmissions. In this context, each phase is divided in rounds, in turn divided in time slots, as explained in Chapter 2, Section 2.2. Each of the rounds is dedicated to serve the users in the set $\mathcal{G}^{(p,r)}$, with all groups of the rounds of phase p with the same cardinality G_p .

For ease of exposition, and following the notation of other variables, the block rows of the SSM $\boldsymbol{\Omega}_j$ corresponding to each of the phases will be denoted by $\boldsymbol{\Omega}_j^{(p)}$, with

$$\boldsymbol{\Omega}_j^{(p,q)} = \text{stack} \left(\boldsymbol{\Omega}_j^{(p)}, \dots, \boldsymbol{\Omega}_j^{(q)} \right). \quad (5.1)$$

defined in (2.15). Moreover, for simplicity we will maintain the notation for the complete SSM, i.e:

$$\boldsymbol{\Omega}_j \triangleq \boldsymbol{\Omega}_j^{(1:P)} = \text{stack} \left(\boldsymbol{\Omega}_j^{(1)}, \dots, \boldsymbol{\Omega}_j^{(P)} \right), \quad (5.2)$$

as previously defined.

5.1.1 Broadcast Channel

In the K -user BC there is only cell, thus there is only one transmitter. Then,

$$K_c = 1, \quad K = K_u, \quad c(j) = 1. \quad (5.3)$$

Moreover, the received signal at RX_j during the (p,r) th round, generally expressed in (2.3) for the IBC, simplifies to

$$\mathbf{y}_j^{(p,r)} = \mathbf{H}_j^{(p,r)} \mathbf{V}_j^{(p,r)} \mathbf{x}_j + \mathbf{H}_j^{(p,r)} \sum_{i \neq j} \mathbf{V}_i^{(p,r)} \mathbf{x}_i + \mathbf{n}_j^{(p,r)}, \quad (5.4)$$

where it is worth pointing out that the second subindex of channel matrices has been omitted since there is only one transmitter.

5.1.2 Interference Channel

In Chapter 6, we study the K -user IC, where there is only user per cell, thus each receiver is served by the transmitter with the same index. Then,

$$K_u = 1, \quad K = K_c, \quad c(j) = j, \forall j \quad (5.5)$$

Accordingly, the received signal at RX_j during the (p, r) th round, generally expressed in (2.3) for the IBC, simplifies to

$$\mathbf{y}_j^{(p,r)} = \mathbf{H}_{j,j}^{(p,r)} \mathbf{V}_j^{(p,r)} \mathbf{x}_j + \sum_{i \neq j} \mathbf{H}_{j,i}^{(p,r)} \mathbf{V}_i^{(p,r)} \mathbf{x}_i + \mathbf{n}_j^{(p,r)}. \quad (5.6)$$

5.1.3 Interference Broadcast Channel

The 2-cell 2-user IBC is studied in Chapter 7, with

$$K_c = K_u = 2, \quad K = 4, \quad c(j) = \left\lceil \frac{j}{K_u} \right\rceil. \quad (5.7)$$

Accordingly, the received signal at RX_j during the (p, r) th round, generally expressed in (2.3) for the K_c -cell K_u -user IBC, simplifies to

$$\mathbf{y}_j^{(p,r)} = \mathbf{H}_{j,1}^{(p,r)} \left(\mathbf{V}_1^{(p,r)} \mathbf{x}_1 + \mathbf{V}_2^{(p,r)} \mathbf{x}_2 \right) + \mathbf{H}_{j,2}^{(p,r)} \left(\mathbf{V}_3^{(p,r)} \mathbf{x}_3 + \mathbf{V}_4^{(p,r)} \mathbf{x}_4 \right) + \mathbf{n}_j^{(p,r)}. \quad (5.8)$$

5.1.4 Delayed CSIT Constraint

This constraint is here reviewed for reader's convenience. For simplicity, it will be specified only for the IC, where it is assumed that at the beginning of each phase p , only the set of channels

$$\{\mathbf{H}_{j,i}^{(\varrho,r)}\}_{\varrho=1}^{p-1}, \forall i, j, r,$$

are available at the transmitter side, corresponding to all phases before phase p .

5.2 State-of-the-Art

In frequency division duplexing systems, channel coefficients are usually estimated at the receivers by means of a training period, and then fed back to the transmitters, a procedure that entails both delays and errors. While errors and other practical issues related to feedback will be addressed in the last part of the thesis, here the focus is on feedback received with high delay. Assumed a block fading channel model, where channel remains constant in blocks of duration equal to the channel coherence time, if the feedback delay is greater than the coherence time, the available CSIT becomes completely outdated. Since the channel coherence time is related to user's mobility, until recently it was believed that CSIT was only useful for very low mobility (pedestrian speeds at most) because, otherwise, all strategies based on full CSIT cannot handle the interference.

In this respect, Maddah-Ali and Tse (MAT) [MAT12] introduced recently a new framework where IA concepts can be exploited even when the CSIT is completely outdated, referred to as delayed CSIT. Indeed, they assume *perfect* delayed CSIT, which is now more reliable since in contrast to the current CSIT case, during the time elapsed between transmissions, receivers can report a number of quantization bits sufficient to ensure certain feedback quality. However, there are some drawbacks, e.g. since the current channels are not known, the effective rate at which symbols are sent is simply based on statistics and the particular topology/setting. Moreover, notice that the concept of reciprocity [GCJ08] no longer holds for networks restricted to only delayed CSIT, which in case of full CSIT drastically simplifies the challenge of DoF characterization for all MIMO settings. Therefore, recall that the antenna setting in the sequel will be understood as:

$$\rho = \frac{M}{N}.$$

The MAT scheme was the first application of IA concepts using only delayed CSIT. Originally proposed for the K -user MISO broadcast channel, the communication is carried out along K phases for transmitting b symbols per user. The two main ingredients of their approach are *delayed CSIT precoding* and *user scheduling*, to be reviewed in Section 5.2.1. On the one hand, linear combinations of all b symbols exploiting the delayed CSIT are sent along all the phases, working similarly to the automatic repeat request protocols, where the same message (or packet) is retransmitted until it can reliably be decoded at the receiver side. On the other hand, the scheme imposes that during each phase p users are served in different time instances by groups of $p \leq K$ users, whereas the rest of users listen and learn about the interference. This user scheduling is decided beforehand by a protocol and independently of the available (delayed) CSIT, with the objective of controlling the number of interference terms contributing to the signal observed at each receiver. For example, during the first phase ($p = 1$), users are served in a TDMA fashion, i.e. first the transmitter sends the symbols of user one, then symbols of user two, and so on. The scheme is designed for a MISO setting, with the number of transmitted symbols higher than the receive antennas, thus symbols cannot be linearly decoded after the first phase. However, under the assumption that channels are uncorrelated across users, all users (*served* and *listening*) obtain different and independent linear combinations (LCs) of each set of symbols after the first phase. The obtained LCs of symbols when one user acts as listening user (thus containing non-intended symbols) will be denoted by *overheard interference*. They are known at one or more receivers, where they are seen as interference, and desired by another one. Then, the objective of the following phases is to exploit the delayed CSIT to reconstruct this overheard interference, and then retransmit it since it will be removable at the receivers that already know it. This idea allows that more than one user can be simultaneously served after the first phase.

Inspired by the MAT scheme in [MAT12], shown to be optimal only for the K -user MISO BC, a number of works appeared for studying networks with delayed CSIT, summarized in Table 5.1, and enumerated in the sequel. For the BC, Vaze et al. obtained the DoF characterization of the 2-user MIMO BC in [VV11], while Abdoli et al. derived in [AGK11] the channel DoF for all settings with $\rho \notin (2, 3)$. To the best of our knowledge, this is the last characterization revealed for the BC. Hence, the DoF characterization of the general K -user MIMO BC with (M, N) antennas at the transmitter and each of the receivers, although solved for some specific cases using current inner and outer bounds, is yet to be derived.

Table 5.1: Available results in the literature for networks with delayed CSIT. The last column indicate which settings and where are studied in this dissertation.

	Available results in terms of DoF	Settings studied in this thesis
BC	K -user MIMO [MAT12], 2-user MIMO [VV11] 3-user MIMO for $\rho \notin (2, 3)$ [AGK11]	—
IC	2-user MIMO [VV12b], Inner bounds for the K -user case with $\rho = 1$ [AGK13], $\rho = K$ [HC15]	Chapter 6: K -user MIMO
IBC	Inner bounds for the K_u -user 2-cell IBC [PA14], but not exploiting the advantageous topology of the IBC w.r.t. the IC	Chapter 7: 2-user 2-cell MIMO

For the IC with delayed CSIT, the authors in [VV11] extended their results to the 2-user MIMO IC in [VV12b]. However, having $K > 2$ transmitters is still an open problem. Basically, this is because in the MIMO IC, in contrast to the MIMO BC, each transmitter has only access to its own symbols, thus it can only reconstruct part of the overheard interference. In this context, Maleki et al. proposed a novel approach in [MJS12] for the 3-user SISO IC. Their two-phase scheme, denoted by the retrospective interference alignment (RIA) scheme, provides 3 symbols to each user after a transmission protocol of duration 8 time slots, thus attaining $\frac{3}{8}$ DoF per user. In contrast to the MAT scheme, no *user scheduling* is applied, and all transmitters are active and interfering each other during all the communication time. The main innovation of [MJS12] lies on performing a first phase transmission with *redundancy*, i.e. the receiver obtains more linear combinations than the number of symbols of one user. This allows processing the signal at the receiver side to project it onto singular vector spaces where the desired signals are only interfered by the symbols of one user, i.e. the contribution of one set of non-intended symbols can be removed. Thanks to this operation, hereafter denoted by *partial interference nulling*, interference is easily aligned during the second phase by exploiting delayed CSIT. It is worth pointing out that in contrast to the MAT scheme where desired signals and overheard interference are acquired from different time instants, now they are obtained together, thus after the first phase no interference-free LCs of desired signals are obtained at the receivers.

The work of Maleki et al. in [MJS12] was extended to the K -user case in [MC12] by Maggi and Cottatellucci, but unfortunately their main conclusion was that it is preferable to consider only 3 active transmitter-receiver pairs and applying time-sharing. Consequently, it is not known if the ideas of Maleki et al. are useful for the 3-user SISO case only.

In any case, the DoF inner bound proposed by Maleki et al. was later outperformed by Abdoli et al. in [AGK13], who proposed a precoding scheme for the K -user SISO IC where all the ingredients in [MAT12] and [MJS12] are combined, i.e: *delayed CSIT precoding*, *user scheduling*, and *redundancy transmission*. This scheme will be referred hereafter as the precoding, scheduling, redundancy (PSR) scheme. Developed in K phases, its sum DoF increase with the number of users K , thus considerably improving the result in [MC12]. Moreover, the authors conjectured that in contrast to the full CSIT case, the sum DoF of the IC with delayed CSIT collapse to a constant value as the number of users becomes asymptotically high. More recently, a generalization of the PSR scheme has been proposed by Hao and Clerckx in [HC15] for the K -user MISO IC, with transmitters

equipped with $K - 1$ or more antennas and single-antenna receivers.

The inner bounds proposed in [AGK13] and [HC15] outperform any proposed work for each setting, although at the cost of a long communication delay with low DoF improvement. For example, [MJS12] obtains $\frac{3}{8}$ DoF per user in the 3-user SISO IC with only 8 slots, whereas the scheme in [AGK13] requires 31 slots to increase the achieved DoF to $\frac{12}{31}$, i.e. a 3% of DoF gain. Moreover, it requires 3 phases, thus more uplink resources dedicated for channel feedback. Similarly, for the 6-user MISO IC with 6 antennas at the transmitters, the scheme in [HC15] provides a 40% DoF gain w.r.t. applying the 2-user MAT scheme with time-sharing, but this is at the cost of 1422 instead of 45 slots. Summarizing, it seems that better schemes in terms of DoF are obtained at the expenses of longer transmission time. In this respect, the DoF-delay trade-off comes up as an interesting topic to be investigated, i.e. comparison of schemes not only takes into account the achievable DoF, but also the transmission duration.

Ergodic IA concepts have also been extended to the case of delayed CSIT [KC13]. However, although the DoF results provided in [KC13] outperform some of the material presented here, it has basically the same drawbacks reviewed in Chapter 3: very long delays, and the requirement of time-varying channels. This latter condition is common throughout all the literature on delayed CSIT, and it follows from the assumption that channel feedback will incur a delay larger than channel coherence time. But, is this assumption necessary indeed? Note that in practice the transmitter has no way to know the current channel coefficients. Therefore, one may ask which of the state-of-the-art results are applicable in case there is delayed CSIT, the channel remains constant, but transmitter is not aware of this, thus performing a delayed CSIT strategy anyway.

It is worth pointing out that IA concepts have also been extended to the case of no CSIT, with a kind of IA which is labeled in the literature as Blind IA [GWJ11]. In such a case, proper channel variations are chosen for interference alignment. Although it was initially assumed that they appear naturally [Jaf10], i.e. by proper user selection, some recent works have shown that they can be manipulated or artificially constructed from a constant channel by means of reconfigurable antennas [GWJ11]. In any case, hereafter Blind IA will not be considered since contrary to Ergodic IA it requires constant channels and reconfigurable antennas.

Finally, we review the state-of-the-art for the IBC with delayed CSIT, to be tackled in Chapter 7. Since the IC remains still open for many settings, actually there is only one work treating the more complicated IBC [PA14], but their results are trivial since do not exploit the benefits of having two cooperating transmitters at each cell. Then, transmission strategies exploiting the specific topology of the IBC are yet to be developed.

5.2.1 MAT Scheme

The original scheme proposed by Maddah Ali and Tse in [MAT12] is here reviewed for the 2-user MISO BC, with $M = 2$ antennas at the transmitter, and $N = 1$ antennas at the receivers. The objective of the transmission is to deliver $b = 2$ symbols per user along $P = 2$ phases, see Fig. 5.1, with $\tau = 3$ slots, such that

$$d_j^{(\text{in})} = \frac{2}{3} \quad (5.9)$$

DoF per user are achieved, which coincides with the outer bound in [MAT12], thus is optimal. The main principles employed to achieve this are *user scheduling*, and *delayed CSIT precoding*, as shown next. Generalizing those ideas, it is possible to tackle the K -user case, for which some intuition is shed at the end of this section.

Individual interference sensing phase

Following a TDMA fashion, during this phase only one user is served per round ($G_1 = 1$), with two single-slot rounds, i.e:

$$R_1 = 2, \quad S_1 = 1, \quad \mathcal{G}^{(1,r)} = \{r\}, \quad G_1 = 1. \quad (5.10)$$

The objective is to simultaneously obtain LCs of desired signals, and sensing the interference. This knowledge will be useful for the next phase.

The received signal at RX_j during the $(1,r)$ th round writes as

$$y_j^{(1,r)} = \underline{\mathbf{h}}_j^{(1,r)} \mathbf{V}_r^{(1,r)} \mathbf{x}_r + n_j^{(1,r)}, \quad (5.11)$$

where $\mathbf{V}_r^{(1,r)} \in \mathbb{C}^{2 \times 2}$ is randomly chosen from a predetermined dictionary since in this phase there is no CSIT, $\underline{\mathbf{h}}_j^{(1,r)} \in \mathbb{C}^{1 \times 2}$, and $\mathbf{z}_j^{(1,r)} = \mathbf{y}_j^{(1,r)}$ since there is no per-phase processing. Thanks to this phase, one LC of desired signals is obtained at each receiver, but since two symbols have been transmitted, the message cannot still be linearly decoded.

Now, for $i, j = 1, 2$, let

$$\underline{\mathbf{t}}_{j,i} = \underline{\mathbf{h}}_j^{(1,i)} \mathbf{V}_i^{(1,i)} \in \mathbb{C}^{1 \times 2} \quad (5.12)$$

denote the observed vector at RX_j carrying the symbols of user i during the first phase. Clearly, when $i \neq j$, it represents interference that is available at RX_j whereas it is a desired signal at RX_i , such that if obtained, it would be sufficient to decode the two transmitted symbols. In the sequel, those terms will be denoted by the *overheard interference* (OHI), and will be the basis to construct the transmitted signal for the second phase.

Retrospective interference alignment phase

The second phase consists of one single-slot round, where both users are simultaneously served exploiting the principle of *delayed CSIT precoding*, i.e:

$$R_2 = 1, \quad S_2 = 1, \quad \mathcal{G}^{(2)} = \{1, 2\}, \quad G_2 = 2. \quad (5.13)$$

This means that the signal obtained at each receiver writes as

$$\mathbf{y}_j^{(2)} = \underline{\mathbf{h}}_j^{(2)} \left(\mathbf{V}_1^{(2)} \mathbf{x}_1 + \mathbf{V}_2^{(2)} \mathbf{x}_2 \right) + \mathbf{n}_j^{(2)} \quad (5.14)$$

The key point here is that the alignment constraint

$$\underline{\mathbf{h}}_j^{(2)} \mathbf{V}_i^{(2)} \propto \underline{\mathbf{t}}_{j,i}, \forall j \neq i. \quad (5.15)$$

can be ensured without current CSIT by setting

$$\mathbf{V}_i^{(2)} = \boldsymbol{\sigma}_i \underline{\mathbf{t}}_{j,i}. \quad (5.16)$$

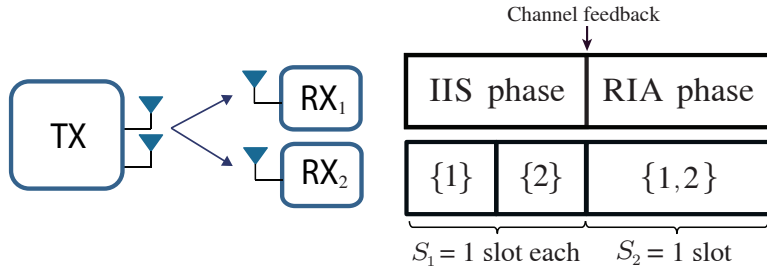


Figure 5.1: MAT for the 2-user BC with $M = 2$, $N = 1$. There are two phases: IIS and RIA. The groups of users being served each round ($\mathcal{G}^{(p,r)}$) is specified.

where $\boldsymbol{\sigma}_i \in \mathbb{C}^{2 \times 1}$ is some arbitrary random vector ensuring the transmit power constraint. The received signals can be represented by the SSM shown next:

$$\Omega_j = \begin{bmatrix} \underline{\mathbf{t}}_{j,1} & \mathbf{0} \\ \mathbf{0} & \underline{\mathbf{t}}_{j,2} \\ \hline \underline{\mathbf{h}}_j^{(2)} \boldsymbol{\sigma}_1 \underline{\mathbf{t}}_{2,1} & \underline{\mathbf{h}}_j^{(2)} \boldsymbol{\sigma}_2 \underline{\mathbf{t}}_{1,2} \end{bmatrix} \begin{array}{l} (1,1)\text{th round} \\ (1,2)\text{th round} \\ \hline \text{2nd phase} \end{array} \quad (5.17)$$

where phases are separated by a dashed line, each block row represents a different round, and each block column represents the subspaces occupied by the signals of each user. For the sake of clarity, in this first example we have annotated at the right hand side which round corresponds to each block row. Notice that thanks to the first phase OHI, each user $j = 1, 2$ may remove the received interference for the second phase since (5.15) has been ensured. Then, each user obtains another LC of its desired symbols, and once it has two LCs of two symbols it is able to linearly decode them.

Generalization to more than 2 users

The MAT scheme is generalized in [MAT12] for an arbitrary number of users K by suitably applying the principles of *user scheduling* and *delayed CSIT precoding*, similarly to toy example presented above. Therefore, in the general case there are K phases, and for each phase p we have:

$$R_p = \binom{K}{p}, \quad S_p = \frac{\text{lcm}(\{1, \dots, K\})}{p \cdot R_p}, \quad G_p = p, \quad (5.18)$$

where $\text{lcm}(\cdot)$ denotes the lowest common multiple of a set of numbers. Notice that the number of rounds guarantee that all possible groups of p users are served, and S_p denotes the number of time slots dedicated to each of them.

The procedure consists in transmitting symbols of order p for phase p , which generate symbols of order $p+1$ to be delivered during phase $p+1$. An order- m symbol refers to a supersymbol which is desired or available (thus can be removed) at m receivers. For example, during the second phase of the 2-user MAT scheme, an order-2 symbol is transmitted, because it is useful for both users. The process of transmitting every phase symbols of higher order ends up at phase K where symbols of order- K , i.e. intended to all

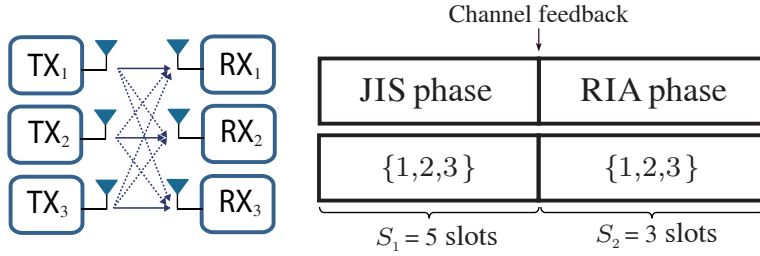


Figure 5.2: RIA for the 3-user SISO IC. There are two single-round phases: JIS and RIA. All users are served during all rounds.

the users, are transmitted by means of TDMA, and not producing additional high-order symbols. Accordingly, the order- m DoF are defined as the efficiency of transmitting order- m symbols through the network. Notice that they account for the DoF obtained with transmitting order- m symbols without interpretation of which user they are intended to. Hence, this formulation works with sum-DoF. By denoting $d^{(m,\text{in})}$ as the order- m sum-DoF inner bound, and according to previous arguments, the following recursive formulation is found[MAT12]:

$$d^{(m,\text{in})} = \frac{K - m + 1}{m} \frac{1}{\binom{K}{m} + \binom{K}{m+1} \frac{m}{d^{(m+1,\text{in})}}}, \quad m = 1 \dots K - 1, \quad (5.19a)$$

$$d^{(K,\text{in})} = 1, \quad (5.19b)$$

$$d^{(1,\text{in})} \equiv d^{(\text{in})}, \quad (5.19c)$$

where the efficiency of transmitting order- m symbols depends on the efficiency of transmitting order- $(m + 1)$ symbols. This divide and conquer approach allows uncoupling the design of each phase, and obtaining a more general framework. Finally, notice that the sum-DoF of order- K are equal to one since we work with normalized DoF.

5.2.2 RIA for the 3-user SISO IC

The original scheme for the 3-user SISO IC proposed by Maleki et al in [MJS12] is here reviewed. The objective of the transmission is to deliver $b = 3$ symbols per user along $P = 2$ phases, see Fig. 5.2, with $\tau = 8$ slots, such that

$$d_j^{(\text{in})} = \frac{3}{8}. \quad (5.20)$$

This scheme is not best in terms of DoF, since other approaches provide higher DoF, e.g. the 3-phase scheme proposed in [AGK13]. However, it is interesting because it allows us to introduce a new ingredient: *redundancy transmission*, which together with *delayed CSIT precoding* constitute the two principles this scheme is built with.

Joint interference sensing phase

The first phase consists of one round of $S_1 = 5$ slots where all users are served, i.e. there is no user scheduling. The objective is that receivers sense information about the interference, to be used in the next phase. Since there is no CSI available at the transmitters,

generic full-rank precoding matrices $\mathbf{V}_i^{(1)} \in \mathbb{C}^{5 \times 3}$ selected from a predetermined dictionary are agreed by all nodes. Each receiver obtains 5 observations, which are processed and then may be written as

$$\mathbf{z}_j^{(1)} = \mathbf{U}_j^{(1)} \mathbf{H}_{j,j}^{(1)} \mathbf{V}_j^{(1)} \mathbf{x}_j + \mathbf{U}_j^{(1)} \left[\mathbf{H}_{j,j+1} \mathbf{V}_{j+1}^{(1)}, \mathbf{H}_{j,j-1}^{(1)} \mathbf{V}_{j-1}^{(1)} \right] \begin{bmatrix} \mathbf{x}_{j+1} \\ \mathbf{x}_{j-1} \end{bmatrix}, \quad (5.21)$$

where the noise term is omitted since we focus on DoF analysis, i.e. at the very high SNR regime. Recall that thanks to the suitable design of the parameters (number of transmitted symbols and duration of the round), the received signal presents some redundancy: there are more observations than variables corresponding to each interference term. This *redundancy transmission* will be exploited in pursuit of *partial interference nulling*, i.e. projecting the received signals onto subspaces where the desired signals are interfered by the symbols of a single user. In this regard, consider the linear receive filters $\mathbf{U}_{j,i}^{(1)} \in \mathbb{C}^{2 \times 5}, i \neq j$, defined such that

$$\mathbf{U}_{j,i}^{(1)} \mathbf{H}_{j,k}^{(1)} \mathbf{V}_k^{(1)} = \mathbf{0}, k \neq \{i, j\} \quad (5.22a)$$

$$\mathbf{U}_{j,i}^{(1)} \mathbf{H}_{j,i}^{(1)} \mathbf{V}_i^{(1)} \neq \mathbf{0}. \quad (5.22b)$$

Notice that receivers have full CSI, so this design is feasible at the end of the first phase. Then, the first-phase receiving filter is given by

$$\mathbf{U}_j^{(1)} = \text{stack}\left(\mathbf{U}_{j,j+1}^{(1)}, \mathbf{U}_{j,j-1}^{(1)}\right) \in \mathbb{C}^{4 \times 5}, \quad (5.23)$$

and satisfies

$$\mathbf{U}_j^{(1)} \left[\mathbf{H}_{j,j+1}^{(1)} \mathbf{V}_{j+1}^{(1)} \mathbf{H}_{j,j-1}^{(1)} \mathbf{V}_{j-1}^{(1)} \right] = \text{bdiag}(\mathbf{T}_{j,j+1}, \mathbf{T}_{j,j-1}), \quad (5.24a)$$

$$\mathbf{T}_{j,i} = \mathbf{U}_{j,i}^{(1)} \mathbf{H}_{j,i}^{(1)} \mathbf{V}_i^{(1)} \in \mathbb{C}^{2 \times 3}, i \neq j \quad (5.24b)$$

where $\mathbf{T}_{j,i}$ is the residual interference from TX_i after applying the linear filter $\mathbf{U}_{j,i}^{(1)}$, i.e. this processing together with the transmitted redundancy allows uncoupling the interference from the different sources at RX_j . Now, for each $i \neq j$ we define

$$\mathcal{T}_{j,i} = \text{rspan}(\mathbf{T}_{j,i}). \quad (5.25)$$

Those subspaces represent the OHI, and similarly to the MAT scheme, will be the basis to construct the second phase transmitted signals. Finally, for the sake of reader's understanding, the processed signals in (5.21) are next written by applying the design for $\mathbf{U}_j^{(1)}$ in (5.22):

$$\mathbf{z}_j^{(1)} = \mathbf{U}_j^{(1)} \mathbf{H}_{j,j}^{(1)} \mathbf{V}_j^{(1)} \mathbf{x}_j + \begin{bmatrix} \mathbf{T}_{j,j+1} & \mathbf{0} \\ \mathbf{0} & \mathbf{T}_{j,j-1} \end{bmatrix} \begin{bmatrix} \mathbf{x}_{j+1} \\ \mathbf{x}_{j-1} \end{bmatrix}, \quad (5.26)$$

ensuring that (5.24a) holds.

Retrospective interference alignment phase

The second phase lasts for $S_2 = 3$ slots where the precoding matrix for TX_i is designed to align the generated interference with the overheard interference at *all* non-intended receivers. In other words, each receiver should be able to remove the interference generated

by $\mathbf{V}_i^{(2)}$ using the overheard interference from the JIS phase, see (5.25). Then, they are designed to satisfy the following set of constraints:

$$\text{rspan} \left(\mathbf{H}_{k,i}^{(2)} \mathbf{V}_i^{(2)} \right) \subseteq \mathcal{T}_{k,i}, \quad \forall k \neq i. \quad (5.27)$$

An easy way to ensure this without using full CSIT is to set

$$\mathbf{V}_i^{(2)} = \boldsymbol{\Sigma}_i^{(2)} \mathbf{T}_i^{(2)}, \quad (5.28a)$$

$$\text{rspan} \left(\mathbf{T}_i^{(2)} \right) = \mathcal{T}_i^{(2)} = \bigcap_{k \neq i} \mathcal{T}_{k,i} = \mathcal{T}_{i+1,i} \cap \mathcal{T}_{i-1,i}, \quad (5.28b)$$

where $\boldsymbol{\Sigma}_i^{(2)} \in \mathbb{C}^{3 \times 1}$ is some arbitrary full rank matrix ensuring the transmit power constraint, and $\mathbf{T}_i^{(2)} \in \mathbb{C}^{1 \times 3}$ is some arbitrary matrix whose rows span the intersection subspace $\mathcal{T}_i^{(2)}$ of dimension one. The received signals along the whole communication at each receiver, can be more easily understood by writing the j th signal space matrix:

$$\boldsymbol{\Omega}_j = \begin{bmatrix} \mathbf{U}_{j,j+1} \mathbf{H}_{j,j}^{(1)} \mathbf{V}_j^{(1)} & \mathbf{T}_{j,j+1} & \mathbf{0} \\ \mathbf{U}_{j,j-1} \mathbf{H}_{j,j}^{(1)} \mathbf{V}_j^{(1)} & \mathbf{0} & \mathbf{T}_{j,j-1} \\ \hline \mathbf{H}_{j,j}^{(2)} \mathbf{V}_j^{(2)} & \mathbf{H}_{j,j+1} \mathbf{V}_{j+1}^{(2)} & \mathbf{H}_{j,j-1}^{(2)} \mathbf{V}_{j-1}^{(2)} \end{bmatrix} \begin{array}{l} \text{Phase 1} \\ \vdots \\ \text{Phase 2} \end{array} \quad (5.29)$$

where the dotted lines separate the blocks rows corresponding to each of the two phases. Recall that here the first phase has two block rows, but they correspond to the signals processed with two different filters, instead of two different rounds for the first phase. Since precoding matrices satisfy conditions in (5.27), each interference term generated during the second phase is aligned with one of the OHI terms of the first phase. Therefore, all the second phase interference can be removed by combining the processed signals, which is interpreted as row operations on the signal space matrix. In turn, notice that the first and second block rows of (5.29) contain desired signals. Then, it can be seen that each time slot provides one independent LC of desired symbols, i.e. three LCs after all, thus all desired symbols can be linearly decoded.

Generalization for more than 2 users

The RIA scheme presented in [MJS12] was later extended to the K -user case in [MC12]. Given our formulation, notice that (5.27) easily generalizes to an arbitrary number of users, as well as (6.12b). In this later case, the subspace $\mathcal{T}_i^{(2)}$ is built as the intersection of $K - 1$ subspaces. Therefore, using suitable parameters the rest of the design follows the same. However, the conclusion of such generalization is that it is better to consider only 3 users and applying time-sharing arguments [MC12].

IC with Delayed CSIT

6

This chapter studies the DoF of the K -user MIMO interference channel with delayed CSIT, see Fig. 6.1. Three linear precoding strategies are envisioned, formulated in such a way that the achievable DoF can be derived as a function of the transmission delay, thus elucidating its achievable DoF-delay trade-off. All strategies are based on the concept of retrospective interference alignment, and built upon three main ingredients: *delayed CSIT precoding*, *user scheduling*, and *redundancy transmission*, reviewed in the previous chapter. Finally, the latter part of this chapter settles that all the proposed strategies work also for constant channels, except for SISO. In such a case, the schemes can be made feasible by resorting to ACS concepts, as applied for full CSIT in Chapter 4. This conclusion removes the time-varying channels assumption usually assumed in all the literature on delayed CSIT.

6.1 Main Contributions

The three main research results attained in this chapter are next exposed.

6.1.1 Proposed Transmission Strategies

Three linear precoding strategies are proposed. For each case, the number of transmitted symbols, and the duration of the phases are obtained as the solution of a DoF maximization problem. This allows formulating the achievable DoF as a function of each setting, i.e. number of users K and antenna configuration ρ . From the obtained results, three different regimes are observed:

- When $\rho \leq 1$, the RIA scheme for the 3-user SISO IC in [MJS12], reviewed in previous chapter (Section 5.2.2), is generalized to the K -user MIMO case. In contrast to the rule of thumb in [MC12], it is shown that considering $L \in \{3, 4, \dots, K\}$ users simultaneously active may increase the attained DoF, where the optimal value of L depends on each antenna setting and the total number of users K .
- For $\rho > 1$, a two-phase scheme is proposed. The idea is similar to the MAT scheme reviewed in previous chapter. In contrast, now in the second phase groups of $G_2 \in \{2, \dots, K\}$ users are served, where the optimal value of G_2 is designed according to ρ and the number of users K in pursuit of DoF boosting. Inspired by the way it is carried out, we denote this scheme as the TDMA groups (TG) scheme.
- For $\rho \approx 1$ and $K = 3$ users, we generalize the PSR scheme in [AGK13] to the MIMO case. Moreover, this scheme turns to be also useful for the K -user MIMO

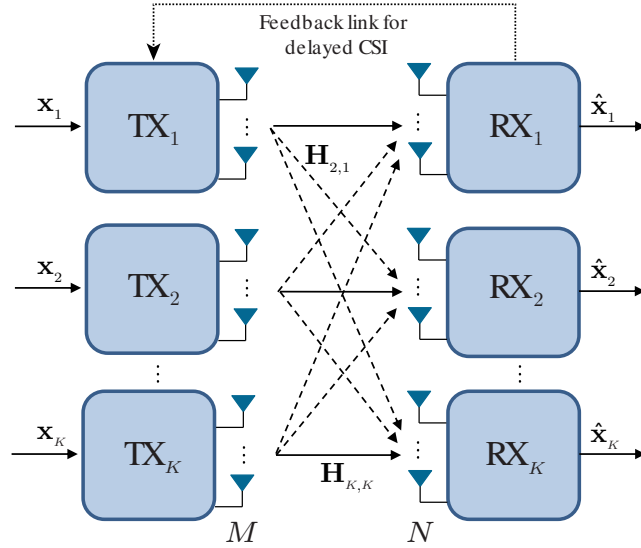


Figure 6.1: The K -user MIMO IC, with (M, N) antennas at the transmitters and receivers, respectively. Solid/Dotted lines denote the links carrying intended/interference signals.

IC when it is combined with time-sharing concepts, i.e. with $L < K$ users being simultaneously served, where the optimal value of L depends on the value of ρ .

The DoF attained by means of the proposed schemes are summarized in Theorem 6.2, Theorem 6.3, whereas the DoF outer bound resulting from combining different SotA results is formulated in Theorem 6.1. For $\rho < \frac{1}{K-1}$, the DoF with full CSIT can be achieved without CSIT by applying zero-forcing concepts at the receiver only, see for example [WGJ14, Section V.A]. For the rest of cases, and for comparison purposes, the following DoF outer bound will be used:

Theorem 6.1 (DoF Outer bound [WSJ14, MAT12]). *For the K -user MIMO IC with delayed CSIT and antenna ratio ρ , the normalized DoF per user are bounded above by:*

$$d_j^{(\text{out})} = \begin{cases} \frac{K-1}{K}\rho & \frac{1}{K-1} \leq \rho < \alpha \\ \frac{\rho}{\rho+1} & \alpha \leq \rho < \frac{1}{\beta} \\ \frac{1}{\beta+1} & \rho \geq \frac{1}{\beta} \end{cases} \quad (6.1)$$

where $\alpha = \frac{K-2}{K^2 - 3K + 1}$ and $\beta = \frac{1}{2} + \frac{1}{3} + \dots + \frac{1}{K}$.

Proof: The first two bounds follow by assuming full CSIT and applying the results in [WSJ14], since this cannot decrease the capacity of a network with delayed CSIT. Similarly, the other bound is based on the idea that cooperation can never hurt the DoF, thus the bounds for the 3-user BC with delayed CSIT in [MAT12] can be applied here. \square

The DoF inner bounds describing the performance of the proposed schemes are next stated and illustrated by means of some examples:

Theorem 6.2 (DoF Inner bound for 3 users). *For the 3-user MIMO IC with delayed CSIT and antenna ratio ρ , the following DoF per user can be achieved:*

$$d_j^{(\text{in})} = \begin{cases} \frac{\rho^3}{2 - \rho} & \frac{1}{2} < \rho \leq \rho_{\text{PSR},1} \\ \frac{2\rho^2}{5\rho^2 - 10\rho + 8} & \rho_{\text{PSR},1} < \rho \leq \rho_{\text{PSR},2} \\ \frac{6\rho}{3\rho + 10} & \rho_{\text{PSR},2} < \rho < \frac{4}{5} \\ \frac{12}{31} & \rho \geq \frac{4}{5} \end{cases} \quad (6.2)$$

where

$$\rho_{\text{PSR},1} = \frac{1}{15} \left(10 + 5^{2/3} \left(\sqrt[3]{2(3\sqrt{6} + 2)} - \sqrt[3]{2(3\sqrt{6} - 2)} \right) \right) \approx 0.7545 \quad (6.3)$$

$$\rho_{\text{PSR},2} = \frac{1}{3} (5 - \sqrt{7}) \approx 0.7847 \quad (6.4)$$

Proof: See Section 6.2.3, describing the 3-user PSR scheme. \square

Theorem 6.3 (DoF Inner bound for K users). *For the K -user MIMO IC with delayed CSIT and antenna ratio ρ , the following DoF per user can be achieved:*

$d_j^{(\text{in})}$	ρ	Scheme
$\frac{\rho}{\rho + 1}$	$\left(\frac{1}{K}, \rho_A(K)\right)$	
$\frac{1}{K} \max\left(\frac{\lambda^2}{\lambda^2 - 1}, (\lambda - 1) \frac{\rho}{\rho + 1}\right)$	$[\rho_A(\lambda), \rho_A(\lambda - 1)], \lambda \in \{4 \dots K\}$	RIA
$\frac{9}{8K}$	$\left(\frac{3}{5}, \rho_x\right]$	
$\frac{3}{K}\Gamma$	$(\rho_x, \rho_y(K))$	3-user PSR
$\frac{\rho}{\rho + (K - 1)}$	$(\rho_y(K), \rho_B(K))$	
$\max\left(\frac{1 + \alpha(\lambda) \cdot (\lambda - 1)}{K + (1 + \lambda \cdot (\lambda - 2)) \cdot \binom{K}{\lambda}}, \frac{\lambda - 1}{K} \frac{\rho}{\rho + (\lambda - 2)}\right)$	$[\rho_B(\lambda), \rho_B(\lambda - 1)], \lambda \in \{3 \dots K\}$	TG
$\frac{2}{K + 1}$	(K, ∞)	

where $\rho_A(\lambda) = \frac{\lambda}{\lambda^2 - \lambda - 1}$, $\rho_x = \sqrt{249} - 15 \approx 0.7797$, Γ denotes the DoF achieved for the 3-user MIMO IC, and stated in Theorem 6.2, applicable to the K -user case by means of time-sharing arguments (see Section 2.4.2), $\rho_y(K) = \frac{36(K-1)}{31K-36}$, $\alpha(\lambda) = \binom{K-1}{\lambda-1}$, and $\rho_B(\lambda) = \frac{1+\alpha(\lambda)\cdot(\lambda-1)}{1+\alpha(\lambda)\cdot(\lambda-2)}$. Note that $\rho_A(3) = \frac{3}{5}$, and $\rho_B(2) = K$, both representing the extremal values of the range of application for the RIA and TG schemes, respectively.

Proof: Each DoF value is achieved by means of the precoding scheme indicated in the last column. Among the proposed schemes, the RIA scheme gets the best performance for $\rho < \rho_x$, and it is described in Section 6.2.1. When ρ is close to one ($M \approx N$), the 3-user PSR scheme combined with time-sharing performs the best. This scheme is described in Section 6.2.3. Finally, the TG scheme addressed in Section 6.2.2 corresponds to the cases $\rho > \rho_y(K)$. \square

Combining Theorems 6.2, 6.3, and 6.1, the inner and outer bound DoF per user for $K = 3$ and $K = 6$ users are summarized in Fig. 6.2 top and bottom, respectively. They are represented for $\rho > \frac{1}{K-1}$, since otherwise the DoF outer bound is attained without the need of CSIT, i.e. TDMA, see e.g. [WGJ14].

Previous inner bound curves are constructed by using two different transmission strategies, yielding the best known DoF for each antenna setting. First, the PSR scheme in [AGK13] for the K -user SISO IC may be trivially extended for $M \neq N$ by turning off the additional antennas, and scaling all the parameters by a factor $\min(M, N)$. Second, the scheme for the 2-user MIMO IC in [VV12b] with delayed CSIT is considered, where the

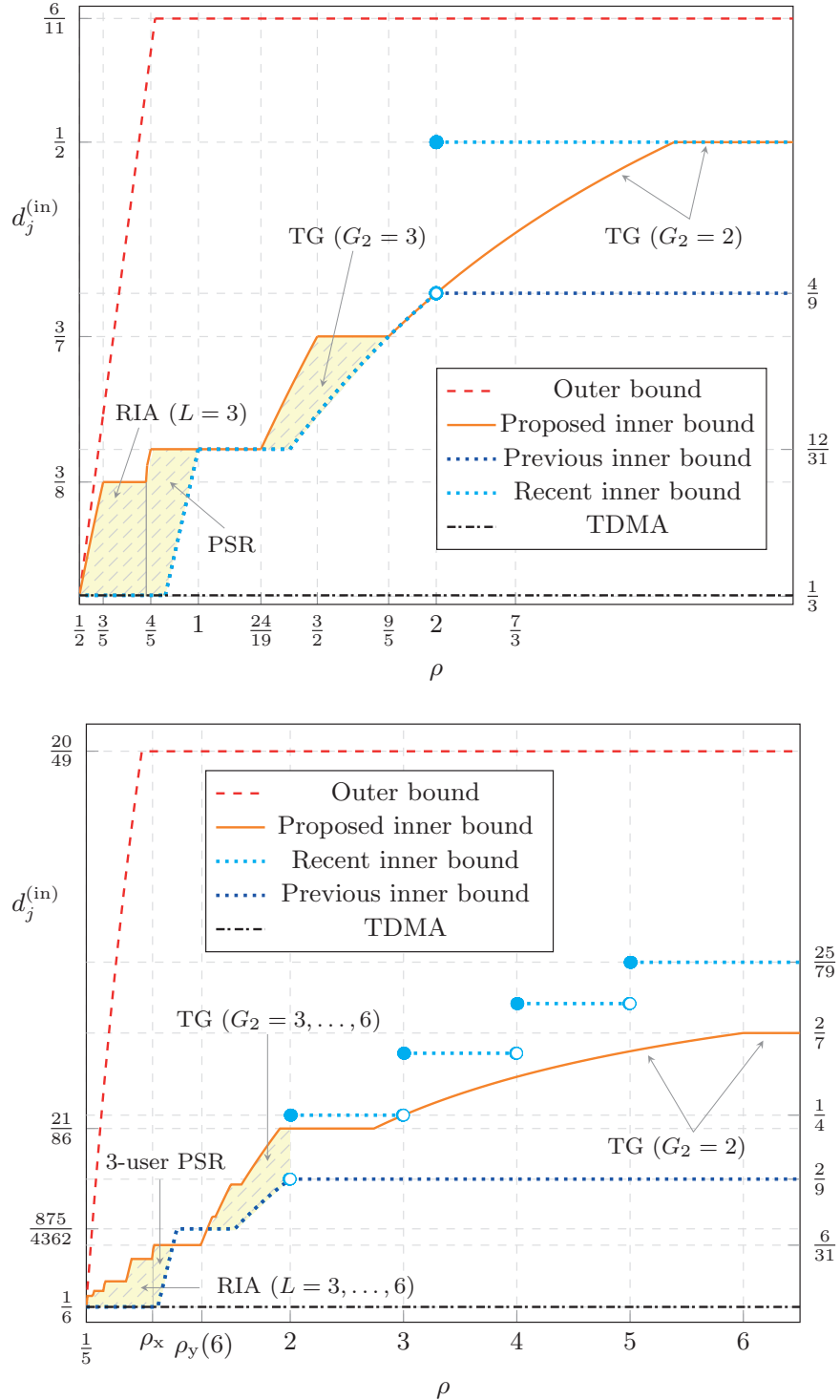


Figure 6.2: Normalized DoF inner and outer bounds per user for the MIMO IC with delayed CSIT, for $K = 3$ (top) and $K = 6$ (bottom). Shaded regions identify where proposed inner bounds improve recent and previous bounds in the state-of-the-art.

equivalent DoF are multiplied by a factor $\frac{2}{K}$, see (2.20). Further, the work of Hao and Clerckx [HC15] appeared during the development of the material in this chapter has been depicted, labeled as the recent inner bound. Although not explicitly stated in their paper, since all the schemes on delayed CSIT scale, it is assumed that the scheme in [HC15] scales with the number of antennas, thus it can be depicted as a function of ρ . Moreover, it is worth pointing out that such scheme assumes *local delayed CSIT* only.

No claim of optimality for the proposed inner bounds is stated, while it is worth pointing out that they outperform current inner bounds for certain antenna settings. Moreover, for the region $\frac{1}{K-1} < \rho < \frac{K}{K^2-K-1}$, the RIA scheme gets close to the best known DoF outer bound.

6.1.2 DoF-Delay Trade-Off

Although the proposed schemes do not obtain the best achievable DoF in comparison with recently appeared SotA, they present a shorter transmission, elucidating a trade-off between DoF and delay. Recall that precoding schemes exploiting delayed CSIT require multi-phase transmissions. For some settings, this entails long communication delays, and a high number of transmitted symbols, thus increasing the complexity of the encoding/decoding operation at transmitters/receivers. In contrast, the proposed schemes are limited to 2 or 3 phases. The aim of this restriction is to obtain simpler transmission strategies exploiting most of the DoF gains provided by having delayed CSIT, but without the need of DoF optimality, which seems to require long and complex communications procedures.

Section 6.3 studies the DoF-delay trade-off of the proposed and some state-of-the-art schemes. Thanks to the DoF-delay trade-off analysis, two main insights are concluded:

- The supremacy in terms of achievable DoF of one scheme w.r.t. another depends on the allowed complexity of the transmission, i.e. number of transmitted symbols or duration of the communication.
- The communication delay can be highly alleviated without high DoF penalties. Many examples are provided showing the balance between optimal (but usually large) parameters and more DoF w.r.t. practical parameters and competitive DoF.

Two methodologies will be used to derive the DoF-delay trade-off curves of the proposed schemes. On the one hand, the different points of the curves are obtained by limiting the maximum number of transmitted symbols. On the other hand, the curves are produced by varying the maximum order of the transmitted symbols. Both methodologies allow us to limit the complexity of the communication procedure, and will be explained in detail in Section 6.4.

6.1.3 Achievable DoF for Constant Channels

One may ask which of the previous results is applicable in case there is delayed CSIT, but the channel remains constant. This is addressed in Section 6.4, where it is proved that: 1) for some settings the schemes in the literature fail, although 2) as for the full CSIT

case, they can be made feasible by resorting to asymmetric complex signaling concepts. The following theorem summarizes this contribution:

Theorem 6.4 (DoF Inner bound with delayed CSIT and constant channels). *All inner bounds proposed in Theorem 6.3 apply for the K -user MIMO IC with delayed CSIT, constant channels, and antenna ratio ρ .*

Proof: See Section 6.4. □

6.2 Proposed Transmission Strategies

Three linear precoding strategies are proposed: RIA, TG, and PSR. For each case, the number of transmitted symbols, and the duration of the phases are obtained as the solution of a DoF maximization problem. This allows formulating the achievable DoF as a function of each setting, i.e. number of users K and antenna configuration ρ .

6.2.1 RIA Scheme ($M < N$)

This two-phase scheme is general for the K -user MIMO case, and proves Theorem 6.3 for $\rho < \rho_x$. Next section gives an intuition behind this transmission strategy. Then, each of the two phases is built. Finally, we present the optimization problem that provides the optimal system parameters for any antenna setting and number of users.

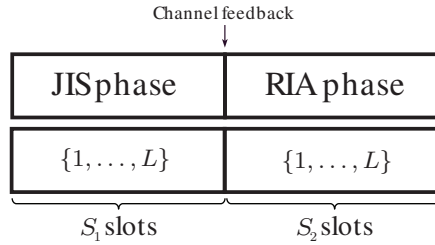


Figure 6.3: Transmission frame for the RIA scheme. $P = 2$ single-round phases, where only L out of the total K users are served, i.e. $\mathcal{G}^{(1)} = \mathcal{G}^{(2)} = \{1, \dots, L\}$. By time-sharing concepts, the rest of users are considered on other frames.

Overview of the precoding strategy

The transmission frame is depicted in Fig. 6.3. In contrast to the original RIA scheme, in both phases only $L \leq K$ users are scheduled for the communication, with $L \in \{3, \dots, K\}$. Delayed-CSIT precoding and redundancy transmission constitute the two main ingredients, with all L users considered being active during the two single-round phases, i.e.:

$$R_1 = R_2 = 1, \quad (6.5)$$

$$G_1 = G_2 = L, \quad (6.6)$$

as specified in Table 6.1.

During the JIS phase the transmitted signals are precoded with coefficients agreed before the communication starts. The objective is that each receiver senses the interference, with

Table 6.1: Served users per round and acquired OHI at RX₁ for each round for the RIA scheme

Phase (p)	Round (r)	$\mathcal{G}^{(p,r)}$	Acquired OHI at RX ₁ after processing
1	1	$\{1, \dots, L\}$	$\mathbf{T}_{1,2} \mathbf{x}_2, \dots, \mathbf{T}_{1,L} \mathbf{x}_L$
2	1	$\{1, \dots, L\}$	—

the objective of being used during the second phase. Thanks to the channel feedback, at beginning of the RIA phase each transmitter is able to reconstruct the interference terms generated at the non-intended receivers in the previous phase. Then, the transmitted signals delivered during the second phase are designed to be aligned with the interference generated during the first phase, i.e. such that do not cause additional interference.

In the sequel, the transmission scheme is described for a particular value of L . After this, we present the methodology used to derive the optimal value of L , as well as the optimal system parameters for each antenna setting ρ . The results are summarized in Table 6.2, showing the optimal system parameters for a given value of L , entailing two different antenna setting regimes: A.I = $\{\frac{1}{K-1} < \rho \leq \rho_A(L)\}$ and A.II = $\{\rho_A(L) < \rho \leq 1\}$. Note that for the regime A.II the achieved DoF are constant with respect to M , and equal to the achievable DoF for $\rho = \rho_A(L)$. Actually, this simply evidences that if a DoF value can be attained for $\rho = \rho_A(L)$, it is also achievable for $\rho > \rho_A(L)$. In particular, those cases may be tackled by scaling equally all the parameters and turning off enough transmit antennas to obtain the desired antenna ratio¹. Consequently, without loss of generalization, in what follows only regime A.I is detailed.

Table 6.2: System parameters for RIA scheme as a function of ρ

	b	S_1	S_2	$d_j^{(\text{in})}$
A.I = $\{\frac{1}{2} < \rho \leq \rho_A(L)\}$	MN	N	M	$\frac{L}{K} \frac{\rho}{\rho+1}$
A.II = $\{\rho_A(L) < \rho < 1\}$	LN	$L^2 - L - 1$	L	$\frac{L}{K} \frac{L}{L^2 - 1}$

Joint interference sensing phase

The first phase lasts for S_1 slots with all transmitters active. Since there is no CSI available at the transmitters, generic full-rank precoding matrices $\mathbf{V}_i^{(1)} \in \mathbb{C}^{MS_1 \times b}$ selected from a predetermined dictionary are agreed by all nodes. As specified in Table 6.2, $b = MN$, $S_1 = N$. Then, each receiver obtains $NS_1 = N^2$ observations, which are processed and write as

$$\mathbf{z}_j^{(1)} = \mathbf{U}_j^{(1)} \mathbf{H}_{j,j}^{(1)} \mathbf{V}_j^{(1)} \mathbf{x}_j + \mathbf{U}_j^{(1)} \left[\mathbf{H}_{j,\mathcal{I}_1^j}^{(1)} \mathbf{V}_{\mathcal{I}_1^j}^{(1)} \dots \mathbf{H}_{j,\mathcal{I}_{L-1}^j}^{(1)} \mathbf{V}_{\mathcal{I}_{L-1}^j}^{(1)} \right] \begin{bmatrix} \mathbf{x}_{\mathcal{I}_1^j} \\ \vdots \\ \mathbf{x}_{\mathcal{I}_{L-1}^j} \end{bmatrix}, \quad (6.7)$$

where $\mathcal{I}^j = \{1, \dots, L\} \setminus \{j\}$, and \mathcal{I}_k^j is the k th index of the set \mathcal{I}^j , and as explained above the noise term is omitted since we focus on DoF analysis.

¹This methodology might not be possible if parameters are limited to some value for the sake of e.g. low complexity or communication delay, as in Section 6.3.

We impose by design that the parameters satisfy $NS_1 > (L - 2)b$, thus there is some redundancy: the receiver has more observations than variables corresponding to interference. This redundancy can be exploited in pursuit of partial interference nulling, i.e. projecting the received signals onto subspaces where the desired signals are interfered by the symbols of a single user. In this regard, let define the receiving filter $\mathbf{U}_j^{(1)} \in \mathbb{C}^{\varphi_0 \times NS_1}$, $\forall i \neq j$, with

$$\begin{aligned}\varphi_0 &= (L - 1)\varphi_1, \\ \varphi_1 &= NS_1 - (L - 2)b = N(N - (L - 2)M),\end{aligned}$$

which consists of the composition of $L - 1$ linear filters $\mathbf{U}_{j,i}^{(1)} \in \mathbb{C}^{\varphi_1 \times NS_1}$, $i \neq j$, defined such that

$$\mathbf{U}_{j,i}^{(1)} \mathbf{H}_{j,k}^{(1)} \mathbf{V}_k^{(1)} = \mathbf{0}, \quad k \neq \{i, j\} \quad (6.8a)$$

$$\mathbf{U}_{j,i}^{(1)} \mathbf{H}_{j,i}^{(1)} \mathbf{V}_i^{(1)} \neq \mathbf{0}, \quad (6.8b)$$

$$\mathbf{U}_j^{(1)} = \text{stack}(\mathbf{U}_{j,\mathcal{I}_1^j}^{(1)}, \dots, \mathbf{U}_{j,\mathcal{I}_{L-1}^j}^{(1)}), \quad (6.8c)$$

$$\mathbf{U}_j^{(1)} [\mathbf{H}_{j,\mathcal{I}_1^j}^{(1)} \mathbf{V}_{\mathcal{I}_1^j}^{(1)} \dots \mathbf{H}_{j,\mathcal{I}_{L-1}^j}^{(1)} \mathbf{V}_{\mathcal{I}_{L-1}^j}^{(1)}] = \text{bdiag}(\mathbf{T}_{j,\mathcal{I}_1^j}, \dots, \mathbf{T}_{j,\mathcal{I}_{L-1}^j}), \quad (6.8d)$$

$$\mathbf{T}_{j,i} = \mathbf{U}_{j,i}^{(1)} \mathbf{H}_{j,i}^{(1)} \mathbf{V}_i^{(1)} \in \mathbb{C}^{\varphi_1 \times b}, \quad i \neq j \quad (6.8e)$$

where $\mathbf{T}_{j,i}$ is the residual interference from TX_i after applying the linear filter $\mathbf{U}_{j,i}^{(1)}$, i.e. this processing together with the transmitted redundancy allows uncoupling the interference from the different sources at RX_j . Now, let define for each $i \neq j$ the subspace

$$\mathcal{T}_{j,i} = \text{rspan}(\mathbf{T}_{j,i}). \quad (6.9)$$

Those subspaces represent the *overheard interference* the signals of the second phase will be aligned with, and they are available at RX_j after the first phase. As an example, Table 6.1 shows in its last column the acquired OHI at RX_1 . Notice that all these terms can be constructed using only delayed CSIT, thus transmitters will be able to construct them at the beginning of the second phase. Finally, for the sake of reader's understanding, the processed signals in (6.7) are written by applying the design for $\mathbf{U}_j^{(1)}$ in (6.8):

$$\mathbf{z}_j^{(1)} = \mathbf{U}_j^{(1)} \mathbf{H}_{j,j}^{(1)} \mathbf{V}_j^{(1)} \mathbf{x}_j + \begin{bmatrix} \mathbf{T}_{j,\mathcal{I}_1^j} \mathbf{x}_{\mathcal{I}_1^j} \\ \vdots \\ \mathbf{T}_{j,\mathcal{I}_{L-1}^j} \mathbf{x}_{\mathcal{I}_{L-1}^j} \end{bmatrix}. \quad (6.10)$$

Retrospective interference alignment phase

The second phase lasts for $S_2 = M$ slots where the precoding matrix for TX_i is designed to align the generated interference with the overheard interference at *all* non-intended receivers. In other words, each receiver should be able to remove the interference generated by $\mathbf{V}_i^{(2)}$ using the overheard interference from the JIS phase, see (6.9). Then, they are designed to satisfy the following set of constraints:

$$\text{rspan}(\mathbf{H}_{k,i}^{(2)} \mathbf{V}_i^{(2)}) \subseteq \mathcal{T}_{k,i}, \quad \forall k \in \mathcal{G}^{(2)} \setminus \{i\}. \quad (6.11)$$

An easy way to ensure this without using full CSIT is to set

$$\mathbf{V}_i^{(2)} = \boldsymbol{\Sigma}_i^{(2)} \mathbf{T}_i^{(2)}, \quad (6.12a)$$

$$\text{rspan}(\mathbf{T}_i^{(2)}) = \mathcal{T}_i^{(2)} = \bigcap_{\forall k \in \mathcal{G}^{(2)} \setminus \{i\}} \mathcal{T}_{k,i}, \quad (6.12b)$$

where $\boldsymbol{\Sigma}_i^{(2)} \in \mathbb{C}^{MS_2 \times \varphi_2}$ is some arbitrary full rank matrix ensuring the transmit power constraint, and $\mathbf{T}_i^{(2)} \in \mathbb{C}^{\varphi_2 \times b}$ is some arbitrary matrix whose rows span the intersection subspace $\mathcal{T}_i^{(2)}$ of dimension

$$\varphi_2 = b - (L-1)(b-\varphi_1) \quad (6.13a)$$

$$= N((L-1)N - L(L-2)M), \quad (6.13b)$$

derived using the identity described in the Notations Section. The received signals along the whole communication at each receiver, can be more easily understood by writing the j th signal space matrix:

$$\boldsymbol{\Omega}_j = \begin{bmatrix} \mathbf{U}_{j,\mathcal{I}_1^j} \mathbf{H}_{j,j}^{(1)} \mathbf{V}_j^{(1)} & \mathbf{T}_{j,\mathcal{I}_1^j} & \dots & \mathbf{0} \\ \vdots & \vdots & \ddots & \vdots \\ \mathbf{U}_{j,\mathcal{I}_{L-1}^j} \mathbf{H}_{j,j}^{(1)} \mathbf{V}_j^{(1)} & \mathbf{0} & \dots & \mathbf{T}_{j,\mathcal{I}_{L-1}^j} \\ \hline \mathbf{H}_{j,j}^{(2)} \mathbf{V}_j^{(2)} & \mathbf{H}_{j,\mathcal{I}_1^j}^{(2)} \mathbf{V}_{\mathcal{I}_1^j}^{(2)} & \dots & \mathbf{H}_{j,\mathcal{I}_{L-1}^j}^{(2)} \mathbf{V}_{\mathcal{I}_{L-1}^j}^{(2)} \end{bmatrix},$$

where the dotted lines separate the blocks rows corresponding to each of the two phases. Note that combination of processed signals may be interpreted as row operations on the signal space matrix. Since precoding matrices satisfy conditions in (6.11), each interference term generated during the second phase is aligned with one of the overheard interference terms of the first phase. Therefore, all the second phase interference can be removed, and N LCs of desired symbols free of interference are retrieved at each receiver per time slot, i.e. $NS_2 = MN = b$ LCs after all. In the next section, the constraints to be satisfied by all parameters for each antenna setting will be presented, including that all such b LCs are linearly independent, and thus all desired symbols can be linearly decoded.

Finally, after explaining this precoding scheme we are able to highlight the main difference of the IC w.r.t. the BC. In this case, each transmitter has only access to its own symbols, thus can only reconstruct part of the overheard interference. Consequently, the interference can only be aligned individually, i.e. two users cannot align their signals simultaneously at one receiver with the signals of one slot, since the transmitted signals travel through different channels. This is why a partial interference nulling is applied to the first phase received signals by means of the processing filter $\mathbf{U}_j^{(1)}$, such that only one interference term affects the desired signals on the processed signal space. In terms of the signal space matrix, this means that block columns corresponding to interference should have at most one non-zero element per block row.

System parameters optimization

Optimal system parameters for each antenna setting and number of users are derived next. First, the optimal value of L can be found by exhaustive evaluation of the expressions in

Theorem 6.3. Since for high values of K there will be many regions, the Algorithm 6.1 in the next page is provided to alleviate the search for the optimal L to only two candidates. The motivation behind each of its different steps is next explained.

First, the real number x is the positive solution of inverting the definition of $\rho_A(L)$, defined in Theorem 6.3. Then, since the inner bound is a piecewise function, x represents the value of L between two steps. For this reason, using the ceil and floor functions the two closest integers are selected as candidates, evaluating the achievable DoF for each of them. Finally, the best integer value L is chosen taking into account the extreme cases.

Algorithm 6.1: L solver

$$\textbf{Step 1: } x := \frac{1}{2} \left((1 + \rho^{-1}) + \sqrt{(1 + \rho^{-1})^2 + 4} \right)$$

$$\textbf{Step 2: } y := \lfloor x \rfloor \frac{\rho}{\rho+1}, z := \frac{1}{K} \frac{\lceil x \rceil^2}{\lceil x \rceil^2 - 1}$$

$$\textbf{Step 3: } L(\rho) = \begin{cases} K & x \geq K \\ 3 & x \leq 3 \\ \lfloor x \rfloor & 3 < x < K, y > z \\ \lceil x \rceil & \text{otherwise} \end{cases}$$

Assuming a particular value for L , we formulate the following DoF optimization problem:

$$\mathcal{P}_1 : \underset{\{b, S_1, S_2\} \in \mathbb{Z}^+}{\text{maximize}} \quad \frac{L}{KN} \frac{b}{S_1 + S_2} \quad (6.14a)$$

$$\text{s.t.} \quad MS_1 \geq b \quad (6.14b)$$

$$NS_1 > (L - 2)b \quad (6.14c)$$

$$NS_2 \geq b \quad (6.14d)$$

$$LMS_2 \geq b \quad (6.14e)$$

$$L\varphi_2 \geq b, \quad (6.14f)$$

with $\varphi_2 = (L - 1)NS_1 - L(L - 2)b$. This problem provides the optimal values for b , S_1 , and S_2 when the RIA scheme is employed. The objective function corresponds to the number of symbols divided by the channel uses, and a factor due to time-sharing and DoF normalization. On the other hand, the following four constraints are introduced to ensure linear feasibility:

Transmit rank during the JIS phase (6.14b): During the first phase, MS_1 linear combinations of the b symbols are transmitted using M antennas, and during S_1 slots. Then, for linear decodability of the desired symbols, no more symbols than the number of transmit dimensions can be sent.

JIS phase redundancy (6.14c): After the first phase, the linear filters $\mathbf{U}_{j,i} \in \mathbb{C}^{\varphi_1 \times NS_1}$ in (6.8), $\varphi_1 = NS_1 - (L - 2)b$, are applied assuming some redundancy has been transmitted. Then, we force $\varphi_1 > 0$ or, equivalently, (6.14c).

Receiver space-time dimensions (6.14d): Each receiver should have enough space-time dimensions to allocate all the desired and interference signals without space over-

lapping. First, notice that the interference received during the JIS phase occupies at most NS_1 dimensions. This subspace remains the same after the RIA phase, since all the interference generated during the RIA phase is aligned. On the other hand, the desired signals occupy at most b dimensions at each receiver. Hence, we must have

$$\underbrace{b}_{\text{desired dim.}} + \underbrace{NS_1}_{\text{interference dim.}} \leq \underbrace{NS_1 + NS_2}_{\text{total dimensions}}$$

Rank of desired signals after zero-forcing (6.14e)-(6.14f): For ease of exposition, the signal space matrix Ω_j at each receiver is here rewritten:

$$\Omega_j = \begin{bmatrix} \mathbf{U}_{j,\mathcal{I}_1^j} \mathbf{H}_{j,j}^{(1)} \mathbf{V}_j^{(1)} & \mathbf{T}_{j,\mathcal{I}_1^j} & \cdots & \mathbf{0} \\ \vdots & \vdots & \ddots & \vdots \\ \mathbf{U}_{j,\mathcal{I}_{L-1}^j} \mathbf{H}_{j,j}^{(1)} \mathbf{V}_j^{(1)} & \mathbf{0} & \cdots & \mathbf{T}_{j,\mathcal{I}_{L-1}^j} \\ \hline \mathbf{H}_{j,j}^{(2)} \mathbf{V}_j^{(2)} & \mathbf{H}_{j,\mathcal{I}_1^j}^{(2)} \mathbf{V}_{\mathcal{I}_1^j}^{(2)} & \cdots & \mathbf{H}_{j,\mathcal{I}_{L-1}^j}^{(2)} \mathbf{V}_{\mathcal{I}_{L-1}^j}^{(2)} \end{bmatrix} \begin{array}{l} \downarrow \varphi_1 \\ \downarrow \varphi_1 \\ \downarrow NS_2 \end{array},$$

where the block rows corresponding to the first phase have φ_1 rows each, whereas the block row of the second phase has NS_2 rows. Now, recall that the precoding matrices $\mathbf{V}_i^{(2)}$ lie on a subspace of dimension $t = \min(MS_2, \varphi_2) < \varphi_1$, see (6.12a)-(6.13). Then, if the interference is to be removed, each of the $L - 1$ block rows corresponding to the JIS phase must be projected onto the corresponding subspace of dimension t and linearly combined with the block row of the second phase. This is done by means of the linear filter \mathbf{W}_j , obtaining

$$\text{rank}(\mathbf{W}_j \mathbf{U}_j \mathbf{H}_{j,j} \mathbf{V}_j) = \min(L \cdot \min(MS_2, \varphi_2), b).$$

Since any linear precoding scheme requires $\text{rank}(\mathbf{W}_j \mathbf{U}_j \mathbf{H}_{j,j} \mathbf{V}_j) \geq b$, this yields to

$$L \cdot \min(MS_2, \varphi_2) \geq b \Rightarrow \begin{cases} LMS_2 \geq b \\ L\varphi_2 = L((L-1)NS_1 - L(L-2)b) \geq b \end{cases}.$$

Next, we analytically derive the solution of problem \mathcal{P}_1 in (6.14). For any given value of b , the objective function in (6.14a) is strictly decreasing with S_1 and S_2 , i.e. their optimum values are their minimum feasible values. Therefore, since S_2 appears in (6.14d) and (6.14e) only, its optimum value S_2^* is given by

$$S_2^* = \left\lceil b \max\left(\frac{1}{N}, \frac{1}{ML}\right) \right\rceil$$

This establishes two regions, with the threshold $\rho = \frac{1}{L}$. However, it can be seen that taking $S_2^* = \left\lceil \frac{b}{ML} \right\rceil$ and solving the problem produces a DoF value which is always outperformed by taking $S_2^* = \left\lceil \frac{b}{N} \right\rceil$ and increasing the value of L . Hence, we definitely take

$$S_2^* = \left\lceil \frac{b}{N} \right\rceil. \quad (6.15)$$

On the other hand, the optimum value of S_1 is set to satisfy one of the constraints (6.14b), (6.14c), and (6.14f) with equality:

$$S_1^* = \left\lceil \max\left(\frac{b}{M}, \frac{b+1}{N}, \frac{b}{NL}(L^2 - L - 1)\right) \right\rceil = \left\lceil b \cdot \max\left(\frac{1}{M}, \frac{1}{NL}(L^2 - L - 1)\right) \right\rceil. \quad (6.16)$$

While in Section 6.3 a maximum-value constraint for b will be included, here the problem is solved for unbounded b , i.e. it is simply chosen such that all parameters are integer values. Accordingly, one optimal solution is specified in Table 6.2. Note that the threshold $\rho_A(L) = \frac{L}{L^2 - L - 1}$ follows from the two possible choices for S_1^* , with $b = MN$ or $b = NL$, for each case.

6.2.2 TG Scheme ($M > N$)

The two-phase TG scheme obtains the performance described by Theorem 6.3 for $\rho > \rho_y(K)$. Next section gives an intuition behind this strategy, illustrating how each of the two phases is built, and finally we present the optimization problem that provides the optimal system parameters for any antenna setting and number of users.

Overview of the precoding strategy

This approach is designed according to two main ingredients: *delayed CSIT precoding and user scheduling*. In contrast to the RIA scheme, now all users are considered in each transmission block ($L = K$), and scheduled through the different rounds. During the first phase, time resources are orthogonally distributed among users, thus $G_1 = 1$, such that interference can be sensed individually. For this reason, this phase will be labeled as the individual interference sensing (IIS) phase. Notice also that in addition to sensing the interference, this phase provides free of interference observations of the desired signals to each receiver.

Each round of the second phase is dedicated to a different group of G_2 users, which for simplicity in the notation will be simply denoted as G . The objective is similar to the second phase of the RIA scheme (Section 6.8), and for this reason it is also denoted hereafter as the RIA phase. Based on the channel feedback, each active transmitter is able to send LCs of symbols that can be removed at the non-intended active receivers by exploiting the overheard interference from the IIS phase. As an example, the transmission frame for the case $K = 4$, $G = 3$ is depicted in Fig. 6.4.

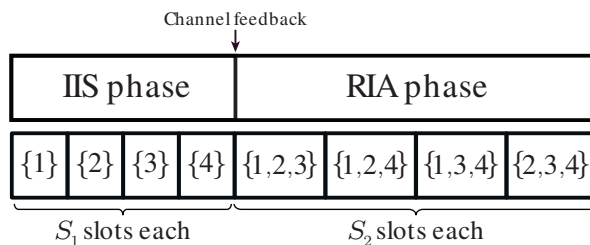


Figure 6.4: Transmission frame for the TG scheme with $K = 4$, $G = 3$. Each of the $P = 2$ phases has four rounds of S_1 and S_2 slots each. Active groups $\mathcal{G}^{(p,r)}$ are represented for each round of the two phases.

Summarizing, we have

$$R_1 = K, \quad R_2 = \binom{K}{G}, \quad (6.17)$$

$$G_1 = 1, \quad G_2 \triangleq G. \quad (6.18)$$

Note that the transmitted signals during each round of the second phase are designed such that they can be removed at the $G - 1$ non-intended active receivers. Consequently, they do not generate additional OHI. Moreover, notice that low values of G relax the constraints on the design, i.e. the number of receivers where the transmitted signals should be aligned, but also increase the number of rounds. This is a trade-off that should be balanced by the optimal value of G . The derivation of the optimal system parameters, as well as G is deferred to last subsection, with results summarized in Table 6.3. For each value of G , it can be seen that there exist two different antenna setting regimes: B.I = $\{1 < \rho \leq \rho_B(G)\}$ and B.II = $\{\rho > \rho_B(G)\}$, with $\rho_B(G) = \frac{1+\alpha(G)\cdot(G-1)}{1+\alpha(G)\cdot(G-2)}$. Following similar arguments as for the RIA scheme, only the case B.I will be addressed in the sequel, and a particular value for G is assumed. Therefore, for ease of notation simply

$$\alpha \triangleq \alpha(G) = \binom{K-1}{G-1}$$

will be used during the following two sections.

Table 6.3: System parameters for TG scheme as a function of ρ

	b	S_1	S_2	$d_j^{(\text{in})}$
B.I = $\{1 < \rho \leq \rho_B(G)\}$	αMN	αN	$M - N$	$\frac{G}{K} \frac{\rho}{\rho + (G-1)}$
B.II = $\{\rho > \rho_B(G)\}$	$(1 + \alpha \cdot (G - 1))N$	$1 + \alpha \cdot (G - 2)$	1	$\frac{1 + \alpha \cdot (G - 1)}{K + (G(G - 2) + 1) \binom{K}{G}}$

Individual interference sensing phase

Each TX_i sends linear combinations of its $b = \alpha MN$ symbols during the $S_1 = \alpha N$ time slots of the $(1, i)$ th round, thus RX_j obtains

$$\mathbf{y}_j^{(1,i)} = \mathbf{H}_{j,i}^{(1,i)} \mathbf{V}_i^{(1,i)} \mathbf{x}_i, \quad (6.19)$$

where $\mathbf{H}_{j,r}^{(1,r)} \in \mathbb{C}^{NS_1 \times MS_1}$, and the precoding matrices $\mathbf{V}_r^{(1,r)} \in \mathbb{C}^{MS_1 \times b}$ are chosen as some generic full-rank matrices. Since no redundancy was transmitted ($b < NS_1$), none per-phase receiving filter is applied, i.e. equivalently we have $\mathbf{U}_j^{(1)} = \mathbf{I}_{N\tau_1}$. Moreover, similarly to (6.8e)-(6.9) we define

$$\mathbf{T}_{j,i} = \mathbf{H}_{j,i}^{(1,i)} \mathbf{V}_i^{(1,i)} \quad (6.20a)$$

$$\mathcal{T}_{j,i} = \text{rspan}(\mathbf{T}_{j,i}), \quad (6.20b)$$

as the *overheard interference* generated by TX_i at RX_j , with $\dim(\mathcal{T}_{j,i}) = NS_1 = \alpha N^2$. As an example, we show in Table 6.4, the OHI obtained at RX_1 after each round when $K = 4$ and $G = 3$. In contrast to the previous scheme, now this term is individually obtained since there is only one active transmitter per round. Specifically, each receiver observes $NS_1 = \alpha N^2$ linear combinations of the desired symbols, as well as $\alpha N^2(K - 1)$ linear combinations of OHI, and since $NS_1 < b$, linear decodability is not possible yet.

Table 6.4: Served users per round and acquired OHI at RX₁ for each round for the TG scheme with $K = 4$ and $G = 3$.

Phase (p)	Round (r)	$\mathcal{G}^{(p,r)}$	Acquired OHI at RX ₁
1	1	{1}	—
	2	{2}	$\mathbf{T}_{1,2} \mathbf{x}_2$
	3	{3}	$\mathbf{T}_{1,3} \mathbf{x}_3$
	4	{4}	$\mathbf{T}_{1,4} \mathbf{x}_4$
2	1	{1, 2, 3}	—
	2	{1, 2, 4}	—
	3	{1, 3, 4}	—
	4	{2, 3, 4}	$\mathbf{H}_{1,2}^{(2,4)} \mathbf{V}_2^{(2,4)} \mathbf{x}_2 + \mathbf{H}_{1,3}^{(2,4)} \mathbf{V}_3^{(2,4)} \mathbf{x}_3 + \mathbf{H}_{1,4}^{(2,4)} \mathbf{V}_4^{(2,4)} \mathbf{x}_4$

Retrospective interference alignment phase

The objective of the RIA phase is to exploit the overheard interference, i.e. the subspaces $\mathcal{T}_{j,i}$ available at the non-intended receivers, to construct signals that can be canceled even without knowing the current CSI. The design pursues that for each round r of the second phase, the interference generated is aligned at *all* the G receivers in $\mathcal{G}^{(2,r)}$. For this reason, the optimal value of G depends on each antenna setting and the total number of users K .

According to this objective, the signal transmitted during the $(2, r)$ th round by each active transmitter $i \in \mathcal{G}^{(2,r)}$ should satisfy the following set of constraints:

$$\text{rspan} \left(\mathbf{H}_{k,i}^{(2,r)} \mathbf{V}_i^{(2,r)} \right) \subseteq \mathcal{T}_{k,i}, \forall k \in \mathcal{G}^{(2,r)} \setminus \{i\}. \quad (6.21)$$

This can be ensured by setting

$$\begin{aligned} \mathbf{V}_i^{(2,r)} &= \boldsymbol{\Sigma}_i^{(2,r)} \mathbf{T}_i^{(2,r)}, \\ \text{rspan} \left(\mathbf{T}_i^{(2,r)} \right) &= \mathcal{T}_i^{(2,r)} = \bigcap_{k \in \mathcal{G}^{(2,r)} \setminus \{i\}} \mathcal{T}_{k,i}, \end{aligned} \quad (6.22a)$$

where $\boldsymbol{\Sigma}_i^{(2,r)} \in \mathbb{C}^{MS_2 \times \varphi}$ is some arbitrary full rank matrix ensuring the transmit power constraint, and $\mathbf{T}_i^{(2,r)} \in \mathbb{C}^{\varphi \times b}$ is a matrix whose rows lie on the intersection subspace of dimension

$$\begin{aligned} \varphi &= (G - 1)NS_1 - (G - 2)b \\ &= \alpha N (N(G - 1) - (G - 2)M). \end{aligned} \quad (6.23a)$$

The main difference between the second phase of this scheme w.r.t. to the second phase of the RIA scheme is that the transmitted signals should be removable only at the non-intended active receivers, instead that at all receivers². This can be seen by comparing (6.12b) with (6.22a): instead of the intersection of all but one subspaces, during each

²Another difference is that here transmitters require only *local* instead of *global* delayed CSIT.

round each transmitter sends signals that lie on the intersection of $G - 1$ subspaces. In order to illustrate how the signals are received and aligned, the signal space matrix at each receiver for the case $K = 4$, $G = 3$ is next shown:

$$\Omega_j = \begin{bmatrix} \mathbf{T}_{j,1} & \mathbf{0} & \mathbf{0} & \mathbf{0} \\ \mathbf{0} & \mathbf{T}_{j,2} & \mathbf{0} & \mathbf{0} \\ \mathbf{0} & \mathbf{0} & \mathbf{T}_{j,3} & \mathbf{0} \\ \mathbf{0} & \mathbf{0} & \mathbf{0} & \mathbf{T}_{j,4} \\ \hline \mathbf{H}_{j,1}^{(2,1)} \mathbf{V}_1^{(2,1)} & \mathbf{H}_{j,2}^{(2,1)} \mathbf{V}_2^{(2,1)} & \mathbf{H}_{j,3}^{(2,1)} \mathbf{V}_3^{(2,1)} & \mathbf{0} \\ \vdots & \vdots & \vdots & \vdots \\ \mathbf{0} & \mathbf{H}_{j,2}^{(2,4)} \mathbf{V}_2^{(2,4)} & \mathbf{H}_{j,3}^{(2,4)} \mathbf{V}_3^{(2,4)} & \mathbf{H}_{j,4}^{(2,4)} \mathbf{V}_4^{(2,4)} \end{bmatrix}. \quad (6.24)$$

Thanks to conditions in (6.21), all the interference captured during the RIA phase can be removed using the overheard interference from the IIS phase. Now, recall that α represents the number of groups of the RIA phase to which each user belongs. Therefore, the RIA phase provides $\alpha \cdot \min(N S_2, \varphi) = \alpha \cdot N(M - N)$ extra observations of the desired symbols. Finally, by combining the $N S_1 = \alpha N^2$ linear combinations retrieved from the IIS phase with that obtained during this phase, each receiver obtains $b = \alpha \cdot MN$ LCs of its desired symbols.

Remark: It can be seen that when $\rho < \rho_B(G)$ only a subspace of dimension $N(M - N) < \varphi$ of $\mathcal{T}_i^{(2,r)}$ is revealed to each receiver. This is in contrast with the case $\rho > \rho_B(G)$ where the entire subspaces $\mathcal{T}_i^{(2,r)}$ must be delivered to RX_i in order to obtaining a sufficient number of observations, and thus ensure linear decodability.

System parameters optimization

Given a value of ρ , the optimal value of G for the TG scheme may be obtained by means of the steps described in Algorithm 6.2. The philosophy here is similar to the one in Algorithm 6.1, and thus its description is omitted to avoid redundancy. The parameters, e.g. number of symbols b and number of slots per round S_1, S_2 , given G, K , and ρ , are derived by means of the following DoF optimization problem:

$$\mathcal{P}_2 : \underset{\{b, S_1, S_2\} \in \mathbb{Z}^+}{\text{maximize}} \quad \frac{1}{N} \frac{b}{K S_1 + \binom{K}{G} S_2} \quad (6.25a)$$

$$\text{s.t.} \quad M S_1 \geq b \quad (6.25b)$$

$$N S_1 < b \quad (6.25c)$$

$$N S_2 \leq (G - 1) N S_1 - (G - 2)b \quad (6.25d)$$

$$N(S_1 + \alpha(G) \cdot S_2) \geq b. \quad (6.25e)$$

While the objective function corresponds to number of symbols delivered per user divided by the duration of the communication, and normalized, the different constraints imposed to ensure linear feasibility are next described:

Algorithm 6.2: G solver

Step 1: For a given value of ρ , find $x \in \{2, \dots, K\}$ minimizing

$$\rho - \frac{1+\alpha(x) \cdot (x-1)}{1+\alpha(x) \cdot (x-2)}, \text{ with } \rho \geq \frac{1+\alpha(x) \cdot (x-1)}{1+\alpha(x) \cdot (x-2)}, \alpha(x) = \binom{K-1}{x-1}$$

Step 2: $y := \frac{1+\alpha(x) \cdot (x-1)}{K+(x(x-2)+1)\binom{K}{x}}, z := \frac{x+1}{K} \frac{\rho}{\rho+x}$

Step 3: $G(\rho) = \begin{cases} x & x \in \{2, K\} \\ x & 2 < x < K, y > z \\ x-1 & \text{otherwise} \end{cases}$

Transmit rank during the IIS phase (6.25b): During the first phase, MS_1 linear combinations of the b symbols are transmitted using M antennas, and during S_1 slots. Then, for linear decodability of the desired symbols, no more symbols than the number of transmit dimensions can be sent, thus we force $MS_1 \geq b$.

Need of RIA phase (6.25c): Since the first phase provides NS_1 interference-free linear observations of the desired symbols, we force $NS_1 < b$.

Non-redundant RIA phase (6.25d): The precoding matrices for each round of the second phase lie on a subspace of dimension φ , see (6.22a) and (6.23a), and they are used during S_2 slots. Then, to avoid redundancy on the received signals, we force that no more than φ linear combinations are obtained at the receivers, i.e. $S_2 < \varphi$.

Linear combinations at the end of the transmission (6.25e): Each round of the first phase provides NS_1 LCs of desired symbols to each receiver, while each round of the second phase $\min(MS_2, NS_2, \varphi) = NS_2$, which follows from $M > N$ the previous constraint. Hence, since each user is active during $\alpha(G)$ rounds of the RIA phase the number of interference-free linear combinations of desired symbols obtained at the end of the transmission are $NS_1 + \alpha(G) \cdot NS_2$, and they should be enough for linearly decoding the b desired symbols.

This problem will be handled as problem \mathcal{P}_1 . First, S_2 is removed by setting it to its minimum feasible integer value, i.e.

$$S_2^* = \left\lceil \frac{1}{\alpha(G)} \left(\frac{b}{N} - S_1 \right) \right\rceil, \quad (6.26)$$

dictated by (6.25e). Then, (6.25d) forces that:

$$(G-1)NS_1 - (G-2)b \geq N \left\lceil \frac{1}{\alpha(G)} \left(\frac{b}{N} - S_1 \right) \right\rceil \geq N \frac{1}{\alpha(G)} \left(\frac{b}{N} - S_1 \right), \quad (6.27)$$

Therefore, S_1 may be written as follows:

$$S_1^* = \left\lceil b \cdot \max \left(\frac{1}{M}, \frac{1}{N} \frac{1+\alpha(G) \cdot (G-2)}{1+\alpha(G) \cdot (G-1)} \right) \right\rceil, \quad (6.28)$$

where B.I and B.II follow from choosing one of the two values above, with the threshold given by $\rho_B(G) = \frac{1+\alpha(G) \cdot (G-1)}{1+\alpha(G) \cdot (G-2)}$.

6.2.3 3-user PSR Scheme ($M \approx N$)

The scheme of $P = 3$ phases proposed in [AGK13] for the 3-user SISO IC is generalized to the 3-user MIMO case, proving Theorem 6.2. Moreover, Theorem 6.3 for $(\rho_x, \rho_y(K))$ follows from applying this scheme together with time-sharing concepts. Next section gives an intuition behind this strategy. Then, each of the phases is built, and finally we present the optimization problem that provides the optimal system parameters for any antenna setting.

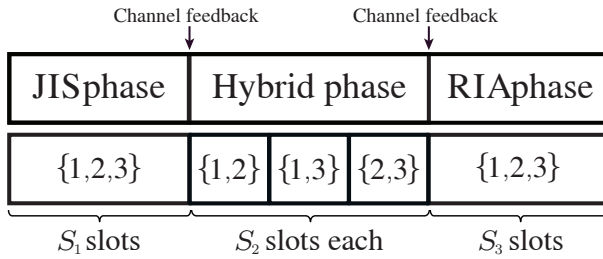


Figure 6.5: Transmission frame for the PSR scheme. Each phase p has $\binom{K}{p}$ rounds of S_p slots. Active groups $\mathcal{G}^{(p,r)}$ are represented for each round of the three phases.

Overview of the precoding strategy

This approach is designed according to the three ingredients exploited so far: *delayed CSIT precoding*, *user scheduling*, and *redundancy transmission*. For this reason, it is denoted as the Precoding, Scheduling, Redundancy scheme. The first and third phases will be labeled as the JIS and RIA phases, as those phases for the RIA scheme. In a similar manner, the objective is to jointly sense the interference for the former and to transmit signals do not causing additional interference for the latter, i.e. aligned with the overheard interference. This is achieved by exploiting only *delayed CSIT precoding* and *redundancy transmission*, thus all users are active during those phases. But, a *hybrid phase* developed by pairs is introduced as the second phase. The objective of the hybrid phase is twofold. First, each transmitter based on channel feedback reconstructs the overheard information created at each receiver during the JIS phase to deliver desired linear combinations of symbols. Second, some redundancy is sent in order to create the overheard interference terms that will be used during the last phase. Hence, all the three ingredients are mixed up in this phase in pursuit of DoF maximization. According to all these ideas, we have:

$$R_1 = R_3 = 1, \quad R_2 = \binom{3}{2} = 3, \quad (6.29)$$

$$G_1 = G_3 = 3, \quad G_2 = 2, \quad (6.30)$$

also summarized in Fig. 6.5. The optimal system parameters are derived at the end of this section, and specified in Table 6.5. Recall that $\rho_{PSR,1} \approx 0.7545$, $\rho_{PSR,2} \approx 0.7847$, see (6.3) and (6.4), which means that regimes C.II and C.III require $M, N > 10$. Moreover, it can be seen that this scheme is always outperformed by the RIA scheme for regime C.I. Therefore, the most significant finding in this case is that the DoF inner bound for SISO ($d_j^{(\text{in})} = \frac{12}{31}$) is valid whenever $\rho \geq \frac{4}{5}$. Consequently, next sections focus on regime C.IV for simplicity on the description.

Table 6.5: System parameters for the PSR scheme as a function of ρ

	b	S_1	S_2	S_3	$d_j^{(in)}$
C.I = $\{\frac{1}{2} < \rho \leq \rho_{PSR,1}\}$	M^3	M^2	$M(N - M)$	$2(N - M)^2$	$\frac{\rho^3}{2-\rho}$
C.II = $\{\rho_{PSR,1} < \rho \leq \rho_{PSR,2}\}$	$2M^2N$	$2MN$	$2N(N - M)$	$5M^2 - 6MN + 2N^2$	$\frac{2\rho^2}{5\rho^2 - 10\rho + 8}$
C.III = $\{\rho_{PSR,2} < \rho < \frac{4}{5}\}$	$6MN$	$6N$	$4N - 3M$	$4(3M - 2N)$	$\frac{6\rho}{3\rho + 10}$
C.IV = $\{\rho \geq \frac{4}{5}\}$	$12N$	15	4	4	$\frac{12}{31}$

Joint interfering sensing phase

The first phase lasts for S_1 slots where transmitters have no CSI, thus they transmit with generic full-rank precoding matrices $\mathbf{V}_i^{(1)} \in \mathbb{C}^{MS_1 \times b}$ selected from a predetermined dictionary known by all nodes. The development of this phase is exactly the same as for the RIA scheme, with the dimensions specified in Table 6.5, where $b = 12N$, $S_1 = 15$. Then, similarly we define the receiving filter $\mathbf{U}_j^{(1)} \in \mathbb{C}^{2\varphi_1 \times NS_1}$, $\forall i \neq j$, with

$$\varphi_1 = \min(NS_1 - b, b) = 3N, \quad (6.31)$$

which consists of the composition of two linear filters $\mathbf{U}_{j,i}^{(1)} \in \mathbb{C}^{\varphi_1 \times NS_1}$, $i \neq j$, defined such that (6.8) is satisfied. Then, $\mathbf{T}_{j,i} = \mathbf{U}_{j,i}^{(1)} \mathbf{H}_{j,i}^{(1)} \mathbf{V}_i^{(1)} \in \mathbb{C}^{\varphi_1 \times b}$, $i \neq j$ is again defined representing the residual interference from TX_i after applying the linear filter $\mathbf{U}_{j,i}^{(1)}$, and subspaces $\mathcal{T}_{j,i} = \text{rspan}(\mathbf{T}_{j,i})$. Next table summarizes the acquired OHI at RX₁ along the whole communication.

Table 6.6: Served users per round and acquired OHI at RX₁ for each round for the 3-user PSR scheme.

Phase (p)	Round (r)	$\mathcal{G}^{(p,r)}$	Acquired OHI at RX ₁ after processing
1	1	{1}	—
	2	{2}	$\mathbf{T}_{1,2} \mathbf{x}_2$
	3	{3}	$\mathbf{T}_{1,3} \mathbf{x}_3$
2	1	{1, 2}	—
	2	{1, 3}	—
	3	{2, 3}	$\mathbf{F}_{3,2}^{\{1\}} \mathbf{x}_2, \mathbf{F}_{2,3}^{\{1\}} \mathbf{x}_3$
3	1	{1, 2, 3}	—

Hybrid phase

The transmission is developed by pairs, where each pair transmits during $S_2 = 4$ slots. The objective of this phase is twofold. First, each transmitter exploits the overheard information available at each receiver after the JIS phase to deliver desired linear combinations of symbols, similarly to the second phase of the TG scheme (Section 6.20) when

$G = 2$. Second, each transmitter sends some redundancy in order to create overheard interference that will be seized during the last phase.

Consider the $(2, r)$ th round, with active users $\mathcal{G}^{(2,r)} = \{i, j\}$. The transmitted signals are designed such that

$$\text{rspan}\left(\mathbf{H}_{i,j}^{(2,r)} \mathbf{V}_j^{(2,r)}\right) \subseteq \mathcal{T}_{i,j}, \quad \text{rspan}\left(\mathbf{H}_{j,i}^{(2,r)} \mathbf{V}_i^{(2,r)}\right) \subseteq \mathcal{T}_{j,i}, \quad (6.32)$$

thus the precoding matrices are set to

$$\mathbf{V}_i^{(2,r)} = \boldsymbol{\Sigma}_i^{(2,r)} \mathbf{T}_{j,i}, \quad \mathbf{V}_j^{(2,r)} = \boldsymbol{\Sigma}_j^{(2,r)} \mathbf{T}_{i,j}, \quad (6.33)$$

where $\boldsymbol{\Sigma}_i^{(2,r)}, \boldsymbol{\Sigma}_j^{(2,r)} \in \mathbb{C}^{MS_2 \times \varphi_1}$ are some arbitrary full rank matrices ensuring the transmit power constraint. For each active pair, $NS_2 = 4N$ LCs of symbols are received, although the rank of the transmitted signals is

$$\text{rank}\left(\mathbf{V}_i^{(2,r)}\right) = \min(MS_2, \dim(\mathcal{T}_{j,i})) = \varphi_1 = 3N, \quad (6.34)$$

thus there exists some redundancy on the received signals. In this case the per-phase receiving filters are defined as follows:

$$\begin{aligned} \mathbf{U}_1^{(2)} &= \text{bdiag}\left(\mathbf{I}, \mathbf{I}, \text{stack}\left(\mathbf{U}_{1,2}^{(2)}, \mathbf{U}_{1,3}^{(2)}\right)\right), \\ \mathbf{U}_2^{(2)} &= \text{bdiag}\left(\mathbf{I}, \text{stack}\left(\mathbf{U}_{2,1}^{(2)}, \mathbf{U}_{2,3}^{(2)}\right), \mathbf{I}\right), \\ \mathbf{U}_3^{(2)} &= \text{bdiag}\left(\text{stack}\left(\mathbf{U}_{3,1}^{(2)}, \mathbf{U}_{3,2}^{(2)}\right), \mathbf{I}, \mathbf{I}\right). \end{aligned}$$

where $\mathbf{U}_{j,i}^{(2)} \in \mathbb{C}^{\varphi_2 \times NS_2}$, with

$$\varphi_2 = \min(NS_2 - \varphi_1, \varphi_1) = N. \quad (6.35)$$

Note that the received signal is modified only for the round where all transmitted signals are interference. The objective of this processing is to obtain signal spaces where the desired signals are interfered by only one user, which will be useful to align the interference during the last phase. For example, the processed signal at the first receiver for the $(2, 3)$ th round writes as:

$$\mathbf{z}_1^{(2,3)} = \begin{bmatrix} \mathbf{U}_{1,2}^{(2)} \\ \mathbf{U}_{1,3}^{(2)} \end{bmatrix} \begin{bmatrix} \mathbf{H}_{1,2}^{(2,3)} \mathbf{V}_2^{(2,3)}, \mathbf{H}_{1,3}^{(2,3)} \mathbf{V}_3^{(2,3)} \end{bmatrix} \begin{bmatrix} \mathbf{x}_2 \\ \mathbf{x}_3 \end{bmatrix} = \begin{bmatrix} \mathbf{F}_{3,2}^{\{1\}} & \mathbf{0} \\ \mathbf{0} & \mathbf{F}_{2,3}^{\{1\}} \end{bmatrix} \begin{bmatrix} \mathbf{x}_2 \\ \mathbf{x}_3 \end{bmatrix}, \quad (6.36)$$

where $\mathbf{F}_{k,i}^{\{j\}} \in \mathbb{C}^{\varphi_2 \times b}$ is defined as

$$\mathbf{F}_{k,i}^{\{j\}} = \mathbf{U}_{j,i}^{(2)} \mathbf{H}_{j,i}^{(2,r)} \mathbf{V}_i^{(2,r)} = \mathbf{U}_{j,i}^{(2)} \mathbf{H}_{j,i}^{(2,r)} \boldsymbol{\Sigma}_i^{(2,r)} \mathbf{T}_{k,i} \quad (6.37)$$

$$\mathcal{F}_{k,i}^{\{j\}} = \text{rspan}(\mathbf{F}_{k,i}^{\{j\}}) \subset \mathcal{T}_{k,i}, \quad (6.38)$$

i.e. $\mathcal{F}_{k,i}^{\{j\}}$ is the remaining contribution of $\mathbf{V}_i^{(2,r)}$ at RX_j after suppressing the signal corresponding to user k , i.e. the other active transmitter during the $(2, r)$ th round. Moreover, it represents the subspace of $\mathcal{T}_{k,i}$ (completely known at RX_k) that is known

thanks to this phase at RX_j , as summarized for RX_1 in Table 6.6. For a better reader's understanding, let us write the signal space matrix obtained at RX_1 after this phase:

$$\Omega_1^{(1:2)} = \begin{bmatrix} \mathbf{U}_{1,2}^{(1)} \mathbf{H}_{1,1}^{(1)} \mathbf{V}_1^{(1)} & \mathbf{T}_{1,2} & \mathbf{0} \\ \mathbf{U}_{1,3}^{(1)} \mathbf{H}_{1,1}^{(1)} \mathbf{V}_1^{(1)} & \mathbf{0} & \mathbf{T}_{1,3} \\ \hline \mathbf{H}_{1,1}^{(2,1)} \mathbf{V}_1^{(2,1)} & \mathbf{H}_{1,2}^{(2,1)} \mathbf{V}_2^{(2,1)} & \mathbf{0} \\ \mathbf{H}_{1,1}^{(2,2)} \mathbf{V}_1^{(2,2)} & \mathbf{0} & \mathbf{H}_{1,3}^{(2,2)} \mathbf{V}_3^{(2,2)} \\ \mathbf{0} & \mathbf{F}_{3,2}^{\{1\}} & \mathbf{0} \\ \mathbf{0} & \mathbf{0} & \mathbf{F}_{2,3}^{\{1\}} \end{bmatrix}. \quad (6.39)$$

where the dotted lines separate the signals corresponding to each phase.

Finally, the number of interference-free LC of desired signals each receiver can retrieve after this phase is summarized. On the one hand, since at each receiver the signals of each round occupy $NS_2 = 4N$ dimensions, and the interference has rank $\varphi_1 = 3N$ only, there exists almost surely a φ_2 -dimensional subspace where interference can be projected to. Then, from the two pairs $2 \cdot \min(\varphi_1, \varphi_2) = 2N$ LCs are obtained. On the other hand, since precoding matrices are designed to align the interference (conditions in (6.32)), RX_j will be able to combine the first phase processed signals with the second phase received signals to cancel the interference. Consequently, $2\varphi_1 = 6N$ additional interference-free LCs of desired signals are retrieved, and only $b - 8N = 4N$ more LCs are required for ensuring linear decodability.

Retrospective interference alignment phase

The third phase lasts for $S_3 = 4$ slots, where all users are active. The objective is to design the transmitted signals based on the information commonly known at the non-intended receivers after the first two phases. The precoding matrices for this phase are constructed as follows:

$$\mathbf{V}_1^{(3)} = \boldsymbol{\Sigma}_1^{(3)} \begin{bmatrix} \mathbf{F}_{2,1}^{\{3\}} \\ \mathbf{F}_{3,1}^{\{2\}} \end{bmatrix}, \quad \mathbf{V}_2^{(3)} = \boldsymbol{\Sigma}_2^{(3)} \begin{bmatrix} \mathbf{F}_{1,2}^{\{3\}} \\ \mathbf{F}_{3,2}^{\{1\}} \end{bmatrix}, \quad \mathbf{V}_3^{(3)} = \boldsymbol{\Sigma}_3^{(3)} \begin{bmatrix} \mathbf{F}_{1,3}^{\{2\}} \\ \mathbf{F}_{2,3}^{\{1\}} \end{bmatrix} \quad (6.40)$$

where $\boldsymbol{\Sigma}_i^{(3)} \in \mathbb{C}^{MS_3 \times 2\varphi_2}$. This design ensures that all the generated interference is already known at both non-intended receivers, thus receivers will be able to remove it. Moreover, each receiver observes $NS_3 = 4N$ linear combinations of the transmitted signals of rank

$$\text{rank}(\mathbf{V}_i^{(3)}) = \dim(\mathcal{F}_{j,i}^{\{k\}} + \mathcal{F}_{k,i}^{\{j\}}) \quad (6.41a)$$

$$= \dim(\mathcal{F}_{j,i}^{\{k\}}) + \dim(\mathcal{F}_{k,i}^{\{j\}}) = 2\varphi_2 = 2N, i \neq j \neq k. \quad (6.41b)$$

Then, the same idea as for the second phase applies here: some redundancy is transmitted in order to apply zero-forcing concepts at the receiver. Following the same notation as before, two linear filters $\mathbf{U}_{j,i}^{(3)} \in \mathbb{C}^{\varphi_3 \times NS_3}, j \neq i$, are applied at each receiver, with

$$\varphi_3 = \min(NS_3 - 2\varphi_2, 2\varphi_2) = 2N, \quad (6.42)$$

For brevity and clarity, the final signal space matrix at RX₁ is next shown:

$$\Omega_1 = \begin{bmatrix} \mathbf{U}_{1,2}^{(1)} \mathbf{H}_{1,1}^{(1)} \mathbf{V}_1^{(1)} & \mathbf{T}_{1,2} & \mathbf{0} \\ \mathbf{U}_{1,3}^{(1)} \mathbf{H}_{1,1}^{(1)} \mathbf{V}_2^{(1)} & \mathbf{0} & \mathbf{T}_{1,3} \\ \hline \mathbf{H}_{1,1}^{(2,1)} \mathbf{V}_1^{(2,1)} & \mathbf{H}_{1,2}^{(2,1)} \mathbf{V}_2^{(2,1)} & \mathbf{0} \\ \mathbf{H}_{1,1}^{(2,2)} \mathbf{V}_1^{(2,2)} & \mathbf{0} & \mathbf{H}_{1,3}^{(2,2)} \mathbf{V}_3^{(2,2)} \\ \mathbf{0} & \mathbf{F}_{3,2}^{\{1\}} & \mathbf{0} \\ \mathbf{0} & \mathbf{0} & \mathbf{F}_{2,3}^{\{1\}} \\ \hline \mathbf{U}_{1,2}^{(3)} \mathbf{H}_{1,1}^{(3)} \mathbf{V}_1^{(3)} & \mathbf{U}_{1,2}^{(3)} \mathbf{H}_{1,2}^{(3)} \mathbf{V}_2^{(3)} & \mathbf{0} \\ \mathbf{U}_{1,3}^{(3)} \mathbf{H}_{1,1}^{(3)} \mathbf{V}_1^{(3)} & \mathbf{0} & \mathbf{U}_{1,3}^{(3)} \mathbf{H}_{1,3}^{(3)} \mathbf{V}_3^{(3)} \end{bmatrix}, \quad (6.43)$$

where the signals received during the RIA phase are processed using $\mathbf{U}_{1,2}^{(3)}$ and $\mathbf{U}_{1,3}^{(3)}$, see the last two blocks rows. Now it is easy to see that all the interference is aligned. For example, consider the 1st, 5th and 7th block rows. Since

$$\text{rspan} \left(\mathbf{U}_{1,2}^{(3)} \mathbf{H}_{1,2}^{(3)} \mathbf{V}_2^{(3)} \right) \subseteq \text{rspan} \left(\mathbf{V}_2^{(3)} \right), \quad (6.44a)$$

$$\text{rspan} \left(\mathbf{V}_2^{(3)} \right) \subseteq \mathcal{F}_{3,2}^{\{1\}} + \mathcal{F}_{1,2}^{\{3\}}, \quad (6.44b)$$

$$\mathcal{F}_{1,2}^{\{3\}} \subset \mathcal{T}_{1,2}, \quad (6.44c)$$

the signals corresponding to the 1st and 5th block rows can be used to remove the interference from the signals represented by the 7th block row. Then, $2\varphi_2$ LCs of desired signals are retrieved. Following similar arguments for rows 2nd, 6th, and 8th, $2N$ extra LCs are obtained. Combining the $4\varphi_2 = 4N$ LCs of desired signals obtained from this phase with the $8N$ LCs from previous phases, each receiver obtains enough LCs for linearly decode all of its $b = 12N$ desired symbols.

System parameters optimization

The parameters for the PSR scheme are derived by means of the following DoF optimization problem:

$$\mathcal{P}_3 : \underset{\{b, \varphi_1, \varphi_2, \varphi_3\} > 0}{\text{maximize}} \quad \frac{b}{b + 4\varphi_1 + 5\varphi_2 + \varphi_3} \quad (6.45a)$$

$$\text{s.t.} \quad \rho(\varphi_1 + b) \geq b \quad (6.45b)$$

$$4\varphi_1 \geq b \quad (6.45c)$$

$$\rho(\varphi_1 + \varphi_2) \geq \varphi_1 \quad (6.45d)$$

$$\varphi_2 \leq \varphi_1 \quad (6.45e)$$

$$2(\varphi_1 + \varphi_2) < b \quad (6.45f)$$

$$\rho(\varphi_3 + 2\varphi_2) \geq 2\varphi_2 \quad (6.45g)$$

$$2(\varphi_1 + \varphi_2 + \varphi_3) \geq b \quad (6.45h)$$

$$\varphi_3 \leq 2\varphi_2 \quad (6.45i)$$

formulated in terms of $\varphi_i > 0, i = 1, 2, 3$, where the number of slots can be retrieved by applying the following change of variables:

$$\varphi_1 = NS_1 - b, \quad \varphi_2 = NS_2 - \varphi_1, \quad \varphi_3 = NS_3 - 2\varphi_2. \quad (6.46)$$

While the objective function corresponds to $\frac{b}{N\tau}$ in terms of the new variables, the constraints imposed to ensure linear feasibility are next described:

Transmit rank during the JIS phase (6.45b): Similarly to other schemes, $MS_1 \geq b$ is imposed to ensure the transmit rank.

Linear combinations on the system (6.45c): After the first phase processing, $4\varphi_1$ linear combinations of the symbols of each user are distributed along the receivers: $2\varphi_1$ at the intended receiver (known coupled with interference), and φ_1 at each non-intended receiver. Then, since the rest of phases are just retransmissions, a necessary condition is that at least obtaining all of them the b desired symbols should be linearly decodable.

Transmit rank during the hybrid phase (6.45d): Written in terms of the new variables, it is forced $MS_2 \geq \varphi_1$, since the rank of the transmitted signals during each second phase round is equal to φ_1 , see (6.34).

Bounded redundancy during the hybrid phase and need of RIA phase (6.45e) and (6.45f): After the hybrid phase, each receiver is able to retrieve $\varphi_1 + \varphi_2$ interference-free LCs of desired symbols from each of the two rounds where desired LCs of signals are sent. First, exploiting the redundancy on the received signals due to $\varphi_2 = NS_2 - \varphi_1 > 0$, $\min(\varphi_1, \varphi_2)$ linear combinations can be retrieved by zero-forcing concepts. Then, we force (6.45e), since having $\varphi_2 > \varphi_1$ does not provide additional LCs. This constraint bounds the value of S_2 , and it is also imposed by $\mathcal{F}_{k,i}^{\{j\}} \subset \mathcal{T}_{k,i}$, as assumed in (6.38).

On the other hand, φ_1 LCs are obtained through RIA concepts, by projecting the signals of the corresponding round of the hybrid phase onto a subspace of dimension φ_1 , and combining them with the JIS phase processed signals. Consequently, at the end of the hybrid phase $2(\varphi_1 + \varphi_2)$ independent observations are obtained. (6.45f) ensures that still some extra LCs are required, and thus RIA phase is necessary.

Transmit rank during the RIA phase (6.45g): Written in terms of the new variables, it is forced $MS_3 \geq 2\varphi_2$, see (6.33).

Linear combinations at the end of the transmission (6.45h) and bounded redundancy during the RIA phase (6.45i): The signal received during the RIA phase is processed to decouple the interference, see (6.43). Those processed signals combined with the rest of available overheard interference provide $2 \cdot \min(\varphi_3, 2\varphi_2)$ extra observations of the desired symbols. First, (6.45i) is forced to bound the value of S_3 , and because in this case more redundancy does not provide additional LCs. Second, the number of interference-free LCs of desired signals each receiver is able to retrieve at the end of the transmission is equal to $2 \cdot (\varphi_1 + \varphi_2 + \varphi_3)$, and it should be enough to linearly decode all the b desired symbols.

The problem \mathcal{P}_3 in (6.45) is next solved. Before proceeding, let us introduce the following

proposition:

Proposition 6.4 *Consider the following two linear inequalities:*

$$ax + by \geq cz, \quad (6.47a)$$

$$dx + ey \leq fz, \quad (6.47b)$$

where $\{a, b, c, d, e, f\}$ are positive given parameters, and $\{x, y, z\}$ represent unknown variables. Then, any solution satisfying both inequalities also satisfies:

$$cdx + cey \leq fax + fby. \quad (6.48)$$

This trivial proposition is useful because it allows suppressing variables from linear constraints. Actually, it is the basis of the Fourier-Motzkin Elimination method, see [DE73].

Consider the application of Proposition 1 to (6.45g), (6.45h), and (6.45i), such that variable φ_3 is removed. This leads to the following two constraints:

$$2(\varphi_1 + 3\varphi_2) \geq b, \quad (6.49)$$

$$\varphi_2(1 - 2\rho) \geq 0, \quad (6.50)$$

where the second constraint forces $\rho \geq \frac{1}{2}$. Now, let us apply again the proposition to (6.45e), (6.45f), and the new constraint (6.49) in order to remove φ_2 . Again, two new constraints are produced:

$$\begin{aligned} 8\varphi_1 &\geq b \\ \varphi_1(1 - 2\rho) &\geq 0, \end{aligned}$$

which are loose with respect to the rest of constraints. Then, the value of φ_1 is completely determined by (6.45b) and (6.45c), as follows:

$$\varphi_1 = b \max\left(\frac{1}{4}, \frac{1 - \rho}{\rho}\right), \quad (6.51)$$

thus establishing two regions: $\rho \geq \frac{4}{5}$ and $\rho < \frac{4}{5}$. For a given value of φ_1 , the optimal φ_2 is decided according to (6.45e) and (6.49), as follows:

$$\varphi_2 = \max\left(\varphi_1 \frac{1 - \rho}{\rho}, \frac{1}{6}(b - 2\varphi_1)\right). \quad (6.52)$$

Finally, the optimal value of φ_3 is set according to

$$\varphi_3 = \max\left(2\varphi_2 \frac{1 - \rho}{\rho}, \frac{b}{2} - \varphi_1 - \varphi_2\right). \quad (6.53)$$

It can be checked that the control constraints (6.45f) and (6.45g) are always satisfied following these rules. The values in Table 6.5 are obtained by inverting the change of variables and taking the value of b such that S_1 , S_2 , and S_3 are integer values.

6.3 DoF-Delay Trade-Off

The precoding schemes exploiting delayed CSIT require multi-phase transmissions. For some settings, this entails long communication delays, and a high number of transmitted symbols, thus increasing the complexity of the encoding/decoding operation at transmitters/receivers. This section studies the DoF-delay trade-off of the proposed and some state-of-the-art schemes. Thanks the DoF-delay trade-off analysis, two main insights are concluded:

- The supremacy in terms of achievable DoF of one scheme w.r.t. another depends on the allowed complexity of the transmission, i.e. number of transmitted symbols or duration of the communication. For example, when $\rho = 1$, $K = 3$, the RIA scheme outperforms the PSR scheme given a maximum number of time slots allowed for the communication.
- The communication delay can be highly alleviated without high DoF penalties. Many examples are provided showing the balance between optimal (but usually large) parameters and maximum DoF w.r.t. practical parameters and competitive achievable DoF.

Two methodologies are used in the sequel to study the DoF-delay trade-off of the proposed schemes. First, the following three sections analyze this trade-off by limiting the maximum number of symbols per user that can be transmitted to B , i.e. by introducing the following constraint into the system parameters optimization problems:

$$b \leq B.$$

The case where this constraint is omitted or, equivalently, $B \rightarrow \infty$, will be hereafter denoted as the *unbounded case*. For each scheme, a simplified version of the DoF optimization problem for finite B is provided. Then, at least two examples are evaluated for each case, one for $K = 3$ and one for $K = 6$, which are useful to benchmark one of the values of ρ in Fig. 6.2 as a function of B .

On the other hand, Section 6.3.4 proposes an alternative approach for comparing the proposed schemes to the PSR scheme in [AGK13] and its extension to MISO for $K > 3$ in [HC15]. Notice that the first methodology could also be used, but currently we do not have derived DoF optimization problems for those schemes, which remains as future work.

Adopting this second methodology, the DoF-delay trade-off is studied by limiting the order of the transmitted symbols. Although the formulation up to this section works with order-1 symbols and order-1 DoF, the works in the literature usually follow the high-order symbol framework, see e.g. [MAT12], reviewed in Section 5.2.1. Inspired by this formulation, we propose to bound the schemes in [AGK13] and [HC15] to maximum order Θ by forcing:

$$d_j^{(\Theta, \text{in})} = 1. \quad (6.54)$$

6.3.1 RIA Scheme

A closed-form solution for S_1 and S_2 was obtained in Section 6.2.1, see (6.15) and (6.16). For unbounded b , the value of L was obtained given ρ and K by means of Algorithm 6.1. However, for finite B the optimal value of L becomes a function of B . In this regard, the achievable DoF for the RIA scheme write as follows:

$$d_j(B) = \frac{1}{KN} \max(f_{\text{RIA},1}(B), f_{\text{RIA},2}(B)), \quad (6.55a)$$

$$f_{\text{RIA},1}(x) = \underset{b \leq x, L}{\text{maximize}} \frac{bL}{\lceil \frac{b}{M} \rceil + \lceil \frac{b}{N} \rceil}, \quad (6.55b)$$

$$f_{\text{RIA},2}(x) = \underset{b \leq x, L}{\text{maximize}} \frac{bL}{\lceil \frac{b}{N} \frac{L^2 - L - 1}{L} \rceil + \lceil \frac{b}{N} \rceil}, \quad (6.55c)$$

where $f_{\text{RIA},1}(x)$ and $f_{\text{RIA},2}(x)$ represent the achievable DoF for each side of the stepping function in Figs. 6.2-top and 6.2-bottom, or in Theorem 6.3. Since the value of L depends on B , it is not possible to derive a threshold as $\rho_A(L)$. Then, we maximize w.r.t. L and b , and then just take the maximum between the two sides of the stepping function.

The maximization problem as a function of B has been solved for the two settings: $(M, N, K) = (4, 7, 3)$, and $(M, N, K) = (3, 4, 6)$, where the solutions follow the expressions given in (6.55a)-(6.55b). The achievable DoF w.r.t. the communication delay are depicted in Fig. 6.6-top for $B = 1 \dots b^*$, where b^* denotes for each case the optimal value of b for the unbounded case. Moreover, the DoF achieved without the need of CSIT are also included for comparison. First, notice that since $L \in \{3, \dots, K\}$, the only possible value for the first setting is $L = 3$. In such a case, since $\rho < \rho_A(3) = \frac{3}{5}$, it follows

$$d_j(B) = \frac{1}{KN} f_{\text{RIA},1}(B).$$

The more interesting conclusion from this analysis is that the number of required slots can be dramatically reduced without high DoF penalties. In particular, the number of time slots may be halved (from 11 to 5), while 94% of the maximum DoF are attained (from 0.3636 to 0.3429). In contrast, for the setting $(M, N, K) = (3, 4, 6)$ the value of L changes as a function of B , as highlighted in Fig. 6.6, top-right. Notice that in this case the number of slots required to outperform TDMA is huge, and DoF gains are insignificant.

The reader may have noticed that the cases with $\rho > \frac{3}{5}$ have been omitted. In this regard, two additional examples will be shown for the RIA scheme in Section 6.3.3, deferred to that section in order to compare together the RIA and PSR schemes performance for limited B .

6.3.2 TG Scheme

Closed form solutions for S_1^* and S_2^* were found in Section 6.23, see (6.26) and (6.28), next restated for reader's convenience. Note that S_2^* depends on the value taken for S_1^* , which depend on the antenna ratio and B . In this case, the achievable DoF for a given

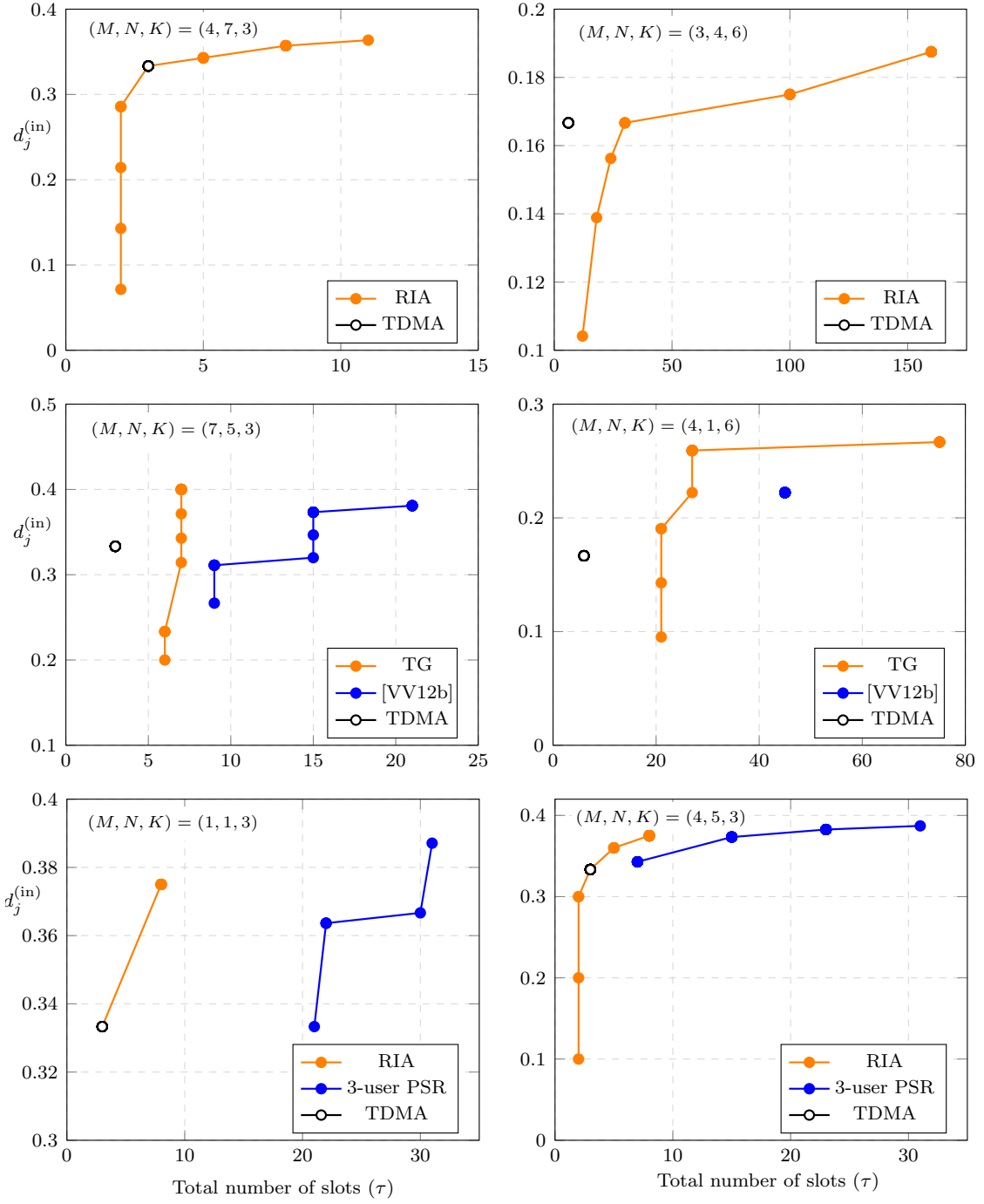


Figure 6.6: Achievable DoF of the proposed schemes vs duration of the transmission τ for different values of B . The DoF achieved without the need of CSIT or using previous schemes in the literature are also depicted for comparison purposes.

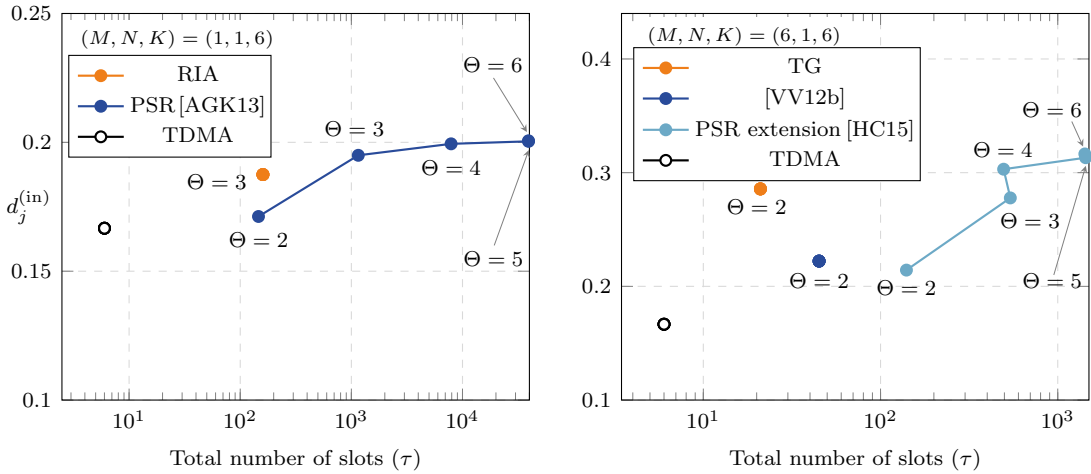


Figure 6.7: Achievable DoF of the proposed schemes vs duration of the transmission τ for different values of the maximum order of the transmitted symbols Θ . The DoF achieved without the need of CSIT or using previous schemes in the literature are also depicted for comparison purposes.

B write as follows:

$$d_j(B) = \underset{b \leq B, G}{\text{maximize}} \frac{1}{N} \frac{b}{KS_1^* + \binom{K}{G} S_2^*}, \quad (6.56a)$$

$$S_1^* = \left\lceil b \cdot \max \left(\frac{1}{M}, \frac{1}{N} \frac{1 + \alpha(G) \cdot (G - 2)}{1 + \alpha(G) \cdot (G - 1)} \right) \right\rceil, \quad (6.56b)$$

$$S_2^* = \left\lceil \frac{1}{\alpha(G)} \left(\frac{b}{N} - S_1^* \right) \right\rceil, \quad \alpha(G) = \binom{K - 1}{G - 1}. \quad (6.56c)$$

Two settings are simulated and shown in Fig. 6.6-middle: $(M, N, K) = (7, 5, 3)$, and $(M, N, K) = (4, 1, 6)$. While the curves have been obtained by solving the problem \mathcal{P}_2 in (6.25), one can check that they follow the expressions in (6.56a)-(6.56c). For comparison purposes, in addition to the TDMA performance, the scheme in [VV12b] for the 2-user IC has been considered. This scheme is applied to the K -user case by means of time-sharing, which dramatically increases the communication delay. In order to obtain its performance for different values of B , a DoF maximization problem has been formulated. The problem is very similar to the TG scheme with $G = 2$, and thus omitted.

In both cases it is observed how DoF gains are provided by the wise use of delayed CSIT w.r.t. no CSIT by increasing the duration of the communication τ . Two remarkable observations can be drawn, one for each setting. For the setting $(M, N, K) = (7, 5, 3)$ the DoF attained using delayed CSIT for both strategies are similar for the unbounded case. However, this is at the cost of a high communication delay for the scheme in [VV12b]. If otherwise τ is reduced, then the TG scheme clearly outperforms any other strategy.

On the other hand, for the setting $(M, N, K) = (4, 1, 6)$, it can be observed that the unbounded case requires $\tau = 75$ slots, while similar DoF gains can be obtained using only $\tau = 27$ slots, and also outperforming any other scheme. This is one of the main conclusions obtained from our analysis: while the best DoF are attained using a high number of time slots, usually one solution with reduced number of time slots can be found without high DoF penalties. The reader may have noticed that no case with $\rho > K - 1$

has been considered because the scheme in [HC15] surpasses the proposed TG scheme. One example for $K = 6$ will be addressed in Section 6.3.4.

6.3.3 PSR Scheme

The performance of the PSR scheme is compared to the RIA scheme for $K = 3$ users. Since the region of most interest for this scheme is $\rho > \frac{4}{5}$, we consider two representative antenna settings: $(M, N) = (4, 5)$, and SISO ($M = N = 1$). In this case, following the expressions given in Section 6.2.3 it is easy to see that:

$$\begin{aligned} S_1^* &= \left\lceil \frac{\varphi_1 + b}{N} \right\rceil = \left\lceil \frac{5}{4} \frac{b}{N} \right\rceil, \\ S_2^* &= \left\lceil \frac{\varphi_1 + \varphi_2}{N} \right\rceil = \left\lceil \frac{b}{3N} \right\rceil = \left\lceil \frac{2\varphi_2 + \varphi_3}{N} \right\rceil = S_3^*, \\ d_j(B) &= \underset{b \leq B}{\text{maximize}} \frac{1}{N} \frac{b}{S_1^* + 3S_2^* + S_3^*}. \end{aligned} \quad (6.57a)$$

The performance for the two settings is depicted in Fig. 6.6-bottom. The most remarkable result is that whenever B is below b^* , the RIA outperforms the PSR scheme. Moreover, notice that for the unbounded case a similar DoF performance (from 0.387 to 0.375) is obtained for RIA w.r.t. the PSR scheme with only a quarter of the number of slots (from 31 to 8).

6.3.4 DoF with Limited Order of Symbols

In order to compare the DoF-delay trade-off of the proposed schemes for $K > 3$ to other approaches in the literature, the DoF are depicted for different values of the maximum order of symbols Θ in Fig. 6.7. Two settings for $K = 6$ are considered: SISO at left, and $(M, N) = (6, 1)$ (MISO) at right. First, since the scale may be confusing, it is worth to remark that the first operation point of the PSR scheme outperforming the RIA scheme requires 1154 slots ($\Theta = 3$), in contrast to the 160 slots required by the latter. Also, it is remarkable how the number of slots grow when the order of the transmitted symbols is not limited, with negligible DoF gains. For example, when $\Theta = 4$ the achievable DoF require a quarter of the unbounded case communication delay (from 39258 to 7898), and provide a 95% of the unbounded case achievable DoF.

For the MISO case, the supremacy of the proposed schemes in terms of practical terms is evident. While the TG scheme requires only 21 slots, the first operation point outperforming its DoF performance ($\Theta = 4$) requires 495 slots. Also, notice that the gains from this latter point w.r.t. the unbounded case are negligible, while the number of slots increase threefold.

As a conclusion, it is observed that in pursuit of approaching the DoF outer bound it is better to increase the number of phases and the order to the transmitted symbols. However, when practical issues come into play, it is preferable to penalize the achievable DoF for the sake of complexity and communication latency.

6.4 Achievable DoF for Constant Channels

The literature on delayed CSIT always assumes that channel feedback incurs a delay larger than channel coherence time, i.e. the current channel is completely uncorrelated w.r.t. the channel that has been reported. However, this assumption is not always realistic in practice, since the transmitter has no way to know if the channel has changed. In this regard, this section studies the extreme case where the channel is constant, the transmitter is not aware of this, and performs a delayed CSIT strategy anyways. Then, the next sections prove Theorem 6.4, stating that all results so far also apply for constant channels.

The difference in the system model between constant and time-varying channels is that all block diagonal compositions of channels are simplified to Kronecker products. Let $\mathring{\mathbf{H}}_{j,i} \in \mathbb{C}^{N \times M}$ denote the channel between TX_i and RX_j for all τ slots of the communication, since the channels are constant. Then, we have

$$\mathbf{H}_{j,i} = \mathbf{I}_\tau \otimes \mathring{\mathbf{H}}_{j,i}.$$

It is instructive to particularize it to the SISO case, where channels become scaled identity matrices, i.e:

$$\mathbf{H}_{j,i} = \mathbf{I}_\tau \otimes \mathring{h}_{j,i} = \mathring{h}_{j,i} \mathbf{I}_\tau, \quad (6.58)$$

which exhibits lower diversity than MIMO channels.

6.4.1 RIA Scheme

This section proves that the RIA scheme described in Section 6.2.1 fails for the SISO case if channels are constant and $L = 3$. Next section will show that this scheme can be made feasible by means of exploiting asymmetric complex signaling concepts. Similar arguments allow showing feasibility for any other antenna setting with probability one.

During the first phase of the RIA scheme, all transmitters are active, using predetermined precoding matrices $\mathbf{V}_i^{(1)} \in \mathbb{C}^{5 \times 3}$, and interfering to all users. The received signal is processed using the per-phase linear filters $\mathbf{U}_{i,j} \in \mathbb{C}^{2 \times 5}$, in such a way that the desired signals are only mixed with interference from another user. Consider the signal space matrix for the signals received during the first phase:

$$\Omega_i^{(1)} = \begin{bmatrix} \mathbf{U}_{i,i+1} h_{i,i} \mathbf{V}_i^{(1)} & \mathbf{U}_{i,i+1} h_{i,i+1} \mathbf{V}_{i+1}^{(1)} & \mathbf{0} \\ \mathbf{U}_{i,i-1} h_{i,i} \mathbf{V}_{i-1}^{(1)} & \mathbf{0} & \mathbf{U}_{i,i+1} h_{i,i-1} \mathbf{V}_{i-1}^{(1)} \end{bmatrix} \quad (6.59)$$

where indices in this section are assumed to be in the set $\{1, 2, 3\}$, applying the modulo-3 operation only if necessary. Notice that matrices $\mathbf{U}_{i,j}$ satisfy

$$\text{rspan}(\mathbf{U}_{i,j}) = \text{null}\left(\text{span}(\mathbf{V}_k^{(1)})\right), \forall i, j \neq k, i \neq j, \quad (6.60)$$

i.e. $\mathbf{U}_{i,j}$ removes the interference generated at RX_i by user $k \neq j$, but not the interference from user j . Due to definition (6.60), there are only three different per-phase filters. Indeed, they correspond to the null space of each $\mathbf{V}_i^{(1)}$, which will be denoted as $\bar{\mathbf{V}}_i^{(1)} \in \mathbb{C}^{2 \times 5}$ for ease of description. Accordingly, the signal space matrix for the whole

communication writes as

$$\boldsymbol{\Omega}_i = \begin{bmatrix} h_{i,i} \bar{\mathbf{V}}_{i-1}^{(1)} \mathbf{V}_i^{(1)} & h_{i,i+1} \bar{\mathbf{V}}_{i-1}^{(1)} \mathbf{V}_{i+1}^{(1)} & \mathbf{0} \\ h_{i,i} \bar{\mathbf{V}}_{i+1}^{(1)} \mathbf{V}_{i-1}^{(1)} & \mathbf{0} & h_{i,i-1} \bar{\mathbf{V}}_{i+1}^{(1)} \mathbf{V}_{i-1}^{(1)} \\ \hline h_{i,i} \boldsymbol{\Sigma}_i^{(2)} \mathbf{T}_i^{(2)} & h_{i,i+1} \boldsymbol{\Sigma}_{i+1}^{(2)} \mathbf{T}_{i+1}^{(2)} & h_{i,i-1} \boldsymbol{\Sigma}_{i-1}^{(2)} \mathbf{T}_{i-1}^{(2)} \end{bmatrix}, \quad (6.61)$$

where the precoding matrices for the second phase are computed following (6.12a) and (6.12b), here repeated for reader's convenience:

$$\begin{aligned} \mathbf{V}_i^{(2)} &= \boldsymbol{\Sigma}_i^{(2)} \mathbf{T}_i^{(2)}, \\ \text{rspan}(\mathbf{T}_i^{(2)}) &= \mathcal{T}_i^{(2)} = \mathcal{T}_{i+1,i} \cap \mathcal{T}_{i-1,i}, \end{aligned}$$

where $\mathbf{T}_{j,i} \in \mathbb{C}^{2 \times 3}$, with $\mathbf{T}_{i+1,i} = h_{i+1,i} \bar{\mathbf{V}}_{i-1}^{(1)} \mathbf{V}_i^{(1)}$ and $\mathbf{T}_{i-1,i} = h_{i-1,i} \bar{\mathbf{V}}_{i+1}^{(1)} \mathbf{V}_i^{(1)}$. This design allows that the interference generated during the RIA phase be aligned with the JIS phase overheard interference at both non-intended receivers. Now, since $\mathbf{T}_{i+1,i}$ and $\mathbf{T}_{i-1,i}$ are independent, its intersection will be of dimension one with probability one. Then, there exist two vectors $\boldsymbol{\theta}_i, \boldsymbol{\vartheta}_i \in \mathbb{C}^{2 \times 1}$ such that $\mathbf{T}_i^{(2)}$ can be written as

$$\mathbf{T}_i^{(2)} \doteq \boldsymbol{\theta}_i^T \bar{\mathbf{V}}_{i-1}^{(1)} \mathbf{V}_i^{(1)} \doteq \boldsymbol{\vartheta}_i^T \bar{\mathbf{V}}_{i+1}^{(1)} \mathbf{V}_i^{(1)}, \quad (6.62)$$

where \doteq is short for equality of row spans. Notice that $\boldsymbol{\theta}_i$ and $\boldsymbol{\vartheta}_i$ correspond to the vectors that project $\bar{\mathbf{V}}_{i-1}^{(1)} \mathbf{V}_i^{(1)}$ and $\bar{\mathbf{V}}_{i+1}^{(1)} \mathbf{V}_i^{(1)}$ to its intersection subspace, respectively. The following lemma states a key property satisfied by these vectors:

Lemma 6.5. *If the vectors $\boldsymbol{\theta}_i, \boldsymbol{\vartheta}_i$, $i = 1, 2, 3$ are computed satisfying the properties in (6.62), then $\boldsymbol{\theta}_i \doteq \boldsymbol{\vartheta}_{i+1}$.*

Proof: Only the proof for $i = 1$ will be shown. The proof for $i = 2, 3$ follows the same steps thus it is omitted. First, notice that (6.62) for $i = 1, 2$ can be written as follows:

$$\boldsymbol{\theta}_1^T \bar{\mathbf{V}}_3^{(1)} - \boldsymbol{\vartheta}_1^T \bar{\mathbf{V}}_2^{(1)} \subset \bar{\mathbf{V}}_1^{(1)} \Rightarrow \boldsymbol{\theta}_1^T \bar{\mathbf{V}}_3^{(1)} - \boldsymbol{\vartheta}_1^T \bar{\mathbf{V}}_2^{(1)} = \boldsymbol{\lambda}^T \bar{\mathbf{V}}_1^{(1)}, \quad (6.63)$$

$$\boldsymbol{\vartheta}_2^T \bar{\mathbf{V}}_3^{(1)} - \boldsymbol{\theta}_2^T \bar{\mathbf{V}}_1^{(1)} \subset \bar{\mathbf{V}}_2^{(1)} \Rightarrow \boldsymbol{\vartheta}_2^T \bar{\mathbf{V}}_3^{(1)} - \boldsymbol{\theta}_2^T \bar{\mathbf{V}}_1^{(1)} = \boldsymbol{\varphi}^T \bar{\mathbf{V}}_2^{(1)}. \quad (6.64)$$

for some $\boldsymbol{\lambda}, \boldsymbol{\varphi} \in \mathbb{C}^{2 \times 1}$, which is equivalent to

$$[\boldsymbol{\lambda}^T, \quad \boldsymbol{\vartheta}_1^T, \quad \boldsymbol{\theta}_1^T] \begin{bmatrix} \bar{\mathbf{V}}_1^{(1)} \\ \bar{\mathbf{V}}_2^{(1)} \\ -\bar{\mathbf{V}}_3^{(1)} \end{bmatrix} = \mathbf{0}, \quad [\boldsymbol{\theta}_2^T, \quad \boldsymbol{\varphi}^T, \quad \boldsymbol{\vartheta}_2^T] \begin{bmatrix} \bar{\mathbf{V}}_1^{(1)} \\ \bar{\mathbf{V}}_2^{(1)} \\ -\bar{\mathbf{V}}_3^{(1)} \end{bmatrix} = \mathbf{0}. \quad (6.65)$$

Hence, $\boldsymbol{\theta}_1$ and $\boldsymbol{\vartheta}_2$ are the last two components of any vector lying on the null space of the 6×5 full rank matrix on the right hand side. Since it has dimension one, the last two components will always be proportional, thus $\boldsymbol{\theta}_1 \doteq \boldsymbol{\vartheta}_2$. \square

Linear feasibility requires that $\text{rank}(\mathbf{W}_j \boldsymbol{\Omega}_j^{\text{des}}) = b$. This will be settled in the negative for user one, while non-feasibility for the rest of users may be similarly proved. In this

regard, consider the product:

$$\mathbf{W}_1 \boldsymbol{\Omega}_1^{\text{des}} = \mathbf{W}_1 \mathbf{U}_1 \mathbf{H}_1 \mathbf{V}_1 = \mathbf{W}_1 \begin{bmatrix} h_{1,1} \bar{\mathbf{V}}_3^{(1)} \mathbf{V}_1^{(1)} \\ h_{1,1} \bar{\mathbf{V}}_2^{(1)} \mathbf{V}_1^{(1)} \\ \vdots \\ h_{1,1} \boldsymbol{\Sigma}_1^{(2)} \mathbf{T}_1^{(2)} \end{bmatrix}, \quad (6.66)$$

as the result of taking the first block column of the SSM in (6.61) multiplied by the receiving filter \mathbf{W}_1 . The objective of this filter is to remove the interference by combining the rows of the signal space matrix. One simple solution is

$$\mathbf{W}_1 = \begin{bmatrix} \boldsymbol{\Sigma}_2^{(2)} \boldsymbol{\vartheta}_2^T & \boldsymbol{\Sigma}_3^{(2)} \boldsymbol{\theta}_3^T & \mathbf{I} \end{bmatrix}, \quad (6.67)$$

thus (6.66) writes as

$$\mathbf{W}_1 \boldsymbol{\Omega}_1^{\text{des}} \doteq h_{1,1} \boldsymbol{\Sigma}_2^{(2)} \boldsymbol{\vartheta}_2^T \bar{\mathbf{V}}_3^{(1)} \mathbf{V}_1^{(1)} + h_{1,1} \boldsymbol{\Sigma}_3^{(2)} \boldsymbol{\theta}_3^T \bar{\mathbf{V}}_2^{(1)} \mathbf{V}_1^{(1)} + h_{1,1} \boldsymbol{\Sigma}_1^{(2)} \boldsymbol{\theta}_1^T \bar{\mathbf{V}}_3^{(1)} \mathbf{V}_1^{(1)}. \quad (6.68)$$

First, note that $\boldsymbol{\theta}_1 \doteq \boldsymbol{\vartheta}_2$ according to Lemma 6.5, thus the first and last terms are proportional. Moreover, note that the last term can be written as $h_{1,1} \boldsymbol{\Sigma}_1^{(2)} \boldsymbol{\vartheta}_1^T \bar{\mathbf{V}}_2^{(1)} \mathbf{V}_1^{(1)}$ due to definition (6.62). Then, since $\boldsymbol{\theta}_3 \doteq \boldsymbol{\vartheta}_1$ holds according to Lemma 6.5, it is concluded that all three terms are proportional, thus $\text{rank}(\mathbf{W}_1 \boldsymbol{\Omega}_1^{\text{des}}) = 1 < 3$, and the desired symbols cannot be retrieved.

6.4.2 RIA Scheme with ACS

As for the full CSIT case [CJW10][T⁺14], the application of asymmetric complex signaling concepts enables the feasibility of the RIA scheme either for constant or time-varying channels also for the SISO case. To the best of the authors knowledge, this is the first claim that improper signaling may be useful for precoding schemes using delayed CSIT. This section provides a sketch of the proof, omitted in its full version to avoid redundancy with the cited references.

In case of using asymmetric complex signaling, the channel can be modeled in terms of real magnitudes (see [T⁺14]), such that $2b$ *real symbols* are transmitted to each user along 2τ slots, and the channel model in (6.58) translates to

$$\mathbf{H}_{j,i} = \mathbf{I}_\tau \otimes |\dot{h}_{j,i}| \dot{\Phi}_{j,i} = |\dot{h}_{j,i}| \boldsymbol{\Phi}_{j,i} \in \mathbb{R}^{2\tau \times 2\tau}, \quad (6.69)$$

where $\phi_{j,i}$ is the phase of the complex channel gain $\dot{h}_{j,i}$, and

$$\dot{\Phi}_{j,i} = \begin{bmatrix} \cos(\phi_{j,i}) & -\sin(\phi_{j,i}) \\ \sin(\phi_{j,i}) & \cos(\phi_{j,i}) \end{bmatrix} \in \mathbb{R}^{2 \times 2}, \quad (6.70)$$

$$\boldsymbol{\Phi}_{j,i} = \mathbf{I}_\tau \otimes \dot{\Phi}_{j,i}. \quad (6.71)$$

Matrices $\boldsymbol{\Phi}_{j,i}$ break the diagonal structure of channel matrices. This is of interest because in previous section the same interference was generated at both unintended receivers thereby the same per-phase filter was used to remove it, see (6.60). Nonetheless, in this case different per-phase filters should be used, thus the connections among vectors $\boldsymbol{\theta}_i, \boldsymbol{\vartheta}_i$ stated by Lemma 6.5 no longer hold, and feasibility is ensured for any channel realization. Similar arguments apply to the MIMO case.

6.4.3 TG Scheme

We review the foundations of this scheme, described in Section 6.2.2 for $M > N$, in order to show that it also works for constant channels. During the IIS phase transmitters are scheduled in a TDMA fashion. Therefore, for each RX_j obtains

$$\begin{aligned}\mathbf{y}_j^{(1,r)} &= \mathbf{H}_{j,r}^{(1,r)} \mathbf{V}_r^{(1,r)} \mathbf{x}_r = \left(\mathbf{I}_{S_1} \otimes \mathring{\mathbf{H}}_{j,i} \right) \mathbf{V}_r^{(1,r)} \mathbf{x}_r, \\ \mathbf{T}_{j,i} &= \left(\mathbf{I}_{S_1} \otimes \mathring{\mathbf{H}}_{j,i} \right) \mathbf{V}_i^{(1,i)},\end{aligned}$$

where the precoding matrices $\mathbf{V}_i^{(1,i)} \in \mathbb{C}^{MS_1 \times b}$ are chosen to be some generic full-rank matrices, with $\mathbf{V}_i^{(1,r)} = \mathbf{0}$ for $r \neq i$. Since $M > N$, and $NS_1 < b$ by design, it is easy to see that all ranks are preserved even for constant channels, i.e. $\text{rank}(\mathbf{T}_{j,i}) = NS_1, \forall i$, and all such pieces of overheard interference generate generic subspaces $\mathcal{T}_{j,i}$.

Now, let us recall that the precoders for each round of the RIA phase, see (6.22a), are linear combinations of $\mathbf{T}_i^{(2,r)}$, obtained as a basis of

$$\text{rspan} \left(\mathbf{T}_i^{(2,r)} \right) = \mathcal{T}_i^{(2,r)} = \bigcap_{k \in \mathcal{G}^{(2,r)} \setminus \{i\}} \mathcal{T}_{k,i}$$

which will also preserve the rank. Therefore, we conclude that this scheme does not require the time-varying channels assumption, since each receiver can acquire enough linear combinations of desired symbols even in case of constant channels.

6.4.4 3-user PSR Scheme

The first phase of this scheme is similar to that for the RIA scheme. In contrast, there are three phases and the second phase is developed by pairs. Feasibility is easily shown for MIMO channels, whereas the SISO setting fails. Since the scheme delivers exactly 12 LCs of the $b = 12$ desired symbols to each receiver, by simply showing that some of those LCs are linearly dependent is sufficient to show the non-feasibility. In this regard, next we show that not all LCs delivered during the first round of the second phase are linearly independent. Consider the signal space matrix for the second phase, particularized for this case:

$$\Omega_1^{(2)} = \left[\begin{array}{ccc} h_{1,1} \bar{\mathbf{V}}_3^{(1)} \mathbf{V}_1^{(1)} & \mathbf{T}_{1,2} & \mathbf{0} \\ h_{1,1} \bar{\mathbf{V}}_2^{(1)} \mathbf{V}_1^{(1)} & \mathbf{0} & \mathbf{T}_{1,3} \\ \hline h_{1,1} \Sigma_1^{(2,1)} \mathbf{T}_{2,1} & h_{1,2} \Sigma_2^{(2,1)} \mathbf{T}_{1,2} & \mathbf{0} \\ h_{1,1} \Sigma_1^{(2,2)} \mathbf{T}_{3,1} & \mathbf{0} & h_{1,1} \Sigma_3^{(2,2)} \mathbf{T}_{1,3} \\ \mathbf{0} & \mathbf{F}_{3,2}^{\{1\}} & \mathbf{0} \\ \mathbf{0} & \mathbf{0} & \mathbf{F}_{2,3}^{\{1\}} \end{array} \right], \quad (6.72)$$

where the same notation as for the RIA case has been used, and in this case we have $\mathbf{T}_{2,1} = h_{2,1} \bar{\mathbf{V}}_3^{(1)} \mathbf{V}_1^{(1)} \in \mathbb{C}^{3 \times 12}$.

Two methods for delivering LCs of desired symbols were used in the second phase, see Section 6.2.3. First, recall that $\Sigma_1^{(2,1)} \in \mathbb{C}^{4 \times 3}$, thus zero-forcing the interference received

during the first round of the second phase, RX_1 obtains

$$\boldsymbol{\lambda}^T h_{1,1} \boldsymbol{\Sigma}_1^{(2,1)} \mathbf{T}_{2,1} \mathbf{x}_1 \quad (6.73)$$

for some $\boldsymbol{\lambda} \in \mathbb{C}^{4 \times 1}$ that satisfies $\boldsymbol{\lambda}^T \boldsymbol{\Sigma}_2^{(2,1)} = \mathbf{0}$. Clearly, such LC of desired signals lies on $\text{rspan}(\mathbf{T}_{2,1})$.

On the other hand, four LCs of desired signals may be obtained by combining the JIS phase received signals with the signals received during the first round of the hybrid phase:

$$\left(h_{1,2} \boldsymbol{\Sigma}_2^{(2,1)} h_{1,1} \bar{\mathbf{V}}_3^{(1)} \mathbf{V}_1^{(1)} + h_{1,1} \boldsymbol{\Sigma}_1^{(2,1)} \mathbf{T}_{2,1} \right) \mathbf{x}_1 = \left(\frac{h_{1,2}}{h_{2,1}} \boldsymbol{\Sigma}_2^{(2,1)} + \boldsymbol{\Sigma}_1^{(2,1)} \right) h_{1,1} \mathbf{T}_{2,1} \mathbf{x}_1.$$

Those LCs form a basis of the three-dimensional subspace $\text{rspan}(\mathbf{T}_{2,1})$, thus actually would provide only three *independent* desired LCs of desired symbols. However, since the LC obtained by the first method lies also in $\text{rspan}(\mathbf{T}_{2,1})$, after this round user one acquires only three instead of four *independent* desired LCs, and linear feasibility is discarded.

Nonetheless, this problem can be fixed by exploiting asymmetric complex signaling, since the per-phase receiving filters for the second phase are distinct across users, similarly to what occurs for the RIA scheme. Then, the PSR scheme can be made feasible even for SISO constant channels.

6.5 Conclusion

Three fundamental tools have been envisioned in the context of delayed CSIT for designing linear precoding strategies: *delayed CSIT precoding*, *user scheduling*, and *redundancy transmission*. Based on them, this chapter proposes three precoding strategies, evaluated as a function of the antenna ratio ρ .

For $\rho < 1$, the RIA scheme initially proposed for the 3-user SISO IC ($\rho = 1$) has been generalized to the K -user MIMO case. This scheme exploits *delayed CSIT precoding* and *redundancy transmission*. In contrast to the conjecture in [MC12], our results show that state-of-the-art DoF can be improved by considering $L \geq 3$ active pairs. Moreover, we have shown that for the region $\frac{1}{K-1} < \rho < \frac{K}{K^2-K-1}$ our proposed inner bound using the RIA scheme gets very close to the best known outer bound.

Moreover, we have generalized the PSR scheme for 3 users from SISO to MIMO, which combines the three tools: *delayed CSIT precoding*, *user scheduling*, and *redundancy transmission*. This scheme provides the best achievable DoF when the number of antennas at the transmitter and receiver are similar ($\rho \approx 1$) not only for the 3-user MIMO IC, but also for the K -user MIMO IC by applying time-sharing concepts. Nevertheless, a MIMO generalization for $K > 3$ users remains open.

In case the transmitter has more antennas than the receiver ($\rho > 1$), we propose the TG scheme improving state-of-the-art for $1 < \rho < K - 1$. Linear precoding and user scheduling are carefully designed for DoF boosting, where the first phase is carried out orthogonally among users, whereas the second phase is developed in groups of $G \leq K$ users. The proper value of G lies on the trade-off between the constraints imposed by interference alignment, and the increase on the number of rounds, in turn depending on the antenna ratio ρ and the number of users K .

The DoF-delay trade-off of the proposed schemes has been studied and compared to SotA by limiting either the number or the order of the transmitted symbols. The first method builds upon the formulation of the parameters of each scheme (number of transmitted symbols and duration of the phases) as the solution of a DoF constrained maximization problem, and as a function of the number of users and antenna ratio. In this regard, the analysis shows that although the PSR scheme and its extensions attain higher DoF values for some settings, this is at the cost of long transmission delays. Consequently, it has been shown that the gains provided by the PSR scheme is not worth the increase of complexity both at the transmitter and the receiver side, as compared to the proposed schemes.

Finally, the later part of this chapter has concluded that the time-varying channels assumption, which is common along all the literature on delayed CSIT, is indeed not necessary, except for the SISO case. This implies that delayed CSIT strategies can be used even if the channel remains constant. For the particular SISO case, we have proved that the two schemes in the literature [MJS12][AGK13] failed, which can be fixed by the applying asymmetric complex signaling concept.

IBC with Delayed CSIT

7

The potential of Retrospective Interference Alignment has been exposed for DoF boosting of broadcast and interference channels with delayed CSIT. However, it is not known if it may be adapted to more complex topologies like the IBC. This chapter studies the MIMO IBC with delayed CSIT, 2 cells and 2 users per cell. Although some of the schemes designed for other channels may be applied, the specific topology of the IBC has not been exploited yet. In this regard, we propose a precoding strategy that includes the concept of *redundancy transmission*, employed in previous chapter for the IC, by taking into account that users of each cell are served by a common transmitter.

7.1 Main Contribution

The main result attained in this chapter is summarized in Fig. 7.2, where DoF inner and outer bounds using delayed CSIT, as well as the optimal DoF for no CSIT (TDMA) are depicted. Three different inner bounds are considered:

- achieved by using the proposed scheme,
- based on consolidated state-of-the-art for the IC and BC,
- based on very recent results for the IC appeared simultaneously to the development of the material in this chapter.

Each of those inner bounds is next specified. First, the performance of the proposed scheme is summarized next:

Theorem 7.1 (DoF Inner bound). *For the 2-cell 2-user MIMO IBC with delayed local CSIT and antenna ratio ρ , the following normalized DoF per user can be achieved:*

$$d_j^{(\text{in})} = \begin{cases} \frac{\rho^3}{\rho^3 + 3\rho^2 + 3\rho + 8} & \rho_A \leq \rho < \rho_B \\ \frac{3\rho^2}{5\rho^2 + 7\rho + 3} & \rho_B \leq \rho < \rho_C \\ \frac{9\rho}{16\rho + 20} & \rho_C \leq \rho < 4 \\ \frac{3}{7} & \rho \geq 4 \end{cases} \quad (7.1)$$

with $\rho_A \approx 2.6413$, $\rho_B \approx 3.1557$, and $\rho_C \approx 3.5414$.

Proof: See Section 7.2. □

Notice that the proposed scheme performance improves the consolidated state-of-the-art for $\rho > 2.9413$, and recent results for $\rho > \rho_C$. The performance for $\rho < \rho_A$ is not derived since in such a case it is better using other approaches from the SotA.

For $\rho > 1$, consolidated SotA refers to applying the TG scheme with $G = 2$ described for the IC in Chapter 6, Section 6.2.2. Notice that in such a case, the IBC is interpreted as

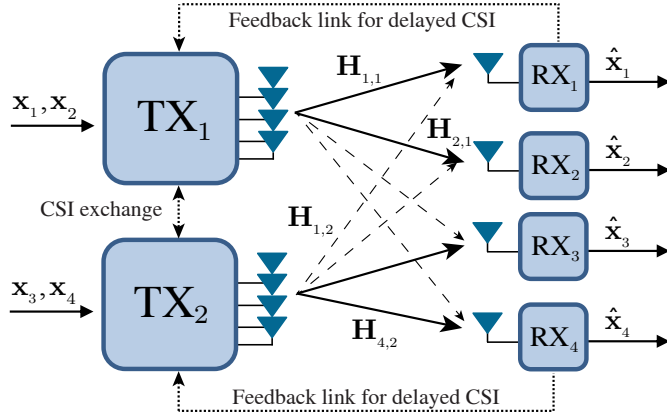


Figure 7.1: The 2-cell 2-user MIMO IBC, with $M = 4$, $N = 1$ antennas at the transmitters and receivers, respectively. Solid/Dotted lines denote the links carrying intended/interference signals.

a 4-user IC, thus not exploiting the common transmitter at each cell. On the other hand, recent SotA corresponds to applying recent results for the IC. For $\rho < 2$, the schemes described in previous chapter are applied. Otherwise, [HC15] is employed.

It is worth pointing out that although the proposed scheme provides lower DoF than the scheme in [HC15], the latter requires a higher number of time slots, which hinders its implementation as studied in previous chapter. For example, for $\rho = 4$ the proposed scheme requires $\tau = 28$, whereas the scheme in [HC15] is developed in $\tau = 65$, i.e. more than twice the number of slots.

Moreover, for comparison purposes we derive the following DoF outer bound:

Theorem 7.2 (DoF Outer bound). *For the 2-cell 2-user MIMO IBC with delayed CSIT and antenna ratio $\rho > \frac{1}{2}$, the normalized DoF per user are bounded above by:*

$$d_j^{(\text{out})} = \begin{cases} \frac{\rho}{2} & \frac{1}{2} \leq \rho < \frac{2}{3} \\ \frac{1}{3} & \frac{2}{3} \leq \rho < 1 \\ \rho/3 & 1 \leq \rho < \frac{4}{3} \\ 2\frac{\rho}{3\rho+2} & \frac{4}{3} \leq \rho < 3/2 \\ 6\frac{\rho}{11\rho+3} & 3/2 \leq \rho < 2 \\ \frac{12}{25} & \rho \geq 2 \end{cases}$$

Proof: It corresponds to the minimum between two trivial upper bounds. First, assuming transmitter cooperation, the IBC turns into a 4-user MIMO BC with $2M$ antennas at the transmitter, whose DoF were derived in [MAT12]. This bound applies for $\rho > \frac{4}{3}$. The second outer bound corresponds to assuming current CSIT [SY13], and applies for $\rho < \frac{4}{3}$. \square

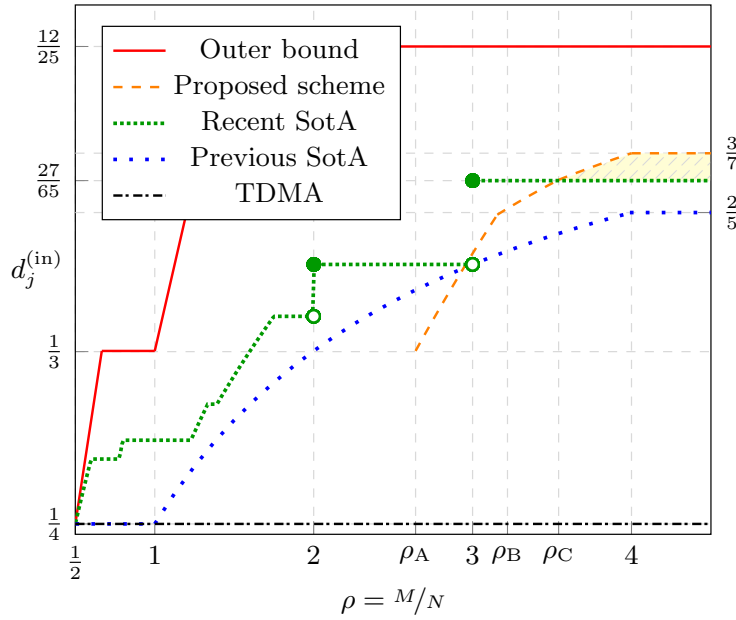


Figure 7.2: Normalized DoF per user inner and outer bounds for the 2-cell 2-user MIMO IBC with delayed CSIT. Only $\rho > \frac{1}{2}$ is shown. Otherwise, the optimal DoF are attained without the need of CSIT [SY13]. The proposed scheme outperforms all other SotA for $\rho > \rho_C$, with $\rho_C \approx 3.5414$.

7.2 Proposed Transmission Strategy

Similarly to the proposed strategies presented in previous chapter, we divide its description in two parts. First, it is presented for the $(M, N) = (4, 1)$ specific antenna setting, easing reader's understanding¹, see Fig. 7.1. Then, it is generalized to a general antenna setting by means of the formulation of a DoF maximization problem with linear constraints.

7.2.1 Case M=4, N=1

Our DoF maximization problem, to be presented in the next section, assumes the following:

$$P = 4, \quad R_p = \binom{4}{p}, \quad (7.2)$$

as summarized in Table 7.1. Then, the number of transmitted symbols, and the duration of each round of each phase should be optimized. For this antenna setting, we obtain that $\frac{3}{7}$ DoF per user can be achieved by delivering $b = 12$ symbols to each user along $\tau = 28$ time slots.

Phase 1

The first phase is divided in $R_1 = 4$ rounds, each of them dedicated to transmit LCs of symbols of one user during $S_1 = 3$ time slots. The precoding matrices used during this

¹In this setting, with single-antenna receivers, the number of transmitted symbols, and duration of the symbols is relatively short. Then, it is one of the more amenable antenna regimes to follow for non-familiar readers, among the ones where the proposed scheme outperforms the SotA.

round are predefined and randomly chosen from a dictionary before the communication. Consequently, after the first phase each receiver acquires $S_1 = 3$ LCs of desired symbols, thus $b - S_1 = 9$ additional LCs are required. Interestingly, those remaining LCs are distributed along the listening receivers, who observe 3 LCs of each non-desired set of symbols. These LCs will be the basis to align the interference during the next phases, while providing new LCs of desired symbols. They represent the *overheard interference* for the first phase, denoted by

$$\mathbf{T}_{j,i} = \mathbf{H}_{j,c(i)}^{(1,i)} \mathbf{V}_i^{(1,i)} \in \mathbb{C}^{3 \times 12}, \quad (7.3)$$

$$\mathcal{T}_{i,j} = \text{rspan}(\mathbf{T}_{j,i}), \quad (7.4)$$

i.e. the signals intended to RX_i and observed at RX_j , see Table 7.1 for the OHI collected at RX_1 . Moreover, notice that all these 12 distributed LCs can be assumed linearly independent with probability one due to the channel randomness. Finally, for better readability we show the signal space matrix for RX_1 :

$$\Omega_1^{(1)} = \text{bdiag}(\mathbf{T}_{1,1}, \mathbf{T}_{1,2}, \mathbf{T}_{1,3}, \mathbf{T}_{1,4}) = \begin{bmatrix} \mathbf{T}_{1,1} & \mathbf{0} & \mathbf{0} & \mathbf{0} \\ \mathbf{0} & \mathbf{T}_{1,2} & \mathbf{0} & \mathbf{0} \\ \mathbf{0} & \mathbf{0} & \mathbf{T}_{1,3} & \mathbf{0} \\ \mathbf{0} & \mathbf{0} & \mathbf{0} & \mathbf{T}_{1,4} \end{bmatrix}. \quad (7.5)$$

Phase 2

Users are served by pairs during this phase, with $R_1 = 6$ single-slot rounds. The first phase OHI is exploited to deliver a LC of desired symbols aligned at the non-intended receiver. Consider the round r dedicated to RX_i and RX_j , i.e. $\mathcal{G}^{(2,r)} = \{i, j\}$. Then, transmitted signals are designed such that

$$\text{rspan}\left(\mathbf{H}_{j,c(i)}^{(2,r)} \mathbf{V}_i^{(2,r)}\right) \subseteq \mathcal{T}_{j,i}, \quad \text{rspan}\left(\mathbf{H}_{i,c(j)}^{(2,r)} \mathbf{V}_j^{(2,r)}\right) \subseteq \mathcal{T}_{i,j},$$

i.e. the signals obtained at each receiver are aligned with the previously received OHI. Similarly to Section 6.2.2, one simple solution using only delayed CSIT is given by

$$\mathbf{V}_i^{(2,r)} = \Theta_i^{(2,r)} \mathbf{T}_{j,i}, \quad \mathbf{V}_j^{(2,r)} = \Theta_j^{(2,r)} \mathbf{T}_{i,j}, \quad (7.6)$$

where $\Theta_i^{(2,r)}, \Theta_j^{(2,r)} \in \mathbb{C}^{4 \times 3}$ are some random full rank matrices ensuring the transmit power constraint.

The OHI obtained during this phase is generally written as

$$\underline{\mathbf{m}}_{j,i}^{(k)} = \underline{\mathbf{h}}_{k,c(i)}^{(2,r)} \mathbf{V}_i^{(2,r)} \in \mathbb{C}^{1 \times 12}, \quad (7.7)$$

with $\text{rspan}(\underline{\mathbf{m}}_{j,i}^{(k)}) \subset \mathcal{T}_{j,i}$, r such that $\mathcal{G}^{(2,r)} = \{i, j\}$, and $k \notin \mathcal{G}^{(2,r)}$. In other words, $\underline{\mathbf{m}}_{j,i}^{(k)}$ is the LC of $\mathbf{T}_{j,i}$ observed at RX_k . For instance, $\underline{\mathbf{m}}_{4,3}^{(1)} = \underline{\mathbf{h}}_{1,2}^{(2,6)} \Theta_3^{(2,6)} \mathbf{T}_{4,3}$ is the LC of $\mathbf{T}_{4,3}$ observed at RX_1 .

From each user's perspective, the rounds of the first two phases can be classified in two classes: serving or listening round, as specified in Table 7.1. During the serving

Table 7.1: Served users per round, type of each round from the perspective of RX₁, and acquired OHI at RX₁ for each round

Phase (p)	Round (r)	$\mathcal{G}^{(p,r)}$	Type of Round for RX ₁	Acquired OHI at RX ₁
1	1	{1}	Serving	—
	2	{2}	Listening	$\mathbf{T}_{1,2} \mathbf{x}_2$
	3	{3}	Listening	$\mathbf{T}_{1,3} \mathbf{x}_3$
	4	{4}	Listening	$\mathbf{T}_{1,4} \mathbf{x}_4$
2	1	{1, 2}	Serving	—
	2	{1, 3}	Serving	—
	3	{1, 4}	Serving	—
	4	{2, 3}	Listening	$\underline{\mathbf{m}}_{3,2}^{(1)} \mathbf{x}_2 + \underline{\mathbf{m}}_{2,3}^{(1)} \mathbf{x}_3$
	5	{2, 4}	Listening	$\underline{\mathbf{m}}_{4,2}^{(1)} \mathbf{x}_2 + \underline{\mathbf{m}}_{2,4}^{(1)} \mathbf{x}_4$
	6	{3, 4}	Listening	$\underline{\mathbf{m}}_{4,3}^{(1)} \mathbf{x}_3 + \underline{\mathbf{m}}_{3,4}^{(1)} \mathbf{x}_4$
3	1	{1, 2, 3}	Mixed	$\underline{\mathbf{m}}_{3,2}^{(1)} \mathbf{x}_2, \underline{\mathbf{m}}_{2,3}^{(1)} \mathbf{x}_3$
	2	{1, 2, 4}	Mixed	$\underline{\mathbf{m}}_{4,2}^{(1)} \mathbf{x}_2, \underline{\mathbf{m}}_{2,4}^{(1)} \mathbf{x}_4$
	3	{1, 3, 4}	Serving	—
	4	{2, 3, 4}	Listening	$\underline{\mathbf{f}}_{1,2} \mathbf{x}_2 + \underline{\mathbf{f}}_{1,3} \mathbf{x}_3 + \underline{\mathbf{f}}_{1,4} \mathbf{x}_4$
4	—	{1, 2, 3, 4}	Serving	—

rounds, extra linear combinations of desired signals are obtained, free of interference or with aligned interference that can be removed using the previously acquired OHI. In contrast, during the listening rounds, only interference is observed, to be used as overheard interference during the next phases. Note that after the second phase some of the overheard interference is *coupled*. For example, during the fourth round at RX₁, the overheard interference obtained is given by

$$\mathbf{y}_1^{(3,2)} = \mathbf{i}_1^{(3,2)} = \underline{\mathbf{m}}_{3,2}^{(1)} \mathbf{x}_2 + \underline{\mathbf{m}}_{2,3}^{(1)} \mathbf{x}_3. \quad (7.8)$$

Therefore, only a LC is known, but not each of the two terms individually. This is specified in Table 7.1, and can be analyzed in a more compact way by means of the second phase SSM at RX₁, given by

$$\Omega_1^{(2)} = \begin{bmatrix} \underline{\mathbf{m}}_{2,1}^{(1)} & \underline{\mathbf{m}}_{1,2}^{(1)} & \mathbf{0} & \mathbf{0} \\ \underline{\mathbf{m}}_{3,1}^{(1)} & \mathbf{0} & \underline{\mathbf{m}}_{1,3}^{(1)} & \mathbf{0} \\ \mathbf{0} & \underline{\mathbf{m}}_{3,2}^{(1)} & \underline{\mathbf{m}}_{2,3}^{(1)} & \mathbf{0} \\ \mathbf{0} & \underline{\mathbf{m}}_{4,2}^{(1)} & \mathbf{0} & \underline{\mathbf{m}}_{2,4}^{(1)} \\ \mathbf{0} & \mathbf{0} & \underline{\mathbf{m}}_{4,3}^{(1)} & \underline{\mathbf{m}}_{3,4}^{(1)} \end{bmatrix}. \quad (7.9)$$

Finally, from the received signals represented by (7.5) and (7.9), each user is able to retrieve 3 new LCs of desired symbols by combining the current received signals and previous OHI.

Phase 3

Each of the $R_3 = 4$ single-slot rounds of this phase is dedicated to one of the four possible triplets of users, see Table 7.2. In contrast to the first two phases, three different types of rounds may be defined during the third phase. In case of RX₁, the third and fourth rounds are serving and listening rounds, respectively, following the definition above. However, the first and second rounds correspond to an intermediate situation, denoted as *mixed rounds*. In those cases, desired signals are received but combined with interference terms that cannot be removed. This is because they come from different transmitters, i.e. observed through different channels, and because the OHI is known coupled. The contribution of this phase is then twofold: 1) to provide one LC of desired signals free of interference during the serving round, and 2) to decouple the OHI from the second phase during the mixed rounds. On the one hand, although the second phase OHI is known coupled it can be removed whenever all the interference is generated by the same transmitter. Since there is one serving round of duration one slot per user, one LC of desired signals free of interference is acquired. On the other hand, the interference for the mixed rounds cannot be entirely removed, but allows *decoupling the interference*, i.e. acquire each of the OHI terms individually, which will be useful for the last phase. As an example, see rounds (3, 1) and (3, 2) in Table 7.1, where the OHI collected at RX₁ during the communication is exposed.

Table 7.2: OHI transmitted during each third phase round

r	$\mathcal{G}^{(3,r)}$	$\mathcal{G}^{(3,r)}(1)$	$\mathcal{G}^{(3,r)}(2)$	$\mathcal{G}^{(3,r)}(3)$
1	{1, 2, 3}	{ $\underline{\mathbf{m}}_{2,1}^{(3)}, \underline{\mathbf{m}}_{3,1}^{(2)}$ }	{ $\underline{\mathbf{m}}_{1,2}^{(3)}, \underline{\mathbf{m}}_{3,2}^{(1)}$ }	{ $\underline{\mathbf{m}}_{1,3}^{(2)}, \underline{\mathbf{m}}_{2,3}^{(1)}$ }
2	{1, 2, 4}	{ $\underline{\mathbf{m}}_{2,1}^{(4)}, \underline{\mathbf{m}}_{4,1}^{(2)}$ }	{ $\underline{\mathbf{m}}_{1,2}^{(4)}, \underline{\mathbf{m}}_{4,2}^{(1)}$ }	{ $\underline{\mathbf{m}}_{1,4}^{(2)}, \underline{\mathbf{m}}_{2,4}^{(1)}$ }
3	{1, 3, 4}	{ $\underline{\mathbf{m}}_{3,1}^{(4)}, \underline{\mathbf{m}}_{4,1}^{(3)}$ }	{ $\underline{\mathbf{m}}_{1,3}^{(4)}, \underline{\mathbf{m}}_{4,3}^{(1)}$ }	{ $\underline{\mathbf{m}}_{1,4}^{(3)}, \underline{\mathbf{m}}_{3,4}^{(1)}$ }
4	{2, 3, 4}	{ $\underline{\mathbf{m}}_{3,2}^{(4)}, \underline{\mathbf{m}}_{4,2}^{(3)}$ }	{ $\underline{\mathbf{m}}_{2,1}^{(3)}, \underline{\mathbf{m}}_{3,1}^{(2)}$ }	{ $\underline{\mathbf{m}}_{2,1}^{(3)}, \underline{\mathbf{m}}_{3,1}^{(2)}$ }

To illustrate all these arguments mathematically, let consider the precoding matrix design for the third round², dedicated to users in $\mathcal{G}^{(3,3)} = \{1, 3, 4\}$:

$$\mathbf{V}_1^{(3,3)} = \boldsymbol{\theta}_1^{(3,3)} \underline{\mathbf{m}}_{3,1}^{(4)} + \boldsymbol{\theta}_2^{(3,3)} \underline{\mathbf{m}}_{4,1}^{(3)}, \quad (7.10a)$$

$$\mathbf{V}_3^{(3,3)} = \boldsymbol{\theta}_1^{(3,3)} \underline{\mathbf{m}}_{1,3}^{(4)} + \boldsymbol{\theta}_3^{(3,3)} \underline{\mathbf{m}}_{4,3}^{(1)}, \quad (7.10b)$$

$$\mathbf{V}_4^{(3,3)} = \boldsymbol{\theta}_2^{(3,3)} \underline{\mathbf{m}}_{1,4}^{(3)} + \boldsymbol{\theta}_3^{(3,3)} \underline{\mathbf{m}}_{3,4}^{(1)}, \quad (7.10c)$$

where $\boldsymbol{\theta}_i^{(3,r)} \in \mathbb{C}^{4 \times 1}$ is some vector with random entries and ensuring the transmit power

²To avoid redundancy, we intentionally focus on this round in order to make use of (7.9). The design for the rest of rounds is easily derived according to Table 7.2.

constraint, thus the interference generated at RX₁ is:

$$\underline{\mathbf{i}}_1^{(3,3)} = \underline{\mathbf{h}}_{1,2}^{(3,3)} \left(\mathbf{V}_3^{(3,3)} \mathbf{x}_3 + \mathbf{V}_4^{(3,3)} \mathbf{x}_4 \right) \quad (7.11a)$$

$$= \underline{\mathbf{h}}_{1,2}^{(3,3)} \left(\boldsymbol{\theta}_1^{(3,3)} \underline{\mathbf{m}}_{1,3}^{(4)} \mathbf{x}_3 + \boldsymbol{\theta}_3^{(3,3)} \left[\underline{\mathbf{m}}_{4,3}^{(1)}, \underline{\mathbf{m}}_{3,4}^{(1)} \right] \begin{bmatrix} \mathbf{x}_3 \\ \mathbf{x}_4 \end{bmatrix} + \boldsymbol{\theta}_2^{(3,3)} \underline{\mathbf{m}}_{1,4}^{(3)} \mathbf{x}_4 \right). \quad (7.11b)$$

By exploiting the phase 2 OHI, see Table 7.1, the terms proportional to the row vector $[\underline{\mathbf{m}}_{4,3}^{(1)}, \underline{\mathbf{m}}_{3,4}^{(1)}]$ can be removed, while the rest of terms are aligned with the first phase OHI. Then, all the interference terms in (7.11) are removed, and one additional LC of desired symbols is retrieved. Unfortunately, the trick in (7.11) can be done only if all the interference comes from the same transmitter, i.e. all the interference terms are observed through the same channel, as in a BC. To see this, consider the interference generated at RX₁ during the (3, 1)th round:

$$\underline{\mathbf{i}}_1^{(3,1)} = \underline{\mathbf{h}}_{1,1}^{(3,1)} \left(\boldsymbol{\theta}_1^{(3,1)} \underline{\mathbf{m}}_{1,2}^{(3)} + \boldsymbol{\theta}_3^{(3,1)} \underline{\mathbf{m}}_{3,2}^{(1)} \right) \mathbf{x}_2 + \quad (7.12a)$$

$$+ \underline{\mathbf{h}}_{1,2}^{(3,1)} \left(\boldsymbol{\theta}_2^{(3,1)} \underline{\mathbf{m}}_{1,3}^{(2)} + \boldsymbol{\theta}_3^{(3,1)} \underline{\mathbf{m}}_{2,3}^{(1)} \right) \mathbf{x}_3. \quad (7.12b)$$

As explained at the beginning of this section, since $\underline{\mathbf{m}}_{3,2}^{(1)}$ and $\underline{\mathbf{m}}_{2,3}^{(1)}$ are known coupled (see Table 7.1), they cannot be simultaneously canceled in (7.12). Nonetheless, RX₁ is able to acquire them individually thanks to this round, denoted as interference uncoupling.

Finally, the OHI for this phase is defined as follows:

$$\underline{\mathbf{f}}_{j,i} = \underline{\mathbf{h}}_{j,c(i)}^{(3,r)} \mathbf{V}_i^{(3,r)} \in \mathbb{C}^{1 \times 12}, \quad (7.13)$$

with r defined such that $i \notin \mathcal{G}^{(3,r)}$. In other words, $\underline{\mathbf{f}}_{j,i}$ is the LC of symbols of RX_i observed at RX_j during the unique third phase round where RX_j is a listening user. Note that $\text{rspan}(\underline{\mathbf{f}}_{j,i}) \subset \text{rspan}(\text{stack}(\underline{\mathbf{m}}_{l,i}^{(k)}, \underline{\mathbf{m}}_{k,i}^{(l)}))$, where all indices take different values. For example, the row span of $\underline{\mathbf{f}}_{4,2} = \underline{\mathbf{h}}_{4,1}^{(3,1)} \mathbf{V}_1^{(3,1)} = \underline{\mathbf{h}}_{4,1}^{(3,1)} \left(\boldsymbol{\theta}_1^{(3,1)} \underline{\mathbf{m}}_{1,2}^{(3)} + \boldsymbol{\theta}_3^{(3,1)} \underline{\mathbf{m}}_{3,2}^{(1)} \right)$ lies on $\text{rspan}(\text{stack}(\underline{\mathbf{m}}_{1,2}^{(3)}, \underline{\mathbf{m}}_{3,2}^{(1)}))$. For a better understanding, the SSM corresponding to the first three phases is shown in Table 7.3.

Table 7.3: OHI terms transmitted during the last phase

i	$\underline{\mathbf{f}}_{\mathcal{I}^i(3),i}$	$\underline{\mathbf{f}}_{\mathcal{I}^i(2),i}$	$\underline{\mathbf{f}}_{\mathcal{I}^i(1),i}$
1	$\{\underline{\mathbf{m}}_{2,1}^{(3)}, \underline{\mathbf{m}}_{3,1}^{(2)}\}$	$\{\underline{\mathbf{m}}_{2,1}^{(4)}, \underline{\mathbf{m}}_{4,1}^{(2)}\}$	$\{\underline{\mathbf{m}}_{3,1}^{(4)}, \underline{\mathbf{m}}_{4,1}^{(3)}\}$
2	$\{\underline{\mathbf{m}}_{1,2}^{(3)}, \underline{\mathbf{m}}_{3,2}^{(1)}\}$	$\{\underline{\mathbf{m}}_{1,2}^{(4)}, \underline{\mathbf{m}}_{4,2}^{(1)}\}$	$\{\underline{\mathbf{m}}_{3,2}^{(4)}, \underline{\mathbf{m}}_{4,2}^{(3)}\}$
3	$\{\underline{\mathbf{m}}_{1,3}^{(2)}, \underline{\mathbf{m}}_{2,3}^{(1)}\}$	$\{\underline{\mathbf{m}}_{1,3}^{(4)}, \underline{\mathbf{m}}_{4,3}^{(1)}\}$	$\{\underline{\mathbf{m}}_{2,3}^{(4)}, \underline{\mathbf{m}}_{4,3}^{(2)}\}$
4	$\{\underline{\mathbf{m}}_{1,4}^{(2)}, \underline{\mathbf{m}}_{2,4}^{(1)}\}$	$\{\underline{\mathbf{m}}_{1,4}^{(3)}, \underline{\mathbf{m}}_{3,4}^{(1)}\}$	$\{\underline{\mathbf{m}}_{2,4}^{(3)}, \underline{\mathbf{m}}_{3,4}^{(2)}\}$

Phase 4

The last phase consists of a single round of $S_4 = 6$ slots, during which all users are simultaneously served. In this case the precoding matrices transmit a rank-3 LC of symbols, thus there is some redundancy, that will be used to cancel the non-aligned interference.

$$\Omega_i^{(1:3)} = \begin{bmatrix} \Omega_i^{(1)} \\ \Omega_i^{(2)} \\ \Omega_i^{(3)} \end{bmatrix} = \begin{bmatrix} \mathbf{H}_{1,1}^{(1,1)} \mathbf{V}_1^{(1,1)} & \mathbf{0} & \mathbf{0} & \mathbf{0} \\ \mathbf{0} & (\mathbf{H}_{1,1}^{(1,2)} \mathbf{V}_2^{(1,2)}) \mathbf{T}_{1,2} & \mathbf{0} & \mathbf{0} \\ \mathbf{0} & \mathbf{0} & (\mathbf{H}_{1,2}^{(1,3)} \mathbf{V}_3^{(1,3)}) \mathbf{T}_{1,3} & \mathbf{0} \\ \mathbf{0} & \mathbf{0} & \mathbf{0} & \mathbf{H}_{1,2}^{(1,4)} \mathbf{V}_4^{(1,4)} \\ \hline \mathbf{H}_{1,1}^{(2,1)} \boldsymbol{\theta}_1^{(2,1)} \mathbf{T}_{2,1} & \mathbf{H}_{1,1}^{(2,1)} \boldsymbol{\theta}_2^{(2,1)} \mathbf{T}_{1,2} & \mathbf{0} & \mathbf{0} \\ \mathbf{H}_{1,1}^{(2,2)} \boldsymbol{\theta}_1^{(2,2)} \mathbf{T}_{3,1} & \mathbf{0} & \mathbf{H}_{1,2}^{(2,2)} \boldsymbol{\theta}_3^{(2,2)} \mathbf{T}_{1,3} & \mathbf{0} \\ \mathbf{H}_{1,1}^{(2,3)} \boldsymbol{\theta}_1^{(2,3)} \mathbf{T}_{4,1} & \mathbf{0} & \mathbf{0} & \mathbf{H}_{1,2}^{(2,2)} \boldsymbol{\theta}_4^{(2,3)} \mathbf{T}_{1,4} \\ \mathbf{0} & \mathbf{H}_{1,1}^{(2,4)} \boldsymbol{\theta}_2^{(2,4)} \mathbf{T}_{3,2} & \mathbf{H}_{1,2}^{(2,4)} \boldsymbol{\theta}_3^{(2,4)} \mathbf{T}_{2,3} & \mathbf{0} \\ \mathbf{0} & \mathbf{H}_{1,1}^{(2,5)} \boldsymbol{\theta}_2^{(2,5)} \mathbf{T}_{4,2} & \mathbf{0} & \mathbf{H}_{1,2}^{(2,5)} \boldsymbol{\theta}_4^{(2,5)} \mathbf{T}_{2,4} \\ \mathbf{0} & \mathbf{0} & (\mathbf{H}_{1,2}^{(2,6)} \boldsymbol{\theta}_3^{(2,6)} \mathbf{T}_{4,3}) \underline{\mathbf{m}}_{4,3}^{(1)} & (\mathbf{H}_{1,2}^{(2,6)} \boldsymbol{\theta}_4^{(2,6)} \mathbf{T}_{3,4}) \underline{\mathbf{m}}_{3,4}^{(1)} \\ \hline \mathbf{H}_{1,1}^{(3,1)} [\boldsymbol{\theta}_1^{(3,1)}, \boldsymbol{\theta}_2^{(3,1)}] \begin{bmatrix} \underline{\mathbf{m}}_{2,1}^{(3)} \\ \underline{\mathbf{m}}_{3,1}^{(2)} \end{bmatrix} & \mathbf{H}_{1,1}^{(3,1)} [\boldsymbol{\theta}_1^{(3,1)}, \boldsymbol{\theta}_3^{(3,1)}] \begin{bmatrix} \underline{\mathbf{m}}_{1,2}^{(3)} \\ \underline{\mathbf{m}}_{3,2}^{(1)} \end{bmatrix} & \mathbf{H}_{1,2}^{(3,1)} [\boldsymbol{\theta}_2^{(3,1)}, \boldsymbol{\theta}_3^{(3,1)}] \begin{bmatrix} \underline{\mathbf{m}}_{1,3}^{(2)} \\ \underline{\mathbf{m}}_{2,3}^{(1)} \end{bmatrix} & \mathbf{0} \\ \mathbf{H}_{1,1}^{(3,2)} [\boldsymbol{\theta}_1^{(3,2)}, \boldsymbol{\theta}_2^{(3,2)}] \begin{bmatrix} \underline{\mathbf{m}}_{2,1}^{(4)} \\ \underline{\mathbf{m}}_{4,1}^{(2)} \end{bmatrix} & \mathbf{H}_{1,1}^{(3,2)} [\boldsymbol{\theta}_1^{(3,2)}, \boldsymbol{\theta}_3^{(3,2)}] \begin{bmatrix} \underline{\mathbf{m}}_{1,2}^{(4)} \\ \underline{\mathbf{m}}_{4,2}^{(1)} \end{bmatrix} & \mathbf{0} & \mathbf{H}_{1,2}^{(3,2)} [\boldsymbol{\theta}_2^{(3,2)}, \boldsymbol{\theta}_3^{(3,2)}] \begin{bmatrix} \underline{\mathbf{m}}_{1,4}^{(2)} \\ \underline{\mathbf{m}}_{2,4}^{(1)} \end{bmatrix} \\ \mathbf{H}_{1,1}^{(3,3)} [\boldsymbol{\theta}_1^{(3,3)}, \boldsymbol{\theta}_2^{(3,3)}] \begin{bmatrix} \underline{\mathbf{m}}_{3,1}^{(4)} \\ \underline{\mathbf{m}}_{4,1}^{(3)} \end{bmatrix} & \mathbf{0} & \mathbf{H}_{1,2}^{(3,3)} [\boldsymbol{\theta}_1^{(3,3)}, \boldsymbol{\theta}_3^{(3,3)}] \begin{bmatrix} \underline{\mathbf{m}}_{1,3}^{(4)} \\ \underline{\mathbf{m}}_{4,3}^{(1)} \end{bmatrix} & \mathbf{H}_{1,2}^{(3,3)} [\boldsymbol{\theta}_2^{(3,3)}, \boldsymbol{\theta}_3^{(3,3)}] \begin{bmatrix} \underline{\mathbf{m}}_{1,4}^{(3)} \\ \underline{\mathbf{m}}_{3,4}^{(1)} \end{bmatrix} \\ \mathbf{0} & \mathbf{H}_{1,1}^{(3,4)} [\boldsymbol{\theta}_1^{(3,4)}, \boldsymbol{\theta}_2^{(3,4)}] \begin{bmatrix} \underline{\mathbf{m}}_{3,2}^{(4)} \\ \underline{\mathbf{m}}_{4,2}^{(3)} \end{bmatrix} & \mathbf{H}_{1,2}^{(3,4)} [\boldsymbol{\theta}_1^{(3,4)}, \boldsymbol{\theta}_3^{(3,4)}] \begin{bmatrix} \underline{\mathbf{m}}_{2,3}^{(4)} \\ \underline{\mathbf{m}}_{4,3}^{(2)} \end{bmatrix} & \mathbf{H}_{1,2}^{(3,4)} [\boldsymbol{\theta}_2^{(3,4)}, \boldsymbol{\theta}_3^{(3,4)}] \begin{bmatrix} \underline{\mathbf{m}}_{2,4}^{(3)} \\ \underline{\mathbf{m}}_{3,4}^{(2)} \end{bmatrix} \\ \mathbf{f}_{1,2} & & & \end{bmatrix}$$

The precoding matrix design for this phase is generally written as:

$$\mathbf{V}_i^{(4)} = \sum_{k=1}^3 \boldsymbol{\theta}_{\mathcal{I}^i(k)}^{(4)} \mathbf{f}_{\mathcal{I}^i(k),i}, \quad (7.14)$$

where $\boldsymbol{\theta}_i^{(4)} \in \mathbb{C}^{4 \times 1}$, $\mathcal{I}^i = \{1, \dots, 4\} \setminus \{i\}$, $\mathcal{I}^i(k)$ is the k th element of \mathcal{I}^i . Table 7.3 shows the different LCs transmitted during this phase. For example:

$$\mathbf{V}_3^{(4)} = \boldsymbol{\theta}_4^{(4)} \mathbf{f}_{4,3} + \boldsymbol{\theta}_2^{(4)} \mathbf{f}_{2,3} + \boldsymbol{\theta}_1^{(4)} \mathbf{f}_{1,3} \quad (7.15a)$$

$$= \boldsymbol{\theta}_4^{(4)} \left(\underline{\mathbf{h}}_{4,2}^{(3,1)} \left(\boldsymbol{\theta}_2^{(3,1)} \underline{\mathbf{m}}_{1,3}^{(2)} + \boldsymbol{\theta}_3^{(3,1)} \underline{\mathbf{m}}_{2,3}^{(1)} \right) \right) \quad (7.15b)$$

$$+ \boldsymbol{\theta}_2^{(4)} \left(\underline{\mathbf{h}}_{2,2}^{(3,3)} \left(\boldsymbol{\theta}_1^{(3,3)} \underline{\mathbf{m}}_{1,3}^{(4)} + \boldsymbol{\theta}_3^{(3,3)} \underline{\mathbf{m}}_{4,3}^{(1)} \right) \right) \quad (7.15c)$$

$$+ \boldsymbol{\theta}_1^{(4)} \left(\underline{\mathbf{h}}_{1,2}^{(3,4)} \left(\boldsymbol{\theta}_1^{(3,4)} \underline{\mathbf{m}}_{2,3}^{(4)} + \boldsymbol{\theta}_3^{(3,4)} \underline{\mathbf{m}}_{4,3}^{(1)} \right) \right). \quad (7.15d)$$

In general, $\mathbf{V}_i^{(4)}$ is constructed by retransmitting each piece of interference received at RX _{k} , with $k \notin \mathcal{G}^{(3,r)}$, for each of the three rounds $(3,r)$ where the signals of RX _{i} were transmitted. The received signal at RX₁ writes as

$$\begin{aligned}
\mathbf{y}_1^{(4)} &= \mathbf{H}_{1,1}^{(4)} \left((\Theta_1^{(4)} \mathbf{f}_{4,1} + \Theta_2^{(4)} \mathbf{f}_{3,1} + \Theta_3^{(4)} \mathbf{f}_{2,1}) \mathbf{x}_1 + (\Theta_1^{(4)} \mathbf{f}_{4,2} + \Theta_2^{(4)} \mathbf{f}_{3,2} + \Theta_4^{(4)} \mathbf{f}_{1,2}) \mathbf{x}_2 \right) + \\
&\quad \mathbf{H}_{1,2}^{(4)} \left((\Theta_1^{(4)} \mathbf{f}_{4,3} + \Theta_2^{(4)} \mathbf{f}_{3,3} + \Theta_4^{(4)} \mathbf{f}_{1,3}) \mathbf{x}_3 + (\Theta_2^{(4)} \mathbf{f}_{3,4} + \Theta_3^{(4)} \mathbf{f}_{2,4} + \Theta_4^{(4)} \mathbf{f}_{1,4}) \mathbf{x}_4 \right), \\
&= \mathbf{H}_{1,1}^{(4)} \left(\left(\Theta_1^{(4)} \mathbf{H}_{4,1}^{(3,1)} [\boldsymbol{\theta}_1^{(3,1)}, \boldsymbol{\theta}_2^{(3,1)}] \begin{bmatrix} \underline{\mathbf{m}}_{2,1}^{(3)} \\ \underline{\mathbf{m}}_{2,1}^{(2)} \end{bmatrix} + \Theta_2^{(4)} \mathbf{H}_{3,1}^{(3,2)} [\boldsymbol{\theta}_1^{(3,2)}, \boldsymbol{\theta}_2^{(3,2)}] \begin{bmatrix} \underline{\mathbf{m}}_{2,1}^{(4)} \\ \underline{\mathbf{m}}_{4,1}^{(2)} \end{bmatrix} + \Theta_3^{(4)} \mathbf{H}_{2,1}^{(3,3)} [\boldsymbol{\theta}_1^{(3,3)}, \boldsymbol{\theta}_2^{(3,3)}] \begin{bmatrix} \underline{\mathbf{m}}_{3,1}^{(4)} \\ \underline{\mathbf{m}}_{4,1}^{(3)} \end{bmatrix} \right) \mathbf{x}_1 + \right. \\
&\quad \left. \left(\Theta_1^{(4)} \mathbf{H}_{4,1}^{(3,1)} [\boldsymbol{\theta}_1^{(3,1)}, \boldsymbol{\theta}_3^{(3,1)}] \begin{bmatrix} \underline{\mathbf{m}}_{1,2}^{(3)} \\ \underline{\mathbf{m}}_{1,2}^{(1)} \\ \underline{\mathbf{m}}_{3,2}^{(2)} \end{bmatrix} + \Theta_2^{(4)} \mathbf{H}_{3,1}^{(3,2)} [\boldsymbol{\theta}_1^{(3,2)}, \boldsymbol{\theta}_3^{(3,2)}] \begin{bmatrix} \underline{\mathbf{m}}_{1,2}^{(4)} \\ \underline{\mathbf{m}}_{4,2}^{(1)} \\ \underline{\mathbf{m}}_{4,2}^{(2)} \end{bmatrix} + \Theta_4^{(4)} \mathbf{H}_{1,1}^{(3,4)} [\boldsymbol{\theta}_1^{(3,4)}, \boldsymbol{\theta}_2^{(3,4)}] \begin{bmatrix} \underline{\mathbf{m}}_{3,2}^{(4)} \\ \underline{\mathbf{m}}_{3,2}^{(3)} \\ \underline{\mathbf{m}}_{4,2}^{(2)} \end{bmatrix} \right) \mathbf{x}_2 \right) + \\
&\quad \mathbf{H}_{1,2}^{(4)} \left(\left(\Theta_1^{(4)} \mathbf{H}_{4,2}^{(3,1)} [\boldsymbol{\theta}_2^{(3,1)}, \boldsymbol{\theta}_3^{(3,1)}] \begin{bmatrix} \underline{\mathbf{m}}_{1,3}^{(2)} \\ \underline{\mathbf{m}}_{2,3}^{(1)} \end{bmatrix} + \Theta_3^{(4)} \mathbf{H}_{2,2}^{(3,3)} [\boldsymbol{\theta}_1^{(3,3)}, \boldsymbol{\theta}_3^{(3,3)}] \begin{bmatrix} \underline{\mathbf{m}}_{1,3}^{(4)} \\ \underline{\mathbf{m}}_{4,3}^{(1)} \end{bmatrix} + \Theta_4^{(4)} \mathbf{H}_{1,1}^{(3,4)} [\boldsymbol{\theta}_1^{(3,4)}, \boldsymbol{\theta}_3^{(3,4)}] \begin{bmatrix} \underline{\mathbf{m}}_{2,3}^{(4)} \\ \underline{\mathbf{m}}_{4,3}^{(2)} \end{bmatrix} \right) \mathbf{x}_3 + \right. \\
&\quad \left. \left(\Theta_2^{(4)} \mathbf{H}_{3,2}^{(3,2)} [\boldsymbol{\theta}_2^{(3,2)}, \boldsymbol{\theta}_3^{(3,2)}] \begin{bmatrix} \underline{\mathbf{m}}_{1,4}^{(2)} \\ \underline{\mathbf{m}}_{2,4}^{(1)} \end{bmatrix} + \Theta_3^{(4)} \mathbf{H}_{2,2}^{(3,3)} [\boldsymbol{\theta}_2^{(3,3)}, \boldsymbol{\theta}_3^{(3,3)}] \begin{bmatrix} \underline{\mathbf{m}}_{1,4}^{(3)} \\ \underline{\mathbf{m}}_{3,4}^{(1)} \end{bmatrix} + \Theta_4^{(4)} \mathbf{H}_{1,1}^{(3,4)} [\boldsymbol{\theta}_2^{(3,4)}, \boldsymbol{\theta}_3^{(3,4)}] \begin{bmatrix} \underline{\mathbf{m}}_{2,4}^{(3)} \\ \underline{\mathbf{m}}_{3,4}^{(2)} \end{bmatrix} \right) \mathbf{x}_4 \right).
\end{aligned}$$

For some column vector $\mathbf{a} \in \mathbb{C}^{6 \times 1}$ (different for each case), the interference terms generated during this phase at RX₁ can be classified in three classes:

- Terms associated to the OHI generated during the first phase at RX₁, i.e. of the form $\mathbf{a} \cdot (\underline{\mathbf{m}}_{1,i}^{(k)} \mathbf{x}_i)$, $\forall k \neq 1, \forall i \neq 1$. All those terms can be removed using the first phase overheard interference, since by definition $\text{rspan}(\underline{\mathbf{m}}_{j,i}^{(k)}) \subset \mathcal{T}_{j,i}$.
- Terms associated to the OHI generated during the second phase, i.e. of the form $\mathbf{a} \cdot (\underline{\mathbf{m}}_{j,i}^{(1)} \mathbf{x}_i)$, $\forall j \neq 1, \forall i$. All those terms can be removed using the second phase OHI terms, which are now decoupled thus individually available thanks to the mixed rounds of the third phase.
- Other terms that cannot be individually removed.

After removing all possible terms using the available OHI, RX₁ obtains

$$\bar{\mathbf{H}}_{1,1}^{(4)} \bar{\mathbf{V}}_1^{(4)} \mathbf{x}_1 + \underbrace{\mathbf{H}_{1,1}^{(4)} \boldsymbol{\theta}_1^{(4)} \mathbf{f}_{1,2}}_{\text{rank 1}} \mathbf{x}_2 + \underbrace{\mathbf{H}_{1,2}^{(4)} \boldsymbol{\theta}_1^{(4)} [\mathbf{f}_{1,3}, \mathbf{f}_{1,4}]}_{\text{inter-cell interference}} \begin{bmatrix} \mathbf{x}_3 \\ \mathbf{x}_4 \end{bmatrix} \quad (7.16)$$

where $\bar{\mathbf{H}}_{1,1}^{(4)} \bar{\mathbf{V}}_1^{(4)} \in \mathbb{C}^{6 \times 12}$ is a full rank matrix containing a combination of the desired signals received during phase 4, and the first two rounds of the phase 3. Now, using the OHI from the last third phase round ($[\mathbf{f}_{1,2}, \mathbf{f}_{1,3}, \mathbf{f}_{1,4}]$) the receiver is able to remove the inter-cell interference terms in (7.16). However, there remain some non-aligned intra-cell interference terms, since in general we cannot ensure that $\mathbf{H}_{1,1}^{(4)} = \mathbf{H}_{1,2}^{(4)}$. Fortunately, $\mathbf{H}_{1,1}^{(4)} \boldsymbol{\theta}_1^{(4)} \mathbf{f}_{1,2} \in \mathbb{C}^{6 \times 12}$ contains a 5-dimensional orthogonal subspace where the signals can be projected, such that 5 LCs of desired signals free of interference may be retrieved from this phase.

Overall, the total number of interference-free LCs of desired symbols at the end of the communication is equal to $3 + 3 + 1 + 5 = 12 = b$, thus $d_j^{(\text{in})} = \frac{12}{28} = \frac{3}{7}$ DoF are achieved.

7.2.2 Generalization to MIMO

Achievability of inner bounds in Theorem 7.1 is based on the generalization of the previous transmission protocol to any antenna setting. To this end, we formulate the following DoF

optimization problem:

$$\mathcal{P}_1 : \underset{\{b, S_1, S_2, S_3\} \in \mathbb{Z}^+}{\text{maximize}} \quad \frac{1}{N} \frac{b}{4S_1 + 6S_2 + 4S_3 + S_4} \quad (7.17a)$$

$$\text{s.t.} \quad \max(MS_1, 4NS_1) \geq b \quad (7.17b)$$

$$4NS_1 \geq b \quad (7.17c)$$

$$MS_2 \geq NS_1 \quad (7.17d)$$

$$MS_3 \geq 2NS_2 \quad (7.17e)$$

$$N(S_1 + 3S_2 + 6 \max(S_2, S_3)) \geq b \quad (7.17f)$$

providing the optimal values for b , $S_i, i = 1, 2, 3$ when the proposed scheme is employed, with $S_4 = \min(6S_2, \frac{b}{N} - S_1 - 3S_2)$, to be derived next. This problem may be solved by using the same methods employed at the end of Section 6.2.3.

The objective function (7.17a) corresponds to the number of symbols b divided by the number of signal dimensions $N\tau$ at the receiver. Moreover, a number of linear constraints are introduced to ensure linear decodability, and are justified next:

Transmit rank in phase 1: During the first phase, MS_1 linear combinations of the b symbols are transmitted using M antennas, and during S_1 slots. Then, for linear decodability of the desired symbols, no more symbols than the number of transmit dimensions can be sent, thus we force (7.17b).

Enough linear combinations in phase 1: After the first phase, NS_1 linear combinations of each user's symbols are distributed along each receiver. Note that no more fresh linear combinations of desired symbols will be introduced to the system, since the rest of phases consists in the retransmission of those linear combinations. Therefore, we force (7.17c), i.e. if each user have access to all $4NS_1$ linear combinations of its symbols, it should be able to linearly decode them.

Transmit rank in phase 2: Since NS_1 linear combinations of overheard interference are retransmitted in the S_2 slots of each phase 2 round, we force (7.17d), in order to ensure that the rank of transmitted OHI is preserved.

Transmit rank in phase 3: Similarly to the first and third constraints, we force (7.17e).

Enough LCs for the whole communication: At most, $N(S_1 + 3S_2 + 6 \max(S_2, S_3))$ linear combinations of desired symbols are delivered to each user. Then, we must have (7.17f).

Finally, we show how the value of S_4 can be obtained in closed form. First, we have that $6S_2$ linear combinations of overheard interference are transmitted per user during the last phase, thus we force:

$$N \cdot 6S_2 \leq N \cdot S_4.$$

Moreover, after the third phase $N(S_1 + 3S_2 + S_3)$ linear combinations of desired symbols are provided to each user, while the last phase delivers $N(S_4 - S_3)$ additional linear

combinations to each of them. This last expression can be easily derived by taking into account the zero-forcing operation. Then, we must have

$$\begin{aligned} N(S_1 + 3S_2 + S_3 + (S_4 - S_3)) &\geq b \\ N(S_1 + 3S_2 + S_4) &\geq b \end{aligned}$$

Taking into account that no more than these two constraints involve S_4 , we pick its minimum feasible, given by:

$$S_4 = \min\left(6S_2, \frac{b}{N} - S_1 - 3S_2\right)$$

7.3 Conclusion

The DoF of the 2-cell 2-user MIMO IBC have been studied for the case of delayed CSIT. We propose a four-phase protocol using only local knowledge, and based on linear precoding and decoding, extending the MAT scheme to be applicable in the IBC. Built on this basis, employing the principles of *delayed CSIT precoding* and *user scheduling*, we introduce the principle of *redundancy transmission*, taking into account the particular topology of the IBC, where users located in the same cell are served by the same transmitter.

Similarly to the schemes proposed for the IC (Chapter 6), we formulate a DoF maximization problem, generalizing the approach to be reliable for any antenna ratio $\rho = \frac{M}{N}$. Hence, the optimal transmission parameters (number of transmitted symbols, and duration of the phases) are derived as a function of ρ as the solution of the optimization problem. After evaluating the solution for each antenna ratio, we conclude that the proposed scheme improves any other work in terms of achievable DoF for $\rho > \rho_C$, with $\rho_C \approx 3.5414$.

Part III

Impact of Limited Feedback

The last part of this dissertation studies the MISO IC under the constraint of finite rate to inform the transmitters about the channel state. First, we introduce a common formulation able to connect the feedback parameters (number of quantization bits or transmission power for the feedback transmission) to the feedback quality. Then, the performance of the TDMA-groups scheme, described in Section 6.2.2 is evaluated under the case of finite-rate CSIT from three different perspectives: i) comparing its performance for digital and analog feedback, ii) for fixed feedback quality ϵ , and iii) in terms of net DoF. The adopted formulation allows drawing interesting conclusions for the first two cases, and analyzing the net DoF independently of the feedback method. Moreover, notice that our analysis moves from a particular to a general vision, since the net DoF take into account not only the impact of feedback quality on the DoF, but also the cost of CSI acquisition. Consequently, the net DoF provide a more accurate analysis, since each technique is affected by the transmission efficiency, its robustness to *quality* and *delay* of channel feedback, as well as to the channel coherence time value.

Technical paper/s related to this part:

M. Torrellas, A. Agustin, and J. Vidal, "On the degrees of freedom of the K -user MISO Interference Channel With Delayed CSIT", IEEE ICASSP, May 2014.

M. Torrellas, A. Agustin, and J. Vidal, "Performance Analysis of Inter-cell Interference Coordination in Small-Cell Networks with long feedback delays", Poster at EuCNC, Bologna, June 2014.

M. Torrellas, A. Agustin, and J. Vidal, "Net DoF analysis for the K -user MISO IC with outdated and imperfect channel feedback", EuCNC, Paris, June 2015.

Preliminaries

8

This chapter reviews some background required to understand the contributions of the last part of the thesis. First, we write the specific system model for the case of finite-rate CSIT, extending and particularizing some of the formulation introduced in Chapter 2, and reviewing the related literature under this type of CSIT. Second, the methods for channel feedback reporting, briefly introduced in Chapter 2, are more in-depth described.

8.1 Specific System Model

Unless otherwise stated, in this part of the thesis all variables will be indexed by means of the block channel structure perspective, as in (2.10), instead of from the point of view of the transmission strategy. This alternative notation hinders the description of transmission strategies, but will be more suitable for the analysis carried out in the sequel. For reader's convenience, we repeat in Fig. 8.1 the figure summarizing the block fading model.

8.1.1 MISO Interference Channel

In the K -user MISO IC there is only one user per cell equipped with a single antenna, thus each receiver is served by the transmitter with the same index. Therefore,

$$K_u = 1, \quad K = K_c, \quad c(j) = j, \forall j. \quad (8.1)$$

We assume that terminals are moving at constant velocity given by

$$v = \frac{\varphi}{T_C}, \quad (8.2)$$

where T_C is the channel coherence time, and φ will be defined as a function of the system parameters. For each time slot t of the block ν , the signal observed at RX_j is expressed as

$$y_j^{[t,\nu]} = \underline{\mathbf{h}}_{j,j}^{[\nu]} \mathbf{s}_j^{[t,\nu]} + \sum_{i \neq j} \underline{\mathbf{h}}_{j,i}^{[\nu]} \mathbf{s}_i^{[t,\nu]} + n_j^{[t,\nu]}, \quad t = 1, \dots, T_C, \quad (8.3)$$

with $\nu = \left\lceil \frac{t}{T_C} \right\rceil$. Moreover, we now consider also the feedback channel, orthogonal to the data channel, and described by:

$$\tilde{\mathbf{y}}_i^{[t,\nu]} = \sum_{j=1}^K \tilde{\mathbf{h}}_{i,j}^{[\nu]} \tilde{s}_j^{[t,\nu]} + \tilde{\mathbf{n}}_i^{[t,\nu]} \quad (8.4)$$

where $\tilde{\mathbf{h}}_{i,j}^{[\nu]} \in \mathbb{C}^{K \times 1}$ denotes the feedback channel gains from RX_j to the antennas of TX_i , and $\tilde{s}_j^{[t,\nu]}$ is the signal transmitted by RX_j during time slot t of the block ν , containing

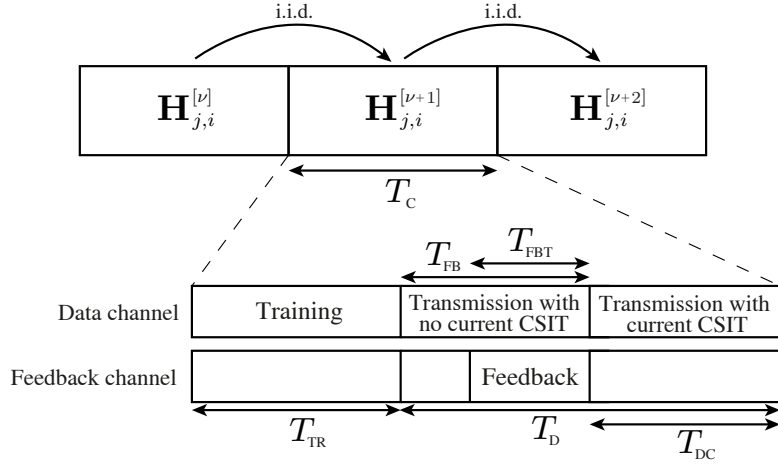


Figure 8.1: Block fading channel model. The channel remains constant in blocks of duration T_C time slots. Every time the channel changes of state, it is estimated by means of a training phase of duration T_{TR} time slots. This information is then fed back through the feedback channel, centered in an orthogonal channel, e.g. another frequency carrier. The transmission of the feedback lasts for T_{FBT} slots, although we assume that the feedback delay is system-fixed and equal to T_{FB} . During this waiting time, the transmitter can use the channel to transmit data without resorting to the current CSIT, i.e. with delayed or without CSIT. Finally, the remaining time of the block (T_{DC}) can be used for transmission exploiting the available information about the current channel state at the transmitter side. The total time of the block that can be used to transmit data is denoted by T_D .

the channel feedback for block ν , and ensuring

$$\mathbb{E} \left[\left| \hat{s}_j^{[t,\nu]} \right|^2 \right] \leq P_{\text{FB}}, \quad (8.5)$$

where P_{FB} is the maximum transmission power at each receiver.

Remark: For ease of exposition, we have assumed that data and feedback channel change its state at the same time. This unrealistic assumption does not affect any of the results in the sequel, and simply makes formulation less cumbersome.

8.1.2 Channel Feedback Quality

Two procedures exist in the literature for reporting the channel estimations from the receiver to the transmitter side: digital and analog feedback, reviewed in Sections 8.2.1 and 8.2.2, respectively. Both procedures introduce some errors on the channel knowledge at the transmitters. The inaccuracy of those methods is described by the feedback quality.

Let $\hat{\mathbf{h}}_{j,i}^{[\nu]}$ denote the estimation available at the transmitter side for channel $\underline{\mathbf{h}}_{j,i}^{[\nu]}$. We assume that this estimation is distributed as a Gaussian variable for both procedures. According to this, the feedback error is given by

$$\tilde{\mathbf{h}}_{j,i}^{[\nu]} = \underline{\mathbf{h}}_{j,i}^{[\nu]} - \hat{\mathbf{h}}_{j,i}^{[\nu]} \sim \mathcal{CN}(0, P_T^{-\epsilon}), \quad (8.6)$$

where P_T is the maximum transmission power at the transmitters, and the exponent $\epsilon \in [0, 1]$ defines the feedback quality: $\epsilon = 1$ implies perfect CSIT, $\epsilon = 0$ entails completely useless or inaccurate CSIT, such that the feedback knowledge gives no information about the actual channel. This definition of quality arises from the context of DoF analysis, which studies the channel at high SNR. Therefore, $\epsilon = 1$ makes the error to vanish as P_T grows, whereas $\epsilon = 0$ makes the error to be as strong as the channel itself.

To the best of the author's knowledge, the first attempt to study the DoF with this framework of imperfect CSIT was in [C⁺10] for the BC with imperfect current CSIT, i.e. when feedback has negligible delay but contains accuracy errors. In such a case, it was shown that null-steering attains ϵK DoF. Consequently, this result suggests that errors on feedback always reduce the channel DoF, although the author in [Jin06] does not claim optimality in terms of DoF for this setting.

More recently, the advances on characterizing the DoF with perfect delayed CSIT have led to the study of multi-user networks, basically the 2-user MISO BC, with different types of CSIT:

- (a) Perfect delayed CSIT and imperfect current CSIT.
- (b) Imperfect delayed CSIT and imperfect current CSIT, with each type of CSIT with a different feedback quality.
- (c) Only imperfect delayed CSIT.

Case (a) was initially studied by Yi et al. in [KC12], and subsequently optimized by Gou and Jafar in [GJ12]. In this latter reference, the authors derived both inner and outer bounds, thus the channel DoF became characterized for the 2-user MISO BC with this type of CSIT. Later, Chen and Elia advanced one step further in [CE13], considering also errors for delayed CSIT, i.e. case (b). Moreover, their work also applies to case (c) if useless current CSIT is considered. Surprisingly, the authors show that above a threshold for ϵ , imperfect delayed CSIT can be sufficient to attain the channel DoF corresponding to the case of perfect delayed CSIT. Regarding the IC, only the journal version [Y⁺14] of [KC12] analyzed the 2-user case, fully characterizing its DoF region for case (a). However, there are no results dealing with the IC for more than 2 users.

8.1.3 Net DoF

The net DoF describe the DoF taking into account all the issues related to channel estimation and feedback. They are given as a function of the channel coherence time, and provide a notion of the *benefits* of using CSIT taking into account the *cost* of having CSIT. While the benefits are basically described in terms of the conventional DoF, the costs are described by the feedback overhead, see (2.32) and feedback efficiency, or *feedback* DoF. In this regard, let F denote the feedback rate, i.e. the amount of resources consumed on the return channel to deliver the feedback. Then, the net DoF $d^{(\text{net})}$ and net bit-rate $B^{(\text{net})}$ are defined as

$$d^{(\text{net})} = d^{(\text{in})} - d^{(\text{FB})} = \lim_{P_T \rightarrow \infty} \frac{B^{(\text{net})}}{\log_2 P_T}, \quad B^{(\text{net})} = B - F, \quad (8.7)$$

where B was defined in (2.17), $d^{(\text{in})}$ also accounts for the overheads, and $d^{(\text{FB})}$ denotes the feedback DoF, defined as

$$d^{(\text{FB})} = \lim_{P_T \rightarrow \infty} \frac{F}{\log_2 P_T}. \quad (8.8)$$

Notice that the DoF are penalized as inaccurate is the available CSIT. On the other hand, the feedback DoF increase if a higher feedback quality should be ensured. Then, all previous variables will depend on the feedback quality ϵ .

Table 8.1: Available results in the literature and contributions of this thesis for the three types of analysis carried out in this part of the thesis.

	Literature	Studied in this thesis
DoF with imperfect FB quality	2-user MISO BC region (any type and quality of CSIT) [CE13], 2-user MISO IC region (perfect delayed CSIT, imperfect current CSIT) [Y ⁺ 14]	Inner bounds for the K -user MISO IC with imperfect delayed CSIT
Performance of analog and digital FB	Digital FB: analysis of ZF for the BC [Jin06] Analog FB: analysis of IA for the IC [AH12]	Simulation results for one strategy using delayed CSIT only
Net DoF	Inner bounds for the K -user BC [XAJ12][LSYW13] Some effects of the block fading channel neglected	Inner bounds for the K -user IC

The concept of net DoF was originally introduced in [XAJ12] for the 2-user BC, comparing the performance of ZF, MAT, and TDMA schemes. For long coherence time values (or very low user speeds), it was concluded that ZF performs the best, whereas for short coherence time (or very fast user speeds) TDMA performs the best. The most interesting conclusion was that for moderate to non-supersonic speedy terminals, MAT raises as the best candidate, i.e. the best balance between the benefit and cost of having CSIT is assuming delayed CSIT.

The net DoF analysis in [XAJ12] includes the errors due to digital feedback with finite quantization bits, but assumes full CSIR after the training period. However, this procedure only provides each receiver with estimations of the channel state for links ending at that receiver, i.e. *local channels*. Since most CSI-based strategies require that receivers have knowledge of all CSI (local and non-local), we denote by *dedicated* training (ded. training) the procedure that provides non-local channels to the receiver side. This issue was added to the net DoF analysis in [LSYW13], also for the 2-user BC, but then imperfect CSIT is not considered. Consequently, a complete analysis taking into account all effects is not available in the literature. Moreover, only the BC has been considered for this type of analysis.

8.2 Feedback Methods

Assuming that the CSI is estimated at the receivers using a pilot-based training signal, two procedures have been proposed in the literature for delivering feedback information from receivers to transmitters, next explained. Notice that we only assume deviation of channel knowledge at the transmitters, whereas receivers have perfect quality CSI after the training period.

8.2.1 Digital Feedback

In current cellular networks, channel feedback (if any) is usually delivered as digital feedback [Jin06]. This procedure entails two steps. First, the channel estimation is quantized to L_B bits. The quantization is performed using a random vector quantization codebook (CB) that is known at the transmitters and the receivers. A random vector quantization codebook consists of 2^{L_B} -dimensional unit norm vectors $\mathbf{c}_i, i = 1 \dots 2^{L_B}$ i.i.d. as $\mathcal{CN}(0, 1)$, where L_B denotes the number of feedback bits per quantized channel. Note that since the phase of a Gaussian vector is uniformly distributed, we can assume that for sufficiently high L_B the 2^{L_B} vectors are uniformly distributed along the unit sphere.

The quantization procedure is performed according to the following criterion:

$$\hat{\mathbf{h}}_{j,i}^{[\nu]} = \arg \max_{\mathbf{c}_i=1 \dots 2^{L_B}} \left\{ \left| \hat{\mathbf{h}}_{j,i}^{[\nu]} \cdot \mathbf{c}_i \right| \right\}, \text{ with } \hat{\mathbf{h}}_{j,i}^{[\nu]} = \frac{\mathbf{h}_{j,i}^{[\nu]}}{\|\mathbf{h}_{j,i}^{[\nu]}\|} \quad (8.9)$$

where $\hat{\mathbf{h}}_{j,i}^{[\nu]}$ denotes the quantization of $\hat{\mathbf{h}}_{j,i}^{[\nu]}$, the normalized channel. Basically, the channel is quantized by selecting the codeword that is closest to the estimated channel vector, where closeness is measured in terms of the chordal distance or, equivalently, the maximum inner product.

Once the quantization operation is performed, the second and last step is the delivery of channel feedback. In this case, it is assumed to be sent through an error-free channel. One possibility for implementation is to send the data through almost error-free control channels usually reserved in wireless networks. Therefore, the channel quantization turns to be the only error source when digital feedback is considered. Note that the total number of bits to be fed back is equal to the codebook size L_B multiplied by the number of cross-channels crossed or to be crossed by the transmitted signals. In other words, if for example TX_i is not active during the block ν , then it is not necessary to feedback the channels $\hat{\mathbf{h}}_{j,i}^{[\nu]}, \forall j$.

Low accurate CSIT may cause high-power non-perfectly aligned interferences at the UEs and drastically reduce the system performance. In terms of DoF, this situation was analyzed in [Jin06] for the BC using null-steering at the transmitter, where the authors concluded that the DoF with perfect CSIT cannot be maintained unless L_B scales with P_T in dB.

8.2.2 Analog Feedback

An alternative way to feed back the CSI is analog feedback, proposed for example in [AH12] for the K -user MIMO IC. In this case, the receivers feed back directly their (perfect accuracy) channel estimations in a dedicated precoded transmission through the feedback channel during T_{FBT} time slots. In our case,

$$T_{\text{FBT}} = \gamma \cdot K^2 (K - 1) \quad (8.10)$$

with $\gamma > 1$, since K channels, and $K - 1$ coefficients per channel are to be reported¹. Notice that in addition to the $K^2 (K - 1)$ coefficients to be transmitted, we also include the term γ , denoting the number of repetitions of the channel feedback transmission. Repeating the feedback allows improving the feedback quality (thus reducing the impact of noise) by coherently combining repetitions of the same transmission, but at the cost of a higher occupation of the feedback channel.

Define $\Phi_j \in \mathbb{C}^{\frac{T_{\text{FBT}}}{K} \times T_{\text{FBT}}}$ such that

$$\Phi_j \Phi_k^H = \delta_{j,k} \mathbf{I}, \quad (8.11)$$

where $\delta_{j,k} = 0$ unless $j = k$. This matrix exists with probability one since any (T_{FBT}) -dimensional space can be split into K orthogonal $(\frac{T_{\text{FBT}}}{K})$ -dimensional subspaces. Therefore, for each time slot $t = 1 \dots T_{\text{FBT}}$ the channel feedback is post-multiplied by the

¹Since the magnitude is not exploited in the schemes considered in this dissertation, for each channel vector of K coefficients, only $K - 1$ coefficients are required.

column t of Φ_j at RX_j . This allows transmitting the feedback simultaneously and such that the different terms can be separated at the transmitter side. As a result, assuming that all transmitters were active during block ν , the signal transmitted by RX_j after the T_{FBT} time slots is written as follows:

$$\tilde{\mathbf{s}}_j^{[\nu]} = \left[\tilde{s}_j^{[1,\nu]}, \dots, \tilde{s}_j^{[T_{\text{FBT}},\nu]} \right] \quad (8.12a)$$

$$= \sqrt{\frac{P_{\text{FB}}}{K-1}} \left[\underline{\mathbf{h}}_{j,1}^{[\nu]}, \dots, \underline{\mathbf{h}}_{j,j-1}^{[\nu]}, \dots, \underline{\mathbf{h}}_{j,j+1}^{[\nu]}, \dots, \underline{\mathbf{h}}_{j,K}^{[\nu]} \right] \Phi_j. \quad (8.12b)$$

Then, the CSI is estimated at the transmitter by applying $\|\tilde{\mathbf{h}}_{i,j}^{[\nu]}\|^{-1} (\tilde{\mathbf{h}}_{i,j}^{[\nu]})^H$ and Φ_j^H by the left and right hand side of the received signal, respectively. After that, each transmitter computes MMSE estimates of the data channels fed back by RX_j , where the quality of such CSI depends on the feedback transmission power P_{FB} ² and the number of repetitions γ of the feedback transmission.

Errors due to analog CSI were analyzed in terms of DoF in [AH12] for the IC using IA, where the authors showed that in order to maintain the perfect CSIT achievable DoF, the transmission power per receiver should scale with the transmission power per transmitter, i.e. $P_{\text{FB}} \propto P_{\text{T}}$. Notice that setting $\gamma > 1$ cannot improve the DoF obtained with $\gamma = 1$, since the number of repetitions is a finite number and we analyze the high SNR regime, although it can improve the performance in terms of bit-rate.

²Recall that noise is assumed to have unit variance, thus P_{FB} also represents the SNR for the feedback channel.

IC with Finite-Rate CSIT

9

The K -user MISO IC is studied under finite-rate CSIT. First, we introduce in Section 9.2 a common formulation able to connect the feedback parameters (number of quantization bits or transmission power for the feedback transmission) to the feedback quality. Then, the performance of the TDMA-groups scheme, described in Section 6.2.2, is evaluated under the case of finite-rate CSIT from three different perspectives. First, in Section 9.3, we analyze its performance by comparing the cases when digital or analog feedback methods are employed. Second, we evaluate the scheme for a fixed feedback quality ϵ in Section 9.4, i.e. feedback parameters are adjusted for each SNR value to guarantee a fixed feedback quality w.r.t. the SNR. Finally, the TG scheme is evaluated in terms of net DoF.

9.1 Main Contributions

9.1.1 A Common Feedback Formulation

When analyzing the errors of feedback, the state-of-the-art usually assumes a feedback setting, and evaluate the performance of the system as a function of it. In the last years, and motivated by the DoF analysis, some works have evaluated the performance of assuming a fixed feedback quality, defined as the exponent of the channel estimation error variance, and decaying with the SNR, as described in Section 8.1.2. As our first contribution, we connect in Section 9.2 both approaches by formulating the feedback quality as a function of the settings of analog or digital feedback. As a byproduct, this formulation will be useful to analyze the net DoF independently of the feedback procedure.

9.1.2 Analog vs Digital Feedback

In Section 9.3, we consider the downlink of a wireless scenario, and evaluate the performance of different strategies in terms mean and outage rate. Specifically, the original IBC is simplified to an IC by orthogonalizing the resources dedicated to in-cell users, and then the inter-cell is managed by: i) the TG scheme based on analog or digital feedback, or ii) a non-CSIT-based strategy. Results show supremacy of analog w.r.t. digital feedback and also the supremacy of both w.r.t. non-CSIT-based strategies.

9.1.3 Impact of Feedback Quality

The TG scheme is evaluated as a function of the feedback quality ϵ in Section 9.4. Our contribution is twofold. First, we derive the achievable DoF for the case of imperfect delayed CSIT, summarized by:

Theorem 9.1. *For the K -user MIMO IC with antenna ratio $\rho = K$, imperfect delayed CSIT, and feedback quality ϵ , the following achievable DoF per user are obtained:*

$$d_j^{(\text{in})} = \frac{2}{K+1} \frac{1 + \epsilon(K-1)}{K}. \quad (9.1)$$

Proof: See Section 9.4. □

Recall that consistently when $\epsilon = 1$ the DoF achieved by the TG scheme under perfect delayed CSIT are obtained, see Theorem 6.3 in Section 6.1. Additionally, we have the following corollary:

Corollary 1. *For any number of users K , the TG scheme outperforms TDMA, whenever $\epsilon > \frac{1}{2}$.*

Proof: It follows by comparing the DoF inner bound achieved by both approaches, i.e. starting from $d_j^{(\text{in})} > \frac{1}{K}$. □

Beyond the theoretical analysis, we have evaluated the bit-rate and outage rate achieved by the TG scheme for different values of ϵ , to be presented in Section 9.4. Since the slope of the bit-rate curves correspond to the achievable DoF proposed in Theorem 9.1, this simulation validates in practical terms the analytical result.

9.1.4 Net DoF Analysis

Our last contribution is addressed in Section 9.5, and may be summarized by the following items:

- The net DoF of 4 protocols are derived as a function of channel coherence time and the quality of channel feedback. They are constructed on the basis of the ZF, TG and TDMA schemes, initially proposed for the cases of current, delayed, and no CSIT: TDMA, TG, ZF-TDMA, and ZF-TG, where the last two combine two strategies: one using current CSIT, and another one to be carried out while the feedback is being transmitted. This will be shown in detail in Section 9.5. Interestingly, we obtain that the derived DoF inner bounds decrease piecewise linearly with user velocity, related to the channel coherence time as in (8.2).
- The CSIR distribution method proposed in [LSYW13] for the BC is extended to the IC.
- Beyond theoretical net DoF analysis, we provide net sum-rate results for the system working at finite SNR and finite feedback quality for two different user velocities.

9.2 A Common Feedback Formulation

When analyzing the errors associated to feedback, the state-of-the-art usually adopts one of the following two approaches:

1. Evaluate the performance of a system when one of the two feedback methods (analog or digital) is employed, using fixed feedback parameters, e.g. number of quantization bits. Moreover, in some cases it is analyzed how these parameters must be chosen to ensure the multiplexing gain or a given rate. This is the approach assumed next in Section 9.3.
2. Evaluate the performance of a system assuming a feedback quality, denoting the exponent of the channel estimation error variance, decaying with the SNR. This approach is employed in Section 9.4, and it is motivated by the DoF analysis.

In this section, we connect both approaches by formulating the feedback quality as a function of the feedback settings of analog or digital feedback. Consequently, we will be able to evaluate the net DoF independently of the feedback procedure using the single parameter ϵ . To this end, the feedback rate will be described in terms of the feedback parameters, to be used to compute the net DoF and net sum-rate in the last section.

Let $T > \tau$ denote the amount of time slots required for the communication, including feedback and training periods, and possibly entailing multiple coherence time blocks. Then, the amount of time resources consumed by feedback are quantified by the feedback rate, and formulated as follows:

$$F = \begin{cases} \frac{L_B}{T} & \text{digital feedback} \\ \frac{T_{FBT}}{T} \log_2 P_{FB} & \text{analog feedback} \end{cases} \quad (9.2)$$

where L_B denotes the number of quantization bits when using digital feedback, whereas T_{FBT} is the duration of the feedback transmission when using analog feedback.

Now, recall the following two results in the literature, derived for current CSIT but easily extendable to the delayed CSIT framework:

- Digital feedback: In [Jin06] the authors showed that the multiplexing gain for ZF cannot be ensured unless the number of bits L_B scales as

$$L_B \propto L_{CH} \log P_T, \quad (9.3)$$

where L_{CH} denotes the number of channels to be reported.

- Analog feedback: In [AH12] the authors showed that analog feedback only ensures the DoF achieved by IA in case

$$P_{FB} \propto P_T, \quad (9.4)$$

Inspired by these works, we propose formulating the feedback quality parameter ϵ for each method, as follows:

$$\epsilon = \begin{cases} \frac{L_B}{L_{CH} \log_2 P_T}, & \text{digital feedback} \\ \alpha + \beta, & \text{analog feedback} \end{cases} \quad (9.5)$$

On the one hand, notice that for digital feedback $\epsilon = 1$ ensures (9.3). On the other hand, we define

$$\alpha = \frac{\log P_{FB}}{\log P_T}, \quad \beta = \frac{\log \gamma}{\log P_T}, \quad (9.6)$$

where α takes into account the increase of quality related to P_{FB} , with (9.4) ensured for $\alpha = 1$. Moreover, β takes into account the number of retransmissions γ of the same packet as a way to improve the feedback quality. However, for finite number of repetitions, $\beta \rightarrow 0$ when $P_T \rightarrow \infty$. Hence, since the DoF analysis assumes an arbitrarily high transmission power, finite γ is useless in terms of DoF, thus $\beta > 0$ ($\gamma > 1$) will be only useful in the context of finite SNR.

9.3 Analog vs Digital Feedback

In this section, the TG scheme is compared for the case of using digital or analog feedback in terms of mean rate and outage rate. Results are benchmarked to a non-CSIT-based strategy, reviewed in the next section. Next, Section 9.3.2 defines the scenario and the three different approaches to be evaluated. Finally, Section 9.3.3 addresses the simulation results.

9.3.1 Review of eICIC

The time domain muting (TDM) enhanced Inter-Cell Interference Coordination (eICIC) has been considered as an interference management strategy for mitigating the inter-cell interference in today's LTE-based systems [WP12]. Basically, it divides the time resources orthogonally between the transmitters, defining a pattern for every transmitter that indicates when it can transmit. Let assume a K -user IC. Then, a muting ratio equal to $\frac{K-1}{K}$ indicates that every transmitter is muted $\frac{K-1}{K}$ part of the time, thus no interference is generated at the receivers. On the other hand, a lower muting ratio forces that more than one transmitter is active at the same time, thus generating some interference at the receivers.

The eICIC approach assumes no CSIT, thus the received interference is treated as noise, and it is not considered any interference management procedure beyond TDM. In this regard, notice that eICIC entails $d^{(in)} = 0$ for any muting ratio lower than $\frac{K-1}{K}$, since the arbitrarily high SNR regime is assumed. Therefore, the eICIC approach is not well suited for networks working at high SNR regime.

9.3.2 Problem Formulation

The downlink of a wireless scenario is considered, which can be modeled by the IBC with $K_c = 4$ cells, each with one transmitter, acting as base-station, and $K_u = 10$ users per cell. In this case, the intra-cell interference is avoided by naive orthogonalization, thus only the inter-cell interference is to be managed, and the problem reduces to the K -user MISO IC with $K = 4$. Three different approaches are considered to deal with the remaining interference, whose frame patterns are depicted in Fig. 9.1, and they are described next:

- The TG scheme with $G = 2$, entailing $P = 2$ phases of $R_1 = 4$ and $R_2 = 6$ single-slot rounds.
- eICIC-A: The eICIC scheme with the same muting ratio.
- eICIC-B: The eICIC scheme with muting ratio $3/4$, equivalent to TDMA.

Notice that employing the first two strategies leads to some interference observed at the

receivers. On the one hand, in case of using the eICIC-A scheme, the received interference is treated as noise. On the other hand, for the TG scheme the receiver will proceed as explained next.

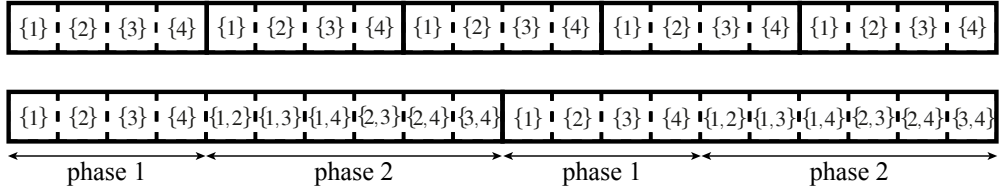


Figure 9.1: The two frame patterns considered for comparison of TG and eICIC. The eICIC scheme with muting ratio $3/4$ uses the frame pattern at top, being equivalent to TDMA. It is repeated 5 times, with each instance of duration 4 slots. The TG scheme and eICIC $3/4 - 1/2$ follow exactly the same frame pattern, shown at bottom, and repeated twice, with each instance of duration 10 slots. Notice that the beyond the served users per slot, the difference between them is how the signals are transmitted using or not the CSIT.

Consider the SSM of interference at RX_j , given by $\boldsymbol{\Omega}_j^{\text{int}} \in \mathbb{C}^{\tau \times \tau}$ (see (2.15)). Remember that in this case $b = 4$ symbols are transmitted per user along $\tau = 10$ time slots. In case of perfect feedback quality, $\text{span}(\boldsymbol{\Omega}_j^{\text{int}})$ lies on a subspace of dimension $\tau - b > b$. Consequently, the receiver can project onto the null space of the interference $(\text{span}(\boldsymbol{\Omega}_j^{\text{int}}))^{\perp}$, of dimension greater or equal to b . Hence, all the interference is canceled without hurting the rank of the desired signals. However, when feedback has errors the subspace orthogonal-to-interference may be of dimension lower than b because there is no guarantee of the IA constraints. For this reason, the receiving filter will be designed as explained next. First, consider the matrix

$$\boldsymbol{\Theta} = [\boldsymbol{\theta}_1, \boldsymbol{\theta}_2, \dots, \boldsymbol{\theta}_\tau] \quad (9.7)$$

whose columns represent the left singular vectors of $\boldsymbol{\Omega}_j^{(\text{int})}$, ordered from the lowest to the highest singular value. Then, the receiving filter \mathbf{W}_j is chosen as:

$$\mathbf{W} = [\boldsymbol{\theta}_1, \boldsymbol{\theta}_2, \dots, \boldsymbol{\theta}_b]^H, \quad (9.8)$$

i.e. the $b = 4$ singulars vectors with lowest singular value. Notice that this design ensures completely null interference only in case of perfect CSIT.

9.3.3 Simulation Results

The three approaches are simulated following the settings in [Hua13]. A quasi-static system level simulator is used according to the parameters for Small Cell Enhancement Scenario 2a. The most relevant parameters are shown in Table 9.1.

In case of using the TG scheme, the two feedback procedures described in Sections 8.2.1 and 8.2.2 are considered, with the maximum values for UE transmission power P_{FB} or codebook size L_B detailed in Table 9.1. A random codebook with Gaussian codewords is employed for digital feedback. System performance is evaluated in terms of *mean bit-rate* (MBR) and 10% *outage rate* (OR) per user. The former is defined as the average of B_j in (2.17), averaging not only among users, but also among channel realizations. On the other hand, the latter represents the bit-rate value above which at least the 90% of the rates are found. These two metrics give insight into the performance and fairness of each technique and feedback procedure working together.

Table 9.1: Simulation parameters

Parameter	Setting
Channel realizations	500
Bandwidth	10 MHz
Carrier frequency	3.5 GHz
Number of cells	4
Number of UEs per cell	10
UEs placement	80% indoor 20% outdoor
Maximum transmission power	BS: 30 dBm UE: [5, 10, 15, 20] dBm
Codebook size	[4, 8, 10, 12, 14, 16] bits
Codewords	Random Gaussian
Antenna Height	BS: 10m UE: 1.5m
Path loss	ITU UMi
Minimum distance (2D distance)	BS to BS: 20m BS to UE: 5m
Noise figure	9dB
Noise density	-174 dBm/Hz
Performance metrics	Mean rate per user Outage rate per user

Fig. 9.2 depicts the performance provided by each scheme on the MBR-OR plane. Results obtained by the eICIC-B scheme are improved in OR terms when the eICIC-B scheme is adopted. This is possible because every user is active during more time slots, where each BS transmits using random beamforming. Therefore, this scheme is able to reduce the impact of bad channel situations. However, the inter-cell interference does not allow gains in MBR terms, since we are in the high SNR regime. In this regard, the TG scheme with perfect delayed CSIT provides the best results in terms of MBR and improves the eICIC-B scheme by 15% gain in OR terms.

Those gains are achieved by managing the inter-cell interference thanks to the feedback report, being progressively reduced depending on which feedback approach and system parameters are employed. As expected, the system performance decreases as the codebook size, or feedback transmission power, respectively, are reduced. For our system parameters, analog clearly outperforms digital FB.

Finally, we observe that eICIC-A exhibits the best OR value as compared to TDMA, i.e. eICIC-B. This is because in our scenario there are some pairs of UEs not really interfering each other, thus scheduling such UEs together provides high contributions. However, UEs highly interfering each other seem to balance those gains. As a result, there exists a trade-off which is translated in approximately the same average rate as compared to TDMA, but an increase in terms of outage rate.

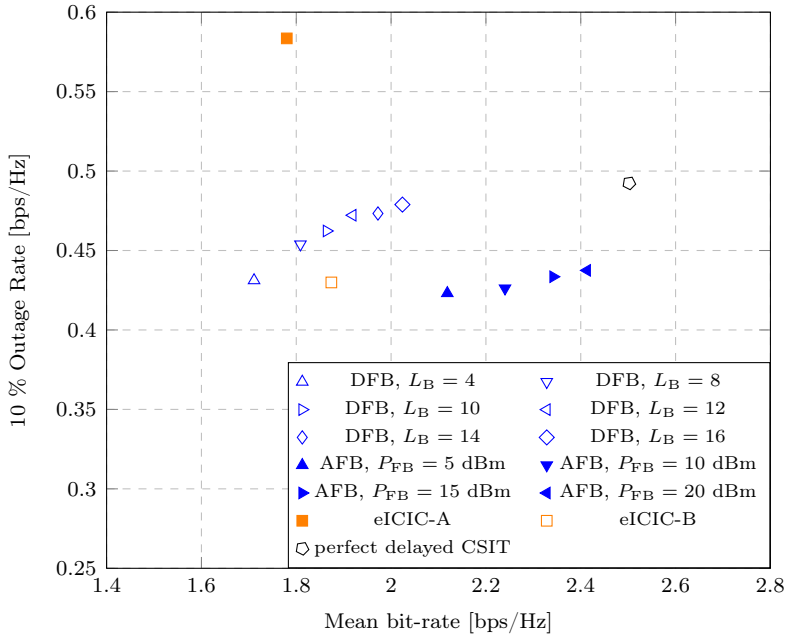


Figure 9.2: Mean bit-rate and 10% Outage Rate per UE for 4 cells of 10 UEs each. Analog and digital feedback procedures are compared to perfect delayed CSIT, and two eICIC-based schemes with different frame patterns are simulated as baselines.

9.4 Impact of Feedback Quality

The TG scheme is now studied when the feedback is acquired with quality ϵ . Notice that thanks to the common formulation proposed in Section 9.2, this analysis hold both for analog or digital feedback. First, the achievable DoF as a function of ϵ are derived in Section 9.4.1, thus proving Theorem 9.1. Next, Section 9.4.2 addresses the evaluation of the scheme in terms of mean and outage rates.

9.4.1 Proof of Theorem 9.1

The proof is presented for the case $M = K$, $N = 1$, although it is easy to see that the result holds for any antenna setting with antenna ratio $\rho = K$, by scaling both the number of transmitted symbols, and time slots. Moreover, the proof is shown for $K = 3$ users, where there are $P = 2$ phases of $R_1 = R_2 = 3$ single-slot rounds. The generalization to K users is straightforward by following a very similar procedure. In this line of arguments, the proof is shown only for RX₁. Also, the channels will be written in terms of phases and rounds for not losing generality. Actually, the DoF performance of this scheme under constant or time-varying channels is equivalent, as addressed in Section 6.4, since the only necessary assumption is independence of channels across users.

We assume that transmitters have no knowledge of feedback quality, thus they transmit as if the feedback was perfect. Then, the signal space matrix of interference at RX₁ is

given by:

$$\Omega_1^{\text{int}} = \begin{bmatrix} \mathbf{0} & \mathbf{0} \\ c_1\sqrt{P_T}\hat{\mathbf{h}}_{1,2}^{(1,2)} & \mathbf{0} \\ \mathbf{0} & c_1\sqrt{P_T}\hat{\mathbf{h}}_{1,3}^{(1,3)} \\ \hline c_2\sqrt{P_T}\hat{\mathbf{h}}_{1,2}^{(1,2)} & \mathbf{0} \\ \mathbf{0} & c_3\sqrt{P_T}\hat{\mathbf{h}}_{1,3}^{(1,3)} \\ c_4\sqrt{P_T}\hat{\mathbf{h}}_{3,2}^{(1,2)} & c_5\sqrt{P_T}\hat{\mathbf{h}}_{2,3}^{(1,3)} \end{bmatrix}, \quad (9.9)$$

where

$$c_1 = \frac{1}{\sqrt{3}}, c_2 = \frac{h_{1,2}^{(2,1)}(1)}{\|\hat{\mathbf{h}}_{1,2}^{(1,2)}\|}, c_3 = \frac{h_{1,3}^{(2,2)}(1)}{\|\hat{\mathbf{h}}_{1,3}^{(1,3)}\|}, c_4 = \frac{h_{1,2}^{(2,3)}(1)}{\|\hat{\mathbf{h}}_{3,2}^{(1,3)}\|}, c_5 = \frac{h_{1,3}^{(2,3)}(1)}{\|\hat{\mathbf{h}}_{2,3}^{(1,3)}\|}, \quad (9.10)$$

and we have assumed that during the second phase transmitters use only one antenna per transmission. Therefore, all constants c_k , $k = 1 \dots 5$ are independent of P_T . Remember that each row in (9.9) corresponds to each round (with only one slot), and each block column to users 2 and 3, respectively.

Let assume that the receiver applies the following receiving filter:

$$\mathbf{W}_1 = \begin{bmatrix} 1 & 0 & 0 & 0 & 0 & 0 \\ 0 & c_2 & 0 & -c_1 & 0 & 0 \\ 0 & 0 & c_3 & 0 & -c_1 & 0 \end{bmatrix} \quad (9.11)$$

such that the residual interference at RX₁ results:

$$\mathbf{W}_1 \Omega_1^{\text{int}} = \begin{bmatrix} \mathbf{0} & \mathbf{0} \\ c_1 c_2 \sqrt{P_T} \tilde{\mathbf{h}}_{1,2}^{(1,2)} & \mathbf{0} \\ \mathbf{0} & c_1 c_3 \sqrt{P_T} \tilde{\mathbf{h}}_{1,3}^{(1,3)} \end{bmatrix}, \quad (9.12)$$

with the estimation error $\tilde{\mathbf{h}}_{j,i}^{(p,r)}$ defined as in (8.6). Therefore, the interference covariance matrix, defined in (2.16), is given by,

$$\mathbf{Q}_1^{\text{int}} = (\mathbf{W}_1 \Omega_1^{\text{int}}) (\mathbf{W}_1 \Omega_1^{\text{int}})^H = \begin{bmatrix} 0 & 0 & 0 \\ 0 & c_6 P_T \|\tilde{\mathbf{h}}_{1,2}^{(1,2)}\|^2 & 0 \\ 0 & 0 & c_7 P_T \|\tilde{\mathbf{h}}_{1,3}^{(1,3)}\|^2 \end{bmatrix} \quad (9.13)$$

where c_6, c_7 are independent of P_T . Notice that this design for the receiving filter ensures completely null interference for perfect CSIT, but some residual terms are obtained otherwise.

Finally, we obtain the achieved DoF by developing the primary definition in (2.19), as follows:

$$\hat{d}_1^{(\text{in})}(\epsilon) \geq \frac{\log \mathbb{E} \{ |\mathbf{Q}_1^{\text{des}}| \} - \log \mathbb{E} \{ |\mathbf{Q}_1^{\text{int}} + \mathbf{W}_1 \mathbf{W}_1^H| \}}{6 \log P} \quad (9.14a)$$

$$= \frac{3 \log P_T - 2(1-\epsilon) \log P_T}{6 \log P_T} = \frac{1+2\epsilon}{6}, \quad (9.14b)$$

with $\mathbf{Q}_j^{\text{des}}$ defined in (2.16), where we have assumed $P_T \rightarrow \infty$, and used the Jensen's inequality [BV04] and basic properties of linear algebra. The DoF value stated in Theorem 9.1 is obtained by generalizing this procedure to the K -user case.

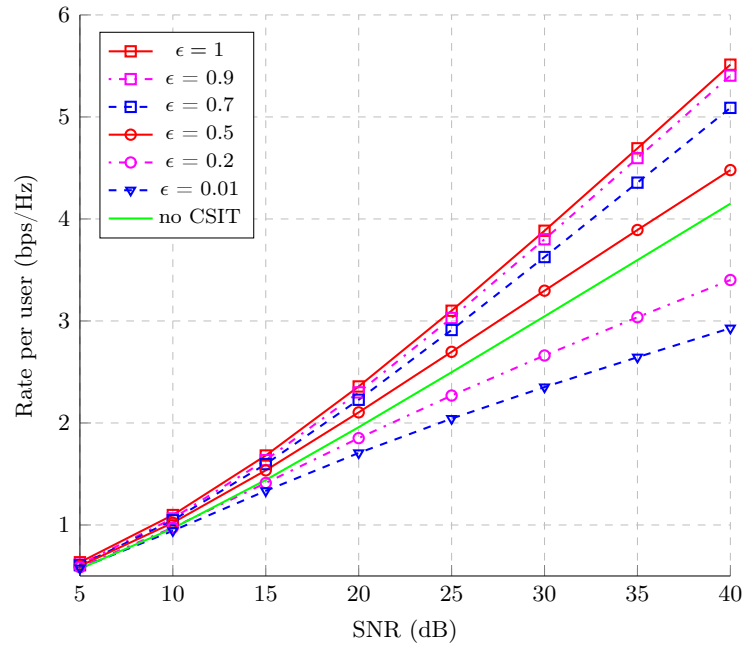


Figure 9.3: Average rate per user vs SNR for different feedback qualities

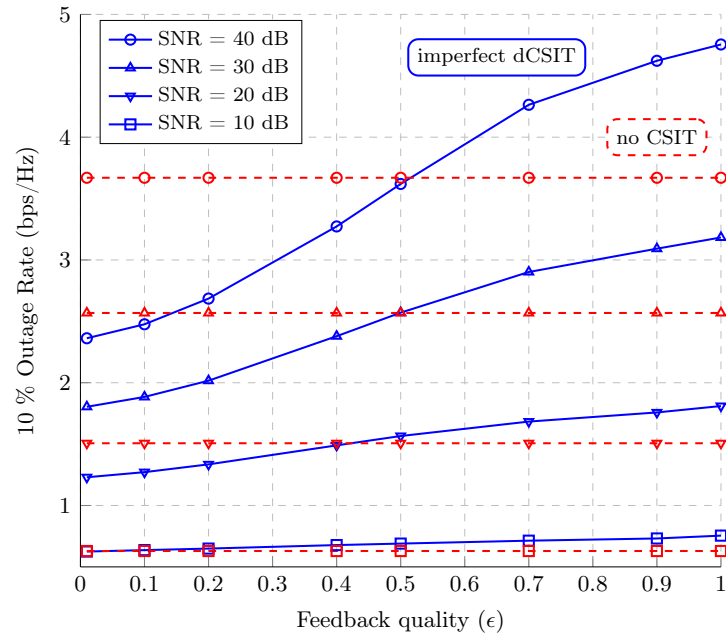


Figure 9.4: Outage rate vs Feedback quality for different SNR values.

9.4.2 Simulation results for Finite SNR

For the 3-user case, we evaluate the TG scheme for different feedback quality and SNR values. Fig. 9.3 shows the rate per user as a function of the SNR, averaged over 2000 channel realizations. We compare our results with the no CSIT case, referring to developing a TDMA strategy during 9 time slots. Notice that the slope for $\epsilon = 0.5$ coincides with that for the no CSIT case, as expected from the DoF expression derived in Theorem 9.1. If, for example, analog feedback is used for feedback transmission, this implies that the TG scheme, based on delayed CSIT, outperforms the no CSIT case as long as P_{FB} is higher than half P_T (both in dB, see (9.3)). It is also remarkable that the no CSIT scheme can be outperformed with the sufficiently high ϵ , even in the low-medium SNR regime. Further, Fig. 9.4 presents the 10% outage rate per user as a function of the feedback quality ϵ . It can be seen that the required feedback quality value for outperforming the TDMA scheme depends on the SNR.

9.5 Net DoF Analysis

We evaluate a number of protocols, presented in Section 9.5.1, in terms of its net DoF in Section 9.5.2. Finally, Section 9.5.3 addresses numerical results in terms of net DoF and net sum-rate.

9.5.1 Problem Formulation

Four protocols will be considered in the sequel, built upon ZF, TG, and TDMA schemes. Their protocol frames are depicted in Fig. 9.5 for both the data and feedback channels, and are briefly described next:

1. **TDMA:** The protocol frame is shown in Fig. 9.5-(a). Since no CSIT is required, there is no feedback. Hence, after the training period, data can directly be transmitted.
2. **ZF-TDMA:** The protocol frame is shown in Fig. 9.5-(b), where each block is divided in four parts. First, a training process is carried out. After that, feedback is transmitted through the feedback channel, thus transmitters must wait. Consequently, the data channel can be used without exploiting the information of the current report of the channel, with TDMA. Once the feedback information is available, transmitters compute the precoding matrices, and deliver the necessary information to the receiver side to ensure correct decodability. This is denoted as the *dedicated training process*. Finally, data is transmitted employing the computed precoding vectors.
3. **Pure TG:** The protocol frame is shown in Fig. 9.5-(d). There are three types of blocks: K for the first phase, $\binom{K}{2}$ for the second phase, and $T_{EDT}^{(TG)}$ extra blocks for dedicated training, with

$$\tau^{(TG)} = K + \binom{K}{2}. \quad (9.15)$$

Since delayed CSIT is assumed, the feedback can be transmitted out of the block. Then, the blocks corresponding to the first phase have only training and data trans-

mission periods. In contrast, in the blocks of the second phase the training period has lower duration since only one antenna is used at the active transmitters. Then, some time slots are used for dedicated training. Finally the extra blocks for dedicated training are divided in two parts: for estimating the current channel coefficients at the receivers, and for transmitting the previous dedicated training coefficients.

4. **ZF-TG:** The protocol frame is shown in Fig. 9.5-(c). Similarly to the previous approach, one can use the TG scheme during the dead times of ZF, since no current CSIT is required. Therefore, we have two types of blocks, $\tau^{(\text{TG})}$ for developing the data transmission for TG, and $T_{\text{EDT}}^{(\text{ZF-TG})}$ extra blocks for transmitting the dedicated training coefficients required for TG.

All of them will be studied in terms of net DoF. To this end, the DoF with overheads $d^{(\text{in})}$ are derived for each case, as well as its feedback DoF $d^{(\text{FB})}$. Then, the net DoF are simply computed as:

$$d^{(\text{net})} = d^{(\text{in})} - d^{(\text{FB})}.$$

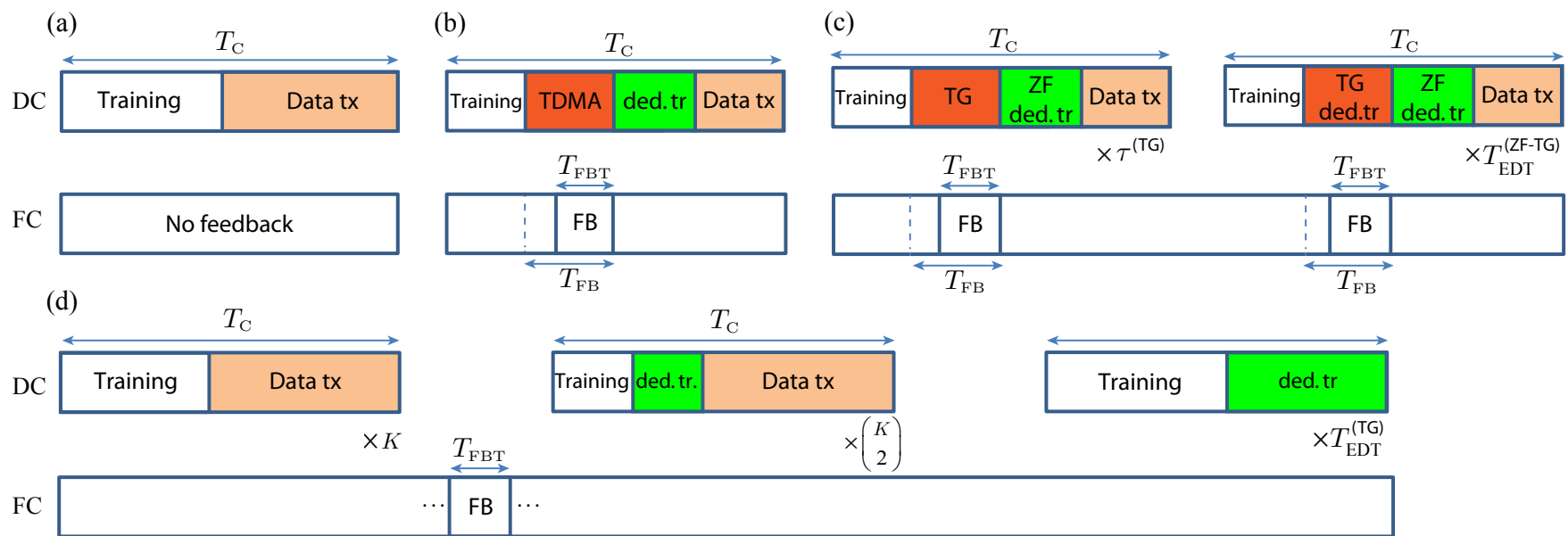


Figure 9.5: Protocol frames for (a) TDMA, (b) ZF-TDMA, (c) ZF-TG, and (d) pure TG for data and feedback channels, DC and FC, respectively.

9.5.2 A Per-Protocol Analysis

TDMA (no CSIT)

The training period lasts for one time slot since only one antenna is used at the transmitter, and no channel feedback is required. Hence

$$d^{(\text{net,TDMA})} = d^{(\text{in,TDMA})} = \frac{T_C - 1}{T_C} = 1 - \frac{1}{T_C}. \quad (9.16)$$

ZF-TDMA (current and no CSIT)

In this case the data channel usage is divided in four parts (see Fig. 9.5-(b)). First, a pilot-based training is carried out during K^2 time slots since all antennas of all transmitters are to be used. Next, feedback is reported and transmitters must wait for T_{FB} time slots. One possibility is to exploit this *dead time* to transmit without current CSIT, e.g. TDMA. Up to the author's best knowledge, the idea of using the dead times of ZF was first introduced in [LSYW12] for the BC. In this case, this adds $T_{\text{FB}} \wedge (T_C - K^2)^+$ DoF per block to the net DoF count.

Once the feedback report is available, each transmitter computes its ZF precoder. Then, one time slot of dedicated training is scheduled, providing to each RX_j its equivalent channel $\boldsymbol{\Omega}_j^{\text{des}}$, i.e. the product of direct channel and ZF precoder.

The DoF achieved by ZF-TDMA, accounting for the overheads, are given by

$$d^{(\text{in,ZF-TDMA})} = \lambda + \kappa, \quad (9.17a)$$

$$\lambda = \epsilon \cdot \left(1 - \frac{K^2 + 1 + T_{\text{FB}}}{T_C}\right)^+, \quad \kappa = \frac{T_{\text{FB}} \wedge (T_C - K^2)^+}{T_C}, \quad (9.17b)$$

where λ are the DoF achieved by the ZF part, taking into account that the DoF with imperfect current CSIT collapse to $K \cdot \epsilon$ [Jin06], whereas κ are the DoF achieved by the TDMA part. On the other hand, $K(K - 1)$ channels are reported, thus the feedback DoF are given by

$$d^{(\text{FB,ZF-TDMA})} = \epsilon \cdot \frac{K(K-1)^2}{T_C} \mathbb{1}(T_C > K^2 + 1 + T_{\text{FB}}), \quad (9.18)$$

where the indicator function $\mathbb{1}$ allows removing the feedback penalty if ZF cannot be done. Finally, the net DoF expression follows from combining (9.17a) and (9.18).

Pure TG (delayed CSIT)

Two different type of blocks are scheduled: for data transmission, and for dedicated training (see Fig. 9.5-d). The first type includes the first and second phases of the precoding scheme, and each block is in turn divided in two parts. The first part corresponds to a training period, while the remaining part of the block corresponds to data transmission without CSIT. The training during the first phase lasts for K time slots, since only one transmitter is active at a time and has K antennas. In contrast, during the second phase there are two simultaneously active transmitters but using only one antenna each. Hence, training consumes only 2 time slots, and the $K - 2$ time slots of excess can be used to transmit dedicated training coefficients, as will be explained later.

For the proper decoding of desired signals, every receiver needs all the CSI used by its associated transmitter for precoding, and the direct channel, although the latter is already known thanks to the training period. The aim of the dedicated training period is to deliver to every receiver the remaining required CSI for decoding. In case of transmitting one channel coefficient at a time, it would take $K^2(K - 1)$ time slots to deliver the $K(K - 1)$ channels. Next, we show that the number of time slots required for dedicated training can be halved. Inspired by [LSYW12] and the TG scheme, we exploit the already available information at the receivers (namely overheard CSI) to transmit the required CSIR. Our approach will be described by means of an example, and later we specify how it is used with the proposed protocol frame.

Consider the channel $\hat{\underline{h}}_{p,q}^{[\nu_1]} (\hat{\underline{h}}_{q,p}^{[\nu_2]})$, available at RX_p (RX_q) thanks to the training phase, and desired at RX_q (RX_p). Notice that we generally write ν_1 and ν_2 since they correspond to different coherence blocks. Assume that $\hat{\underline{h}}_{p,q}^{[\nu_1]}, \hat{\underline{h}}_{q,p}^{[\nu_2]}$ are transmitted as symbols, with no precoding and simultaneously, from TX_p and TX_q , respectively. Therefore, each user obtains a linear combination of $\{\hat{\underline{h}}_{p,q}^{[\nu_1]}, \hat{\underline{h}}_{q,p}^{[\nu_2]}\}$ and the required non-local CSI may be obtained by using the previous available local CSI.

Note that this approach is only reliable in case of digital feedback. This is because in such a case each transmitter obtains the *same imperfect version* of the channels, whereas in case of analog feedback different estimations of the feedback report are obtained at the transmitter side.

Now, since $\binom{K}{2} \cdot (K - 2)$ time slots are saved along the whole second phase, some extra time slots are required for dedicated training, written in general as

$$T_{\text{DT}}^{(\text{TG})} = \binom{K}{2} \cdot (\mu K - K - 2). \quad (9.19)$$

where $\mu = 1, 2$ for digital and analog feedback, respectively. The duration of this process can be longer than the coherence time. Then, since each block requires downlink training, the number of blocks for completing the dedicated training process is

$$T_{\text{EDT}}^{(\text{TG})} = \left\lceil \frac{T_{\text{DT}}^{(\text{TG})}}{T_{\text{C}} - K} \right\rceil, \quad (9.20)$$

assuming K time slots for data channel training per block. Then, data and feedback DoF are written as

$$d^{(\text{in,TG})} = K \frac{(T_{\text{C}} - K)(1 + \epsilon(K - 1))}{T_{\text{C}} \cdot \tau^{(\text{TG})} + K \cdot T_{\text{EDT}}^{(\text{TG})} + T_{\text{DT}}^{(\text{TG})}}, \quad (9.21)$$

$$d^{(\text{FB,TG})} = \epsilon \frac{K(K - 1)^2}{T_{\text{C}} \cdot \tau^{(\text{TG})} + K \cdot T_{\text{EDT}}^{(\text{TG})} + T_{\text{DT}}^{(\text{TG})}}, \quad (9.22)$$

where we use that $T_{\text{C}} - K$ slots are available for data transmission, and $K \frac{1+\epsilon(K-1)}{\tau^{(\text{TG})}}$ DoF are achieved with imperfect delayed CSIT of quality ϵ , see Section 9.1. Note that the same feedback as ZF-TDMA is required but at a reduced rate, thus reducing also the feedback DoF.

ZF-TG (current and delayed CSIT)

Similarly to ZF-TDMA, and ZF-MAT in [LSYW12], the TG scheme may be carried out during the dead times of ZF, since it does not require current CSIT, see its protocol frame in Fig. 9.5-c. The number of blocks for dedicated training are

$$T_{\text{EDT}}^{(\text{ZF-TG})} = \left\lceil \binom{K}{2} \frac{K}{T_{\text{FB}} \wedge (T_{\text{C}} - K^2)} \right\rceil, \quad (9.23)$$

Since each block offers T_{FB} time slots for ZF, we have

$$d^{(\text{in, ZF-TG})} = \lambda + K \frac{T_{\text{FB}} \wedge (T_{\text{C}} - K^2)^+}{T_{\text{C}}} \frac{1 + \epsilon(K-1)}{\tau^{(\text{TG})} + T_{\text{EDT}}^{(\text{ZF-TG})}}.$$

with $d^{(\text{FB, ZF-TG})} = d^{(\text{FB, ZF-TDMA})}$ and λ given in (9.17b).

9.5.3 Numerical Results

The protocols have been evaluated in terms of net DoF and net sum-rate assuming the same LTE-based system parameters in previous section, with $T_s = \frac{1}{168}$ msec as the duration of each time slot, and feedback delay equal to an LTE frame, i.e. 10 msec, equivalent to $T_{\text{FB}} = 1680$ time slots. Moreover, we consider that terminals are moving at constant velocity $v = \frac{\varphi}{T_{\text{C}}}$, with

$$\varphi = \frac{c}{4f_c T_s}, \quad (9.24)$$

where f_c denotes the carrier frequency, c is the speed of light, and T_{C} is measured in number of time slots (dimensionless).

Net DoF

Fig. 9.6 depicts net DoF as a function of user velocity. Those results assume $K = 4$ users, feedback quality $\epsilon = 0.7$, and only $\gamma = 1$ feedback transmissions, since retransmitting the feedback cannot improve the net DoF. Using the proposed common framework (Section 9.2), this translates with, for instance $P_T = 20$ dB, to $B \approx 14$ bits or $P_{\text{FB}} = 14$ dB.

Two regions are clearly observed, interestingly separated at approximately

$$v_T = \frac{\varphi}{T_{\text{FB}}} \approx 7.5 \text{ km/h}. \quad (9.25)$$

This threshold corresponds to the velocity where coherence time is comparable to the feedback delay, since in such a case ZF is no more reliable and the net DoF are severely reduced. ZF-TG performs the best (closely followed by ZF-TDMA) below v_T . Otherwise, pure TG exhibits the best performance. Notice that ZF-TG is outperformed by ZF-TDMA for $v > 60$ km/h. This is essentially because the former transmits an excessive amount of feedback whereas the latter reduces to simply TDMA since ZF cannot be done.

Finally, notice that the net DoF for any protocol are well approximated as piecewise linear functions, whose cut at the y-axis corresponds to the conventional DoF with imperfect CSIT. The derivation of those linear functions can be handled straightforwardly by simple extrapolations using the net DoF expressions.

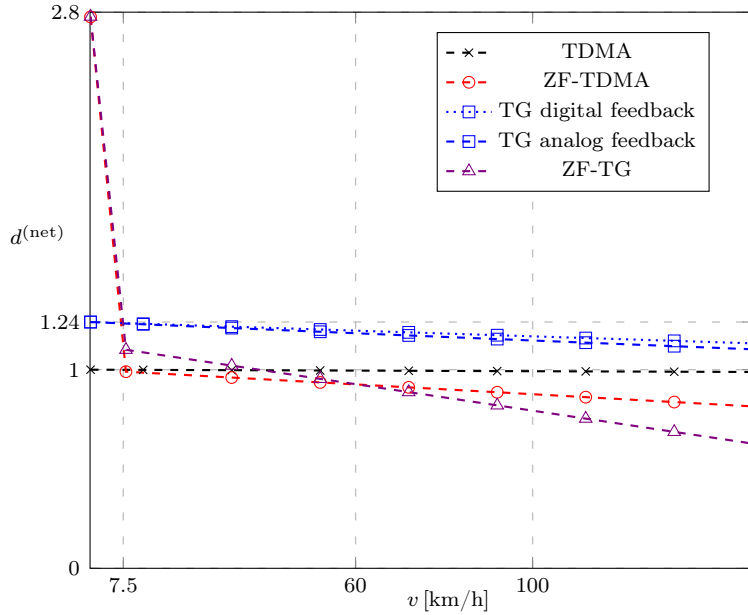


Figure 9.6: Net DoF vs. user velocity for $\epsilon = 0.7$, $K = 4$ users and $T_{FB} = 1680$. Net DoF are independent of the feedback method except for the TG protocol.

Net Sum Rate

Simulation results are depicted in Figs. 9.7 and 9.8 for $v = 3$ km/h and $v = 45$ km/h, respectively, elucidate when previous conclusions apply to settings with finite SNR and finite feedback quality. Results are averaged over 200 channel realizations. Transmissions are repeated such that all protocols employ the same number of channels. The same system parameters as in previous section are used, but now we fix $B = 14$ bits, $P_{FB} = 14$ dB for all SNR values, and evaluate three possible number of feedback repetitions $\gamma = \{1, 5, 10\}$. Some results are omitted to avoid redundancy and simplify the content on figure.

In case of $v = 3$ km/h, ZF is reliable, since $v < v_T$. Therefore, ZF-TG (closely followed by ZF-TDMA) provides the best net sum-rate for low-moderate SNR values ($P_T < 40$ dB). However, both ZF-based protocols decay severely as P_T increases, since the feedback error cannot be bounded using finite B or P_{FB} . For analog feedback, this might be partially solved by increasing the number of repetitions γ , i.e. improving feedback quality at the cost of feedback load. This is beneficial as SNR increases, but not for low SNR, where such amount of feedback penalizes system performance. Consequently, we conclude that there is a trade-off between γ and P_T . In contrast, the TG protocol provides lower performance for the low-medium SNR regime, but it is more resilient to feedback quality, and becomes the best protocol in terms of net sum-rate for $P_T > 40$ dB.

Finally, we also show the case $v = 45$ km/h, depicted in Fig. 9.8. In such a case, ZF is no more reliable ($v > v_T$, see (9.25)), and pure TG performs the best, providing maximum 5-10 % gains w.r.t. TDMA.

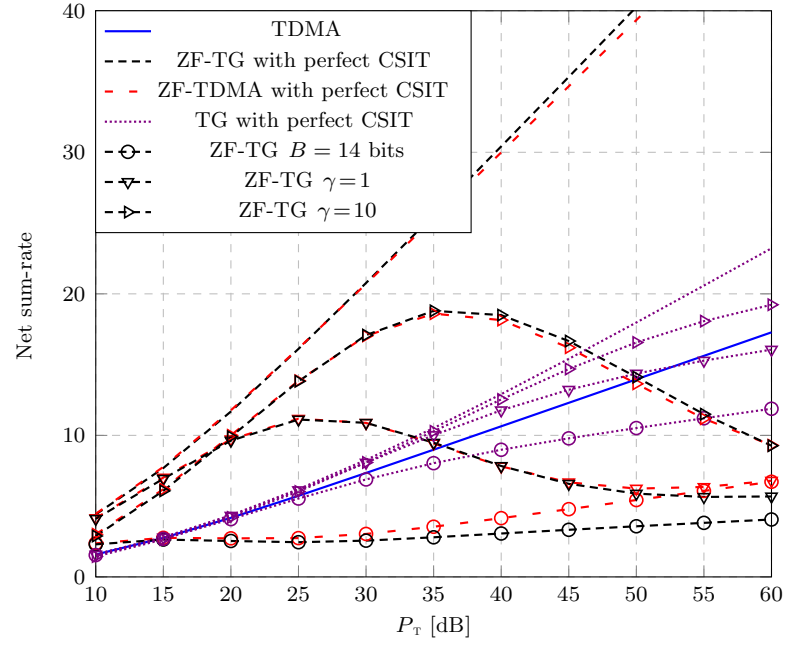


Figure 9.7: Net sum-rate vs. P_T for $v = 3 \text{ km/h}$, with analog feedback employing $P_{FB} = 14 \text{ dB}$. Each protocol is identified by one different color and line style, while markers denote different feedback settings.

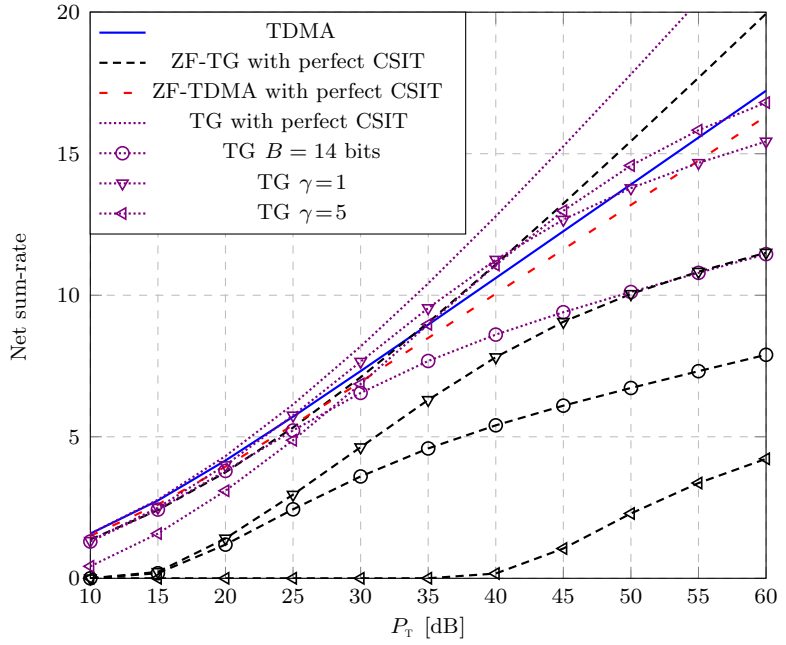


Figure 9.8: Net sum-rate vs. P_T for $v = 45 \text{ km/h}$, analog feedback with $P_{FB} = 14 \text{ dB}$.

9.6 Conclusion

The K -user MISO IC has been studied in case the CSI is obtained by means of finite-rate feedback. First, we have formulated the feedback quality as a function of the parameters of each feedback method. After, the performance of the TG scheme, described in Section 6.2.2, has been evaluated by comparing the cases where digital and analog feedback are employed, and benchmarking the results with eICIC with two different muting ratios. Results show supremacy of analog w.r.t. digital feedback and also the supremacy of both w.r.t. the two no CSIT approaches based on eICIC. Next, we have derived the achievable DoF of the TG scheme for the K -user MISO IC with feedback quality ϵ , obtaining that TDMA is outperformed as long as $\epsilon > \frac{1}{2}$ independently of the number of users K . Finally, we have evaluated the achievable net DoF of four protocols, based on transmission strategies for the cases of current, delayed, and no CSIT. For our system setup, we conclude that the net DoF decrease piecewise linearly with the user velocity. Moreover, and similarly to the conclusions for the BC, we obtain the the introduction of delayed-CSIT-based precoding strategies is beneficial, either for pedestrian or vehicular speeds.

Discussion and Lines of Future Work

Transmission strategies for interfering networks have been proposed and analyzed mainly in terms of DoF throughout this dissertation under different types of topology, MIMO configurations, and CSIT. Our objective has been focused on organizing the dissertation from theoretical towards every time more practical assumptions and key performance metrics, as summarized in Fig. 9.9. In broad terms, notice that in Part I only the channel DoF were studied. Then, we introduce in part II the more practical DoF-delay trade-off, taking also into account the latency and complexity for obtaining such DoF gains. Finally, in the last part of the thesis we have taken into account not only the gains of having CSIT, but also the cost of its acquisition by means of the net DoF metric.

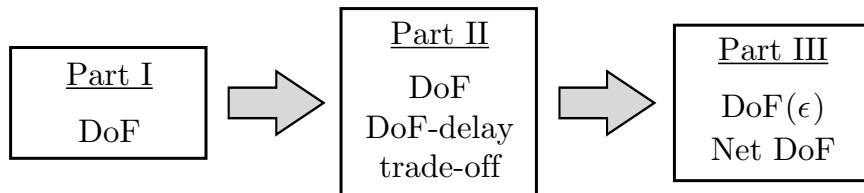


Figure 9.9: Performance metrics employed in each part of the dissertation.

Part I

The starting point of the dissertation has been the analysis of the interference channel in terms of DoF under full CSIT. In such a case, linear strategies proposed in the literature were not able to attain the DoF outer bound if channels are constant and transmitters have one more antenna than receivers, or viceversa ($\rho = \frac{M}{M+1}$). Inspired by the results for the SISO case, we have introduced the principle of asymmetric complex signaling into the machinery of subspace alignment chains, and formally proved that the conjunction of both approaches allows the achievability of the DoF outer bound for $M = 2, 3, \dots, 6$. Moreover, a methodology has been presented easing the proof for any value of M , where we conjecture that the optimal linear DoF can also be attained. This conjecture has been numerically checked for $M = 8, 9$. Consequently, the linear DoF of all antenna settings except for SISO are completely characterized.

Future work related to this first part of the thesis is next summarized:

- Exploring linear strategies for the SISO case, where linear DoF are not yet completely characterized.
- It may be interesting to optimize not only the slope of the sum-rate curve at the high SNR regime, but also the SNR offset. Taking into account the transmit power constraint, this seems to be possible by investigating the design of the support

precoding blocks, with the objective of improving the achievable sum-rate, and as an alternative to the one presented in Section 4.4.2.

- Exploring other practical scenarios under full CSIT whose DoF characterization remains open. For example, the IC with general message demands, i.e. where each transmitter sends a message, and each receiver requests for an arbitrary subset of messages¹, has been characterized for $\rho = 1$, but there are no results for other antenna settings.

Part II

Having perfect knowledge of the current channel state might not be realistic, especially for networks with high channel dynamics where the feedback delay may exceed the channel coherence time. The second part of the thesis has studied how the strategies based on full CSIT are extended to interference networks with delayed CSIT, i.e. when only information about past channel states is available. Chapter 6 has addressed the study of the DoF-delay trade-off for the K -user MIMO IC with delayed CSIT. Three fundamental tools have been identified in the context of delayed CSIT for designing linear precoding strategies: *delayed CSIT precoding*, *user scheduling*, and *redundancy transmission*. Based on them, we have proposed three precoding strategies, evaluated as a function of the antenna ratio ρ . For $\rho < 1$, the RIA scheme (built upon *delayed CSIT precoding* and a *redundancy transmission*, see Section 6.2.1) initially proposed for the 3-user SISO IC ($\rho = 1$) has been generalized to the K -user MIMO case. In contrast to the conjecture in [MC12], our results show that state-of-the-art DoF can be improved by considering $L \geq 3$ active pairs. Moreover, we have shown that for the region $\frac{1}{K-1} < \rho < \frac{K}{K^2-K-1}$ our proposed inner bound using the RIA scheme gets very close to the best known outer bound. Moreover, we have generalized the PSR scheme (built upon *delayed CSIT precoding*, *user scheduling* and a *redundancy transmission*, see Section 6.2.3) for 3 users from SISO to MIMO. This scheme provides the best achievable DoF when the number of antennas at the transmitter and receiver are similar ($\rho \approx 1$) not only for the 3-user MIMO IC, but also for the K -user MIMO IC by applying time-sharing concepts. Nevertheless, a MIMO generalization for $K > 3$ users remains open. In case the transmitter has more antennas than the receiver ($\rho > 1$), we propose the TG scheme (built upon *delayed CSIT precoding* and a *user scheduling*, see Section 6.2.2). The first phase is carried out orthogonally among users, whereas the second phase is developed in groups of $G \leq K$ users. The proper value of G lies on the trade-off between the constraints imposed by interference alignment, and the increase on the number of rounds, in turn depending on the antenna ratio ρ and the number of users K .

Schemes based on delayed CSIT usually obtain large DoF gains as compared to the no CSIT case, but at the cost of long transmission delays. In this regard, we have investigated the sensibility of the DoF for the proposed schemes as a function of the transmission duration, i.e. the DoF-delay trade-off, either by limiting the number of transmitted symbols, or its order, using the nomenclature introduced for the MAT scheme in [MAT12]. The first method builds upon the formulation of the parameters of each scheme (number of transmitted symbols and duration of the phases) as the solution of a DoF constrained maximization problem, and as a function of the number of users and the antenna ratio. In this regard, the analysis shows that although the PSR scheme and its extensions attain

¹Notice that the IC represents the case where each user requests only one and different message.

the best DoF values, this is at the cost of long transmission delays, which increases the complexity both at the transmitter and the receiver. In contrast, the proposed schemes are limited to $P \leq 3$ phases, and provide a better DoF-delay trade-off, i.e. competitive achievable DoF at the cost of not so long transmission delays.

Chapter 6 ends by concluding that the time-varying channels assumption, which is common along all the literature on delayed CSIT, is indeed not necessary, except for the SISO case. This implies that delayed CSIT strategies can be used even if the channel remains constant, which could be the case if the transmitter does not actually know the current channel coefficients. For the particular SISO case, we have proved that the two schemes in the literature failed, which can be fixed by applying asymmetric complex signaling concepts, as applied in the first part of thesis.

Chapter 7 has studied the DoF of the 2-user 2-cell IBC with delayed CSIT. A four-phase protocol based on linear precoding and decoding has been proposed, inspired by the lessons from the BC and IC, and taking into account the particular topology of the IBC, i.e. users from a cell are served by the same transmitter. Specifically, we have introduced the concept of redundancy transmission, originated for the IC, into the MAT scheme, the optimal transmission strategy for the BC. After reviewing the state-of-the-art, the proposed scheme has been shown to outperform any other work in terms of DoF for any antenna ratio $\rho > 3.5414$.

Future work related to the second part of the thesis is next summarized:

- A complete MIMO generalization of the PSR scheme (similar to the one in [HC15]) seems a tentative line of future work. Such generalization for the K -user MIMO IC may lead to tighter DoF results, although may be impractical in terms of communication delay.
- The formulation employed in Chapters 6 and 7 seems to be a good starting point for deriving precoding strategies for the asymmetric MIMO IC, i.e. when not all transmitters and receivers have the same number of antennas. In a similar way, it would be interesting to characterize not only the DoF per user or sum DoF, but also the DoF region for these channels.
- The study of the DoF penalties entailed by the use of local instead of global CSI may be an interesting line of future research.
- For full CSIT, the optimal scheme for the BC, i.e. ZF, extends to the IBC by taking into account the users located in the same cell, in a form of ZF denoted as ZF block-diagonalization [SSH04]. In a similar fashion, we have obtained that the transmission strategy of the BC with delayed CSIT can be extended to the IBC, by following the same arguments, i.e. by taking into account the common transmitters in the set of served users. Then, our contribution opens the door to the application of this principle for the study of scenarios with more cells or users per cell, and using some type of interference uncoupling procedure similar to the one proposed in Chapter 7. In the same line of arguments, we expect that exploiting these ideas the DoF knowledge for other antenna settings could be improved.
- Deriving tighter outer bounds would be also desirable for both channels, since the achievable DoF of the best known schemes are still too far from the trivial upper bounds.

Part III

Concluding the dissertation, we have focused on implementation issues for the TG scheme developed in Chapter 6. First, we have proposed a common framework for dealing with feedback quality regardless of the feedback procedure, see Section 9.2. This allows connecting the approaches of the rest of sections by formulating the feedback quality as a function of the feedback quality parameters of analog or digital feedback. Consequently, the net DoF can be analyzed independently of the feedback procedure.

Next, we study the performance of such scheme for the downlink of a wireless scenario, addressed in Section 9.3. In this case, the network is simplified to a MISO IC by orthogonalizing the resources dedicated to in-cell users, and managing the inter-cell interference by means of three different strategies. Results show supremacy of analog with respect to digital feedback and eICIC-based strategies.

As a third contribution of this part, Section 9.4 has addressed the study of the K -user MISO IC when the transmitters have imperfect, delayed, and local CSIT. Errors on channel feedback have been analyzed by evaluating the performance of the TG scheme in terms of DoF, and as a function of the feedback quality ϵ . We conclude that as long as $\epsilon > \frac{1}{2}$, the proposed scheme outperforms the no CSIT case. Thanks to the common formulation expressed in the last part the thesis, this may be translated as, for example, requiring that the transmission power used for feedback scales as half the transmission power for data, both in dB. Moreover, simulation results are provided, empirically validating the theoretical analysis, and showing the benefits of using delayed CSIT not only in terms of average bit-rate but also in terms of outage rate with respect to the case of uninformed transmitters.

Finally, Section 9.5 has addressed a net DoF analysis of the K -user MISO IC. They represent the most accurate metric for analyzing the performance of the proposed precoding strategy, since the the DoF are written as a function of the coherence time, and taking into account all issues related to channel acquisition at both the transmitter and receiver side: consumption of resources for feedback transmission, consumption of resources for channel training, and feedback delay. First, we have proposed four protocols based on the TG scheme, and the ZF and TDMA principles. Then, the net DoF have been derived as a function of channel coherence time and the quality of channel feedback. Interestingly, our results show that the net DoF decrease piecewise linearly with user velocity. Moreover, we have shown how the CSIR distribution method proposed in [LSYW13] for the BC can be extended to the IC. While the TG scheme has been shown to provide only few gains when combined with ZF for low-speed terminals, it provides considerable gains for vehicular speed terminals with respect to the protocol based on TDMA only, since ZF cannot be done.

Future work related to the last part of the thesis is next summarized:

- Deriving achievable DoF as a function of the feedback quality ϵ for other transmission strategies or antenna settings, as well as deriving outer bounds as a function of ϵ , elucidating how close to the channel DoF are the given inner bounds.
- Using the information about the value of ϵ for the design of the transmission strategy.
- Comparing the net DoF of the TG scheme to other state-of-the-art approaches using both current and delayed CSIT.

- Derive rules-of-thumb based on the information about the user speed for designing the transmission strategy, which is directly related to the channel coherence time.

Bibliography

- [AEKN11] M. Amir, A. El-Keyi, and M. Nafie, *Constrained Interference Alignment and the Spatial Degrees of Freedom of MIMO Cognitive Networks*, IEEE Trans. Inf. Theory, pp. 2994–3004, May 2011.
- [AGK11] M.J. Abdoli, A. Ghasemi, and A.K. Khandani, *On the Degrees of Freedom of Three-User MIMO Broadcast Channel with Delayed CSIT*, IEEE ISIT, Aug. 2011.
- [AGK13] M. Abdoli, A. Ghasemi, and A. Khandani, *On the Degrees of Freedom of K-User SISO Interference and X Channels with Delayed CSIT*, IEEE Trans. Inf. Theory, pp. 6542–6561, Jun. 2013.
- [AH12] O.E. Ayach and R.W. Heath, *Interference Alignment with Analog Channel State Feedback*, IEEE Trans. Wireless Commun., pp. 626–636, Feb. 2012.
- [AV09] V.S. Annapureddy and V.V. Veeravalli, *Gaussian Interference Networks: Sum Capacity in the Low-Interference Regime and New Outer Bounds on the Capacity Region*, IEEE Trans. Inf. Theory, pp. 3032–3050, Jul. 2009.
- [BK98] Y. Birk and T. Kol, *Informed-source coding-on-demand (ISCOD) over broadcast channels*, IEEE INFOCOM, Mar. 1998.
- [BT09] G. Bresler and D. Tse, *3 user interference channel: degrees of freedom as a function of channel diversity*, IEEE Allerton, Sept. 2009.
- [BV04] S. Boyd and L. Vandenberghe, *Convex optimization*, Cambridge University Press, New York, NY, USA, 2004.
- [C⁺10] G. Caire et al., *Multiuser MIMO Achievable Rates With Downlink Training and Channel State Feedback*, IEEE Trans. Inf. Theory, pp. 2845–2866, Jun. 2010.
- [Car75] A Carleial, *A case where interference does not reduce capacity*, IEEE Trans. Inf. Theory, pp. 569–570, Sep. 1975.
- [CE13] J. Chen and P. Elia, *Toward the Performance Versus Feedback Trade-off for the Two-User MISO Broadcast Channel*, IEEE Trans. Inf. Theory, pp. 8336–8356, Dec. 2013.
- [CJ08] V.R. Cadambe and S.A. Jafar, *Interference Alignment and Degrees of Freedom of the K-user Interference Channel*, IEEE Trans. Inf. Theory, pp. 3425–3441, Aug. 2008.

- [CJW10] V.R. Cadambe, S.A. Jafar, and C. Wang, *Interference Alignment With Asymmetric Complex Signaling - Settling the Host-Madsen-Nosratinia Conjecture*, IEEE Trans. Inf. Theory, pp. 4552–4565, Sept. 2010.
- [CK99] M. Capinski and P.E. Kopp, *Measure, integral and probability*, 2003 ed., Springer undergraduate mathematics Series, Springer, Londres, 1999.
- [CT06] T.M. Cover and J.A. Thomas, *Elements of Information Theory*, 2nd. ed., Wiley, Sept. 2006.
- [DE73] G. Dantzig and B. Eaves, *Fourier-Motzkin elimination and its dual*, J. of Combinatorial Theory, pp. 288–297, May 1973.
- [G⁺07] D. Gesbert et al., *Shifting the MIMO Paradigm*, IEEE Signal Processing Magazine, pp. 36–46, Sept. 2007.
- [GCJ08] K. Gomadam, V.R. Cadambe, and S.A. Jafar, *Approaching the Capacity of Wireless Networks through Distributed Interference Alignment*, IEEE GLOBECOM, Nov. 2008.
- [GJ10] T. Gou and S.A. Jafar, *Degrees of Freedom of the K-User M × N MIMO Interference Channel*, IEEE Trans. Inf. Theory, pp. 6040–6057, Dec. 2010.
- [GJ12] ———, *Optimal Use of Current and Outdated Channel State Information: Degrees of Freedom of the MISO BC with Mixed CSIT*, IEEE Communications Letters, pp. 1084–1087, 2012.
- [GK12] A. Gamal and Y. Kim, *Network information theory*, Cambridge University Press, New York, NY, USA, 2012.
- [GMK10] A. Ghasemi, A.S. Motahari, and A.K. Khandani, *Interference alignment for the K-user MIMO interference channel*, IEEE ISIT, Jun. 2010.
- [GWJ11] T. Gou, C. Wang, and S.A. Jafar, *Aiming Perfectly in the Dark-Blind Interference Alignment Through Staggered Antenna Switching*, IEEE Trans. Signal Process., pp. 2734–2744, Jun. 2011.
- [HC15] C. Hao and B. Clerckx, *Degrees-of-freedom of the K-user MISO interference channel with delayed local CSIT*, IEEE ICC, Jun. 2015.
- [HK81] T.S. Han and K. Kobayashi, *A new achievable rate region for the interference channel*, IEEE Trans. Inf. Theory, Jan. 1981.
- [Hua13] HiSilicon Huawei, *Evaluation assumptions for small cell enhancements-physical layer*, R1-130856, 3GPP, Jan. 2013.
- [Jaf05] S.A. Jafar, *Degrees of Freedom in Distributed MIMO Communications*, IEEE Inf. Theory Workshop, Jun. 2005.
- [Jaf10] ———, *Exploiting Channel Correlations - Simple Interference Alignment Schemes with no CSIT*, IEEE Globecom, Dec. 2010.
- [Jaf11] ———, *Interference Alignment: A New Look at Signal Dimensions in a Communication Network*, Found. and Trends in Commun. and Inf. Theory, Jul. 2011.

- [Jin06] N. Jindal, *MIMO Broadcast Channels With Finite-Rate Feedback*, IEEE Trans. Inf. Theory, pp. 5045–5060, Nov. 2006.
- [K⁺11] O.O. Koyluoglu et al., *Interference Alignment for Secrecy*, IEEE Trans. Inf. Theory, pp. 3323–3332, Jun. 2011.
- [KC12] M. Kobayashi and G. Caire, *On the net DoF comparison between ZF and MAT over time-varying MISO broadcast channels*, IEEE ISIT, Jul. 2012.
- [KC13] M.G. Kang and W. Choi, *Ergodic Interference Alignment With Delayed Feedback*, IEEE Signal Process. Lett., pp. 511–514, May 2013.
- [KML04] M. Krunz, A. Muqattash, and S.J. Lee, *Transmission power control in wireless ad hoc networks: challenges, solutions and open issues*, IEEE Network, pp. 8–14, Sept. 2004.
- [KV14] S. Karmakar and M.K. Varanasi, *Capacity region of a class of strong MIMO IC*, CISS, Mar. 2014.
- [L⁺12] Ke L. et al., *Degrees of Freedom Region for an Interference Network With General Message Demands*, IEEE Trans. Inf. Theory, pp. 3787–3797, Jun. 2012.
- [LC13] J.H. Lee and W. Choi, *On the Achievable DoF and User Scaling Law of Opportunistic Interference Alignment in 3-Transmitter MIMO Interference Channels*, IEEE Trans. Wireless Commun., pp. 2743–2753, Jun. 2013.
- [LCR13] J.H. Lee, W. Choi, and B.D. Rao, *Multiuser Diversity in Interfering Broadcast Channels: Achievable Degrees of Freedom and User Scaling Law*, IEEE Trans. Wireless Commun., pp. 5837–5849, Nov. 2013.
- [LS13] C. Lameiro and I. Santamaria, *Degrees-of-freedom for the 4-user SISO interference channel with improper signaling*, IEEE ICC, Jun. 2013.
- [LSYW12] Y. Lejosne, D. Slock, and Y. Yuan-Wu, *Degrees of freedom in the MISO BC with delayed-CSIT and finite coherence time: A simple optimal scheme*, IEEE ICSPCC, Aug. 2012.
- [LSYW13] ———, *Net degrees of freedom of recent schemes for the MISO BC with delayed CSIT and finite coherence time*, IEEE WCNC, Apr. 2013.
- [M⁺14] A.S. Motahari et al., *Real Interference Alignment: Exploiting the Potential of Single Antenna Systems*, IEEE Trans. Inf. Theory, pp. 4799–4810, Aug 2014.
- [MAMK08] M.A. Maddah-Ali, A.S. Motahari, and A.K. Khandani, *Communication Over MIMO X Channels: Interference Alignment, Decomposition, and Performance Analysis*, IEEE Trans. Inf. Theory, pp. 3457–3470, Aug. 2008.
- [MAT12] M.A. Maddah-Ali and D. Tse, *Completely Stale Transmitter Channel State Information is Still Very Useful*, IEEE Trans. Inf. Theory, pp. 4418–4431, Jul. 2012.
- [MC12] L. Maggi and L. Cottatellucci, *Retrospective interference alignment for interference channels with delayed feedback*, IEEE WCNC, Apr. 2012.

- [MJS12] H. Maleki, S.A. Jafar, and S. Shamai, *Retrospective Interference Alignment Over Interference Networks*, J. Sel. Topics Signal Process., pp. 228–240, Jun. 2012.
- [MK09] A.S. Motahari and A.K. Khandani, *Capacity Bounds for the Gaussian Interference Channel*, IEEE Trans. on Inf. Theory, pp. 620–643, Feb. 2009.
- [MMK10] S.H. Mahboubi, A.S. Motahari, and A.K. Khandani, *Layered Interference Alignment: Achieving the total DoF of MIMO X-channels*, IEEE ISIT, Jun. 2010.
- [N⁺12] B. Nazer et al., *Ergodic Interference Alignment*, IEEE Trans. Inf. Theory, pp. 6355–6371, Oct. 2012.
- [OE13] O. Ordentlich and U. Erez, *On the Robustness of Lattice Interference Alignment*, IEEE Trans. Inf. Theory, pp. 2735–2759, May 2013.
- [PA14] J. Parajuli and G. Abreu, *A space-time Tx scheme for two-cell MISO-BC with delayed CSIT*, IEEE ISIT, Jun. 2014.
- [PD12] D.S. Papailiopoulos and A.G. Dimakis, *Interference Alignment as a Rank Constrained Rank Minimization*, IEEE Trans. Signal Process., pp. 4278–4288, Aug. 2012.
- [RLL12] M. Razaviyayn, G. Lyubeznik, and Zhi-Quan Luo, *On the Degrees of Freedom Achievable Through Interference Alignment in a MIMO Interference Channel*, IEEE Trans. Signal Process., pp. 812–821, Feb. 2012.
- [S⁺08] S. Sridharan et al., *Capacity of Symmetric K-User Gaussian Very Strong Interference Channels*, IEEE Globecom, Nov. 2008.
- [SR15] T.K. Sawanobori and R. Roche, *Mobile Data Demand: Growth Forecasts Met*, Jun. 2015, <http://www.ctia.org/docs/default-source/default-document-library/062115mobile-data-demands-white-paper.pdf>.
- [SSH04] Q.H. Spencer, A.L. Swindlehurst, and M. Haardt, *Zero-forcing methods for downlink spatial multiplexing in multiuser MIMO channels*, IEEE Trans. Signal Process., pp. 461–471, Feb. 2004.
- [SY13] G. Sridharan and Wei Yu, *Degrees of freedom of MIMO cellular networks with two cells and two users per cell*, IEEE ISIT, Jul. 2013.
- [T⁺14] M. Torrellas et al., *The DoF of the 3-User ($p, p+1$) MIMO Interference Channel*, IEEE Trans. on Commun., pp. 3842–3853, Nov. 2014.
- [Tel99] I.E. Telatar, *Capacity of Multi-antenna Gaussian Channels*, European Transactions on Telecommunications, pp. 585–595, Nov. 1999.
- [TV05] D. Tse and P. Viswanath, *Fundamentals of wireless communication*, Cambridge University Press, New York, NY, USA, 2005.
- [VV11] C.S. Vaze and M.K. Varanasi, *The Degrees of Freedom Region of the Two-User MIMO Broadcast Channel with Delayed CSIT*, IEEE ISIT, Jul. 2011.

- [VV12a] _____, *The Degree-of-Freedom Regions of MIMO Broadcast, Interference, and Cognitive Radio Channels With No CSIT*, IEEE Trans. Inf. Theory, pp. 5354–5374, Aug. 2012.
- [VV12b] _____, *The Degrees of Freedom Region and Interference Alignment for the MIMO Interference Channel With Delayed CSIT*, IEEE Trans. Inf. Theory, pp. 4396–4417, Jul. 2012.
- [VVK14] S.B. Venkatakrishnan, P. Viswanath, and S. Kannan, *Degrees of Freedom for multiple-multicast traffic*, IEEE ISIT, Jun. 2014.
- [WGJ11] C. Wang, T. Gou, and S.A. Jafar, *On Optimality of Linear Interference Alignment for the Three-User MIMO Interference Channel with Constant Channel Coefficients*, eScholarship Univ. of California, Oct. 2011, Available at: <http://escholarship.org/uc/item/6t14c361>.
- [WGJ14] _____, *Subspace Alignment Chains and the Degrees of Freedom of the Three-User MIMO Interference Channel*, IEEE Trans. Inf. Theory, pp. 2432–2479, May 2014.
- [WP12] Y. Wang and K.I. Pedersen, *Performance Analysis of Enhanced Inter-cell Interference Coordination in LTE-Advanced Heterogeneous Networks*, IEEE VTC Spring, Jul. 2012.
- [WS13] C. Wang and A. Sezgin, *Degrees of Freedom of the Interference Channel with a Cognitive Helper*, IEEE Commun. Letters, pp. 920–923, May 2013.
- [WSJ14] C. Wang, H. Sun, and S.A. Jafar, *Genie Chains: Exploring Outer Bounds on the Degrees of Freedom of MIMO Interference Networks*, ArXiv e-prints, Apr. 2014.
- [WSS06] H. Weingarten, Y. Steinberg, and S. Shamai, *The Capacity Region of the Gaussian Multiple-Input Multiple-Output Broadcast Channel*, IEEE Trans. Inf. Theory, pp. 3936–3964, Sept. 2006.
- [XAJ12] J. Xu, J.G. Andrews, and S.A. Jafar, *MISO Broadcast Channels with Delayed Finite-Rate Feedback: Predict or Observe?*, IEEE Trans. Wireless Commun., pp. 1456–1467, Apr. 2012.
- [Y⁺13] S. Yang et al., *Degrees of Freedom of Time Correlated MISO Broadcast Channel With Delayed CSIT*, IEEE Trans. on Inf. Theory, pp. 315–328, Aug. 2013.
- [Y⁺14] X. Yi et al., *The Degrees of Freedom Region of Temporally Correlated MIMO Networks With Delayed CSIT*, IEEE Trans. on Inf. Theory, pp. 494–514, Jan. 2014.
- [Z⁺14] Y. Zeng et al., *Degrees of Freedom of the Three-User Rank-Deficient MIMO Interference Channel*, IEEE Trans. on Wireless Commun., pp. 4179–4192, Aug. 2014.